SANDIA REPORT SAND84—0799 • Unlimited Release • UC—94cb
Printed March 1984

Final Battery Evaluation Report: Energy Research Corporation Zinc/Bromine Battery

P. C. Butler, D. W. Miller, C. E. Robinson,
Anthony Leo

Prepared by
Sandia National Laboratories
Albuquerque, New Mexico 87185 and Livermore, California 94550
for the United States Department of Energy
under Contract DE-AC04-76DP00789

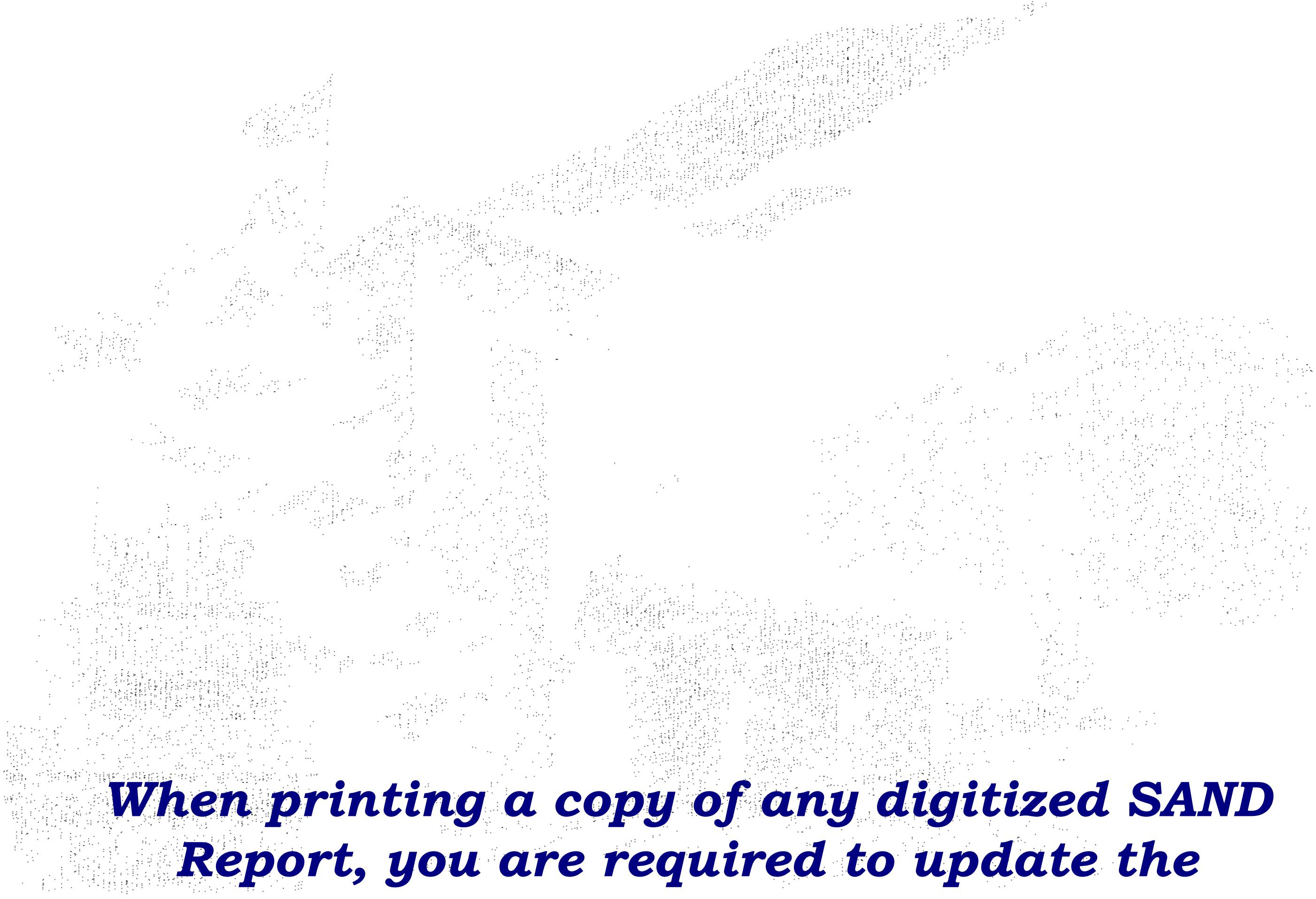

SF2900Q(8-81)

Printed in the United States of America
Available from
National Technical Information Service
U.S. Department of Commerce
5285 Port Royal Road
Springfield, VA 22161

NTIS price codes
Printed copy: A05
Microfiche copy: A01

TABLE OF CONTENTS

LIST OF TABLES

LIST OF FIGURES

Abstract

This final report describes the results of an evaluation of an Energy Research Corporation zinc/bromine, flowing electrolyte battery. This work was performed at Sandia National Laboratories for the U.S. Department of Energy and the Electric Power Research Institute. Included in the report is a description of the battery, charge/discharge cycle test results, failure analysis investigations, and conclusions summarizing what was learned from the evaluation. Extensive appendices are included with detailed descriptions, data, and failure analyses photographs. The battery operated for 163 charge/discharge cycles with an average electrochemical energy efficiency of 54 ± 10%. The primary causes of failure were electrode de-bonding from flow frame assemblies and non-uniform electrolyte flow distribution.

FINAL BATTERY EVALUATION REPORT
ENERGY RESEARCH CORPORATION
ZINC/BROMINE BATTERY

INTRODUCTION

Sandia National Laboratories (SNL) has responsibility for the Exploratory Technology Development and Testing (ETD) lead center for the Electrochemical Branch of the U. S. Department of Energy (DOE). This involves contracting and managing the development of advanced, rechargeable battery systems. Also, an in-house battery test lab evaluates prototype, contract deliverable batteries in order to objectively judge development progress and identify key problem areas. Sealed lead-acid, zinc/bromine, NASA Redox, and nickel/hydrogen batteries have been tested.

This final report will describe the test results for a flowing electrolyte zinc/bromine battery. The battery was built by Gould Laboratories under contract to the Division of Energy Storage of DOE and the Electric Power Research Institute (EPRI). This battery was designed specifically for utility load-leveling applications. Testing was performed by SNL at the request of EPRI free of charge. SNL had expertise in testing flow batteries from Exxon and NASA-Lewis and had all necessary equipment for evaluating the Gould unit. Shortly after delivering the battery to SNL, Gould sold their zinc/bromine technology to Energy Research Corporation (ERC).

The goals of the tests were to evaluate the ERC zinc/bromine technology relative to performance, life, maintenance requirements, and failure mechanisms. This data was valuable to SNL, ERC, Gould, EPRI, and DOE so that an accurate, independent appraisal of the Gould technology could be made. The data has been used to direct battery redesign and in guiding the development program's emphasis.

General battery specifications provided by Gould are given in Table 1. A photograph of the unit is presented in Figure 1. A report is available that describes this technology in detail.(1) The battery operations manual provided by Gould is reproduced in Appendix A and contains other construction details.

The battery consisted of two electrolyte reservoirs which were loosely covered and not sealed, three pumps, associated plumbing, and a 20-cell bipolar cell stack. Each cell was constructed of a vitreous carbon bipolar plate with one side left flat as a zinc substrate and one side contacting a felt flow-through bromine electrode along with a microporous separator. Approximately 36 ℓ of zinc bromide electrolyte were contained in each reservoir. Approximately 10 ℓ of bromine complexing agent was also contained in the catholyte reservoir.

The three magnetically-coupled centrifugal pumps were equipped with 120-V ac motors and operated at maximum output continuously. Electrolyte flow was controlled by throttling valves downstream from the pumps. The battery cooling system consisted of a coil of titanium tubing immersed in the anolyte. Laboratory tap water was used as the cooling medium. Tap water was run continuously while the battery was operating and maintained the system at about 30°C. An upper temperature limit of 35°C was established by Gould due to the temperature sensitivity of the electrode-to-frame bond.

The SNL test lab is described in a previous paper.(2) A block diagram in Figure 2 represents the test equipment used for the testing. A Hewlett-Packard (HP) 85 served as test controller and was interfaced using an HP-IB cable to a HP 3497A data acquisition and relay device. Table 2 lists data items that were measured and stored by the computer system. The 3497A controlled two 25-A, 240-V dc relays, one of which connected the battery into the electrical circuit and one to select either a charge or discharge regime. The battery was

Table 1

ERC/Gould Zinc/Bromine Battery
At Sandia: Specifications

SNL Identification #	168
Energy Rating	6.4 kWh
Capacity Rating	200 Ah
Number of Cells	20
Ave. Discharge Volt	30
Power Rating	800 W
Nominal Electrode Area	1000 Sq. Cm.
Number of Pumps	3
Number of Valves	7
Dimensions (lxdxh)	60x26x30.5 in.

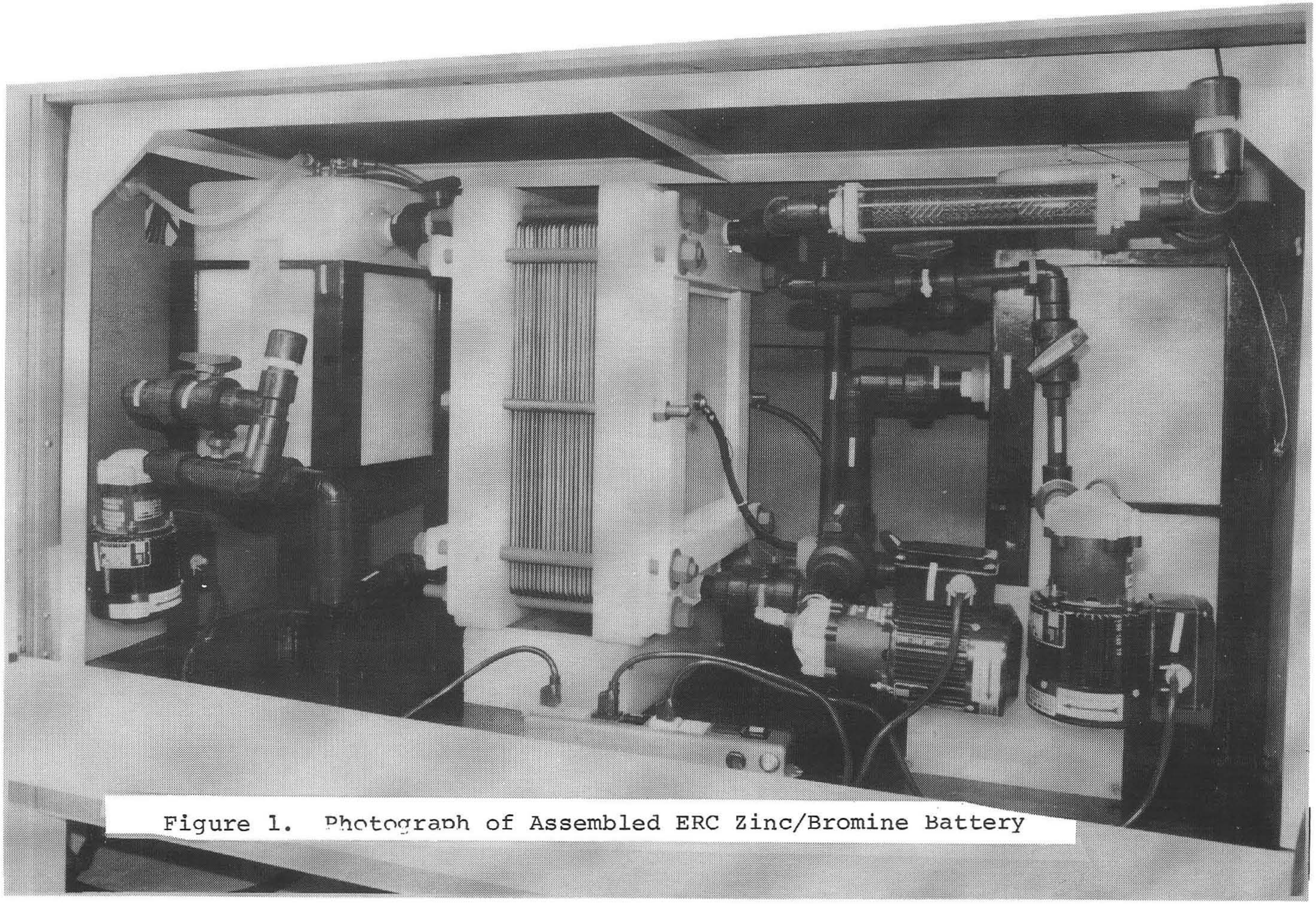

Figure 1. Photograph of Assembled ERC Zinc/Bromine Battery

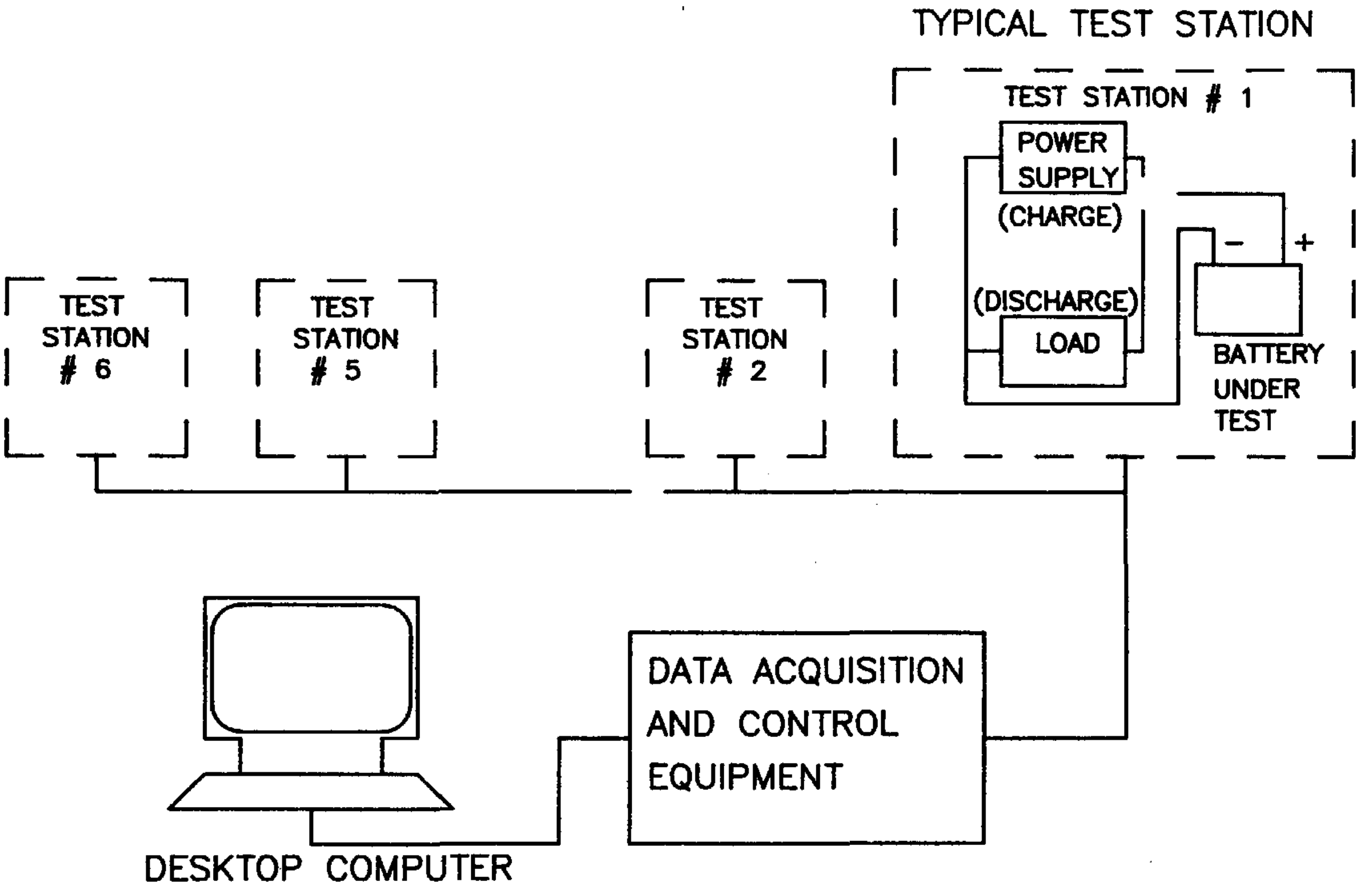

Figure 2. Battery Evaluation Laboratory Test System Block Diagram

Table 2

Data Items Measured by SNL Computer Battery Testing System

Date
Time
Battery Voltage
Battery Current
Battery Temperature
Six spare channels for cell voltages, pressures, etc.

Parameters Calculated During Data Collection

Amp-hours charged and discharged
Watt-hours charged and discharged

charged with two Sorenson power supplies in series. One supply was model DCR40-250 while the other was Model DCR40-125A. The battery was discharged with two acdc Electronics transitorized loads connected in parallel. The model used was EL750BR-2-1.

Data were recorded by the desktop computer in real time on 5-1/4-inch floppy discs. Subsequently, all data were transferred to 8-inch floppy discs and hard discs for archiving purposes. Critical cycle data were placed in a flow battery data base and accessed by a HP 9845B desktop computer. This system permitted the preparation of data lists, graphical data displays, and statistical summaries. Starting at cycle 32, at the request of Gould personnel, a strip chart recorder was used to monitor battery voltage and current. These traces were sent to Gould for analysis.

A test plan (Appendix B) was prepared prior to beginning battery testing. It was based on a similar plan used for evaluating Exxon zinc/bromine batteries. A typical cycle began with the battery completely discharged, i.e., 0 volts. A constant current charge for a specified time period initiated a cycle. Following the charge, the battery was immediately switched to a constant current discharge which was terminated when the battery voltage reached 20 V or 1 volt per cell. At this point, the battery was discharged through a 50-ohm, 1200-W resistor until it reached 0 volts. Cycle coulombic, voltaic, and energy efficiencies were calculated based on the total charge and the discharge to the 20-V cutoff point.

The test plan included a factorial sequence of parametric cycles to evaluate battery performance over a range of four factors. Charge rate, discharge rate, maximum state-of-charge of zinc loading (charge time), and temperature were chosen as critical factors. Table 3 lists the values of the various factors at each of the two levels chosen. A baseline cycle type was selected based on recommendations made by Gould personnel. Cycle type 9 was used as the baseline regime in order to judge variations in battery performance.

Table 3

SNL Cycle Description for ERC $ZnBr_2$ Battery

Cycle Type Identification Number	Cycle Description			
	Charge Current(A)	Discharge Current(A)	Maximum (%) State of Charge	Battery (C) Temperature
1	25	25	50	20
2	25	25	75	20
3	25	25	75	20
4	25	30	75	20
5	30	25	50	20
6	30	25	75	20
7	30	30	50	20
8	30	30	75	20
9(baseline)	25	25	50	30
10	25	25	70	30
11	25	30	50	30
12	25	30	75	30
13	30	25	50	30
14	30	25	75	30
15	30	30	50	30
16	30	30	75	30

Note: Current densities (mA/sqcm): 25A=27; 30A=32

CYCLE TEST DATA

Preliminary cycle data have been presented in previous publications (3, 4). This section will review battery history and observations made during testing. Data will be presented that detail performance over the life of this unit.

The battery was delivered and installed by Gould personnel on November 10-12, 1981. The system was shipped in a Gould van driven to Albuquerque from Chicago by a battery technician. All battery components were installed inside a fume hood.

Zinc bromide electrolyte prepared by Gould was filtered and pumped into the catholyte and anolyte reservoirs. Approximately 36 ℓ was added to the negative (anolyte) side while 46 ℓ was added to the positive (catholyte) side. Ten liters of polybromide (BCL-3) and 800 mℓ of bromine were added to the catholyte. ZDS-11 (720 mℓ) was added to the anolyte.

All three electrolyte pumps were then turned on and flow rates adjusted according to Gould procedures. These rates were determined by measuring electrolyte pressures using a portable transducer at one point in each flow system (catholyte and anolyte). Pressure readings were then correlated, using Gould data, to flow rates. The initial set points were 3 gpm for the anolyte and 2 gpm for the catholyte. Flow rate adjustments and pressure measurement were a source of trouble during life testing, as will be described later.

Following the completion of installation, electrical cycle testing commenced. The baseline cycle described above was used repeatedly to measure battery performance. The test plan required baseline cycle (type 9) testing until stable performance was obtained. After battery operation stabilized, the factorial test cycles were run.

Appendix C contains representative voltage, current, and temperature, plots for several cycles throughout the life of the battery. These plots were generated from archived computer data files. Similar data for any cycle is available if needed. Strip chart recordings of current and voltage were sent to Gould and ERC for analysis and retention.

Figure 3 illustrates coulombic, voltaic, and energy efficiencies versus cycle type and cycle number for the life of this battery. Efficiency values are exclusively electrochemical; losses due to pumps, cooling systems, or any other auxiliaries are not included. Table 4 lists important cycle life events for the battery.

Electrolyte flow rates were adjusted as instructed by Gould on a weekly basis. This procedure involved some spillage of electrolyte and was generally messy. During early cycle testing, pressure readings were relatively stable and correlated well with visual observations. After cycle 30, pressure readings began to increase. Correspondingly, these pressures (flow rates) became more difficult to adjust to nominal values. Flow adjustment was complicated by the numerous valves present on the battery system. Visual inspection of catholyte flow in the polybromide mixing tube indicated decreased flow while pressure increased. Also, the adjustment of polybromide flow depended exclusively on visual observation in the mixing tube. As the changes noted above occurred, polybromide flow rate adjustment became more difficult and less repeatable.

During the first 48 cycles, efficiencies generally declined. This trend was reversed at cycle 48. Two major changes were made in the system at this point. Flow filters in both the catholyte and anolyte pipes had become blocked

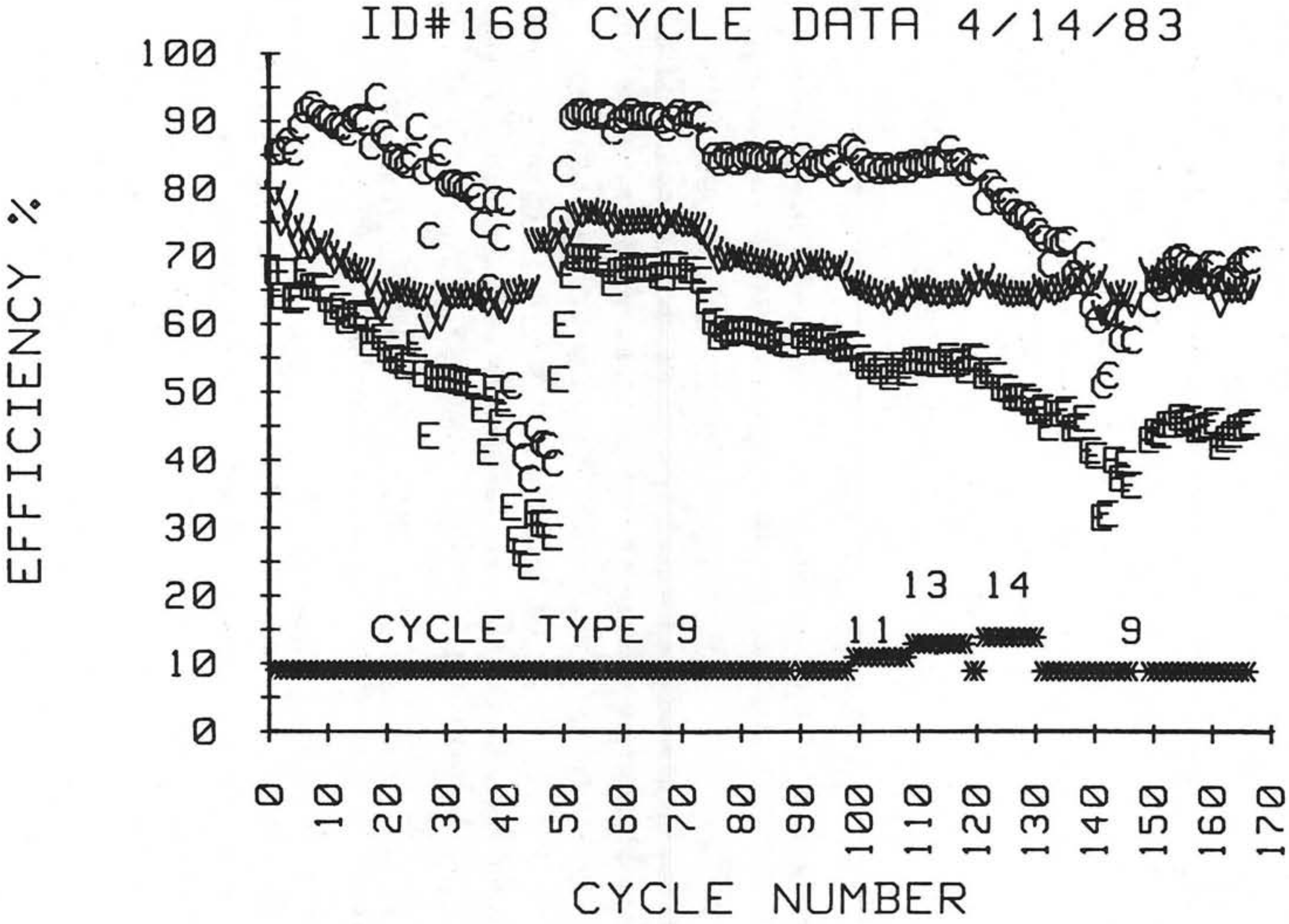

Figure 3. Efficiency and Cycle Type Versus Cycle Number for Battery 168
C = coulombic; V = voltaic; E = energy; X = cycle type identification number

Table 4
Cycle Life Events

Date	Cycle #	Event/Action
11/12/81	0	Installation, start-up with Gould assistance
4/15/82	48	Gould personnel cleaned blocked in-line flow filters on both catholyte and anolyte flow systems. Removed BCL-3 bromine complexer, added BCL-2 complexer. Added three pressure taps.
4/28/82	53	Attempted to seal reservoirs with silicone rubber gaskets.
5/20/82	65	Repaired minor leaks in plumbing. Found that some original pipe sealing compound had discolored. Attempted to use siphon tube between reservoirs. Could not maintain siphon for more than a few hours.
6/9/82	75	Checked in-line flow filters. No blockage.
7/29/82	99	Started factorial test regime
8/30/82	120	Noted that electrolyte reservoir volumes (transfer rate) were harder to control that on previous cycles.
10/12/82	140	Anolyte reservoir overflowed during cycle.
2/2/83	163	Terminated cycle test, began teardown, and failure analysis with ERC and Gould personnel assistance.

with pipe thread sealer and an unidentified, black substance. Sandia personnel were not aware of these filters prior to cycle 48. Gould personnel located and cleaned the filters. Also, the polybromide material (BCL-3) was siphoned out of the reservoir and a new bromine complexing agent (BCL-2) was installed. Three additional pressure taps were installed in the system in an attempt to improve flow rate adjustment accuracy.

Performance improved drastically following these two changes. No other major revisions were made to the battery during cycle life testing. While the efficiencies fluctuated somewhat after cycle 48, no clear-cut cause and effect relationships have been established.

With the addition of more pressure taps, flow rate adjustments became even more messy and accuracy was not obviously improved. Flow rates were adjusted following cycle 48 in order to maintain a balance of volumes in each electrolyte reservoir, rather than by pressure readings.

The factorial test sequence began at cycle number 99. Coulombic efficiency began to decline at cycle number 122. This corresponded to a cycle type (14) requiring a 150-mAh/cm^2 zinc loading. All previous cycles had used 100-mAh/cm^2 zinc loading. After returning to 100-mAh/cm^2 cycles, coulombic efficiency continued to decline before stabilizing. Also after cycle number 122, electrolyte transfer from one reservoir to another increased and became very hard to control.

Electrolyte flow management difficulties and generally low efficiencies after cycle 150 resulted in a decision by Sandia, EPRI, and ERC to terminate cycle testing and begin failure analysis.

The cycle life history is described in more detail in the following tables and figures. Table 5 lists cycle number, coulombic efficiency, voltaic efficiency, energy efficiency, and cycle types. Approximately five cycles have been omitted from all data listings. This was due to data acquisition system errors or test equipment failures. Because in all cases the data were lost, these five will not be included in this report.

Table 6 is a listing of cycle number versus date, end-of-charge voltage (EOC voltage), end-of-discharge temperature (EOD voltage), and end-of-discharge temperature (EOD temperature). The end-of-discharge values serve to verify that the voltage was below 20 V when each discharge terminated and that the electrolyte/battery temperature did not exceed 30-35°C. The end-of-charge voltage shows a correlation of high charge voltage with poor efficiency. During cycles with high efficiency, the end-of-charge voltage typically was just over 40 V. As performance declined prior to cycle 48, and near the end-of-life, charge voltage increased to 42-43 V.

Since the battery failed before the factorial test sequence was completed, a factorial data analysis was not made. Average efficiencies were calculated for the four different cycle regimes used in the tests and are presented in Figure 4. These averages along with standard deviation values are listed in Table 7. Refer to Table 3 to identify the different cycle type identification numbers. No differences in efficiencies are evident between cycle types 11 and 13. These cycle regimes varied charge and discharge rate at the same zinc loading. Cycle type 14, however, increased zinc loading to 150 mAh/cm^2 and coulombic efficiency suffered an irreversible degradation which contributed to a lower average efficiency.

TABLE 5

ERC BATTERY FINAL CYCLE DATE 4/30/83 (REVISED)

Cycle Number	Coulombic Efficiency %	Voltaic Efficiency %	Energy Efficiency %	Cycle Type
1	85.40	79.30	67.70	9
2	85.70	74.80	64.10	9
3	86.97	77.84	67.70	9
4	85.38	74.42	63.54	9
5	89.24	71.73	64.01	9
6	91.63	74.12	67.91	9
7	92.44	70.81	65.46	9
8	91.18	71.91	65.57	9
9	90.39	72.17	65.23	9
10	90.36	70.54	63.74	9
11	89.30	69.20	61.80	9
12	89.18	70.23	62.64	9
13	88.31	68.56	60.55	9
14	90.30	67.90	61.30	9
15	90.59	67.94	61.55	9
16	89.90	67.80	61.00	9
17	86.30	66.20	57.20	9
18	93.62	63.09	59.07	9
19	88.20	62.10	58.10	9
20	87.29	64.46	56.27	9
21	84.70	64.89	54.96	9
22	84.11	65.01	54.68	9
23	83.54	64.45	53.84	9
24	84.81	64.30	54.53	9
25	89.20	64.10	57.18	9
26	82.58	63.77	52.67	9
27	73.05	59.69	43.61	9
28	83.21	62.60	52.08	9
29	85.42	60.86	51.99	9
30	80.78	64.59	52.17	9
31	80.90	64.13	51.88	9
32	80.48	64.21	51.68	9
33	79.94	64.27	51.38	9
34	80.53	63.93	51.49	9
35	78.81	64.53	50.85	9
36	74.71	63.60	47.52	9
37	65.39	63.05	41.23	9
38	78.40	64.52	50.58	9
39	72.81	62.56	45.55	9
40	78.01	61.98	48.35	9
41	50.93	64.87	33.04	9
42	43.65	64.82	28.29	9
43	40.48	64.93	26.28	9
44	37.20	65.45	24.35	9
45	44.58	72.32	32.25	9
46	42.38	72.46	30.71	9
47	42.15	72.39	30.52	9
48	39.55	72.50	28.67	9
49	75.40	68.89	51.94	9
50	82.96	72.31	59.99	9
51	90.72	74.20	67.31	9
52	91.44	76.50	69.95	9
53	91.48	76.21	69.72	9
54	90.98	76.82	69.89	9

TABLE 5

ERC BATTERY FINAL CYCLE DATE 4/30/83 (REVISED)

Cycle Number	Coulombic Efficiency %	Voltaic Efficiency %	Energy Efficiency %	Cycle Type
55	90.80	76.51	69.47	9
56	91.41	76.42	69.85	9
57	90.80	76.00	69.00	9
58	88.60	74.68	66.16	9
59	90.21	75.24	67.88	9
60	90.65	75.04	68.02	9
61	91.50	75.08	68.70	9
62	90.63	75.28	68.22	9
63	91.02	75.23	68.48	9
64	90.60	75.37	68.29	9
65	90.94	75.43	68.59	9
66	90.27	74.56	67.30	9
67	89.09	75.22	67.01	9
68	90.47	76.15	68.90	9
69	91.38	75.23	68.74	9
70	89.70	74.83	67.12	9
71	90.99	74.82	68.09	9
72	91.05	74.73	68.04	9
73	90.45	73.65	66.61	9
74	87.17	72.85	63.51	9
75	84.97	71.17	60.48	9
76	83.99	69.34	58.25	9
77	85.07	69.81	59.39	9
78	84.32	69.66	58.73	9
79	84.10	70.27	59.10	9
80	84.86	69.92	59.34	9
81	85.14	69.48	59.16	9
82	84.97	69.24	58.84	9
83	84.54	69.45	58.71	9
84	84.40	69.02	58.25	9
85	85.28	68.67	58.56	9
86	84.37	68.34	57.66	9
87	84.54	67.74	57.27	9
88	83.67	68.29	57.14	9
89	84.97	68.72	58.40	9
90	83.01	69.22	57.47	9
91	83.94	69.42	58.27	9
92	83.68	69.01	57.75	9
93	84.02	68.46	57.52	9
94	84.77	68.42	58.00	9
95	82.37	69.07	56.90	9
96	82.96	68.07	56.47	9
97	86.31	66.22	57.15	9
98	85.58	66.18	56.64	11
99	84.14	65.49	55.11	11
100	82.98	65.03	53.96	11
101	83.54	64.69	54.05	11
102	82.76	64.25	53.18	11
103	83.52	64.66	54.00	13
104	82.79	63.27	52.38	11
105	82.95	64.13	53.20	11
106	83.65	64.62	54.05	11
107	83.00	63.83	52.98	11
108	84.03	65.17	54.76	11

TABLE 5

ERC BATTERY FINAL CYCLE DATE 4/30/83 (REVISED)

Cycle Number	Coulombic Efficiency %	Voltaic Efficiency %	Energy Efficiency %	Cycle Type
109	83.76	65.51	54.87	13
110	83.70	65.06	54.46	13
111	84.46	64.56	54.52	13
112	83.96	64.70	54.33	13
113	84.00	64.88	54.50	13
114	86.07	64.34	55.38	13
115	84.02	64.66	54.33	13
116	84.27	64.80	54.60	13
117	82.57	64.65	53.38	13
118	83.41	66.36	55.35	9
119	83.33	66.06	55.05	9
120	78.21	67.23	52.58	14
121	81.04	65.77	53.30	14
122	80.04	65.76	52.64	14
123	78.28	64.89	50.79	14
124	78.35	64.63	50.64	14
125	76.69	64.53	49.49	14
126	76.12	64.73	49.27	14
127	76.32	64.75	49.42	14
128	75.27	64.68	48.68	14
129	73.89	64.11	47.37	14
130	72.85	65.72	47.88	9
131	69.03	65.21	45.02	9
132	72.54	64.85	47.04	9
133	72.07	65.31	47.06	9
134	72.64	65.54	47.61	9
135	67.60	66.43	44.91	9
136	66.60	67.76	45.13	9
137	70.40	65.82	46.34	9
138	62.79	66.25	41.59	9
139	60.80	67.19	40.85	9
140	51.23	61.85	31.68	9
141	52.70	61.23	32.27	9
142	61.86	64.99	40.21	9
143	57.99	64.60	37.46	9
144	61.22	64.78	39.66	9
145	57.83	63.09	36.49	9
146	63.34	68.23	43.21	9
147	66.52	66.75	44.40	9
148	65.55	67.03	43.94	9
149	68.17	66.73	45.49	9
150	69.73	65.29	45.52	9
151	70.11	66.36	46.53	9
152	69.10	66.13	45.70	9
153	68.65	67.42	46.28	9
154	66.66	67.16	44.77	9
155	67.81	66.57	45.14	9
156	69.11	65.68	45.39	9
157	68.98	66.70	46.01	9
158	66.92	63.12	42.24	9
159	66.59	65.09	43.35	9
160	67.47	65.25	44.03	9
161	68.92	65.34	45.03	9
162	69.59	65.05	45.27	9
163	69.79	65.68	45.83	9

TABLE 6

ERC BATTERY FINAL CYCLE DATA 4/30/83 (REVISED)

Cycle Number	Date	EOC Voltage	EOD Voltage	EOD (°C) Temperature
1	11/12/81	39.93	16.12	25.13
2	11/12/81	40.64	13.92	29.01
3	11/16/81	40.50	16.16	30.54
4	11/20/81	40.43	18.37	28.93
5	11/30/81	40.96	15.70	28.76
6	12/01/81	41.31	17.47	33.90
7	12/02/81	41.22	12.61	29.79
8	12/03/81	41.91	17.43	31.20
9	12/04/81	42.19	18.99	31.50
10	12/08/81	42.20	19.97	31.18
11	12/09/81	41.92	19.04	29.63
12	12/10/81	41.61	17.43	30.84
13	12/11/81	41.83	17.91	30.12
14	12/17/81	42.27	17.91	30.22
15	12/18/81	42.19	16.21	30.26
16	12/21/81	42.32	19.83	29.77
17	12/22/81	42.44	19.60	29.37
18	01/05/82	42.85	19.39	28.93
19	01/08/82	42.90	17.98	29.81
20	01/11/82	42.92	18.76	29.29
21	01/12/82	42.93	18.58	29.81
22	01/13/82	42.95	19.76	30.04
23	01/14/82	42.94	18.83	30.41
24	01/20/82	42.90	18.22	30.66
25	01/28/82	42.91	19.97	30.21
26	02/02/82	42.91	19.59	30.41
27	02/24/82	43.47	19.93	33.58
28	03/01/82	43.64	19.53	31.24
29	03/02/82	43.41	17.22	29.50
30	03/03/82	43.01	19.99	30.22
31	03/04/82	43.11	19.44	29.10
32	03/04/82	43.28	19.17	30.77
33	03/05/82	43.25	19.84	31.23
34	03/08/82	43.06	18.72	32.29
35	03/09/82	43.17	19.82	31.97
36	03/09/82	43.42	19.25	32.01
37	03/10/82	43.34	19.74	31.78
38	03/11/82	42.78	19.87	32.61
39	03/12/82	43.60	19.63	32.18
40	03/15/82	43.40	19.46	32.50
41	03/16/82	43.40	18.08	31.69
42	03/17/82	43.42	19.57	31.17
43	03/18/82	43.58	19.67	31.42
44	03/19/82	43.47	19.87	31.03
45	03/24/82	41.67	18.31	29.29
46	03/25/82	41.97	19.85	29.71
47	04/01/82	41.43	18.78	29.86
48	04/07/82	41.22	18.90	31.37
49	04/16/82	41.73	18.72	27.53
50	04/22/82	40.78	19.72	28.18
51	04/23/82	40.36	19.53	28.55
52	04/26/82	40.29	16.78	28.66
53	04/28/82	40.42	16.55	28.79
54	04/29/82	40.26	18.99	29.47

TABLE 6

ERC BATTERY FINAL CYCLE DATA 4/30/83 (REVISED)

Cycle Number	Date	EOC Voltage	EOD Voltage	EOD (°C) Temperature
55	04/30/82	40.33	18.91	28.58
56	05/03/82	40.46	19.23	29.35
57	05/04/82	40.50	19.99	28.00
58	05/11/82	40.75	17.22	28.79
59	05/12/82	40.38	18.23	28.05
60	05/13/82	40.56	15.82	27.79
61	05/14/82	40.51	16.45	28.34
62	05/17/82	40.63	18.94	28.81
63	05/18/82	40.58	17.77	29.24
64	05/19/82	40.59	19.16	29.32
65	05/20/82	40.56	19.43	29.52
66	05/24/82	40.62	19.76	29.16
67	05/25/82	40.76	19.79	29.25
68	05/26/82	40.31	18.20	30.25
69	05/27/82	40.63	15.13	29.11
70	06/01/82	40.63	19.69	28.54
71	06/02/82	40.71	16.52	28.55
72	06/03/82	40.62	17.41	28.59
73	06/04/82	40.78	18.73	28.43
74	06/07/82	41.14	18.39	30.15
75	06/08/82	41.35	19.39	29.88
76	06/14/82	41.60	19.62	30.35
77	06/15/82	41.66	17.82	30.59
78	06/16/82	41.71	19.97	30.33
79	06/17/82	41.37	18.09	30.52
80	06/18/82	41.60	19.03	30.65
81	06/21/82	41.63	16.74	30.20
82	06/22/82	41.87	17.84	30.32
83	06/23/82	41.91	18.24	30.86
84	06/24/82	41.77	18.95	30.73
85	07/01/82	41.71	17.43	30.63
86	07/02/82	42.07	19.81	30.30
87	07/06/82	41.93	18.77	30.51
88	07/07/82	41.91	19.44	30.91
89	07/09/82	41.61	18.76	29.93
90	07/14/82	41.82	19.04	31.39
91	07/15/82	41.50	19.00	31.75
92	07/19/82	41.62	19.45	31.38
93	07/20/82	42.07	18.69	30.53
94	07/21/82	41.92	18.93	31.12
95	07/22/82	41.81	18.79	30.98
96	07/23/82	41.63	18.97	30.95
97	07/26/82	42.07	19.47	31.92
98	07/27/82	42.14	19.11	31.67
99	07/28/82	41.98	19.28	31.56
100	07/29/82	41.94	19.58	32.49
101	07/30/82	41.99	19.03	31.22
102	08/02/82	42.27	19.49	31.27
103	08/03/82	42.05	19.38	31.20
104	08/04/82	42.21	19.75	30.92
105	08/06/82	41.97	19.99	31.24
106	08/09/82	42.33	18.86	31.41
107	08/10/82	42.18	19.38	31.46
108	08/11/82	43.30	19.16	30.41

TABLE 6

ERC BATTERY FINAL CYCLE DATA 4/30/83 (REVISED)

Cycle Number	Date	EOC Voltage	EOD Voltage	EOD (°C) Temperature
109	08/12/82	43.22	18.91	30.92
110	08/13/82	43.33	18.87	30.51
111	08/16/82	43.43	18.68	32.54
112	08/17/82	43.48	19.24	31.74
113	08/18/82	43.56	18.02	32.54
114	08/19/82	43.58	19.31	30.54
115	08/20/82	43.41	19.30	30.84
116	08/23/82	43.31	19.15	32.84
117	08/24/82	43.31	19.76	32.67
118	08/25/82	42.23	19.55	30.10
119	08/26/82	42.19	19.06	30.32
120	08/30/82	42.30	19.91	31.78
121	08/31/82	43.34	19.93	30.62
122	09/01/82	42.72	19.10	32.60
123	09/02/82	42.87	19.78	32.22
124	09/07/82	42.67	19.77	32.48
125	09/08/82	42.80	19.96	31.56
126	09/09/82	42.70	19.65	31.68
127	09/13/82	42.84	19.75	31.36
128	09/14/82	42.47	19.63	30.99
129	09/15/82	42.43	19.59	30.67
130	09/16/82	41.91	19.59	31.40
131	09/17/82	42.05	19.73	30.74
132	09/21/82	42.25	19.69	29.11
133	09/22/82	42.06	19.47	30.19
134	09/30/82	42.04	19.75	30.37
135	10/04/82	41.83	19.88	31.25
136	10/05/82	41.34	19.95	32.52
137	10/06/82	42.02	19.68	29.71
138	10/07/82	41.80	19.95	29.99
139	10/11/82	41.95	19.82	29.92
140	10/12/82	41.71	19.73	31.48
141	10/13/82	41.21	19.98	30.23
142	10/27/82	41.46	19.45	29.75
143	10/28/82	41.33	19.91	29.88
144	10/29/82	41.62	19.99	31.33
145	11/01/82	41.26	19.65	30.74
146	12/02/82	41.00	19.60	30.14
147	12/03/82	41.19	19.98	27.93
148	12/06/82	41.18	19.94	28.14
149	12/07/82	41.25	19.75	28.95
150	12/08/82	41.21	19.91	27.55
151	12/09/82	41.46	19.70	27.96
152	12/10/82	41.34	19.78	28.46
153	12/20/82	41.31	19.77	29.20
154	12/21/82	41.38	19.93	29.70
155	12/22/82	41.40	19.20	30.53
156	01/04/83	41.64	19.14	29.80
157	01/10/83	41.13	19.67	30.19
158	01/11/83	42.64	19.62	30.24
159	01/12/83	41.83	19.50	29.70
160	01/13/83	41.70	19.79	29.18
161	01/14/83	41.74	19.83	29.39
162	01/17/83	41.65	19.49	29.59
163	02/02/83	41.86	19.63	30.70

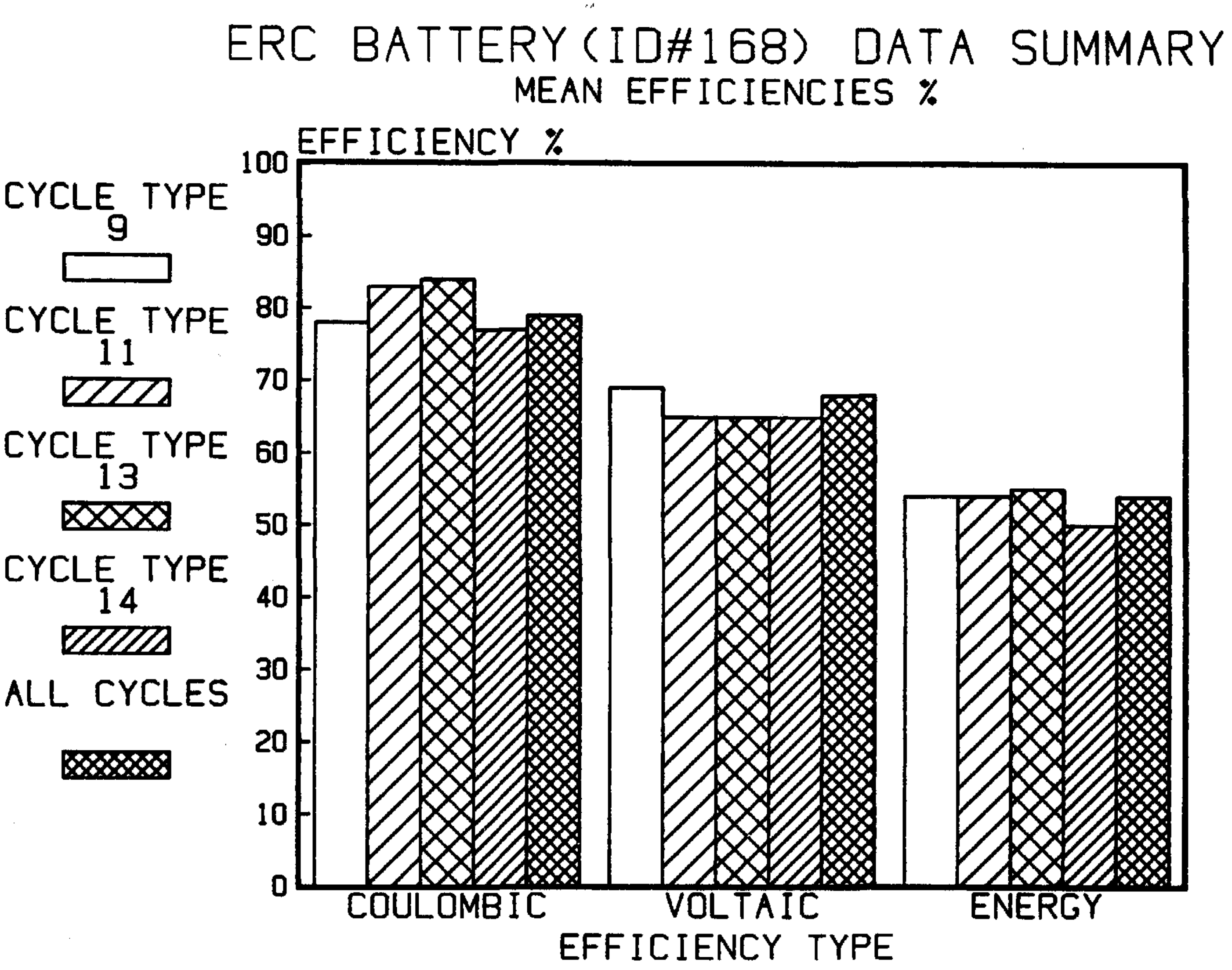

Figure 4. Mean Efficiencies for All Cycle Types Run on Battery 168

Table 7

ERC Battery (ID#168) Cycle Data Summary

Cycle Type	Number of Cycles	Mean Coulombic Efficiency%	Mean Voltaic Efficiency%	Mean Energy Efficiency %
9 (Baseline)	133	78+/-13	69+/-4	54+/-11
11	10	83+/-1	65+/-1	54+/-1
13	10	84+/-1	65+/-1	55+/-1
14	10	77+/-2	65+/-1	50+/-2
All	163	79+/-12	68+/-4	54+/-10

Figures 5 and 6 respectively are plots of amp-hours and watt-hours of charge and discharge versus cycle number. These plots represent the cumulative current and energy values for all charge-discharge cycles. Energy removed during the zinc strip part of a cycle (below 20 V) is not included in these plots.

A plot of cycle number versus cumulative number of calendar days on test is included in Figure 7. Testing typically occurred Monday through Friday, one cycle per day. The battery sat idle on two occasions. Both occurred while Sandia staff awaited information or instruction from either Gould or ERC personnel when a problem was encountered.

Numerous electrolyte chemical analyses were performed during cycle testing. Electrolyte pH was maintained below a value of three except for one occasion. Hydrobromic acid (HBr) was added to the electrolyte to lower the pH when necessary. Figure 8 is a plot of anolyte and catholyte pH versus cycle number while Table 8 is a description of the occurrences of the addition of HBr. Acid was generally added to the catholyte reservoir while the electrolyte pumps were running. Hydrogen ions equilibrate with the anolyte within 30 minutes. Although the pH reached a value of 5 at one point during testing, no solids were observed in the electrolyte during this time and no damage occurred.

Table 9 is a list of the occurrences of the addition of electrolyte to the battery during the test. Electrolyte replenishment was necessary because of several operational problems. Plumbing fittings and connections leaked to different degrees during the test. Also, with certain valve settings and operating conditions, enough back pressure was created inside the battery to cause significant leaks from the electrode stack. This condition was not allowed to

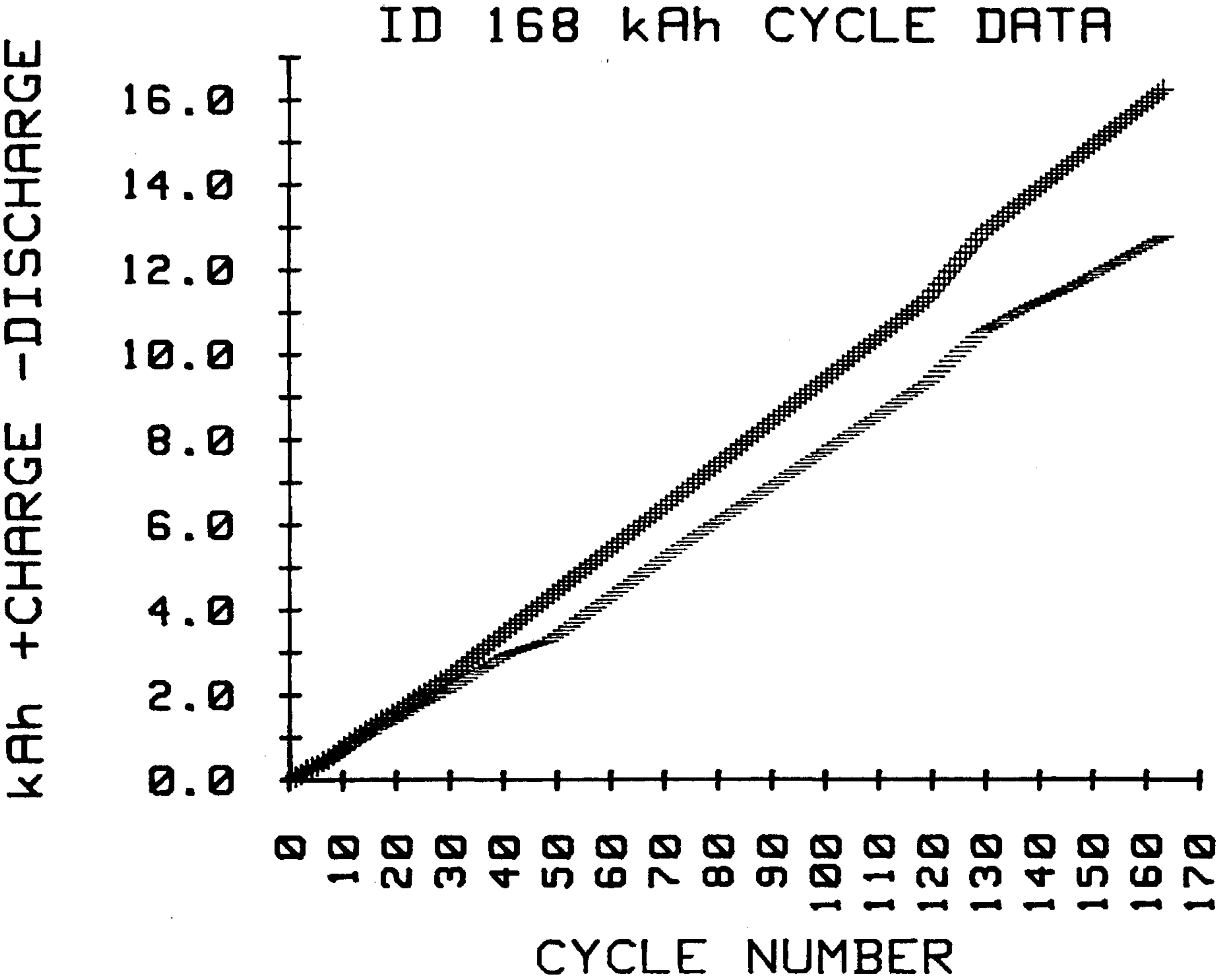

Figure 5. Cumulative Amp-Hours of Charge and Discharge

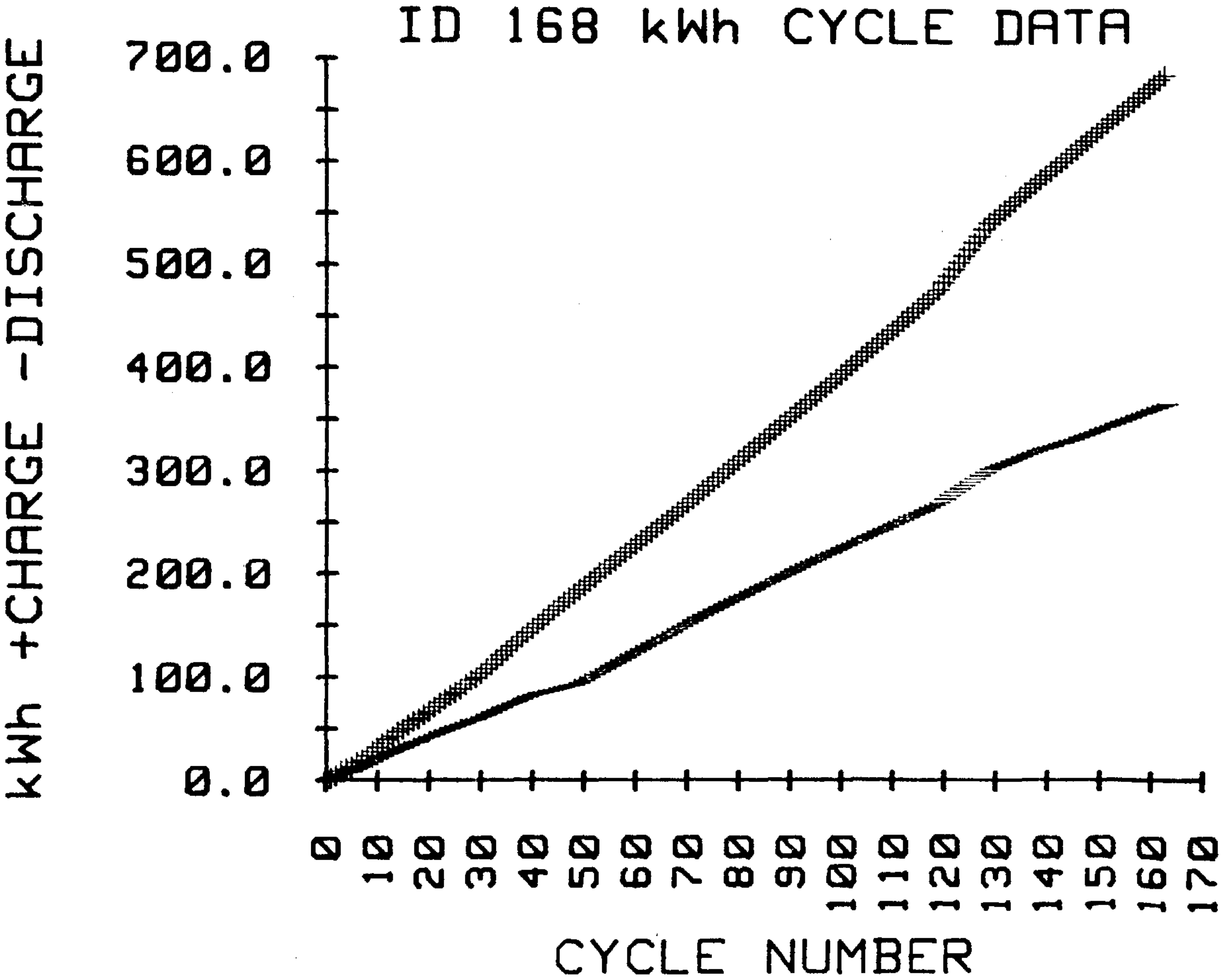

Figure 6. Cumulative Watt-Hours of Charge and Discharge

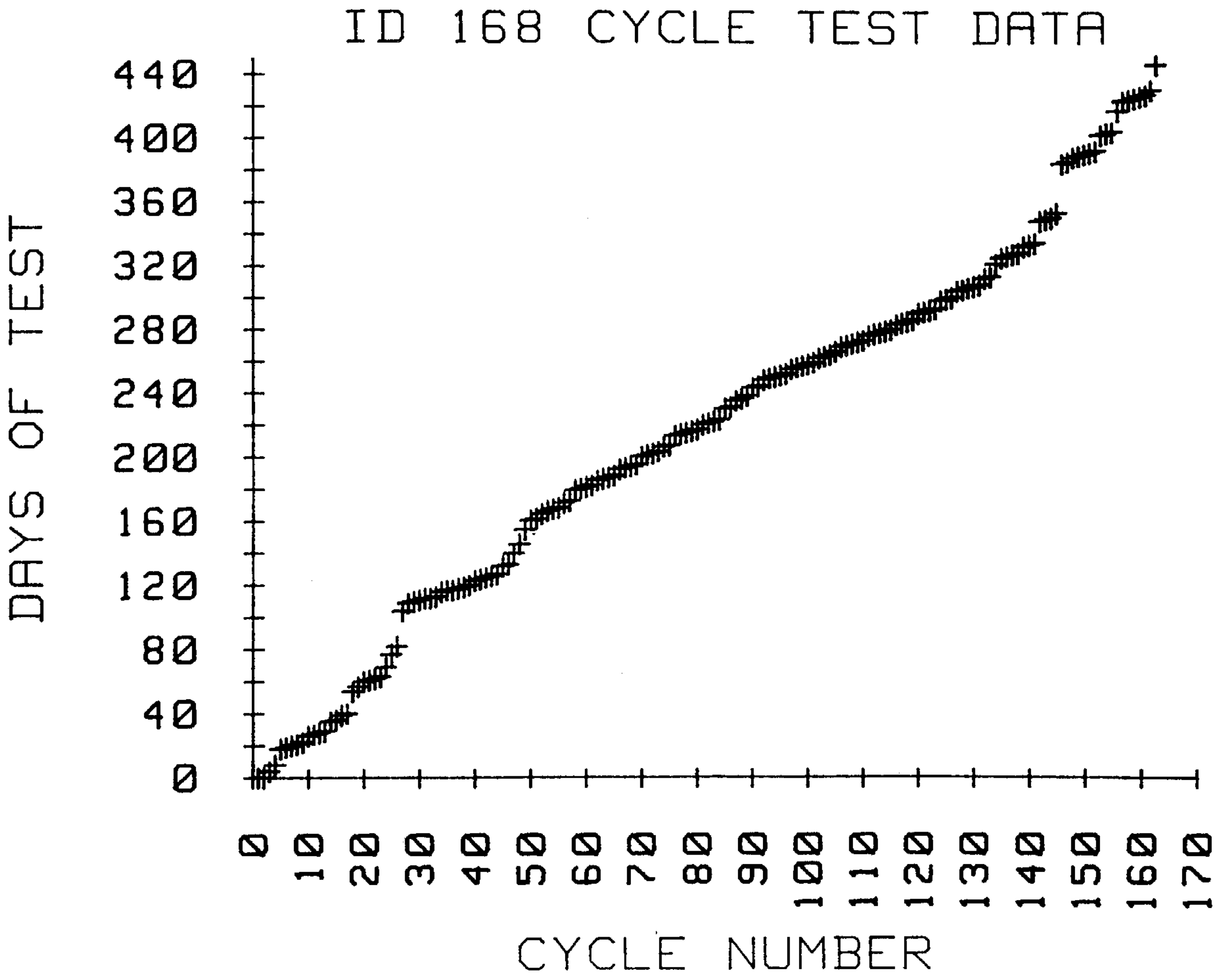

Figure 7. Correlation of Total Number of Days on Test Versus Cycle Number

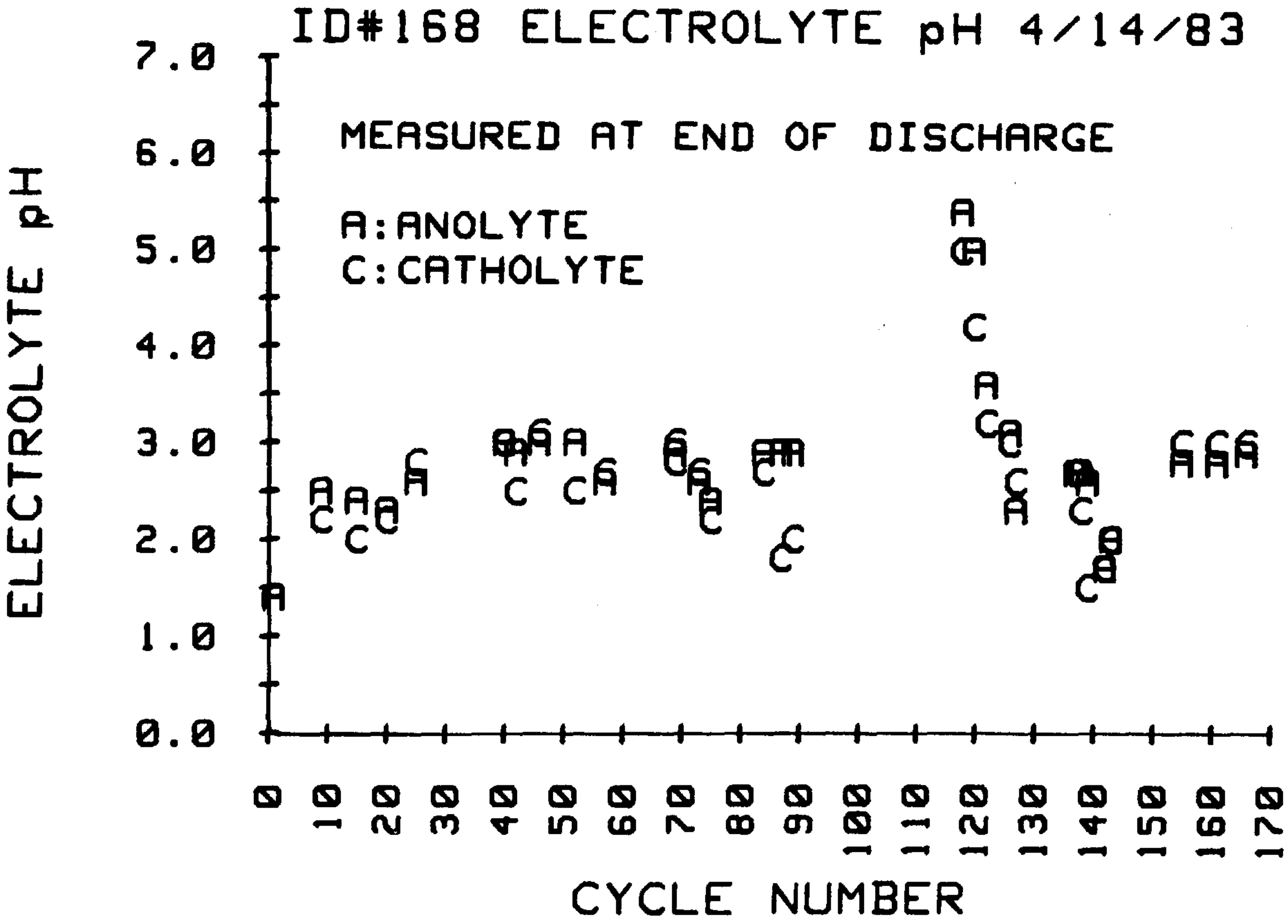

Figure 8. Electrolyte pH Versus Cycle Number

Table 8
Hydrobromic Acid (HBr) Addition

Date	Cycle #	Amount of HBr Added to Catholyte Reservoir (mℓ)
3/16/82	41	50
3/26/82	46	75
5/27/82	69	50
5/28/82	69	50
6/4/82	73	50
6/24/82	84	50
8/24/82	117	50
9/1/82	122	50
9/8/82	125	50*

---

* 50 mℓ added to each reservoir

Table 9

Electrolyte Addition During Cycle Test

		Volume of Electrolyte Added (ℓ)	
Date	Cycle #	Anolyte	Catholyte*
11/11/81	0	36	56
12/16/81	13	8	6
2/25/82	27	?	?
3/16/82	41	5	5
4/16/82	49	--	Removed BCL-3 Added 15ℓ BCL-2/Br_2 mix
4/20/82	50	3.5	3.5
1/12/83	159	0.5	0.5

---

* Includes polybromide in initial fill.

persist for long periods of time. Electrolyte samples were removed periodically and not returned to the battery. Also, due to the identification of a superior bromine complexing agent by Gould staff, the original polybromide material was replaced at cycle 48. Leaks diminished during the later part of the cycle life test. However, on at least one occasion a small amount of electrolyte overflowed a reservoir and had to be replaced by fresh solution.

Gould personnel requested that the battery be operated with an excess of bromine in the catholyte. Samples of electrolytewere removed at the end of charge and a titration performed in duplicate to analyze for bromine. Figure 9 is a plot of results. While the anolyte bromine concentration typically was less than 2 g/ℓ early in life, after cycle 100 it increased to levels approximately that of the catholyte. Bromine catholyte concentrations of about 6 g/ℓ were acceptable and were maintained. Table 10 is a list of the amounts of liquid bromine added to the catholyte during the cycle tests. Regardless of the quantities of bromine added in the early part of testing, bromine concentrations exceeding 6 g/ℓ were not obtained.

During the last cycle (#163), samples of electrolyte were taken every hour starting before the battery began charging. Zinc and bromide were analyzed in anolyte, catholyte, and polybromide solutions. Viscosity and density measurements were made and are tabulated in Appendix D. The cycle was type 9, i.e., a 4-hour, 25-A charge started at time 0 and a discharge at 25 A that started after four hours. The battery reached the 20-V cutoff point immediately prior to hour 7. Figure 10 presents the results of these analyses. It must be remembered that these data were obtained during a period of relatively poor battery performance. The causes of

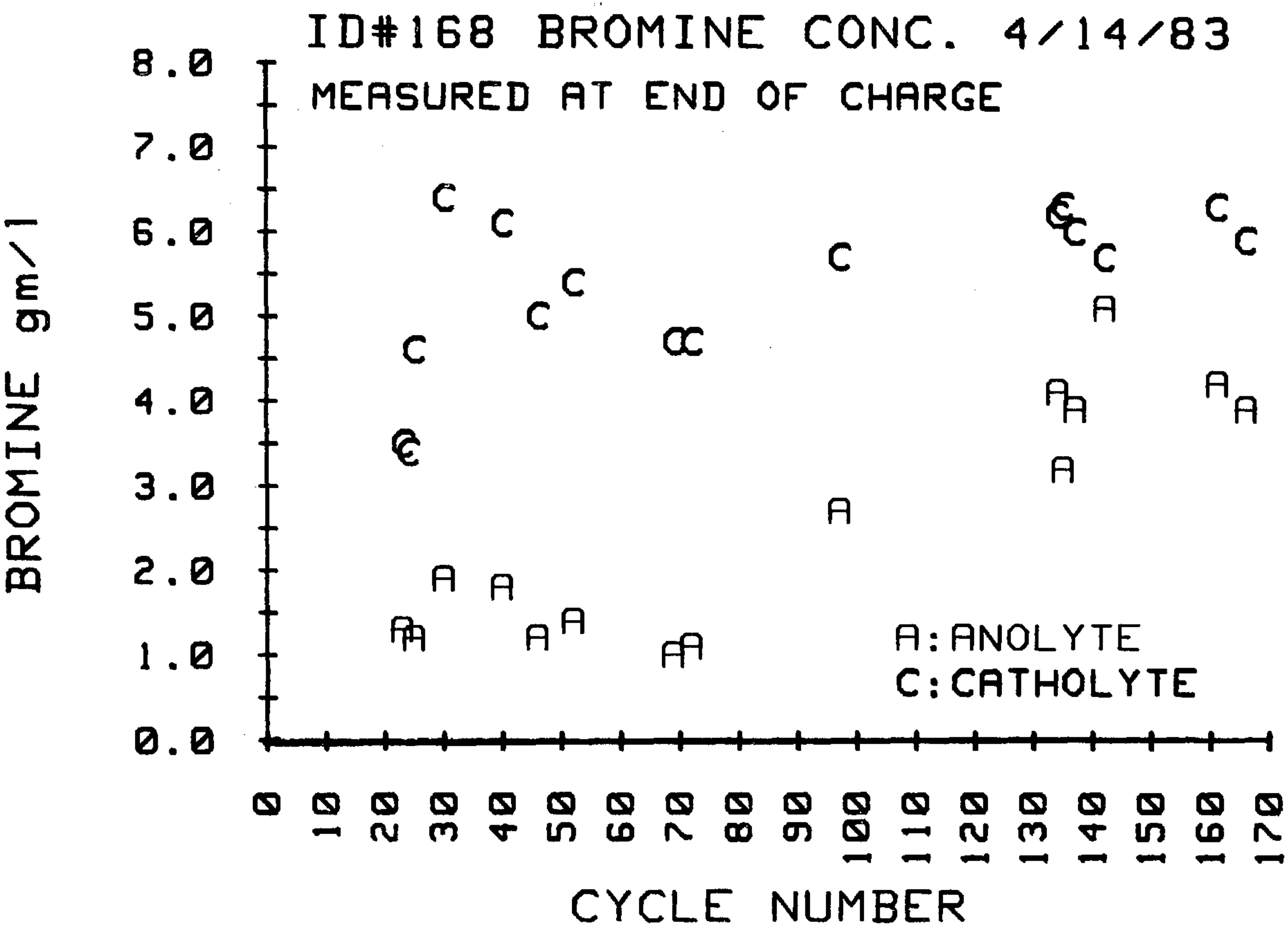

Figure 9. Electrolyte-Free Bromine Concentration Versus Cycle Number

Table 10

Bromine Addition During Cycle Test

Date	Cycle #	Volume Added to Catholyte (mℓ)
1/25/82	24	100
1/26/82	24	100
1/28/82	25	100
1/29/82	25	100
2/2/82	26	42
3/2/82	29	470
3/3/82	30	450
3/16/82	41	200
4/16/82	49	Change bromine complex
6/2/82	71	100
6/4/82	73	200
9/22/82	133	100

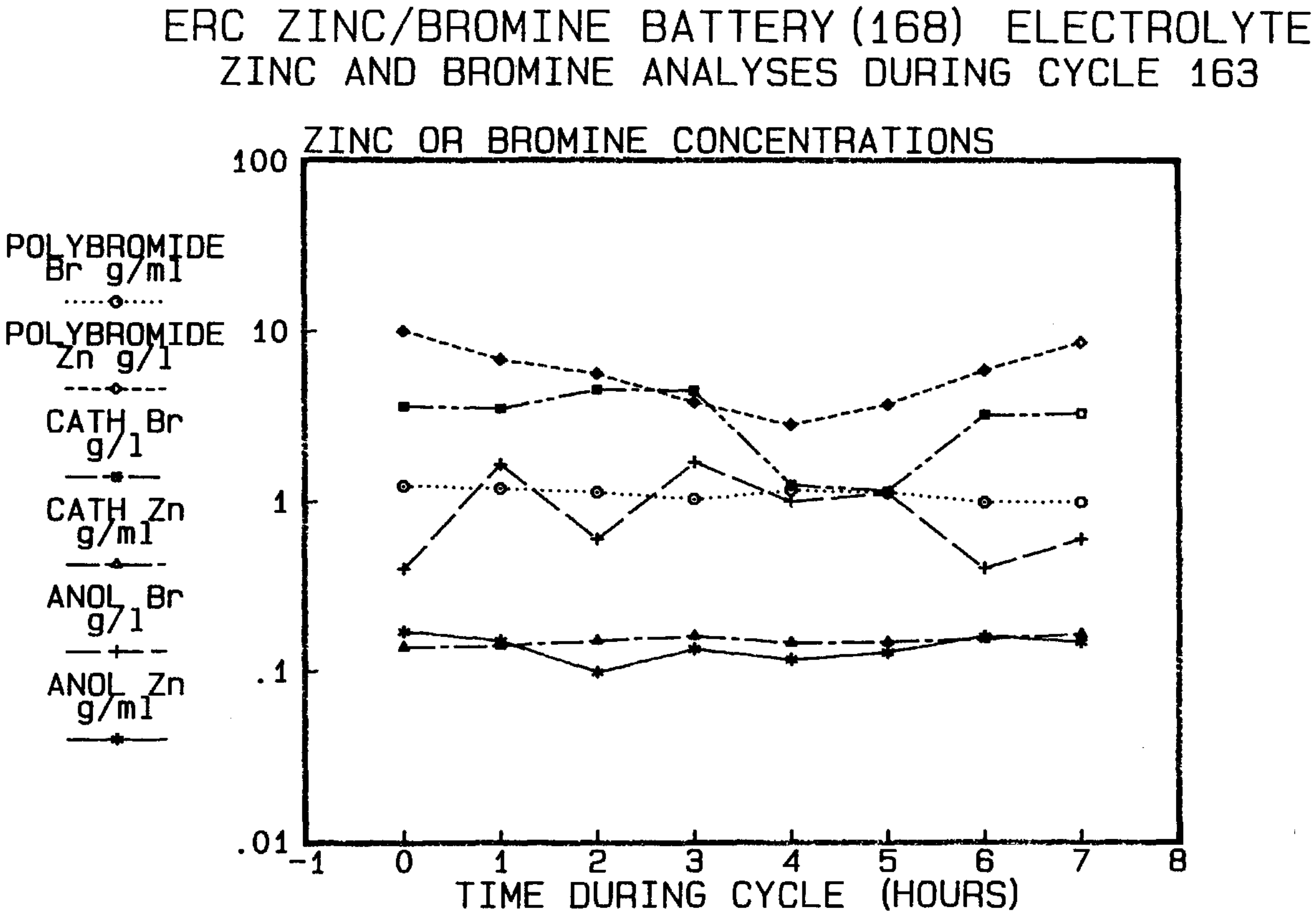

Figure 10. Zinc and Free-Bromine Concentrations During Cycle 163

this poor performance, discussed in the failure analysis section, very likely influenced the results in Figure 10. Random fluctuations occurred in the zinc concentration in the anolyte and catholyte, while a pattern indicated in the polybromide solution. Bromine levels changed in an expected pattern in the anolyte, but randomly varied in the catholyte and were relatively constant in the polybromide. Precision of these results is estimated at ±5%.

Following the life cycle tests, the battery was disassembled and failure analyses begun. This task is described in the next section.

FAILURE ANALYSIS

Disassembly Procedures

Following completion of cycle 163 on February 2, 1983, the battery was prepared for disassembly. On February 16, 1983, it was charged at 25 A for 4 hours according to the usual baseline cycle procedure. At the end of charge, the battery was placed on open circuit and the pumps turned off. The cell stack was isolated from the battery plumbing system and moved to a disassembly fume hood. At that point, following a recommendation by ERC personnel, electrolyte was drained from both sides of the stack and deionized (DI) water was poured into the stack through pipe fittings. A pressurized water feed was not used and, therefore, it was not possible to completely fill the stack with water. The percentage of the stack filled with water was not determined. The battery was left in this condition overnight.

The next day, ERC and Sandia personnel disassembled the battery stack. First, the deionized water was drained. While both anolyte and catholyte solutions were bromine colored as expected, the anolyte solution contained a large quantity of black particles. All solutions were saved for later analysis.

The cell stack retainers were unbolted and all assembly hardware removed. Individual electrodes and separators were removed and inspected one at a time. Each piece was numbered, starting from the negative end plate. The following general observations were made:

1. Zinc deposition was nonuniform on almost all electrodes. Areas near the top and bottom of most electrodes had the poorest zinc deposit. Several electrodes had severe zinc dendrite formations.

Because of non-uniform electrolyte distribution caused by item two below, it is difficult to draw conclusions regarding zinc deposition and shunt currents from these observations.

2. The electrodes were loosely held in the flow frames. Most electrodes were easily lifted out of the frame and few showed signs of being bonded. All electrodes were flat.
3. Copious quantities of a silicone sealer type of material were found throughout the stack assembly.
4. A small quantity of a black coating was found in a limited number of anolyte flow channels. The channels were not blocked.
5. The top half of all separators and bromine electrodes had a heavy layer of salt crystals deposited uniformly on the surfaces.
6. Several separators showed evidence of penetration by zinc dendrites and subsequent localized heating.
7. Electrolyte flow frames had an orange discoloration after removal from the battery. This discoloration gradually faded within a month while the frames were stored in plastic bags. All other plumbing components were in good condition after battery disassembly.

Detailed notes written by Sandia and ERC personnel containing observations, measurements, and topics for further research are given in Appendices E and F. Photographs of all separators and electrodes as they were removed from the stack are included in Appendix G. While the electrode debonding is not obvious from the photographs, it was easily observed. Once the electrodes were removed from the flow frames, they deformed over a two-week period so that they could not be replaced in the flow frames.

All materials were packed in sealed, plastic bags. Representative samples were shipped to ERC for analysis and the rest were saved at Sandia.

ERC Results

Failure analysis activities were divided between Sandia and ERC. The results of the ERC investigations are included here.

Samples of electrode material, separator material and black anolyte residue from the ERC submodule were tested and compared with unused materials (the residue was tested for the presence of ZDS-11 additive). The results were as follows:

Anolyte Residue

A black sludge-like material was collected from the anolyte flow frames. The material was dissolved and tested by atomic absorbtion for the presence of ZDS-11 additive. A level of about 5 ppm was detected in the diluted sample, which is not inconsistent with the level that is normally in the electrolyte. The results suggest no unusual concentration of the additive in the residue.

Separator Material

The separator material was tested for strength and electrical resistivity in electrolyte. Samples were tested for strength in a tensile test machine which stretches the sample at a constant travel rate and records the force and elongation at the break point.

The tapered area on the tensile samples is 1/4" wide by 5/8" long. Results were as follows:

SAMPLE	FORCE AT BREAK, lbs.	ELONGATION %
Uncycled-1	6.1	600
Uncycled-2	7.3	760
Uncycled-3	6.8	740
Average	6.7	700
Cycled-1	6.7	690
Cycled-2	7.5	660
Cycled-3	7.7	740
Average	7.3	700

The data show that the strength of the cycled material is about the same as the uncycled material.

Resistivity of the material in electrolyte was also tested. Resistivity was found to be about 22 cm^2, which is similar to the uncycled DARAMIC, which ranges from 20 to 25 Ω cm^2. Resistivity is measured by determining the voltage drop at 10 mA/cm^2 between Ag-AgBr reference electrodes in electrolyte with and without the presence of separator.

Carbon Electrodes

The strength of the carbon electrodes was measured using a three point flexural strength test. Each sample was supported at two points and pressure was applied at a third point directly in the middle of the two support points. The force at break was measured and divided by the cross-sectional area of the sample to derive the psi flexural strength. The results are shown in the following table.

SAMPLE	THICKNESS, mils	BREAK, lbs.	STRENGTH, psi
Cycled-1	37.4 ±4	5.1	136.4
Cycled-2	35.8 ±8	4.6	128.5
Cycled-3	36.5 ±5	4.8	131.5
Average	36.6	4.8	132.1
Uncycled-1	35.8 ±1	4.1	114.5
Uncycled-2	35.7 ±1	4.5	126.1
Uncycled-3	35.9 ±1	4.2	117.0
Average	35.7	4.3	119.2

The thickness of the cycled electrode material was (on the average) about 2.5% greater than the uncycled material and exhibited much more variability. This could be due to a difference in supplied material, however, an increase in thickness was expected based on stability testing conducted at ERC. The surprising result is that the cycled material is actually about 10% stronger than the uncycled material. This could be due to a filling of open pores with electrolyte salts or to structural changes which occur as the carbon material absorbs Br_2 and swells.

Sandia Results

Scanning electron microscope (SEM) photographs were made of each major battery component. New materials directly comparable to the parts removed from the cell stack were obtained from ERC. Figure 11 is a series of SEM photographs of new and cycled separators at several magnifications. Note the surface cracks evident on the used material. Figure 12 is a series of SEM photographs of a new electrode and used anode surfaces. Areas labeled "dark" were locations where zinc was deposited on the electrode while "light" areas were covered by the plastic grid spacer. The used electrodes had been washed and rinsed with deionized water twice before being photographed. Zinc crystals are visible in some photographs. Figure 13 is composed of SEMs of cathode felt material. The used felt shows signs of compression with several broken fibers. Figure 14 is a series of SEM photographs of a roughened area found on one bromine graphite electrode.

The BET surface area of a new and used separator was measured. The results are summarized below:

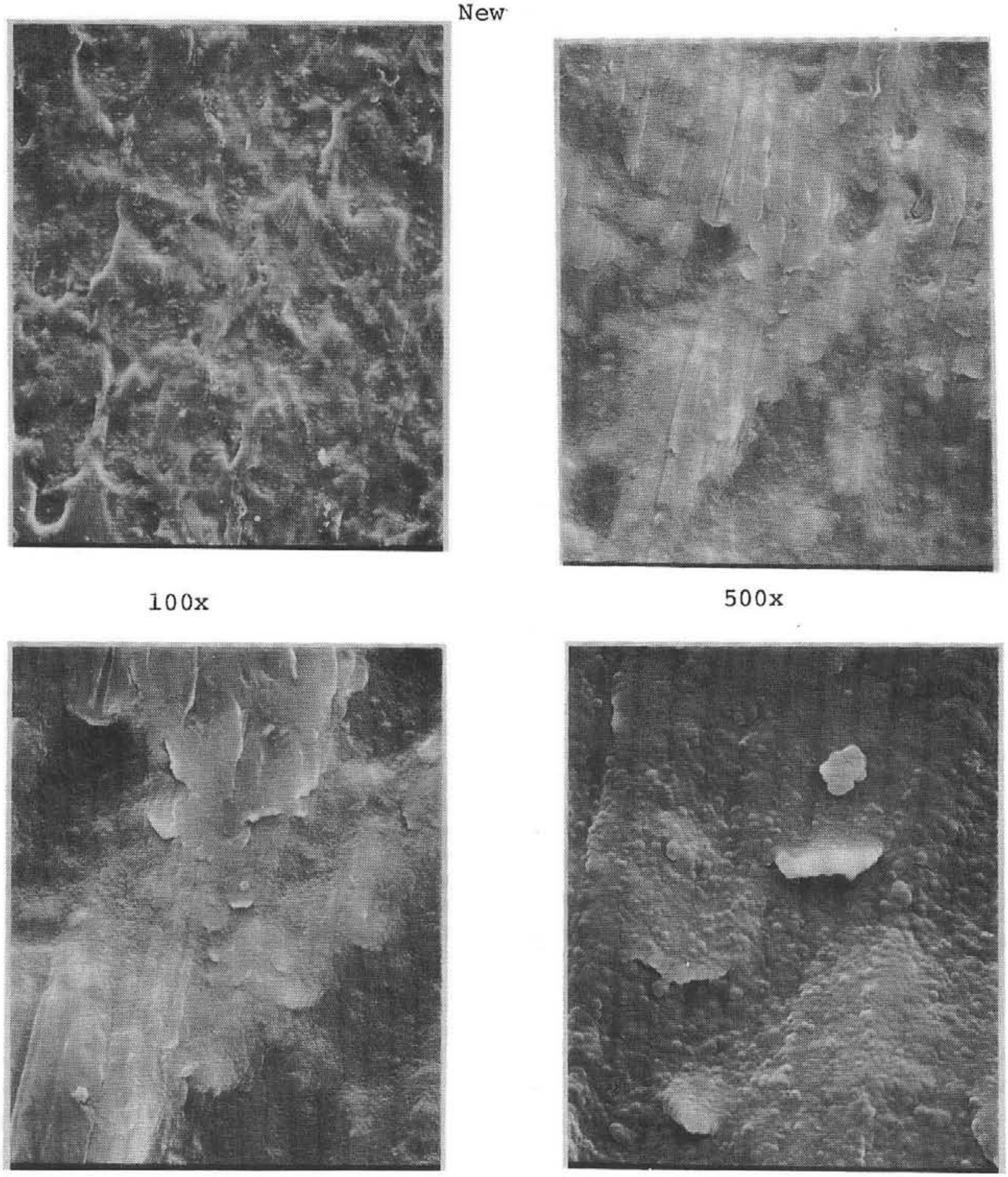

New

100x

500x

1000x

5000x

Figure 11a. SEM of New and Used Separator Material at 100x, 500x, 1000x, and 5000x

Used

100x

500x

1000x

5000x

Figure 11b. SEM of New and Used Separator Material at 100x, 500x, 1000x, and 5000x

New Electrode

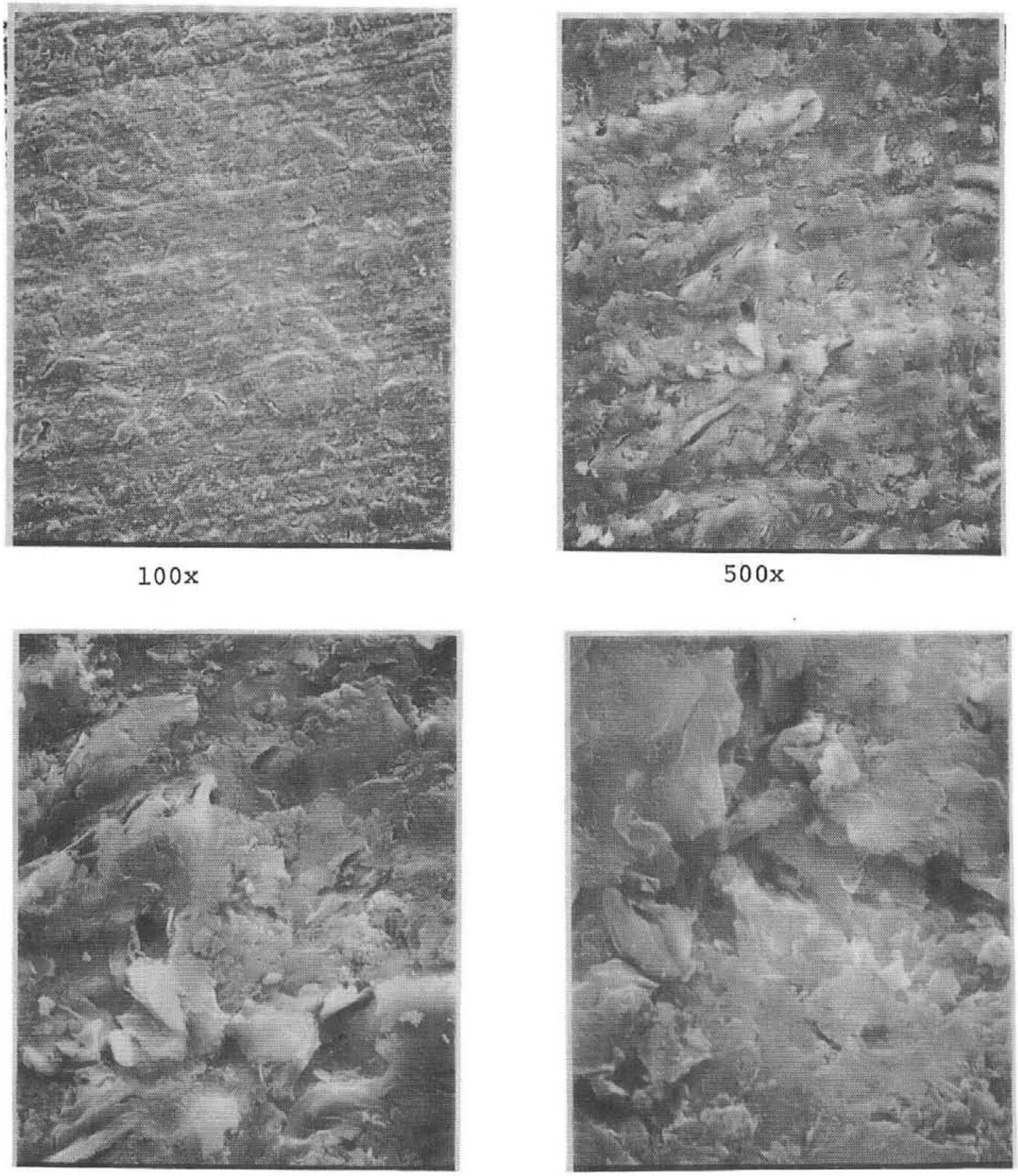

100x

500x

1000x

5000x

Figure 12a. SEM of New, Used, and Zinc-Coated Electrode Materials at several magnifications

Used-Electrode 21 Zinc Deposits

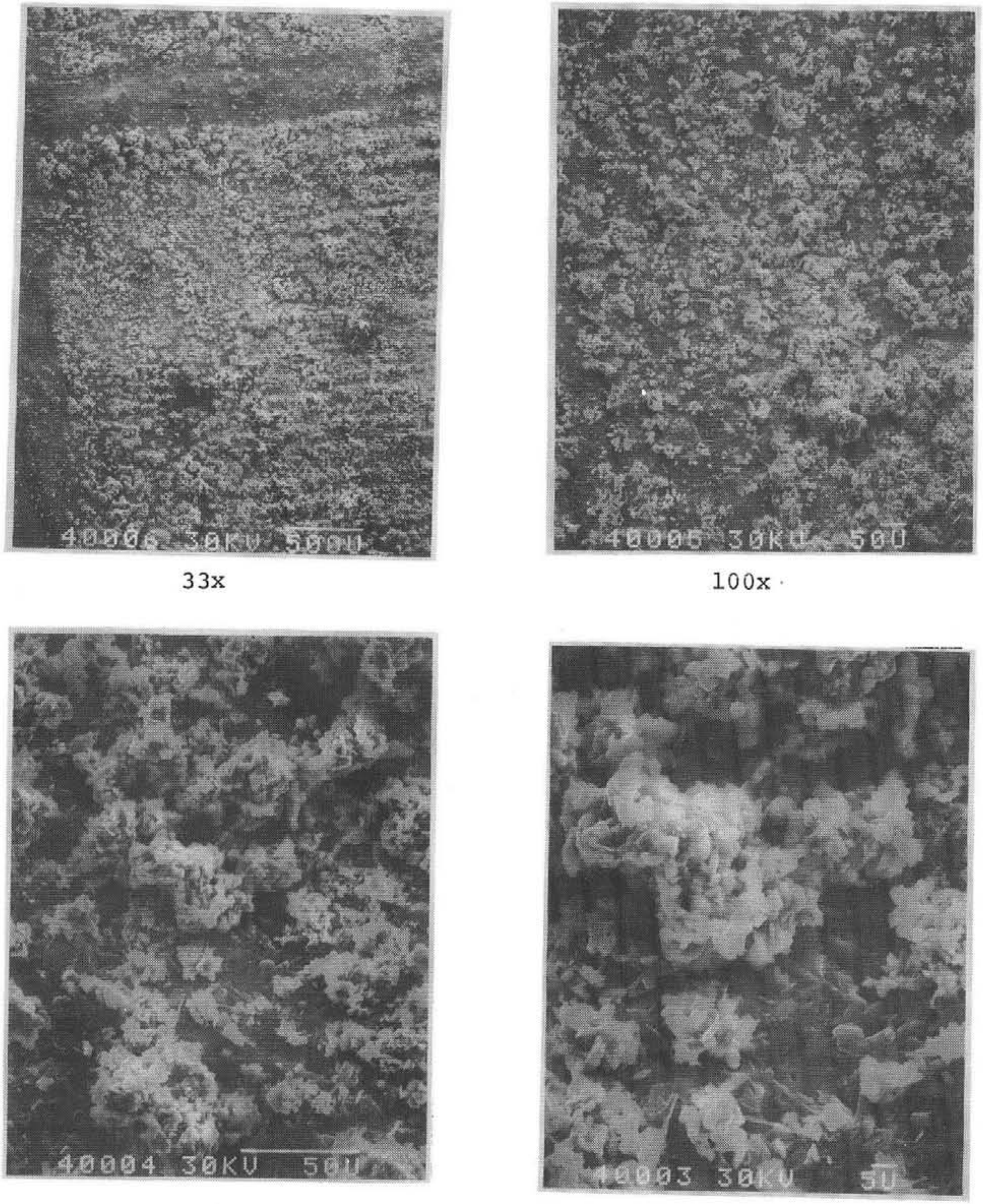

33x

100x

500x

1000x

Figure 12b. SEM of New, Used, and Zinc-Coated Electrode Materials at Several Magnifications

Used Electrode 21 Zinc Dendrites

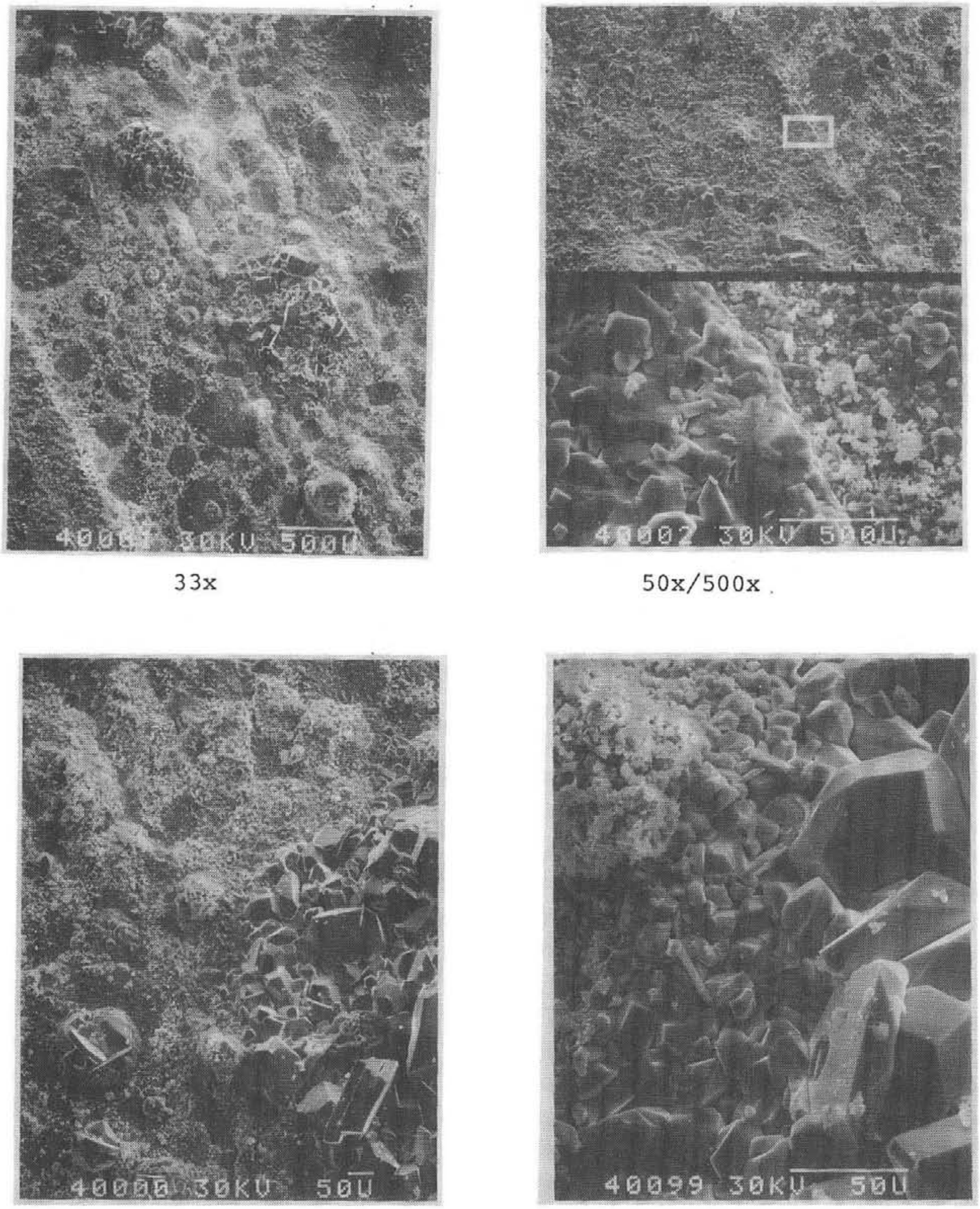

33x

50x/500x

100x

500x

Figure 12c. SEM of New, Used, and Zinc-Coated Electrode Materials at Several Magnifications

Used-Light Areas of Electrode

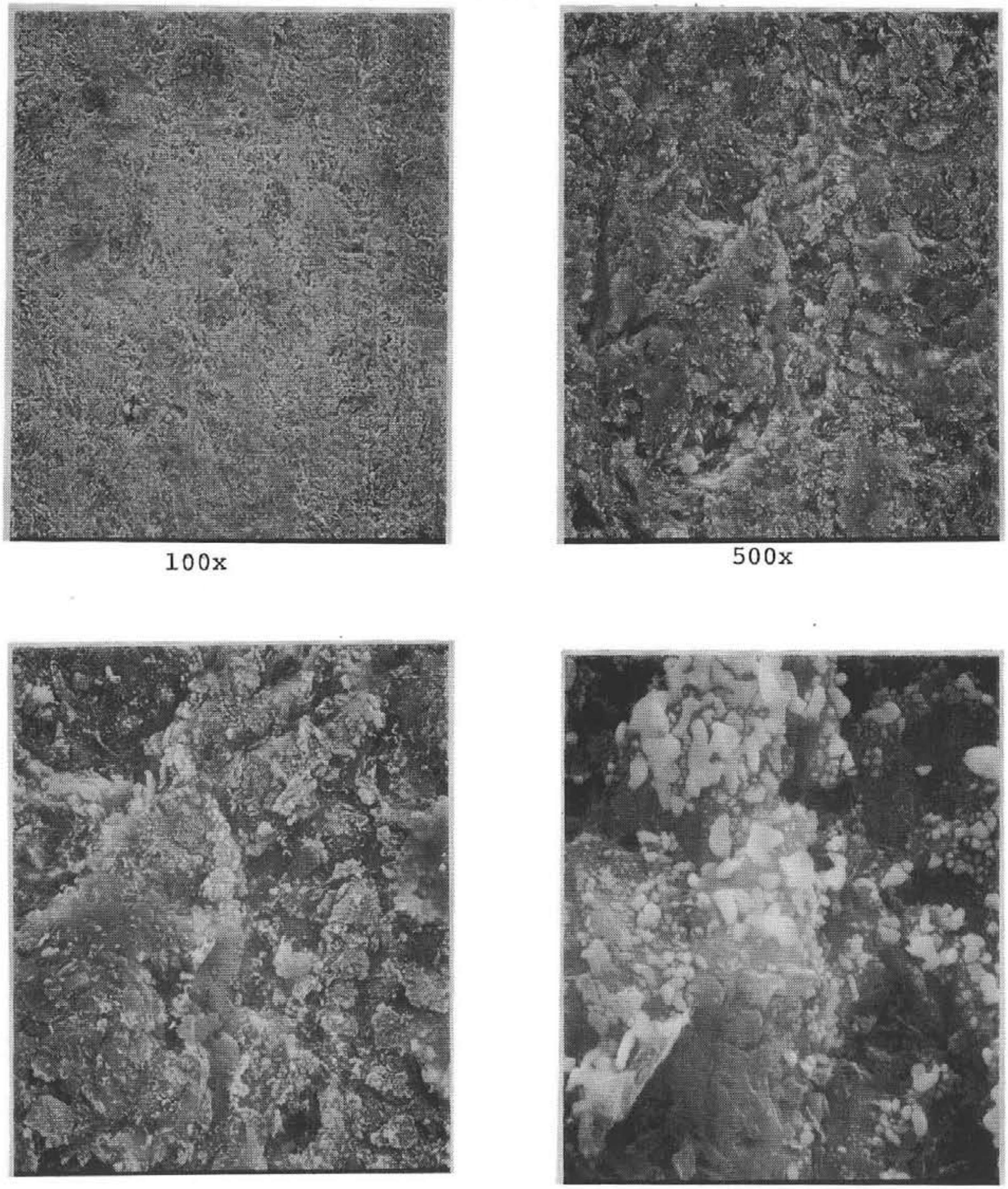

100x

500x

1000x

5000x

Figure 12d. SEM of New, Used, and Zinc-Coated Electrode Materials at Several Magnifications

Used-Dark Areas of Electrode

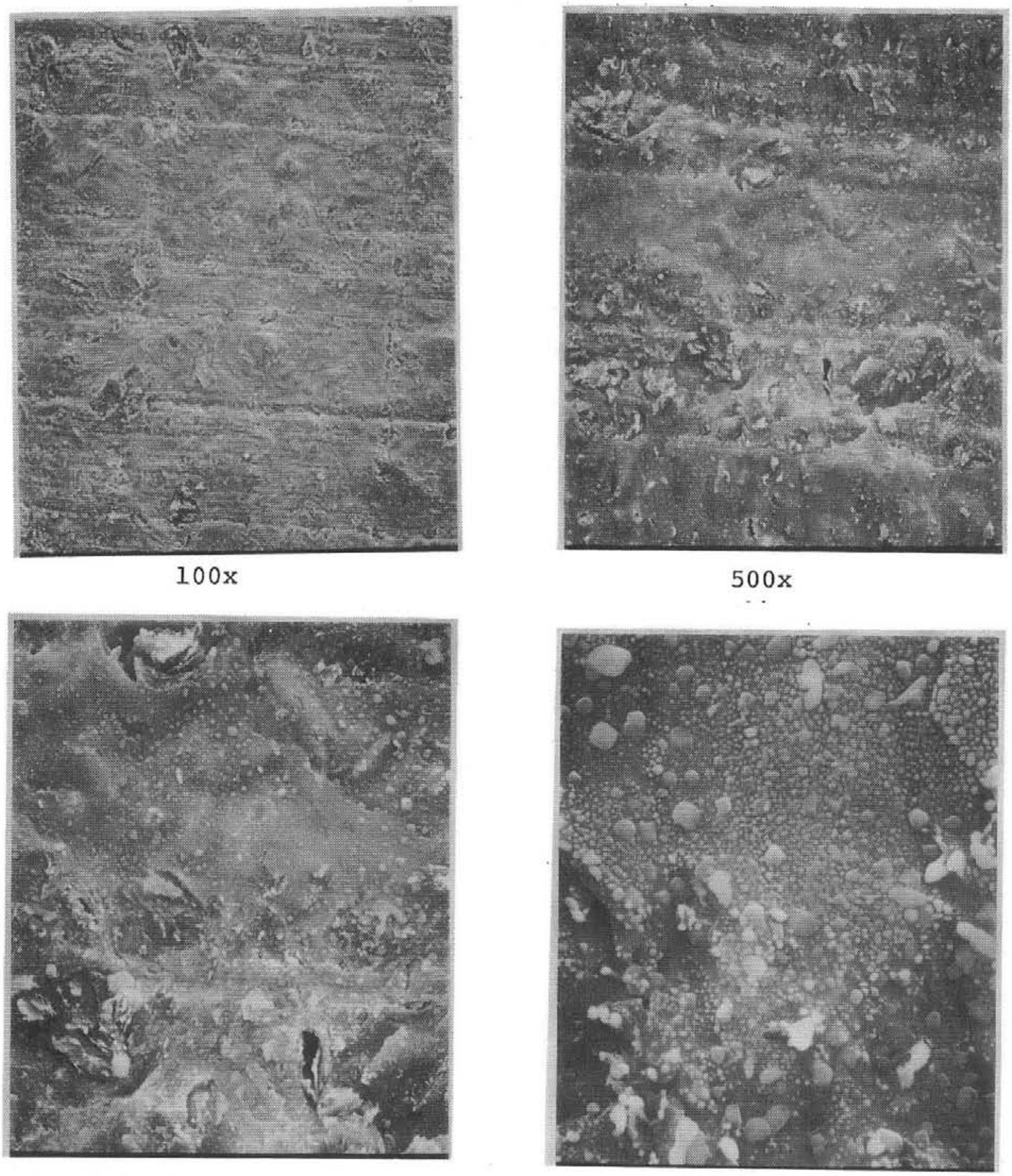

100x

500x

1000x

5000x

Figure 12e. SEM of New, Used, and Zinc-Coated Electrode Materials at Several Magnifications

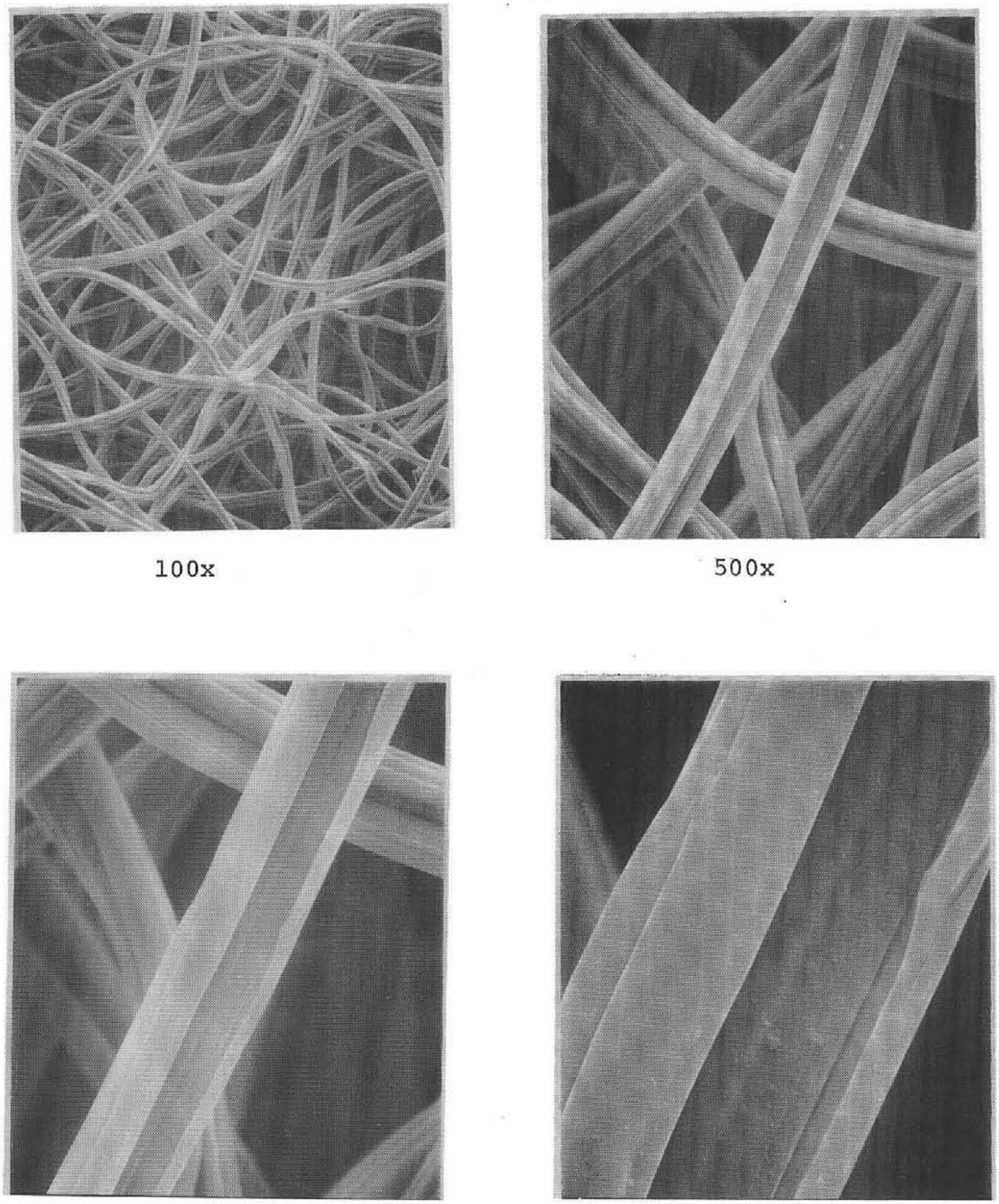

New Felt

100x

500x

1000x

3000x

Figure 13a. SEM of New and Used Carbon Felt From Battery 168 at 100x, 500x, 1000x, and 3000x

Used Felt

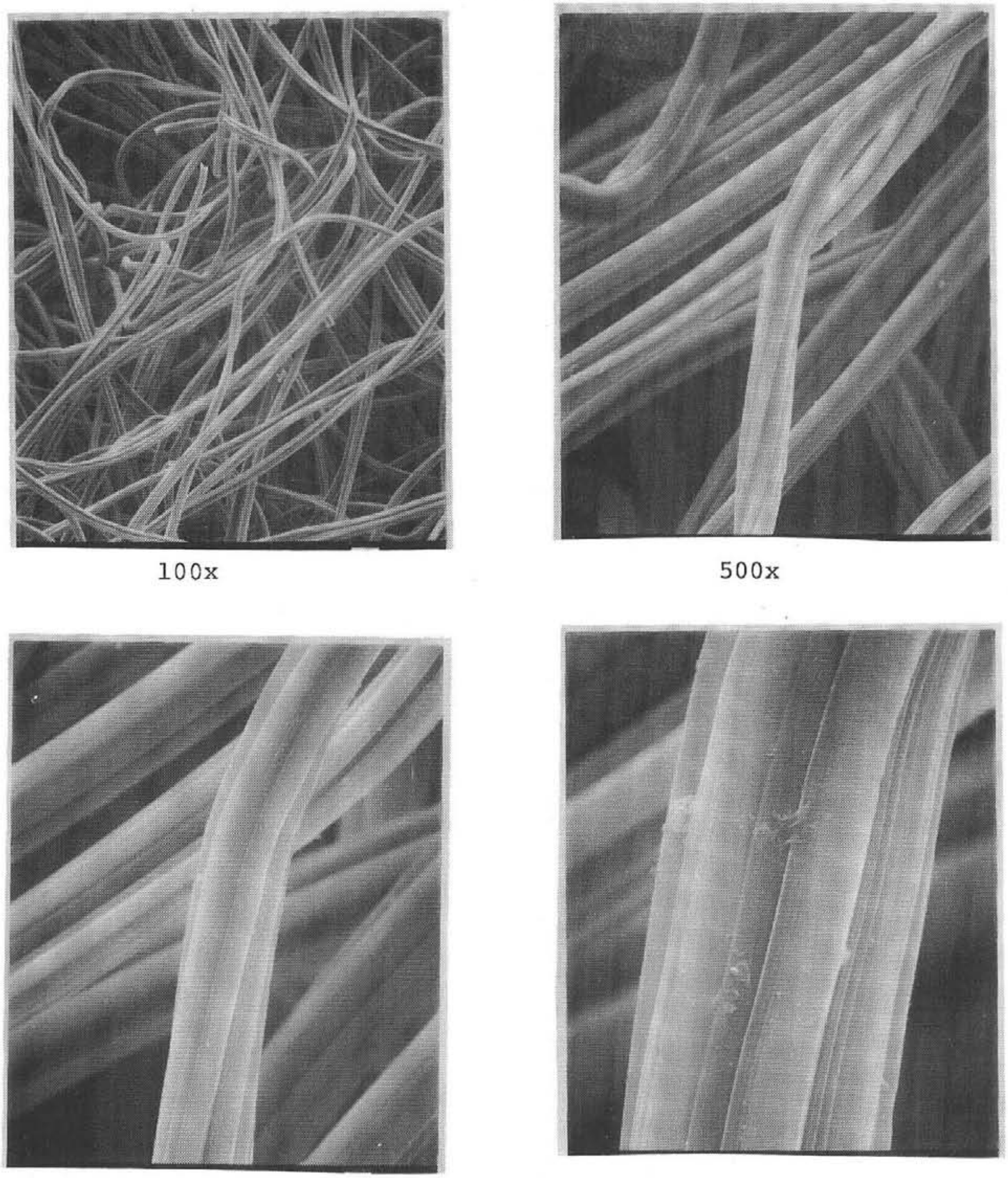

100x

500x

1000x

3000x

Figure 13b. SEM of New and Used Carbon Felt From Battery 168 at 100x, 500x, 1000x, and 3000x

Rough Bromine Electrode

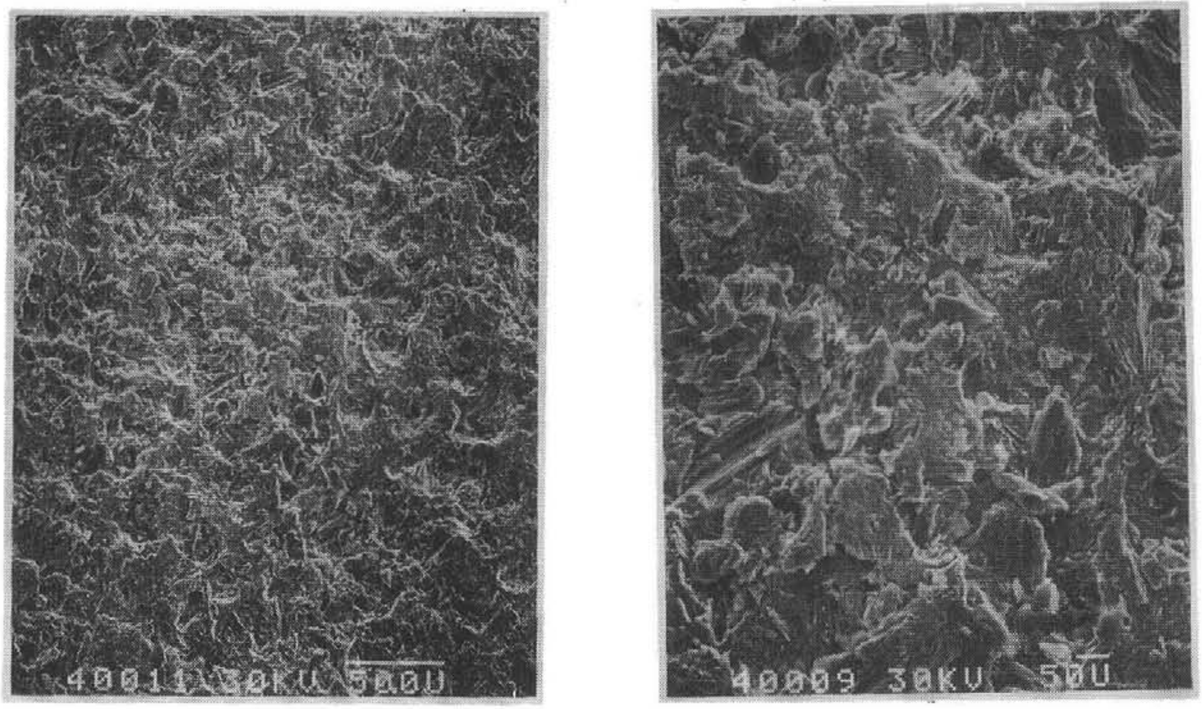

33x

100x

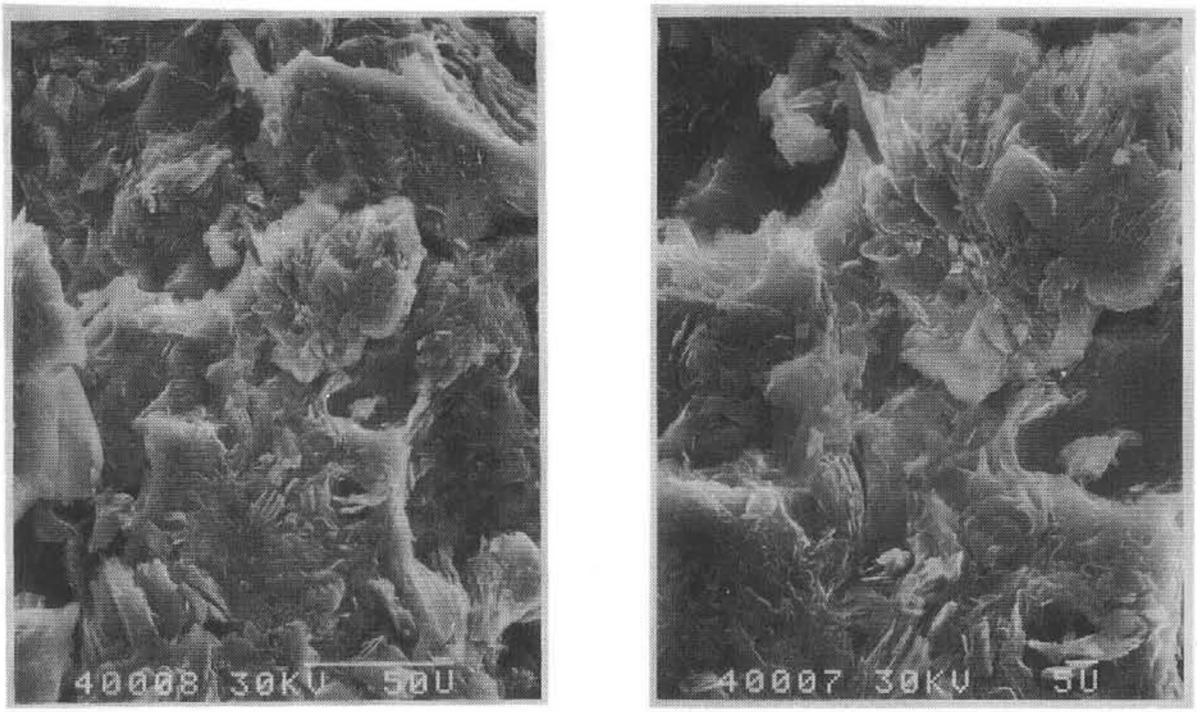

500x

1000x

Figure 14. SEM of Rough Appearing Bromine Electrode 21 at 33x, 100x, 500x, and 1000x

Separator BET Surface Area (m^2/g)
(average of several points)

New	Cycled
47 ± 1	55 ± 1

The slight increase in surface area may be indicative of the cracks and fissures noted in the SEM pictures.

Attempts were made to measure surface area of electrodes, but the electrode area was below the limit of the analyzer. The lower limit of the surface area analyzer used is 0.25 m^2/g. This measurement was attempted without prior knowledge of the vitreous carbon electrode area. In these experiments, both sides of the electrode were exposed. No distinction was noted between the zinc and bromine sides.

Chemical analyses were performed on several samples obtained during disassembly. It was not possible to identify any material because all samples contained mixtures of many species. Table 11 summarizes the data obtained. The used electrolyte did not appear to be contaminated with any inorganic species. The anolyte wash solution had been removed from the stack after sitting overnight, immediately before disassembly. It contained a large concentration of black particles. This sample was analyzed and found to contain a large amount of carbon. The deionized water rinse apparently allowed some of the electrode materials to wash into solution.

The black residue found in some anolyte flow channels was found to contain the same constituents as the electrolyte except that sizable amounts of iron, lead, and aluminum were present. The origin of these elements in this sample is unknown.

Table 11

Chemical Analysis Results
Battery Failure Analyses

	Species										
Sample	Zn	Br	Fe (ppM)	Pb (ppM)	Na (ppM)	Si (ppM)	Al (ppM)	K (ppM)	C wt%	H wt%	N wt%
Anolyte (used)	major	--	2	50	major	2	200	major	--	--	--
Catholyte (used)	major	--	3	150	major	5	200	major	--	--	--
Anolyte wash solids	0.51 wt %	major	--	--	--	--	--	--	47	1.6	0.2
Anolyte flow channel black residue	major	--	1500	1200	1800	4000	3000	major	--	--	--
Frame 3, Electrode 2 white crusty residue	major	--	400	2000	1600	major	2000	major	--	--	--
Frame 4, Electrode 3 crystalline chunk	major	--	900	600	800	<100	900	major	--	--	--
Separator between Frames 3 & 4, white chalky material	major	--	200	<700	400	<200	500	major	--	--	--

Precision: within factor of 2.

A large amount of white crystalline or chalky precipitates were found in many places in the cell stack. The samples seemed to primarily be electrolyte species crystallized with various amounts of iron and lead. The source of these two metals is unknown. These crystals may have formed during the overnight stand when the cell stack was only partially full of water.

A series of samples not included in Table 11 all had the appearance of slightly degraded silicone sealer. Infrared analysis of these materials confirmed that they were of that class of organic compounds.

On March 18, 1983, a representative from Gould responsible for the original construction of the battery visited Sandia and inspected the disassembled components. A summary of his findings are included in Table 12.

Table 12

Gould Representative Inspection of Battery 168, 3/18/83

Kendall, from Gould, visually inspected the battery and noted:

1. Small dendrites, on most electrodes, penetrating the middle of the separators between the two felt pieces.
2. The screens are melted to the separators, indicating the battery got hot.
3. Placing deionized water in the battery, after electrolyte was removed, caused the graphite plates to warp. This caused most of the debonding.
4. The separators were pressed into top of flow frames 1-6, restricting the flow channels.
5. No. 3 separator had a short cut in it.
6. The black residue in the flow frames is dendrite inhibitor and carbon particles from zinc electrode.
7. Frame #6 separator was light grey color, indicating it had dried out.
8. Silicone sealer was used to seal battery stack in many places.
9. Non-uniform zinc deposits due to debonded electrodes which allowed bromine to react with zinc.
10. End plates appeared to be in good shape, and available for reuse.
11. The white/grey crystals in the battery are electrolyte salts.

DISCUSSION OF RESULTS

In general, this battery performance performed according to expectations. Its life and efficiency performance were comparable to other batteries built by Gould with similar designs. Several operational problems were evident and will be discussed.

Efficiency fluctuations occurred several times during battery testing. While one of the fluctuations at cycle 48 has been explained by electrolyte flow blockage and another at cycle 125 by dendrite formation during high zinc loadings, the reason for the step change at cycle 90 has not been discovered. It may have been due to a sudden partial electrode to flow frame debonding permitting electrolyte cross-mixing. It also may be related to bromine addition to the catholyte that was being made just prior to the step change. Excellent efficiency performance was obtained between cycles 50 and 75 relative to other zinc/bromine batteries tested at Sandia.

The plumbing design required frequent valve adjustment to maintain proper electrolyte flow distribution. The severity of this difficulty increased as the battery aged. It was apparently caused by minor pump output variations, flow filter screen blockages, changing stack back pressure, and electrode debonding which permitted electrolyte flow cross-mixing. Electrolyte reservoirs without adequate seals led to fluctuating electrolyte levels because of evaporative losses and also contributed to this problem. Minor plumbing system leaks contributed to additional maintenance requirements.

A further plumbing problem was the lack of dedicated electrolyte flow rate/pressure instrumentation. While a portable pressure transducer was supplied with the battery, it was awkward and messy to use. Also, the correlation of pressure to flow rate appeared unreliable as the battery aged. Valve adjustment to obtain repeatable pressure values was difficult. Similarly, adjustment of polybromide flow rate was based on a visual appearance and difficult to reproduce.

Finally, while the battery was rated at 200 Ah, attempts to cycle the unit at 150 Ah caused immediate dendrite shorting, localized heating, and debonding which led to battery failure. Further investigations appear warranted to increase uniform flow distribution and zinc plating techniques, or anti-dendrite electrolyte additives may be necessary to attain high zinc loading capacities.

Battery failure was most likely due to electrolyte cross flow because of debonded electrodes. This led to non-uniform electrolyte flow distribution and zinc deposition and low efficiencies. High zinc loading cycles caused zinc dendrite shorting and poor efficiency. These design problems appear to be the most critical areas for research effort.

CONCLUSIONS

Sandia personnel consider the Gould/ERC battery test a success. Performance comparable to other state-of-the-art zinc/bromine technology was observed. A great deal was learned about the ERC system and about zinc/bromine batteries in general. Several recommendations for redesign of the battery system will be presented in this section.

Based on operational problems noted above, it will be important to simplify the plumbing system. This will alleviate many manual valve adjustment requirements and improve system performance by assuring more uniform electrolyte flow distribution. Also, improved electrolyte pressure and flow rate instrumentation would improve understanding of battery operation and data analysis of performance problems.

The electrode to flow frame bond must be revised to insure a more durable cell stack and to improve battery life. The use of silicone sealer to bond the electrodes to flow frames, and to seal the edges of the cell stack may not be appropriate for efficient battery production techniques. Over many years of operation, silicone sealer may degrade under exposure to bromine and lead to decreased system performance. Further investigations of methods of sealing the cell stack would be desirable. Seepage was noticed during the entire Sandia test coming from the bottom of the cell stack area. This was only a nuisance in this work, but could be a significant problem on large-scale systems. Improvement of the electrode-flow frame bond should also decrease cell stack sensitivity to thermal excursions.

Similarly, reservoirs should be redesigned to be completely sealed. Plumbing for electrolyte addition and removal should still be available. Sealed reservoirs will decrease electrolyte and bromine evaporative losses and also prevent significant electrolyte cross-flow.

In summary, this battery evaluation has identified several areas for system design improvements. Nothing was discovered which indicated the zinc/bromine technology was fundamentally flawed. With continued system optimization during the next few years, this battery type has an excellent chance of eventual commercial success.

REFERENCES

1. R. A. Putt and A. Attia, Development of Zinc Bromide Batteries for Stationary Energy Storage, EPRI EM-2497, July 1982.

2. A. E. Verardo, P. C. Butler, D. M. Bush, and D. W. Miller, "Testing Batteries for Photovoltaic Power Systems," Proceedings of the 16th Intersociety Energy Conversion Engineering Conference, 1981, p. 680.

3. P. C. Butler, D. W. Miller, and A. E. Verardo, "Flowing Electrolyte Battery Testing and Evaluation," Proceedings of the 17th Intersociety Energy Conversion Engineering Conference, 1982, p. 653.

4. P. C. Butler and D. W. Miller, "Zinc/Bromine Prototype Batteries Evaluation," Proceedings of the 18th Intersociety Energy Conversion Engineering Conference, 1983, p. 1653.

APPENDIX A

Gould Battery Operations Manual

Note: The proprietary information restriction
noted in this appendix has been removed
by Energy Research Corporation.

Copy No. 2

Prepared under DOE Contract No. DE-AC02-78ET29345

800W ZINC-BROMINE SUBMODULE

OPERATIONS MANUAL

August 11, 1981

Gould Inc. - Gould Laboratories
40 Gould Center
Rolling Meadows, Illinois 60008

DISCLAIMER

NOTICE

"Data contained on pages 1 through 21 of this document are proprietary information of Gould Inc. and shall not be disclosed for any purpose not specified in the contract under which this work was performed."

CONTENTS

Appendices:

ILLUSTRATIONS

I. INTRODUCTION

The 800W zinc-bromine submodule is a self-contained, ambient temperature, rechargeable battery system. It is of a bipolar design with flowing electrolyte (Figure 1).

Electrochemical energy is stored through the reduction of zinc ions to zinc metal at the negative electrode and oxidation of bromide ions to bromine at the positive. The free bromine formed on the positive electrode is stored as a liquid chemical complex (polybromide) externally to the submodule. A microporous separator between electrodes slows the diffusion of bromine from the positive to the negative sides, to limit the rate of self discharge. The bulk of the electrolyte and the polybromide are stored externally to the submodule in storage tanks.

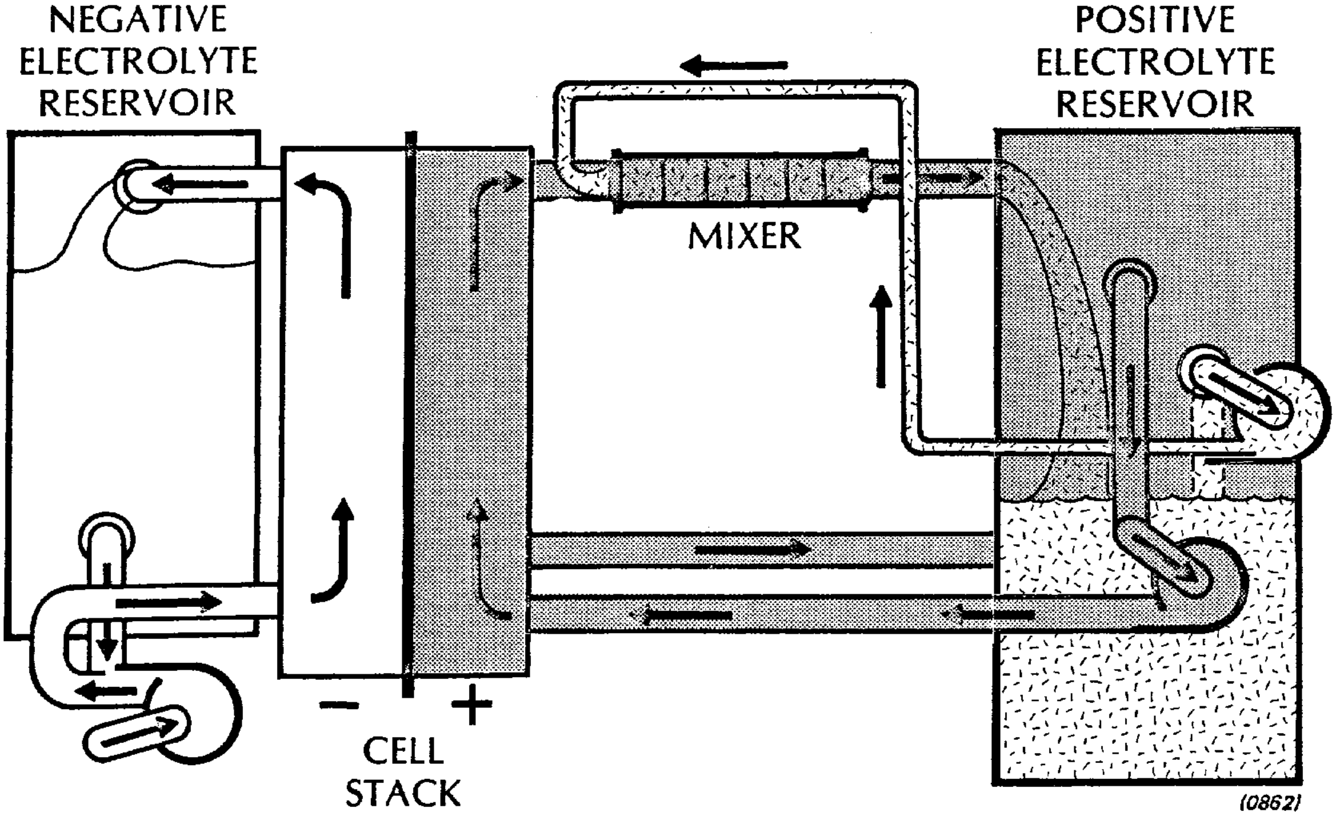

Figure 1 Zinc — Bromine Submodule Flow System

II. SYSTEM DESIGN

The system consists of a submodule, pumps, plumbing and electrolyte storage tanks. The submodule is rated at 800W (discharge) based on an average discharge voltage of 32V at the design current of 25A.

A. The Submodule

The submodule (Figure 2) comprises a filter-press stack of 20 electrodes, each a square of $0.09m^2$ ($\sim 1ft^2$) area, mounted in a polypropylene frame. The frame, in addition to holding the electrode in position and sealing its edges from leakage currents, also provides the important function of directing electrolyte flow to and from the electrode surfaces.

Between each pair of electrodes there is a microporous separator, DARAMIC, to limit the rate of self-discharge. Since the separator is non-rigid, polypropylene spacing ribs are provided on the negative side to hold it off the electrode surface. The spacing function on the positive side is provided by the positive substrate, a carbon-felt material having a high surface area for minimizing polarization of the bromine electrode. The two end plates are made of polypropylene and provide the multiple functions of compressing the cell tightly to prevent leakage, serving as plumbing connections for electrolyte flow, and collecting the electrical current from the two end electrodes.

B. Plumbing and Pumps

Electrolyte and polybromide circulation between the storage tanks and the submodule are via schedule 80 polypropylene pipe and magnetically coupled, centrifugal pumps of polypropylene construction. Plumbing connections are accomplished with socket welding, except for union connections for the pumps, tanks, and submodule to simplify installation and removal.

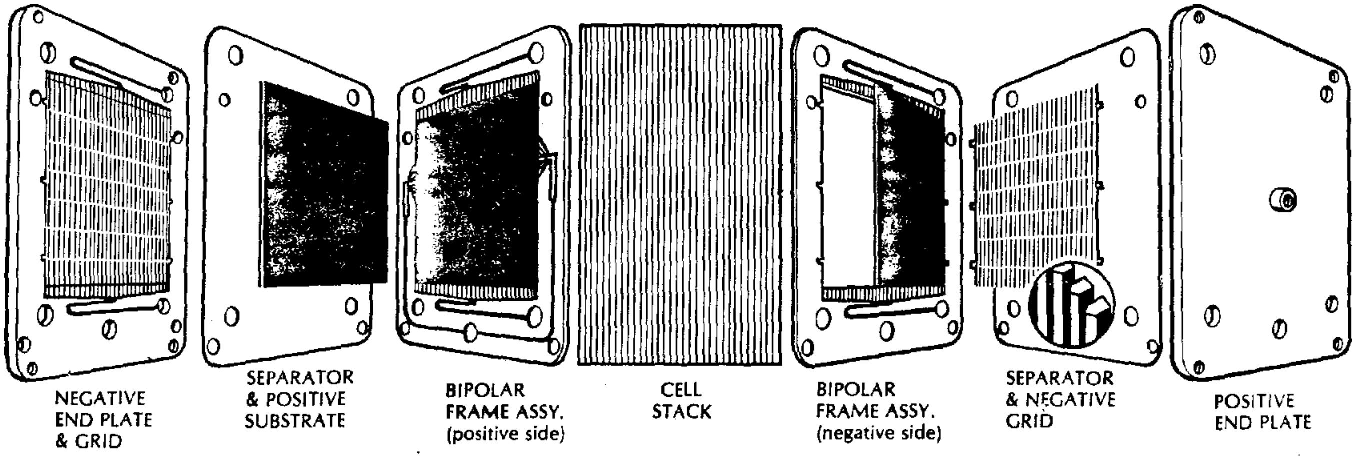

Figure 2 Zinc – Bromine Cell Stack Components

C. Electrolyte

The electrolyte solution comprises the active species zinc and bromide, potassium chloride supporting electrolyte, and water, the solvent.

The electrolyte composition and quantity are designed to provide adequate quantities of species for the electrode reactions and to minimize the internal resistance of the submodule. The design specifications are as follows:

Composition:
1.33M zinc bromide
0.67M zinc chloride
3.00M potassium chloride

Volume:
32ℓ each on the positive and negative sides

An additional specification on the electrolyte is a pH of 2-3.

D. Bromine Storage

Bromine is generated at the positive electrodes during the charge half cycle and consumed during discharge. Control of the bromine concentration in the positive electrolyte is accomplished by complexing the bromine in a second, liquid, polybromide phase. The polybromide phase is stored externally to the submodule. A static mixer (Figure 3) is used to mix the electrolyte and polybromide phases to exchange bromine. Polybromide flow to the mixer is provided by the polybromide pump.

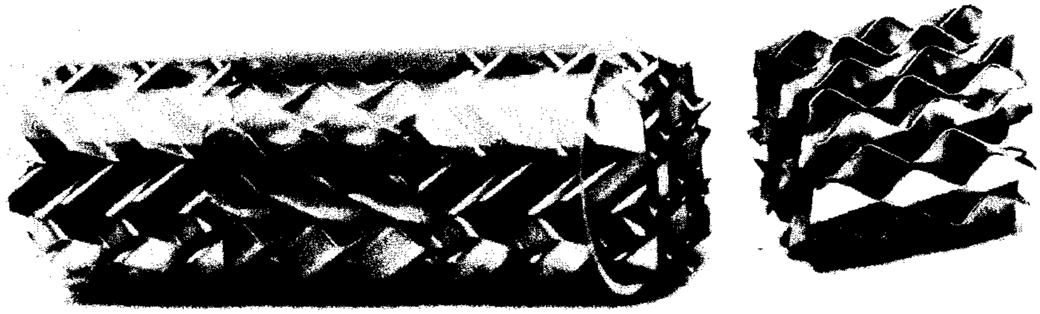

Figure 3 Static Mixer
(Courtesy Koch Engineering)

E. Auxiliaries

A titanium coil has been incorporated into the negative electrolyte tank. When connected up to a cold water line it functions as a cooling coil for the submodule. Without the use of a cooling coil the submodule temperature will exceed 35C, the present temperature limit for the battery. Above this point undue thermal stresses are placed on the electrode/electrode-frame bond, which could result in an electrode debond.

A pressure transducer and its associated power supply are also included with the submodule package. It is used for setting the electrolyte flow rate. A thermocouple is also included for temperature monitoring.

III. OPERATION

A. Components

Supplied by Gould:

1 - 800 W submodule
2 - Electrolyte tanks
4 - Pumps (3 for submodule; 1 for electrolyte transfer) TE-MDX-MT3
1 - Static mixer
1 - Cooling coil
1 - Electrical outlet strip
1 - Electrolyte filter bed
8 - Pressure/sample taps
5 - 1" ball valves
2 - 1/2" ball valves
Var - plumbing
30 gal - Electrolyte
3 gal - Polybromide
1 - Pressure transducer with power supply
1 - Thermocouple with electric ice point
1 - Filtration chamber

all wetted parts
are talc filled
polypropylene

To be supplied by customer:

- Respirator approved for halogens
  (i.e.: NIOSH No.TC-23C-76 with cartridges
  NIOSH No.TC-23C-82)
- Gas mask approved for halogens
  (i.e.: Scott chin style gas mask TC-14G-102 with canister
  600252-08)

5 lb - bromine, rgt. grade
1 gal - Hydrobromic acid, 48%
- Latex gloves

B. Assembly

Assembly involves connecting the tanks, pumps, and submodule together as follows:

1 - Place the submodule in the center of the hood. The negative electrical connection should be on the left hand side.

2 - Place the negative electrolyte tank and pump to the left of the submodule.

3 - Place the positive electrolyte tank, pump, and the polybromide pump to the right of the submodule.

4 - Remove the screw-in plugs from the submodule. Some electrolyte might come out of the bottom ports. This will be from initial check-out testing before the submodule was shipped. Any spillage should be cleaned up and disposed of as described under safety procedures.

5 - The plumbing can now be connected by referring to Figure 4. The plumbing assembly is carried out by connecting part 1 to part 2 etc. All unions should be aligned and hand tightened. Do not over tighten as this can deform the o-ring seating. Ball valves should be in the closed position when assemblying.

6 - After all plumbing connections are made, check to see that all valves are closed including the sample ports.

7 - The pumps should be plugged into the outlet strip.

8 - The coil in the negative tank should be connected to a chill water line of 60F and 10psi supply pressure (the flowrate will not exceed 0.5 gpm at this supply pressure).

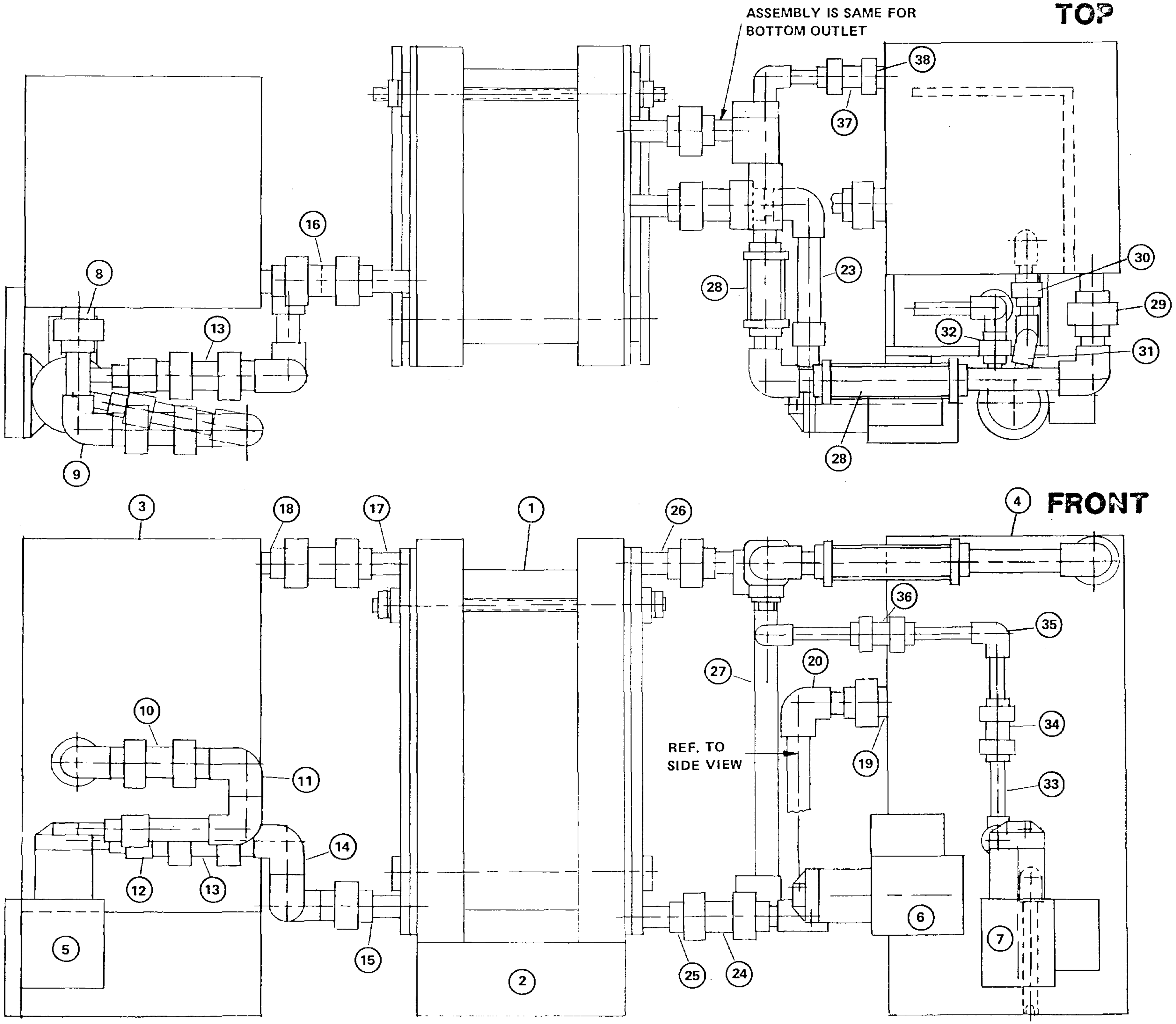

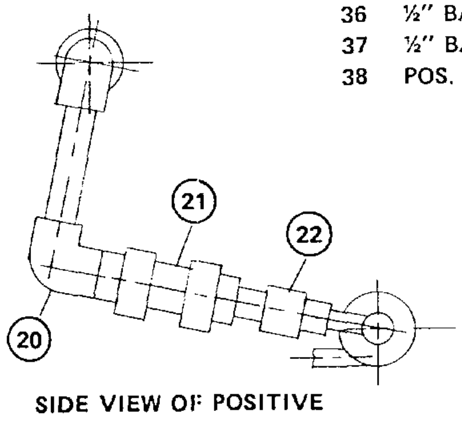

SIDE VIEW OF POSITIVE PUMP INLET FROM TANK

800W Submodule Layout

DESCRIPTION:

1	SUBMODULE
2	SUBMODULE STAND
3	NEG. ELECTROLYTE TANK
4	POS. ELECTROLYTE TANK
5	NEG. ELECTROLYTE PUMP
6	POS. ELECTROLYTE PUMP
7	POLYBROMIDE PUMP
8	NEG. TANK OUTLET
9	PLUMBING
10	1" BALL VALVE
11	PLUMBING – NEG. PUMP INLET
12	NEG. PUMP OUTLET - Pressure tap (orig.)
13	1" BALL VALVE
14	PLUMBING
15	PLUMBING – SUBMODULE INLET, NEG. SIDE
16	1" BALL VALVE
17	PLUMBING – SUBMODULE OUTLET, NEG. SIDE
18	NEG. TANK INLET
19	POS. TANK OUTLET
20	PLUMBING – POS. PUMP INLET
21	1" BALL VALVE
22	POS. PUMP INLET
23	PLUMBING
24	1" BALL VALVE – Pressure tap (orig.)
25	PLUMBING – SUBMODULE INLET, POS. SIDE
26	PLUMBING – SUBMODULE OUTLET, POS. SIDE
27	PLUMBING
28	STATIC MIXER – Pressure tap (cyc.48)
29	POS. TANK INLET
30	POS. TANK, POLYBROMIDE OUTLET
31	PLUMBING – POLYBROMIDE PUMP INLET
32	PLUMBING – POLYBROMIDE PUMP OUTLET
33	PLUMBING
34	½" BALL VALVE
35	PLUMBING
36	½" BALL VALVE - Pressure tap - cyc.48
37	½" BALL VALVE - Pressure tap - cyc.48
38	POS. TANK INLET

(0962)

Figure 4
800W Submodule Layout

C. System Fill

The polybromide and electrolyte come in two drums. The smaller (5 gal) one contains the polybromide and some electrolyte. The larger (55 gal) drum contains electrolyte.

Initially, all valves should be closed. The first step in filling the system is to transfer 7ℓ of polybromide into the positive tank. This is done by manually pouring the polybromide from its shipping container into the positive tank. The electrolyte present with the polybromide should also be transferred into the positive tank.

Next, the electrolyte can be transferred into both the positive and negative tanks. This should be done by use of the transfer pump. In pumping the electrolyte from the drum to the electrolyte tanks it should first be pumped through the filtration chamber before it enters the electrolyte tanks.

Filling of the electrolyte tanks should be up to the mark on each tank. After initial pumping of the electrolyte into the submodule the tank volumes should be readjusted to their appropriate levels.

D. Operation

After the tanks are filled, all valves can be opened. This will allow the electrolyte to enter the plumbing system and the submodule. Allow a few minutes for the electrolyte to fill the submodule. Valves 10, 13, and 24 should then be closed. Valve 37 should be closed half-way. The negative and positive electrolyte pumps can now be turned on.

The required electrolyte flowrate on each side should be 2.5gpm. The flowrate can be set by using the pressure transducer and monitoring the differential pressure across each of the electrolyte pumps. The readout from

neg side 10mV
pos. side 13mV

the transducer is in millivolts. By referring to Figure 5 this can be converted into flowrate. The inlet pressure to the electrolyte pumps is equivalent to ~~6~~mV. Since the required differential millivolt reading for a flowrate of 2.~~5~~gpm is ~~59~~mV, the pump outlet pressure should be ~~65~~mV.

2.0 61

67 neg side
74 pos. side

The flowrate on the negative side should be set first, by monitoring the negative pump outlet pressure and slowly opening valve 13.

CAUTION: Negative electrolyte flow must always be provided to the submodule prior to positive electrolyte flow.

After the negative flowrate has been set, the positive flowrate can be set. This is done by monitoring the outlet pressure of the positive pump and slowly opening valve 24.

Once valves 13 and 24 have been set, there should be no need to readjust them. Control of electrolyte crossover can be handled by throttling valve 16.

Finally, the polybromide flowrate can be set. This is done mainly by visual inspection of the polybromide through the static mixer. The flow should be set with the electrolyte pumps on. The polybromide flow should be such that the static mixer elements are barely visible. During the discharge mode of cycling the polybromide flowrate can be readjusted as necessary. If there is either insufficient or excessive polybromide flow the discharge curve will have a steep negative slope. This will result in both poor coulombic and voltaic efficiencies.

After all flowrates are adjusted, the electrical connections can be made to the appropriately marked terminals. The submodule is now ready for cycling.

The current/voltage program may be set as desired with the following limitations taken into consideration.

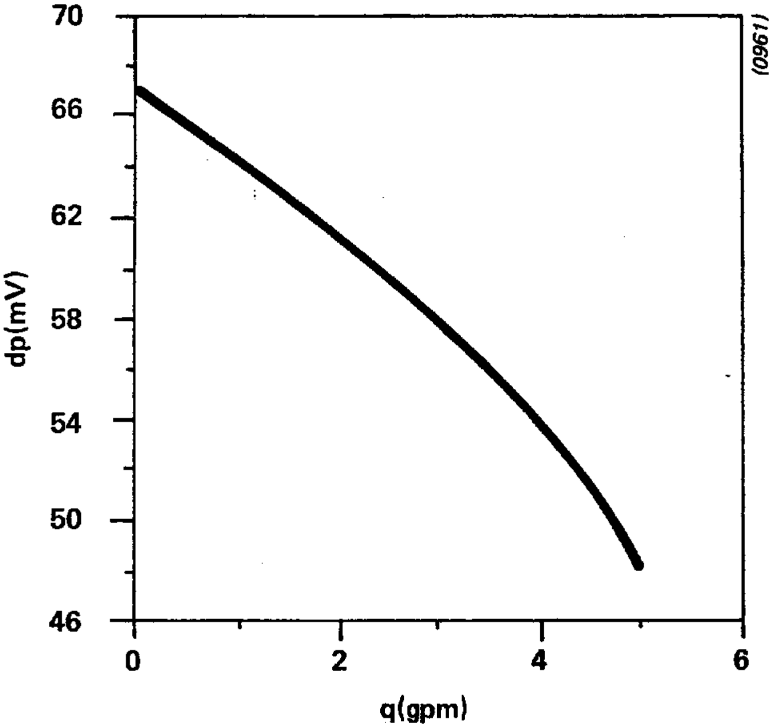

Figure 5 Electrolyte Flowrate through a TE–MDX–MT3 Pump

1. Maximum charge capacity 150Ah
2. Maximum current 25A ~30A
3. Charge should be commenced only on a completely discharged battery (0.0V on open circuit).

These conditions are necessary to minimize the risk of zinc dendrite shorting.

E. Daily Start-Up and Shut-Down Procedures

On a one cycle per day regime, the following procedures should be carried out. It is assumed the flowrates have already been set. If they haven't, refer to the previous section before continuing.

Start-Up - First, turn on the negative electrolyte pump. Allow the electrolyte to exit the submodule before continuing. Next, turn on the positive electrolyte pump. After electrolyte flow has been established on the positive side, the polybromide pump can be turned on. If there is 0.0V on open circuit, cycling may commence. If the open circuit is not 0.0V, the submodule should be placed in the shortout mode.

Shut-Down - The submodule should either be in an open circuit or shortout mode. First, the polybromide pump should be turned off. About 5 minutes after the polybromide pump is turned off, the positive electrolyte pump can be turned off. The time period before turning off the positive pump is necessary to allow residual polybromide to be pumped out of the submodule. Finally, the negative electrolyte pump can be turned off. If the submodule is not completely discharged (i.e., $\leq$5V), it can be left in the shortout mode with the pumps off.

F. Typical Charge-Discharge Program

A typical charge-discharge program is as follows:

1. Charge at 25A for 5 hours. The charge voltage will initially be $\sim$40.00V at 27C, but it will decrease slightly during the course of the charge due to an increase in temperature.

2. Open circuit stand ("charge rest") 10 minutes (optional). The open circuit voltage will be $\sim$35.6V.

3. Discharge at 25A until the voltage reaches 20V. The nominal discharge voltage will be $\sim$30.4V.

4. Shortout ("discharge rest") for 2 hours (required). When the submodule voltage reaches 20V it should be placed into shortout with the pumps left on. This will allow any residual zinc to be removed from the negative electrodes.

Figure 6 is a typical charge-discharge curve for such a cycle.

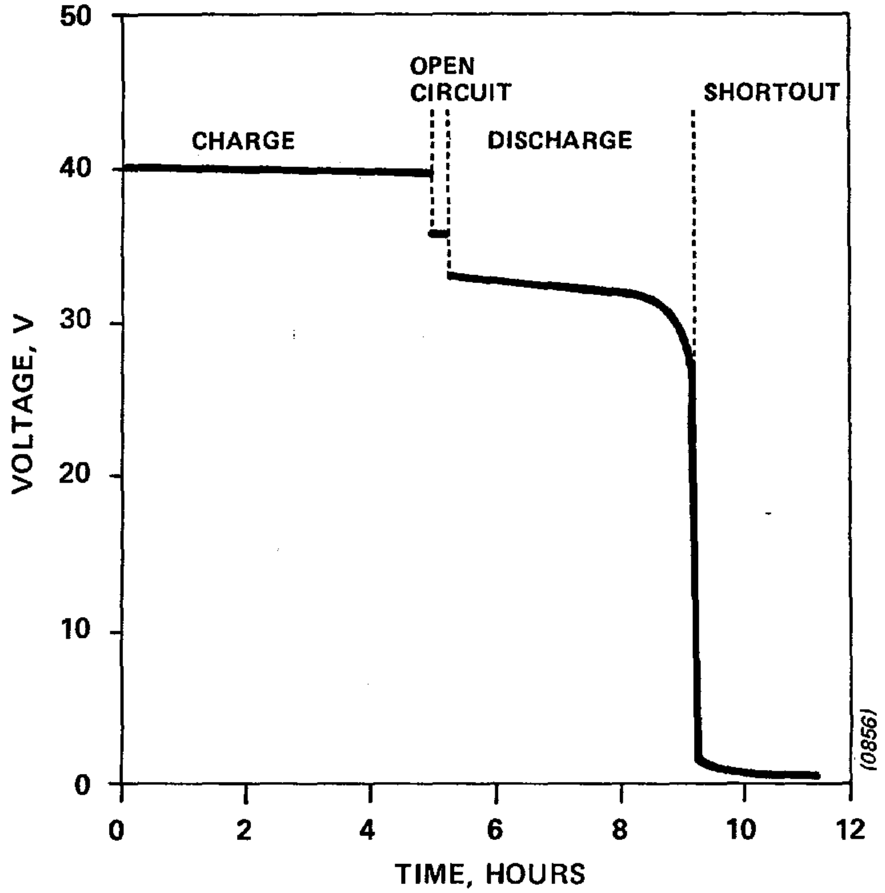

Figure 6 Typical Voltage Profile for 800W Submodule Charge/Discharge Current 25A

G. Operating Parameters

Below are some considerations which apply in selecting submodule operating parameters.

Temperature - The recommended temperature range is 25-35C.

Above 35C thermal stresses are placed on the electrode/electrode-frame bond. This may cause electrode debonding which will result in poor coulombic and voltaic efficiencies and submodule failure. An electrode debonding is unrecoverable and requires a teardown of the submodule.

Current - The current can be between 5A and 25A. Below 5A the corrosion rate of the zinc will exceed the plating rate. Above 25A the chance of zinc dendrite formation is increased. This could lead to dendrite shorting.

Loading - The loading should not exceed 150Ah. Above 150Ah there is an increased chance of zinc dendrite formation which would lead to dendrite shorting.

Flowrate - The flowrate on both sides should be set to 2.5 gpm. Variations of ±0.5 gpm are allowed.

The polybromide flowrate should be set as described on page 12.

IV. MAINTENANCE

The primary maintenance required is as follows:

1. Check electrolyte pH on negative side. This should initially be done on a daily basis at the start of charge. If the pH approaches 3.0, ∿50 ml of hydrobromic acid (48%) should be added to the negative side.

2. Check electrolyte levels. This should be done with the pumps on. If there is a change in the volume of either electrolyte tank the flowrates should be checked and adjusted as necessary. If the flowrates are correct, then valve 16 should be adjusted. By having the valve open, electrolyte crossover will go toward the negative side. As valve 16 is throttled back, electrolyte crossover is shifted toward the positive side.

V. TROUBLESHOOTING

PROBLEM	CAUSE	CURE
1. Rapid, random, voltage spikes, from normal charge voltage to lower value.	Dendrite shoring; zinc dendrites have grown through the separator.	Place submodule in reversal at 5A with pumps on until open circuit voltage is 0.00V.
2. No flow but pump is on.	Pump is decoupled	Shut pump off until motor stops spinning then restart.
3. Leaky fitting	Loose fitting or O-ring misaligned.	Tighten fitting. If it still leaks then O-ring needs replacing.
4. Voltage stepping during discharge.	Debonded electrode or blocked flow channel.	Check open circuit voltage. If open circuit voltage is much lower than $\sim$35V e.g. $\leq$ 33V and there is excessive electrolyte crossover an electrode has debonded. If the open circuit voltage returns to $\sim$35V then a flow channel has become blocked. This sometimes cures itself and is best left alone.
5. Electrolyte crossover	Uneven flow-rates	Check flow-rates and adjust accordingly. Throttle valve 16.
6. Poor coulombic efficiency.	Poor bromine kinetics.	Check positive side bromine concentration. End of charge concentration should be 10-14 g/l. If too low add bromine. Increase polybromide flow.
7. Poor voltaic efficiency	High internal resistance due to excessive polybromide entering submodule.	Decrease polybromide flow.

VI. SAFETY PROCEDURES

1. The submodule should be set up and operated in a reliable fume hood in the event of the escape of bromine vapors.

2. The zinc bromide electrolyte is poisonous if taken internally, and externally causes skin burns on exposure. Latex gloves and safety glasses should be worn any time electrolyte is being handled or when system integrity is to be broken. If accidental contact with the skin occurs, flush well with water. Small quantities (i.e., 1-2ℓ) of electrolyte can be flushed down the drain with copious amounts of water.

3. Bromine is extremely toxic internally and externally. Latex gloves, eye protection, and a respirator should be worn when handling it. It should only be exposed to the atmosphere within a reliable fume hood. Avoid breathing the vapors. It can be neutralized with either a 2M solution of sodium thiosulfate or a 25-50% solution of ammonium hydroxide.

4. Polybromide should be treated like bromine. A good solvent for it is isopropyl alcohol.

APPENDIX A

DETERMINATION OF BROMINE CONTENT IN ELECTROLYTE

spin sample to remove polybromid

A 1.00 ml sample of the aqueous phase is added to 15 ml of a 15 percent by weight potassium iodide solution. The iodine released is titrated with a standard 0.01N thiosulfate solution. Titrate slowly until the solution is colorless. Perform duplicate determinations. Calculate the bromine content as follows:

$$\text{Bromine (g/l)} = \frac{(\text{ml } S_2O_3^{=})(\text{N } S_2O_3^{=})(79.909)}{\text{Sample Volume (ml)}}$$

Bromine concentration range should be:

Start of charge:

neg. side ~ 2-4 gm/l

pos. side ~ 5-7 gm/l

End of charge:

neg. side ~ less than 2 gm/l

pos. side ~ 12-14 gm/l

APPENDIX B: THERMOCOUPLE TEMPERATURE TABLE
TYPE T (Copper-Constantan) Thermocouple

DEG C	0	1	2	3	4	5	6	7	8	9
	Thermoelectric voltage in absolute millivolts									
20	0.789	0.830	0.870	0.911	0.951	0.992	1.032	1.073	1.114	1.155
30	1.196	1.237	1.279	1.320	1.361	1.403	1.444	1.486	1.528	1.569
40	1.611	1.653	1.695	1.738	1.780	1.822	1.865	1.907	1.950	1.992

800W ZINC-BROMINE SUBMODULE

OPERATIONS MANUAL

August 11, 1981

PEN AND INK CORRECTIONS: 3/15/82

p. 11 5th line from bottom:

Replace "Valve 37 should be closed half-way." with "Valve 37 should be throttled from the fully open position until the polybromide droplets in the static mixer are well-dispersed in the electrolyte, but still clearly visible as sub-millimeter diameter droplets. Valve 37 is shut too far if the two-phase flow in the mixer appears as a cloudy emulsion."

p. 12 11th line from bottom:

Replace "The polybromide flow should be such that the static mixer elements are barely visible." with "Set the polybromide flow by throttling valve 34 approximately 45° from the fully open position. Fine adjustment from this point should be made such that the polybromide flow through the static mixer is approximately 25-35% by volume based on visual observation.

p. 12 13th line from the top:

Replace "Control of electrolyte crossover can be handled by throttling valve 16." with "Control electrolyte crossover via minor adjustments to valve 13. For electrolyte crossover positive-to-negative, throttle open valve 13 to increase negative side flow and pressure in the battery, as indicated by a negative pump discharge pressure decrease of 1-3 mV. For negative-to-positive crossover, throttle valve 13 closed to reduce negative side flow and pressure, as indicated by a 1-3 mV pump discharge pressure increase. Valve 16 should be fully open."

p. 15 Item 3

Replace with:

"3. Discharge at 25A until the voltage decreases to zero volts."

p. 15 Item 4

Replace with:

"4. Shortout (discharge rest) for 30 minutes (required), once the battery voltage reaches zero volts in discharge."

Add after p. 22

APPENDIX C

DETERMINATION OF BROMINE CONTENT IN POLYBROMIDE

Obtain a 1.0 ml polybromide sample at end of discharge; place in a 200 ml volumetric flask with 150 ml of fresh electrolyte. Cap and shake to dissolve polybromide completely, then increase volume to 200 ml with fresh electrolyte and mix thoroughly. Titrate this solution for bromine (Appendix A). Calculate bromine content as follows:

$$[\mathrm{Br}_2]\ (\mathrm{g/l})\ \text{in polybromide}$$
$$= (\text{ml thiosulfate})\ [illegible]\ \begin{pmatrix}\text{thiosulfate}\\ \text{normality}\end{pmatrix}\left(\frac{80\text{g Bromine}}{\text{equivalent}}\right)(200\ \text{ml diluted volume}).$$

The bromine content should be as follows:

800 - 850 g/l for bromination level 3 ($Q^+\ Br_3^-$)
950 - 1000 g/l for bromination level 4 ($Q^+Br_4^-$).

If the bromine content is below 800 g/l, add bromine in 200 ml increments to increase its content to 800 - 1000 g/l.

APPENDIX B

Sandia Battery Test Plan

Sandia National Laboratories
Albuquerque, New Mexico 87185

July 7, 1981

Mr. James R. Borta
Gould Inc.
Gould Laboratories
40 Gould Center
Rolling Meadows, IL 60008

Dear Jim:

I am preparing a test plan for the Gould 20-cell zinc-bromine battery to be tested at Sandia. I would appreciate your comments and input on the plan. Specifically, I am interested in the safety aspects of operating the battery under the listed conditions as well as any of the selected parameters that exceed battery design limitations. Also, if you have any suggestions for other experiments for the battery, please feel free to let me know.

The preliminary plan is presented in Figure 1. This experiment is very similar to the one we are running on the Exxon 8-cell 500-Wh zinc-bromine battery. It is a four factor, two level experiment. The factors are charge and discharge rate, maximum state-of-charge (SOC), and battery temperature. The nominal battery values used in determining the parameters were taken from the EPRI report, Development of Zinc-Bromine Batteries for Utility Energy Storage, EPRI EM-1717, March 1981, p. 9. I adjusted the appropriate values for a 20-cell unit. If these values are not applicable to this battery, please let me know. Also is the battery's capacity 200 AH or 180 AH (2000 AH/m^2 x 0.09m^2)?

The battery will be tested under computer control on a continuous basis. The end of discharge voltage will be 1.0V/cell. There will be a two-hour rest period for the battery after every discharge. I intend to run ten cycles of each type. For the 50°C tests, the battery will either be placed in a large oven in our lab, or we will use immersion heaters in the electrolyte reservoirs.

Upon successful completion of this test plan, I would implement a third level into the existing experiment. This would be a lower level, such as a temperature of 5-10°C, a maximum SOC of 30 percent, and lower charge and discharge rates. Also, some electrolyte flow-rate variation might be added. I will submit this plan to you for your review in advance.

As I told you on the phone on June 23, we are now waiting for the installation of our fume hood. This should be the last step before we can begin testing the battery. I estimate that the installation should begin during the next month. I will keep you informed on its progress. I will look forward to hearing from you regarding this test plan.

Sincerely,

Paul C. Butler

Paul C. Butler
Division 2525

PCB:2525:jh

Attachment

bcc:

2525	R. P. Clark
2525	J. L. Chamberlin
2525	D. W. Miller
2533	A. E. Verardo
525	P. C. Butler
2525	Day File

GOULD ZINC-BROMINE 20-CELL BATTERY PRELIMINARY TEST PLAN

FOUR FACTORS -- TWO LEVEL EXPERIMENT

Test No.	Factor A	Factor B	Factor C	Factor D
1	25	25	50	20
2	25	25	80	20
3	25	34	50	20
4	25	34	80	20
5	34	25	50	20
6	34	25	80	20
7	34	34	50	20
8	34	34	80	20
9	25	25	50	50
10	25	25	80	50
11	25	34	50	50
12	25	34	80	50
13	34	25	50	50
14	34	25	80	50
15	34	34	50	50
16	34	34	80	50

Factors

A	Charge Current, A
B	Discharge Current, A
C	Maximum State-of-Charge, %
D	Battery Temperature, °C

Nominal Battery Values

200 AH	(2000 AH/m^2 @ 0.09m^2?)
32V	Average discharge voltage (1.6V/cell)
6.4 kWh	
1.0 kW	
20V	End of discharge voltage (1.0V/cell)

FIGURE 1

Gould Inc., Gould Laboratories
40 Gould Center
Rolling Meadows Illinois 60008
Telephone (312) 640-4400

GOULD

July 30, 1981

Mr. Paul C. Butler
Sandia National Laboratories
Storage Battery Division - 2525
Albuquerque, NM 87185

Dear Paul:

I have reviewed your plan for cycle testing our 800 W zinc-bromine battery. Continuous cycling should be no problem. The two-hour rest period at the end of discharge must be in a short-out mode. This is necessary to allow residual zinc to be removed from the negative electrodes.

The following operating conditions should not be exceeded:

Temperature - should be kept between 25-35 C. Above 35 C there are excessive thermal stresses placed on the electrode bond which could cause electrode debonding. An electrode debonding is unrecoverable and requires a tear-down of the submodule.

Current - should not exceed 30 A. Above 30 A the chance of zinc dendrite formation is increased. This could lead to dendrite shorting.

Loading (state-of-charge) - based on a capacity of 200 Ah, the maximum 50 C should not exceed 75% (150 Ah) of the capacity. Above 150 Ah there is an increased chance of zinc dendrite formation which could lead to dendrite shorting.

50 C ?

In considering a third level of testing involving low temperature, I reccommend it be the last type of test. We have not done any low temperature cycling, and therefore, I am not sure of the effect it will have on the battery.

I am looking forward to visiting your facility in September and implementing the testing program on our 800 W zinc-bromine battery.

Sincerely,

James R. Borta stm

James R. Borta

/stm

APPENDIX C

Battery Voltage, Current, and Temperature Versus Time Plots for Represetnative Cycles

Cycle 3
Gould Zn/Br_2

BATTERY VOLTAGE (VOLTS) VS TIME (HOURS)
TEST ON BATTERY 168 STARTED ON 811116 AT 92343

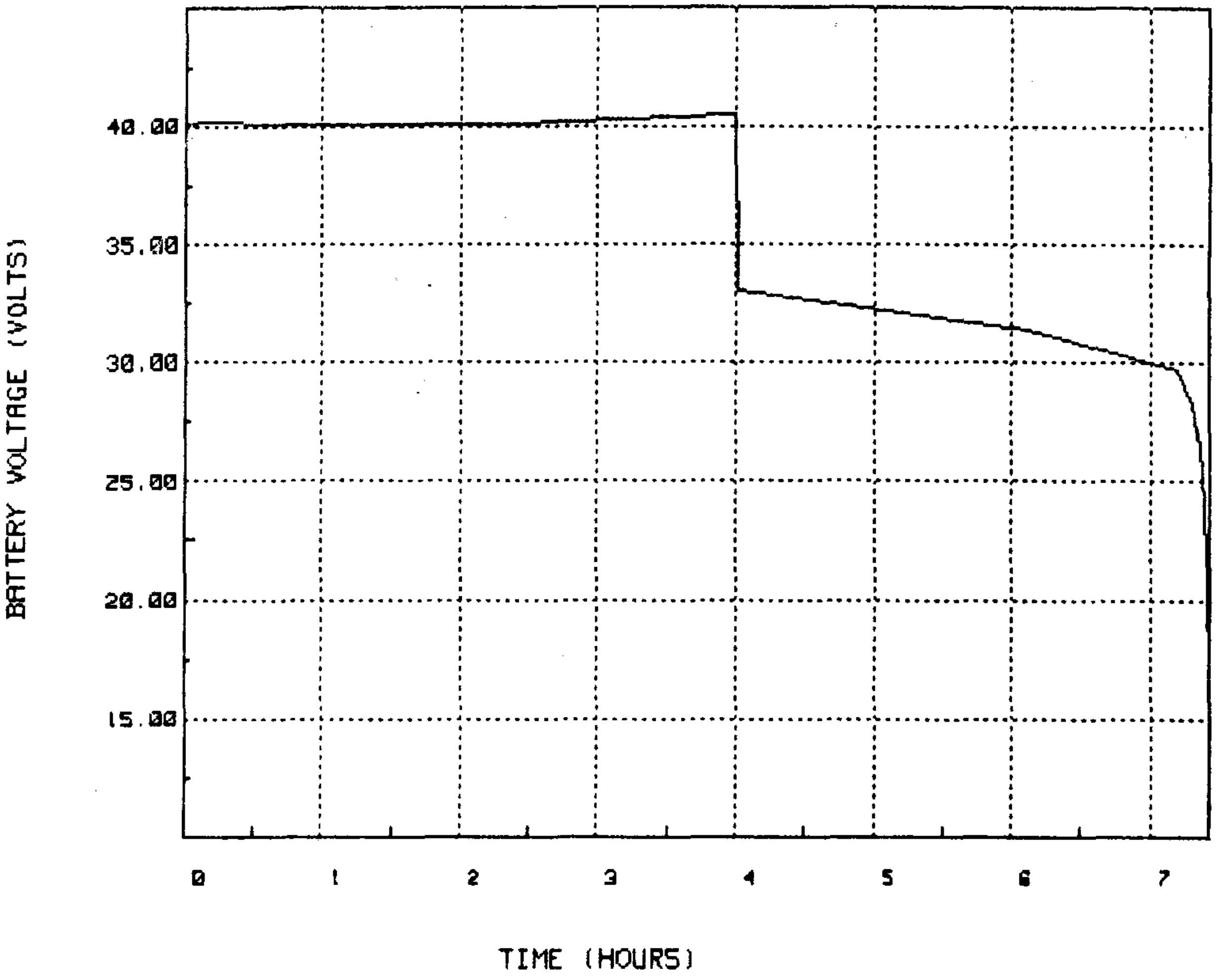

```
TEST ON BATTERY 168 STARTED ON 811116 AT 92343
TIME AT END OF PLOT : 811116 AT 164914
START OF PLOT VOLTAGE=   40.099 VOLTS        AMP-HOURS REMOVED=   -86.610AH
START OF PLOT CURRENT=   25.024AMPS          AMP-HOURS RETURNED=   99.582 AH
END   OF PLOT VOLTAGE=   16.163 VOLTS        WATT-HOURS REMOVED=  -2707.400 WH
END   OF PLOT CURRENT=  -25.115 AMPS         WATT-HOURS RETURNED=  3999.300 WH
```

Cycle 3

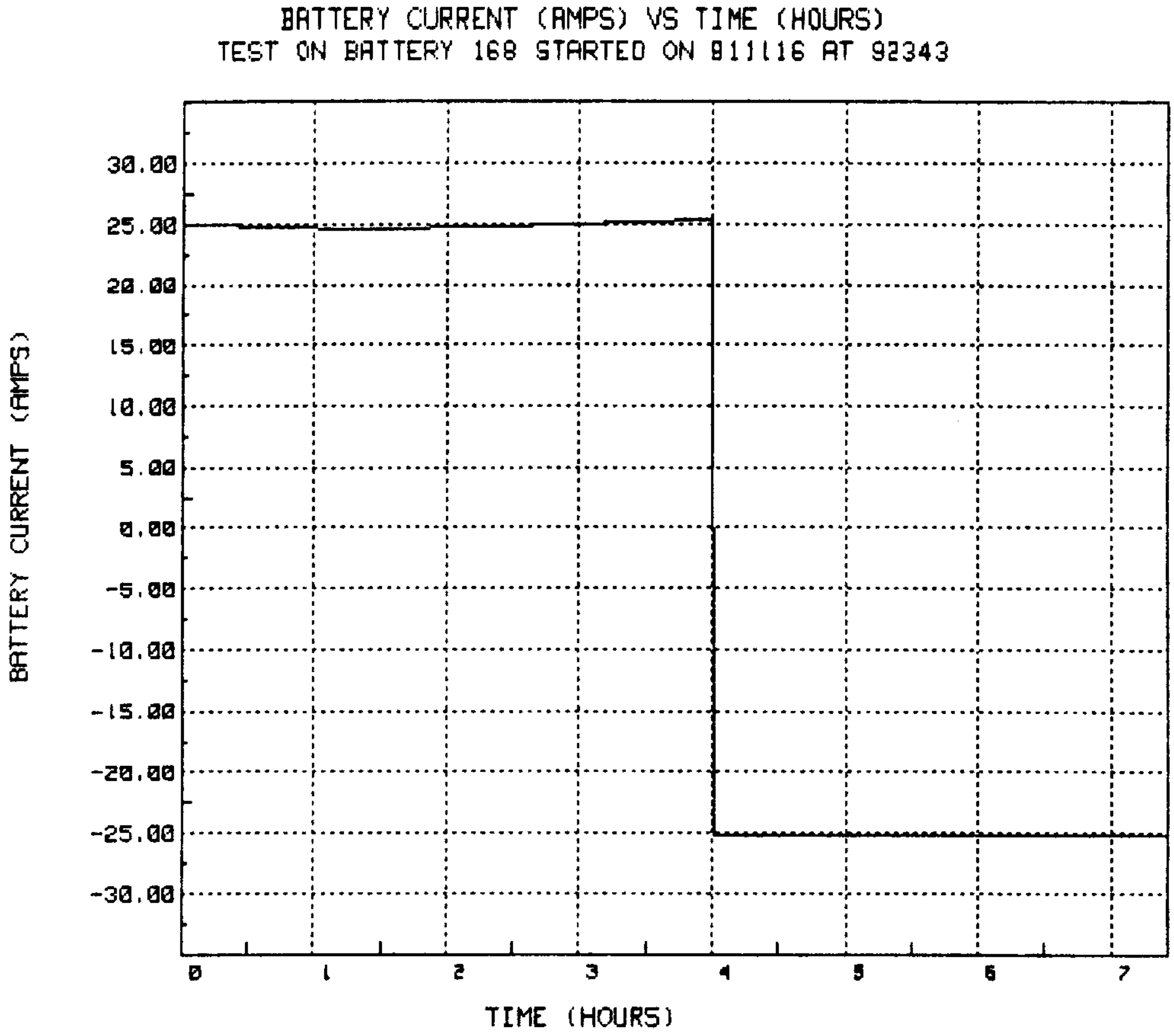
BATTERY CURRENT (AMPS) VS TIME (HOURS)
TEST ON BATTERY 168 STARTED ON 811116 AT 92343
BATTERY CURRENT (AMPS)
30.00
25.00
20.00
15.00
10.00
5.00
0.00
-5.00
-10.00
-15.00
-20.00
-25.00
-30.00
0
1
2
3
4
5
6
7
TIME (HOURS)

Cycle 3

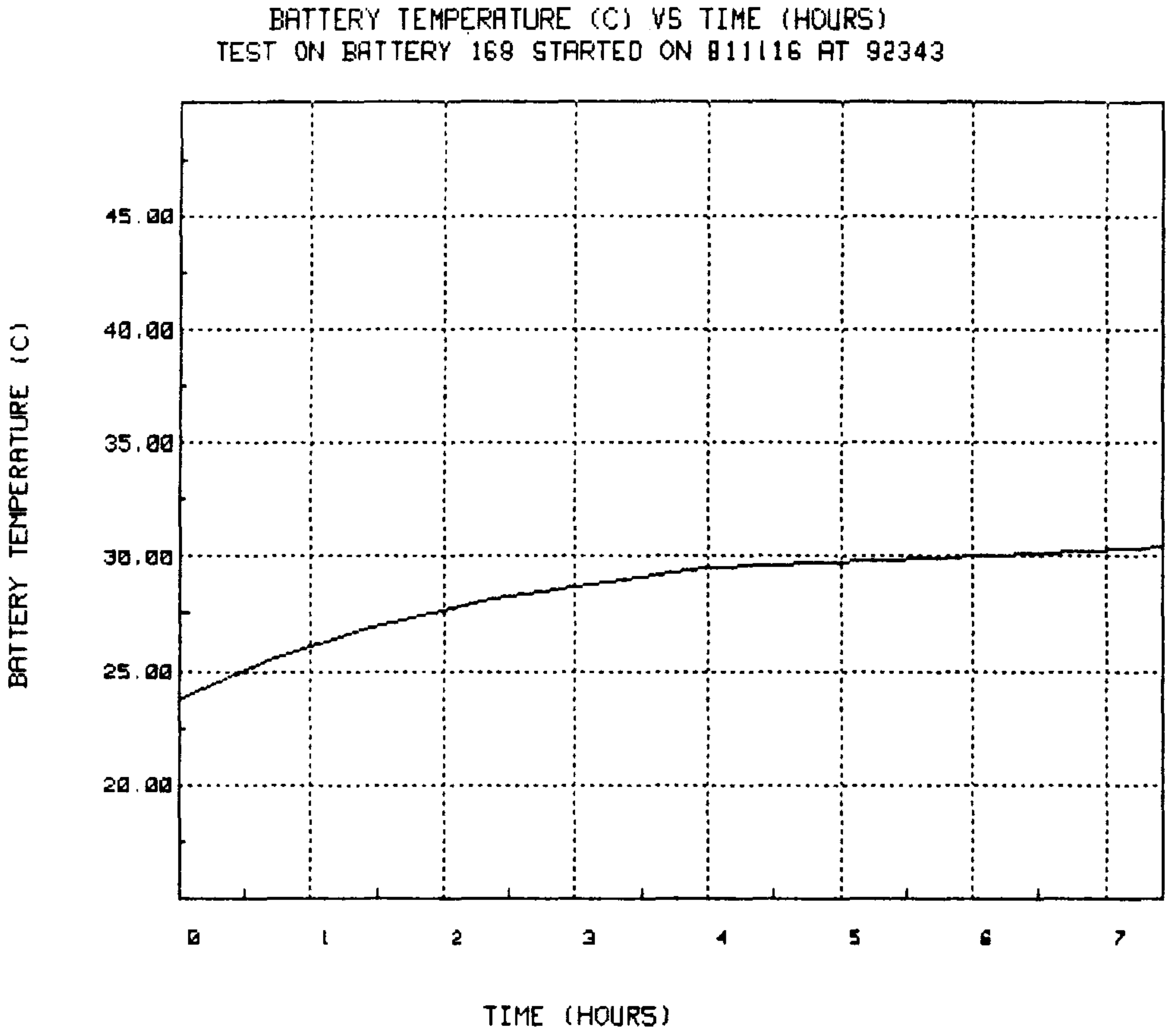
BATTERY TEMPERATURE (C) VS TIME (HOURS)
TEST ON BATTERY 168 STARTED ON 811116 AT 92343
BATTERY TEMPERATURE (C)
45.00
40.00
35.00
30.00
25.00
20.00
0
1
2
3
4
5
6
7
TIME (HOURS)

Cycle 13
Gould Zn/Br_2

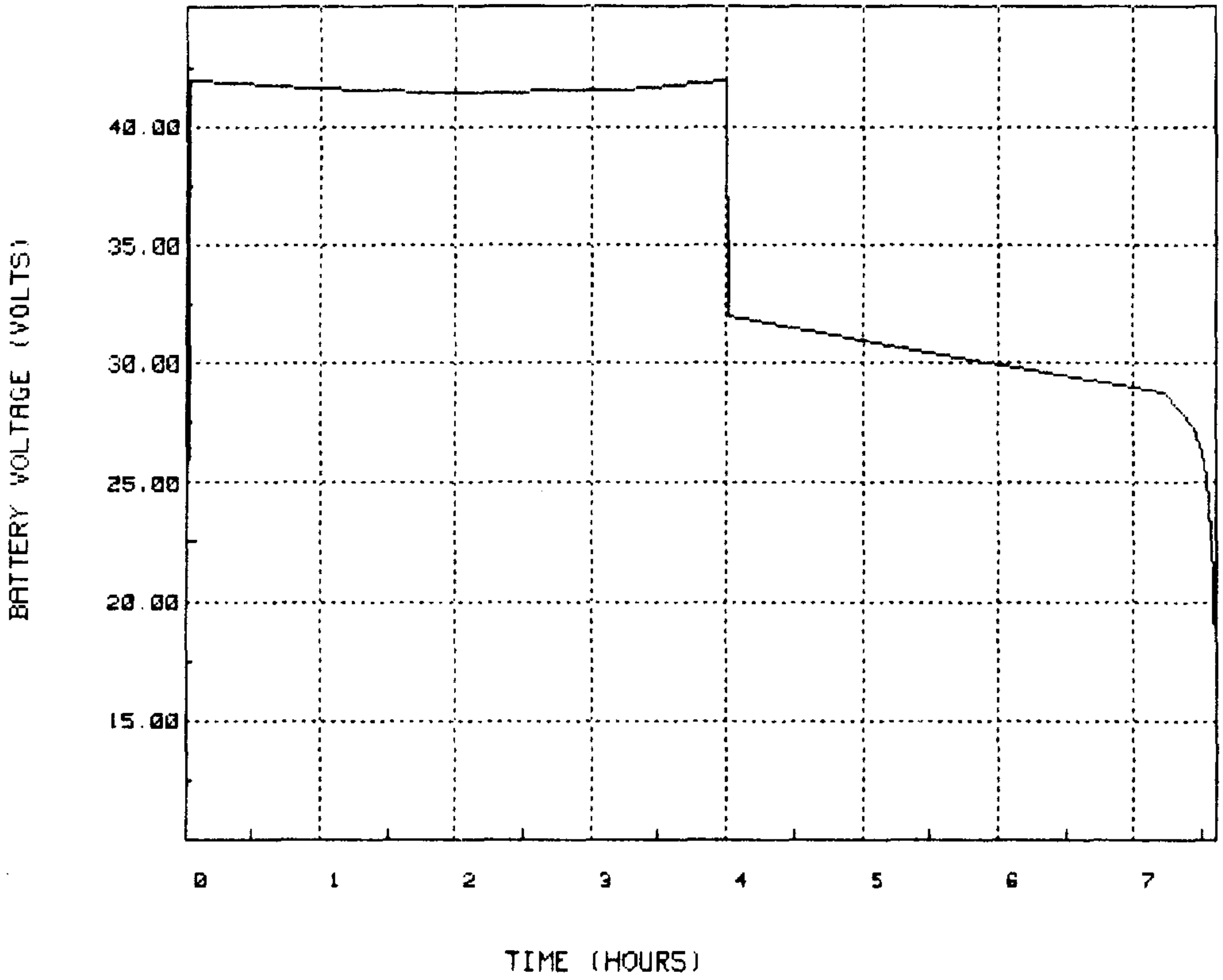

BATTERY VOLTAGE (VOLTS) VS TIME (HOURS)
TEST ON BATTERY 168 STARTED ON 811203 AT 81002

```
TEST ON BATTERY 168 STARTED ON 811203 AT 81002
TIME AT END OF PLOT : 811203 AT 154609
START OF PLOT VOLTAGE=    -.005 VOLTS        AMP-HOURS REMOVED=   -90.328AH
START OF PLOT CURRENT=     .021AMPS          AMP-HOURS RETURNED=   99.069 AH
END   OF PLOT VOLTAGE=   17.427 VOLTS        WATT-HOURS REMOVED=  -2701.600 WH
END   OF PLOT CURRENT=  -25.149 AMPS         WATT-HOURS RETURNED=  4120.400 WH
```

Cycle 13

Gould Zn/Br_2

BATTERY VOLTAGE (VOLTS) VS TIME (HOURS)
TEST ON BATTERY 168 STARTED ON 811211 AT 95448

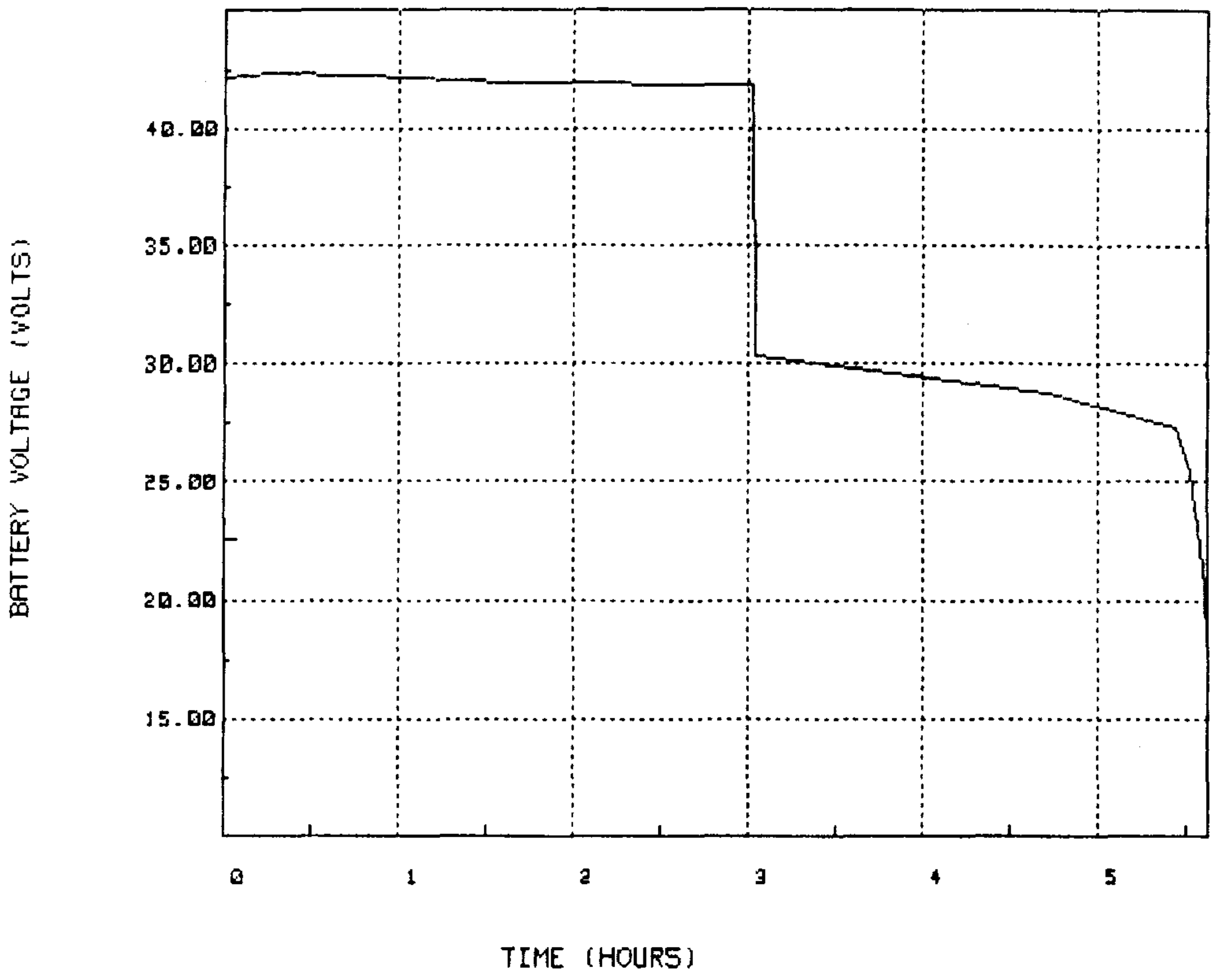

```
TEST ON BATTERY 168 STARTED ON 811211 AT 95448
TIME AT END OF PLOT : 811211 AT 153223
START OF PLOT VOLTAGE=   42.188 VOLTS        AMP-HOURS REMOVED=   -65.056AH
START OF PLOT CURRENT=   24.433AMPS          AMP-HOURS RETURNED=   73.664 AH
END   OF PLOT VOLTAGE=   17.905 VOLTS        WATT-HOURS REMOVED=  -1873.800 WH
END   OF PLOT CURRENT=  -25.042 AMPS         WATT-HOURS RETURNED=  3094.500 WH
```

Cycle 21

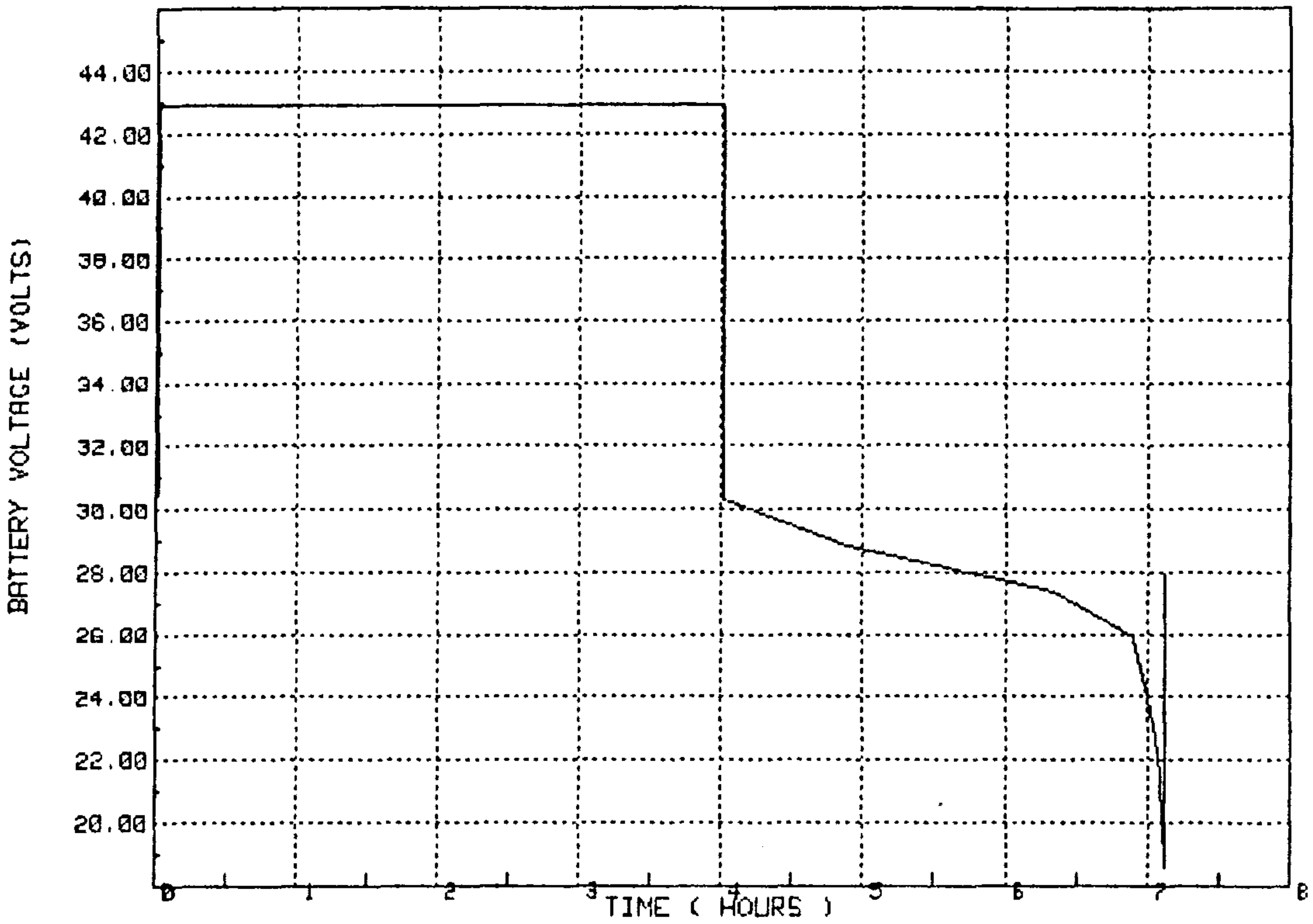

BATTERY VOLTAGE (VOLTS) VS TIME (HOURS)

TEST ON BATTERY 168 TIME AT START OF PLOT : 820112 AT 74954

Cycle 22

BATTERY VOLTAGE (VOLTS) VS TIME (HOURS)

TEST ON BATTERY 168 TIME AT START OF PLOT : 820113 AT 74310

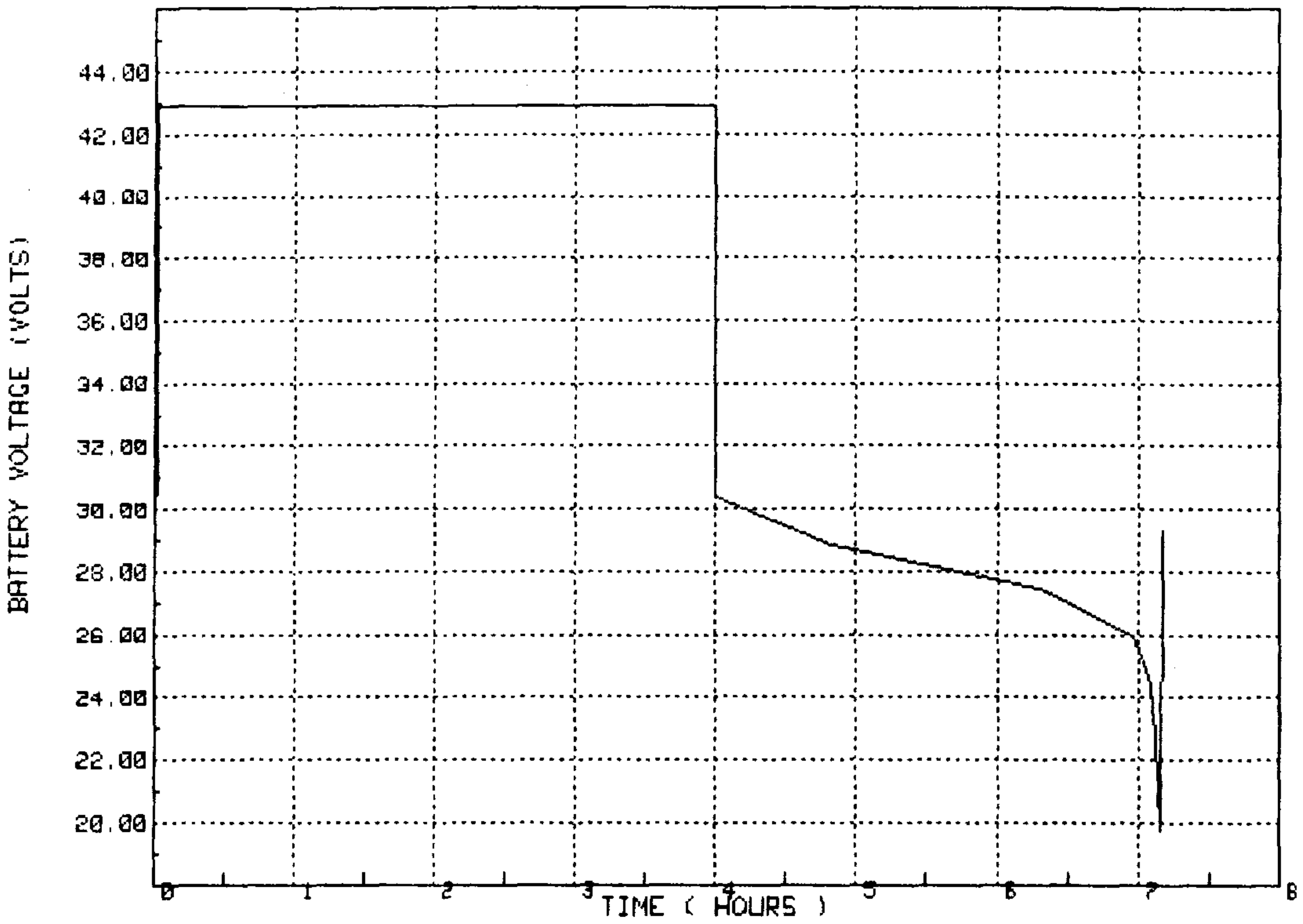

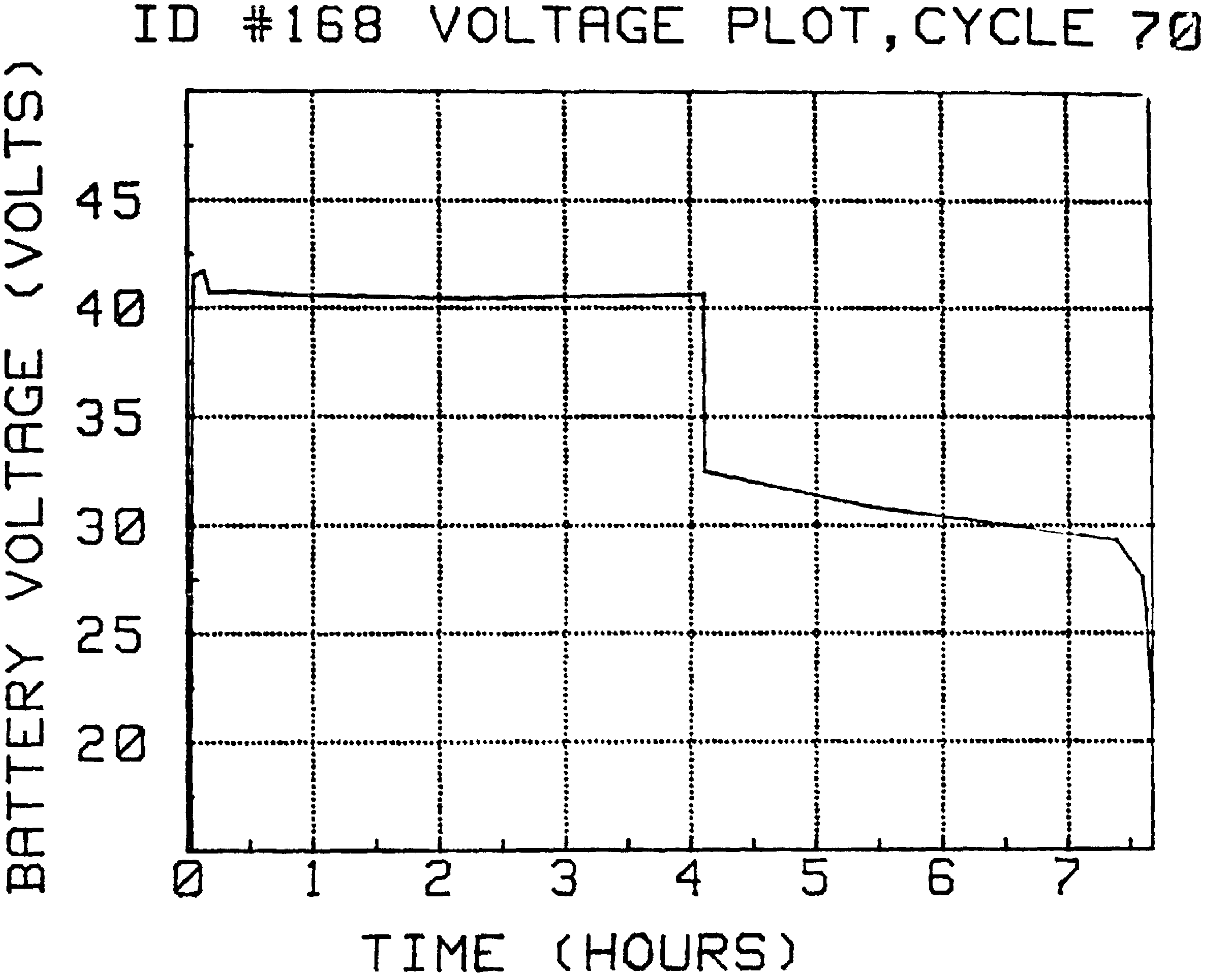
ID #168 VOLTAGE PLOT, CYCLE 70
BATTERY VOLTAGE (VOLTS)
45
40
35
30
25
20
0
1
2
3
4
5
6
7
TIME (HOURS)

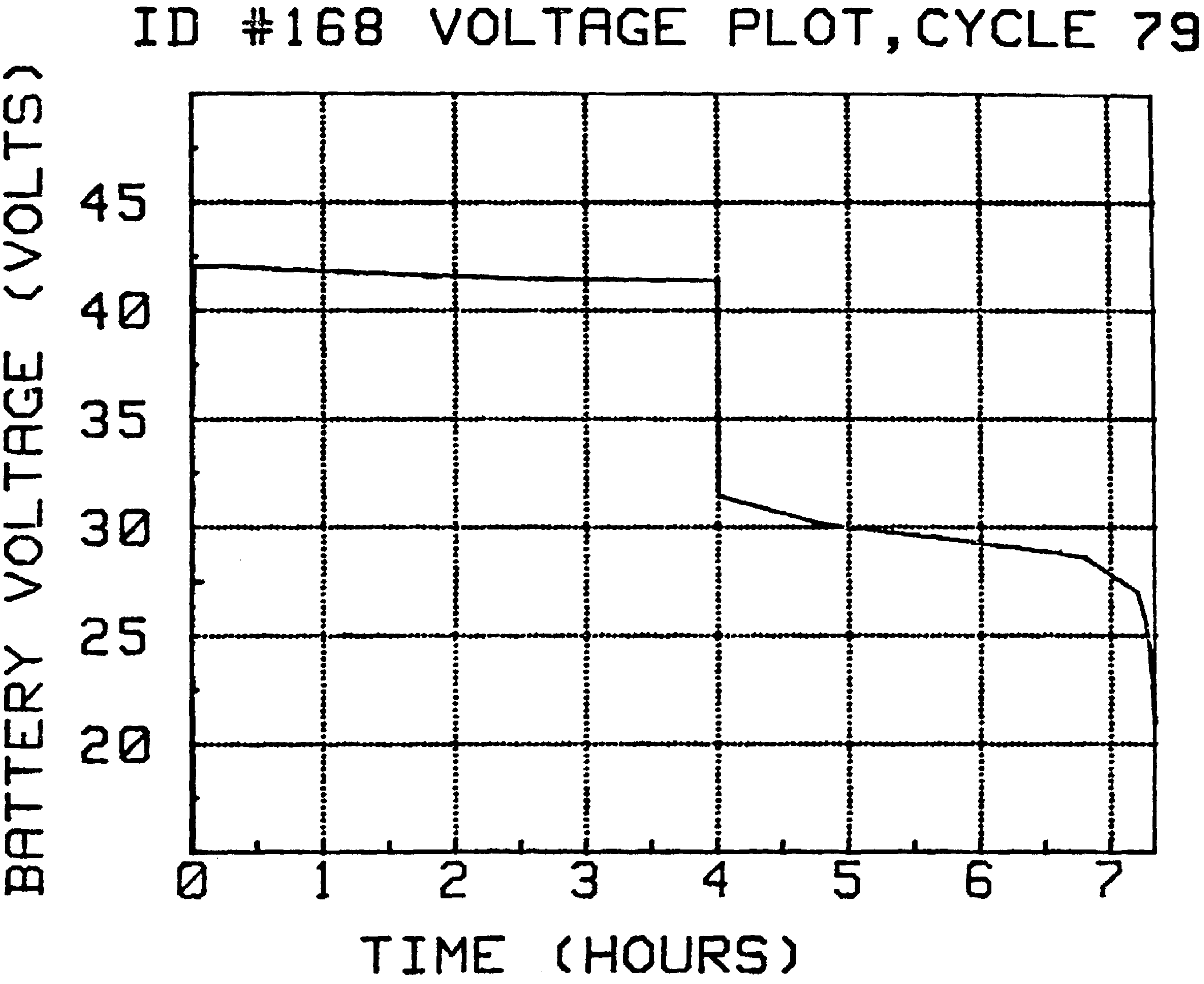

ID #168 VOLTAGE PLOT, CYCLE 79

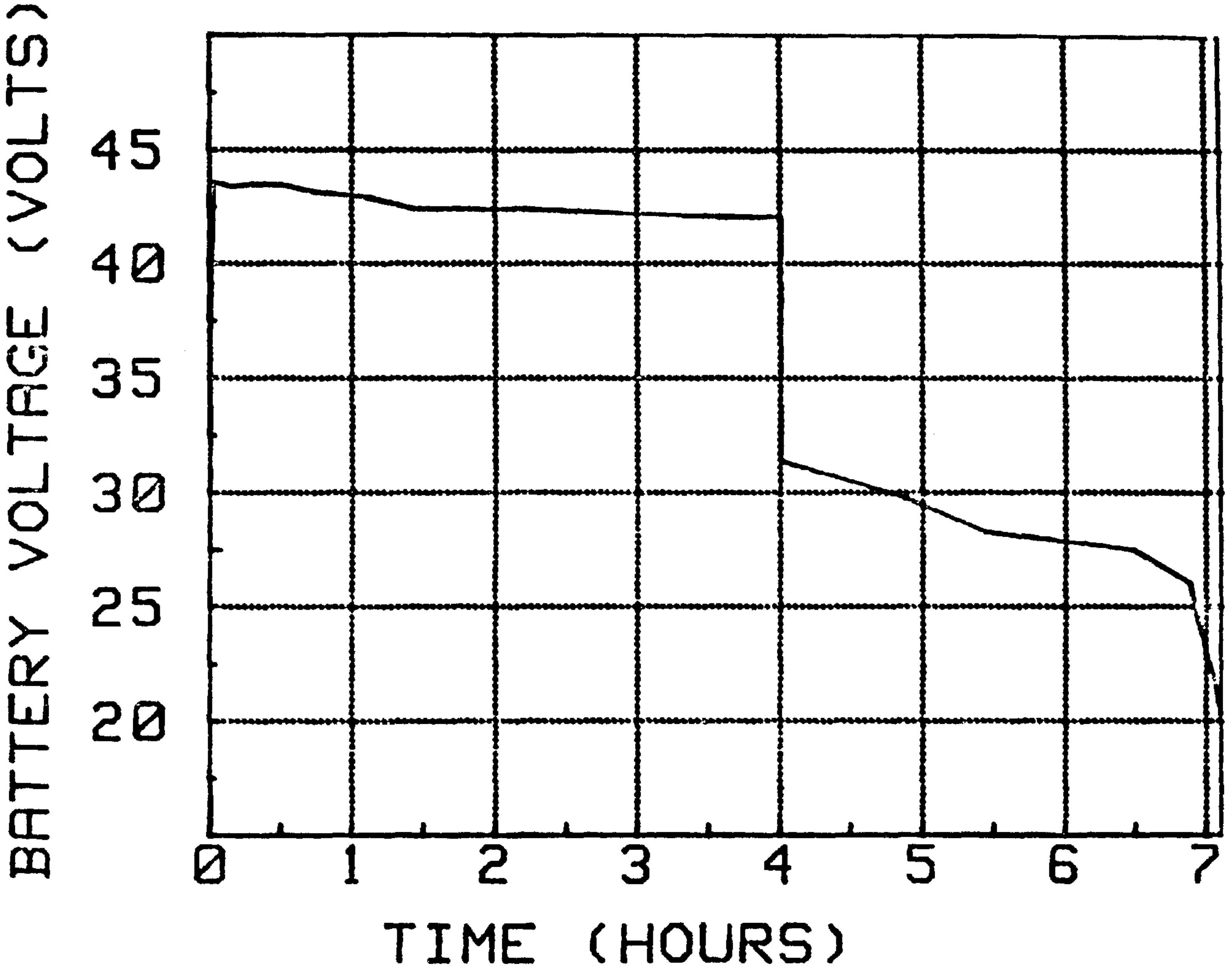

ID #168 VOLTAGE PLOT, CYCLE 98

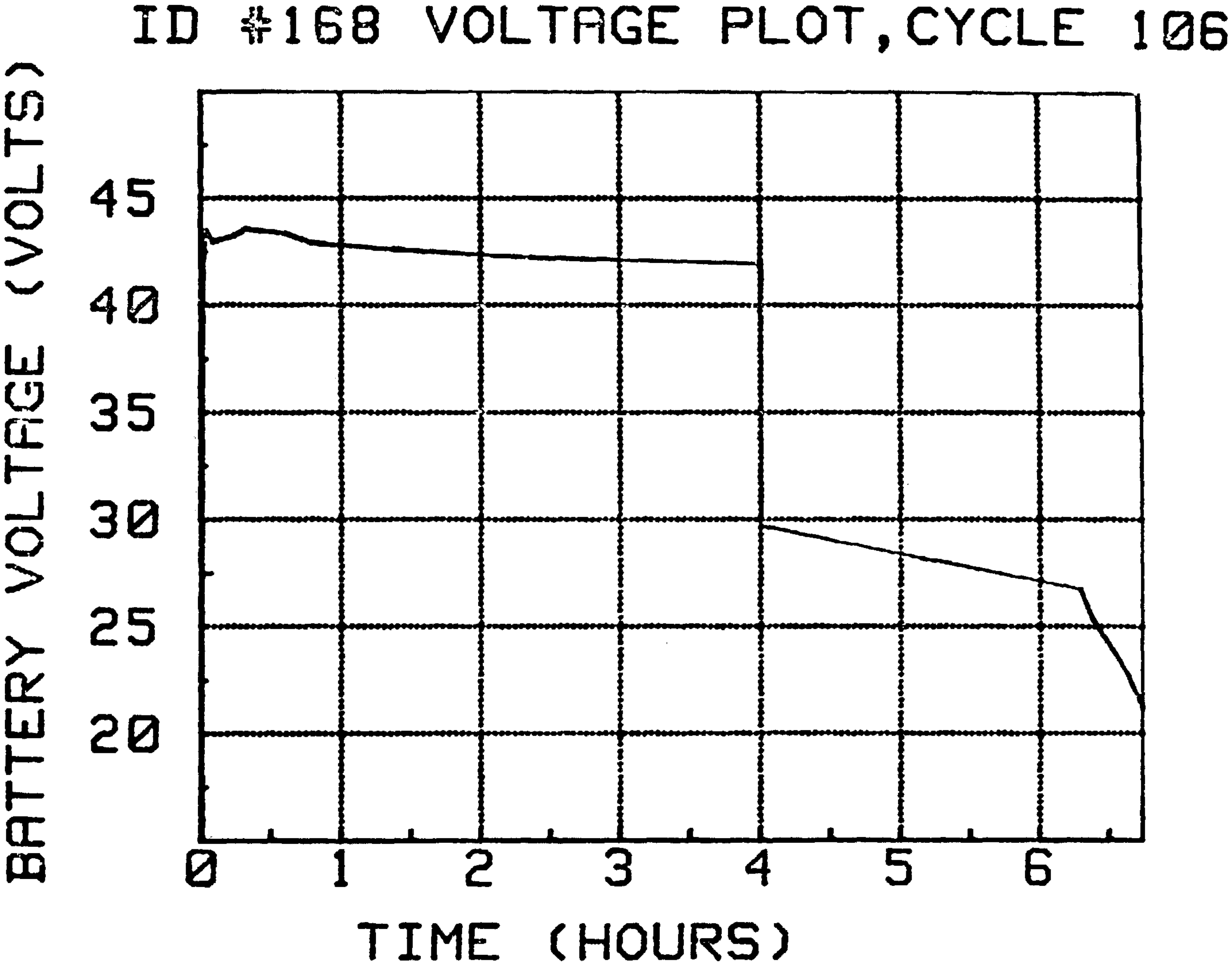
ID #168 VOLTAGE PLOT,CYCLE 106
BATTERY VOLTAGE (VOLTS)
45
40
35
30
25
20
0
1
2
3
4
5
6
TIME (HOURS)

ID #168 VOLTAGE PLOT, CYCLE 114

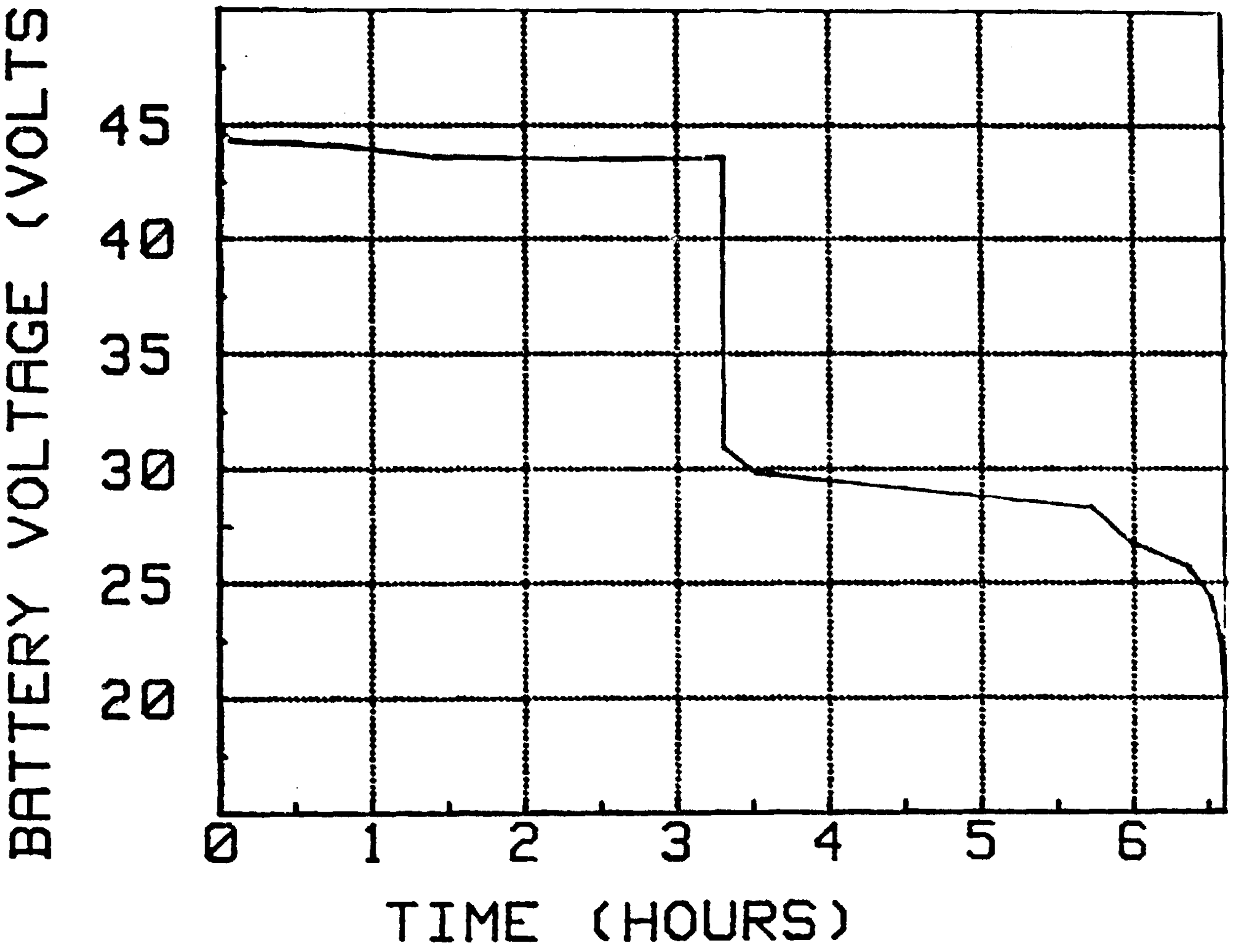

ID #168 VOLTAGE PLOT, CYCLE 120

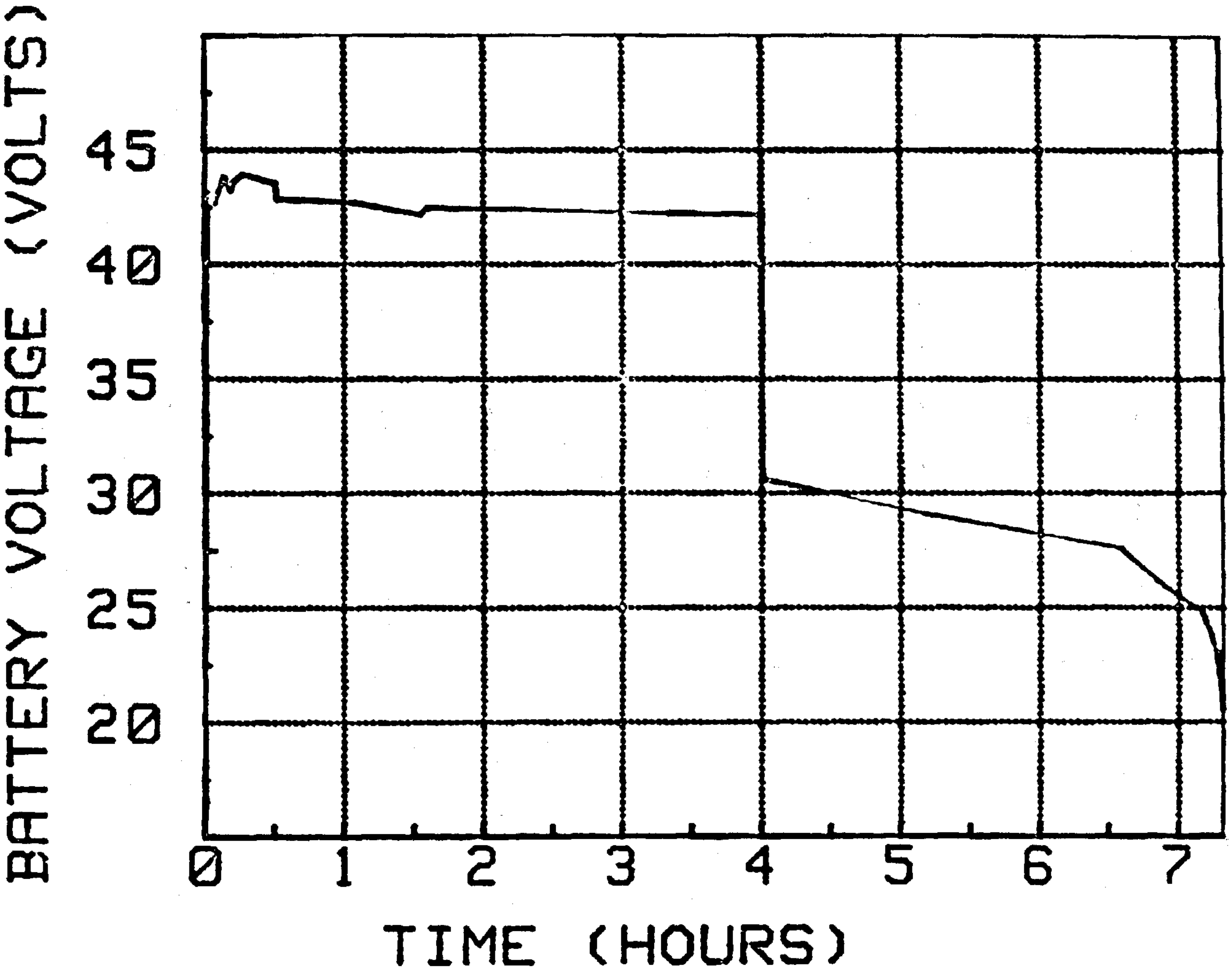

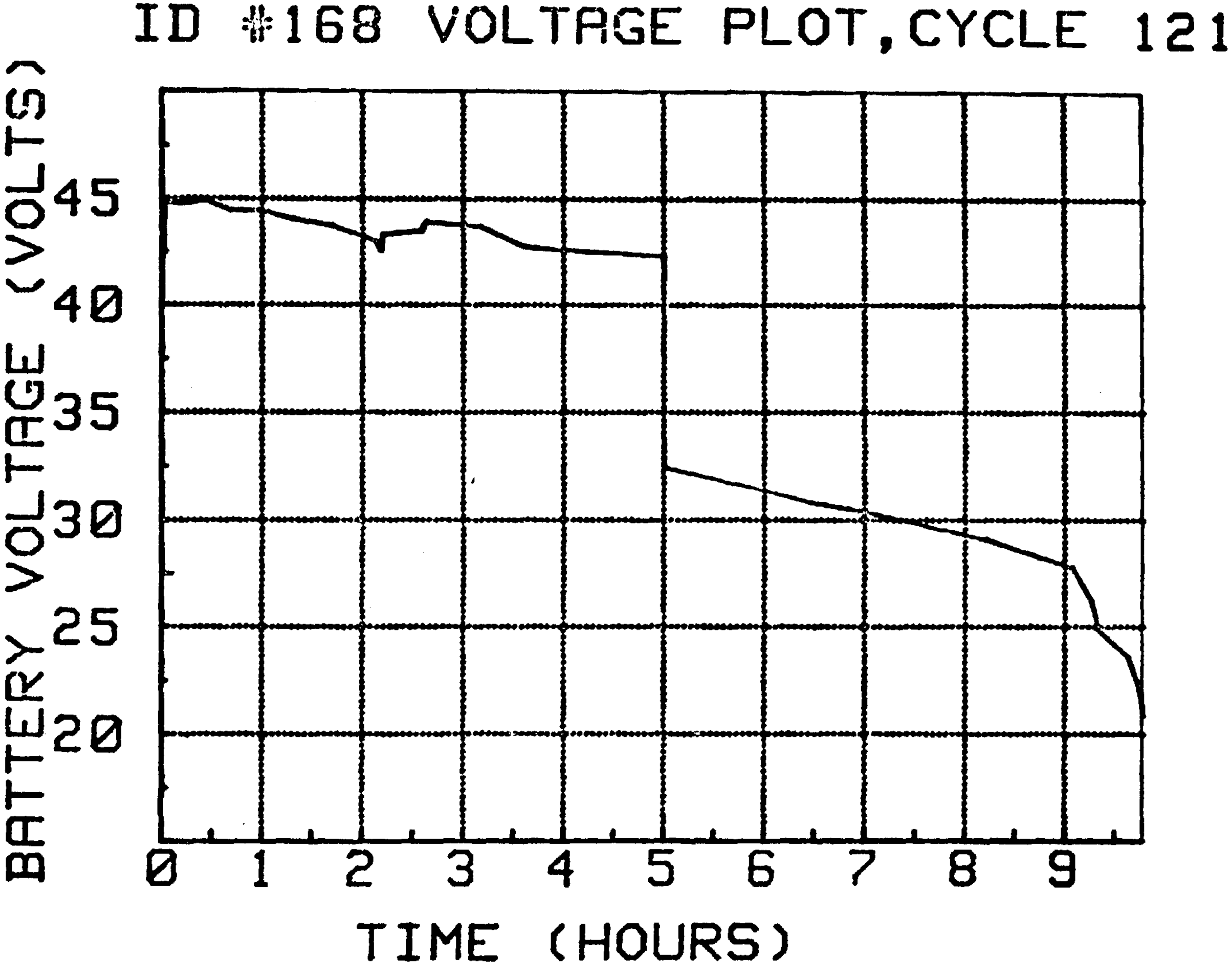
ID #168 VOLTAGE PLOT, CYCLE 121
BATTERY VOLTAGE (VOLTS)
45
40
35
30
25
20
0
1
2
3
4
5
6
7
8
9
TIME (HOURS)

ID #168 VOLTAGE PLOT, CYCLE 129

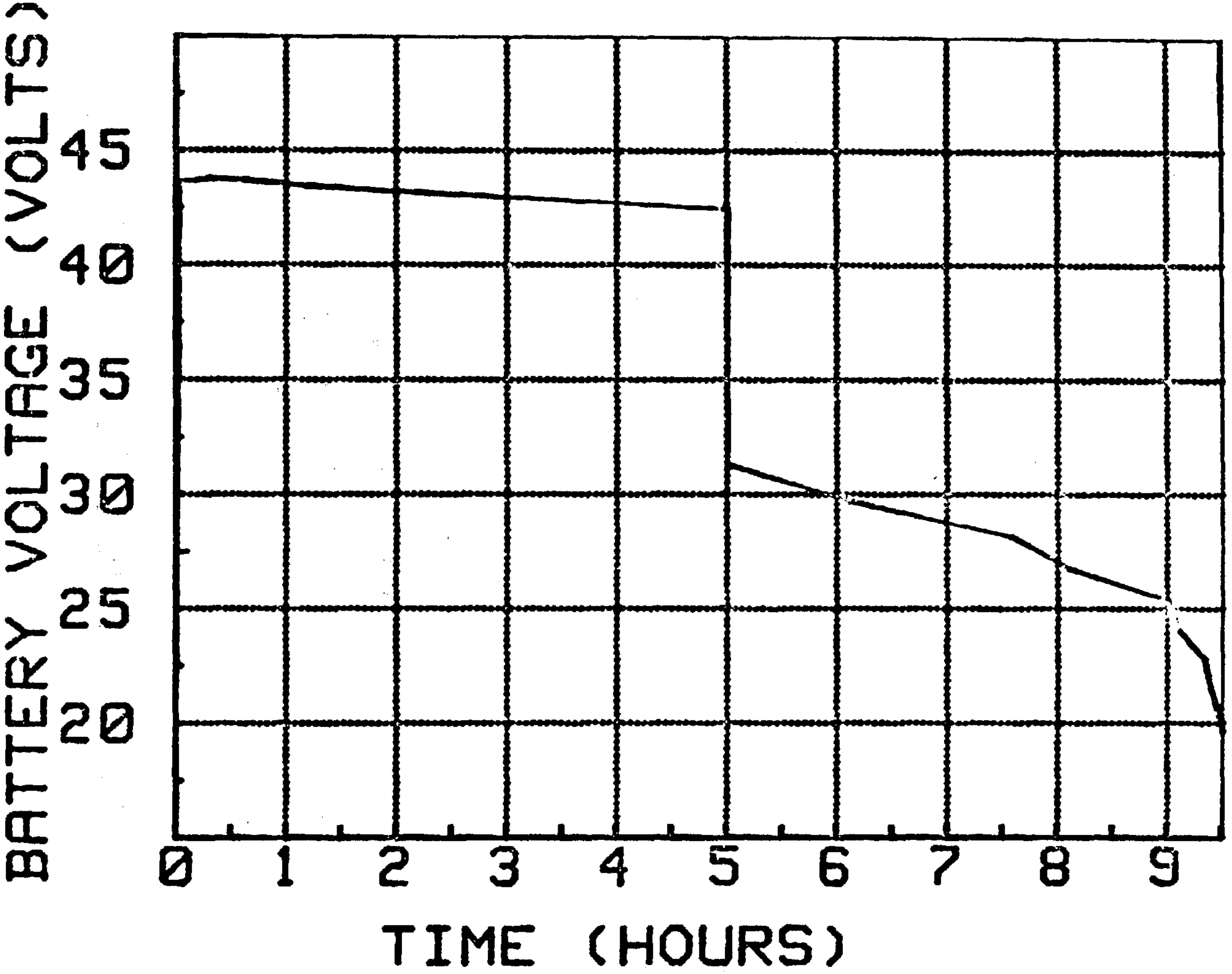

ID # 168 DATA PLOT, CYCLE 141

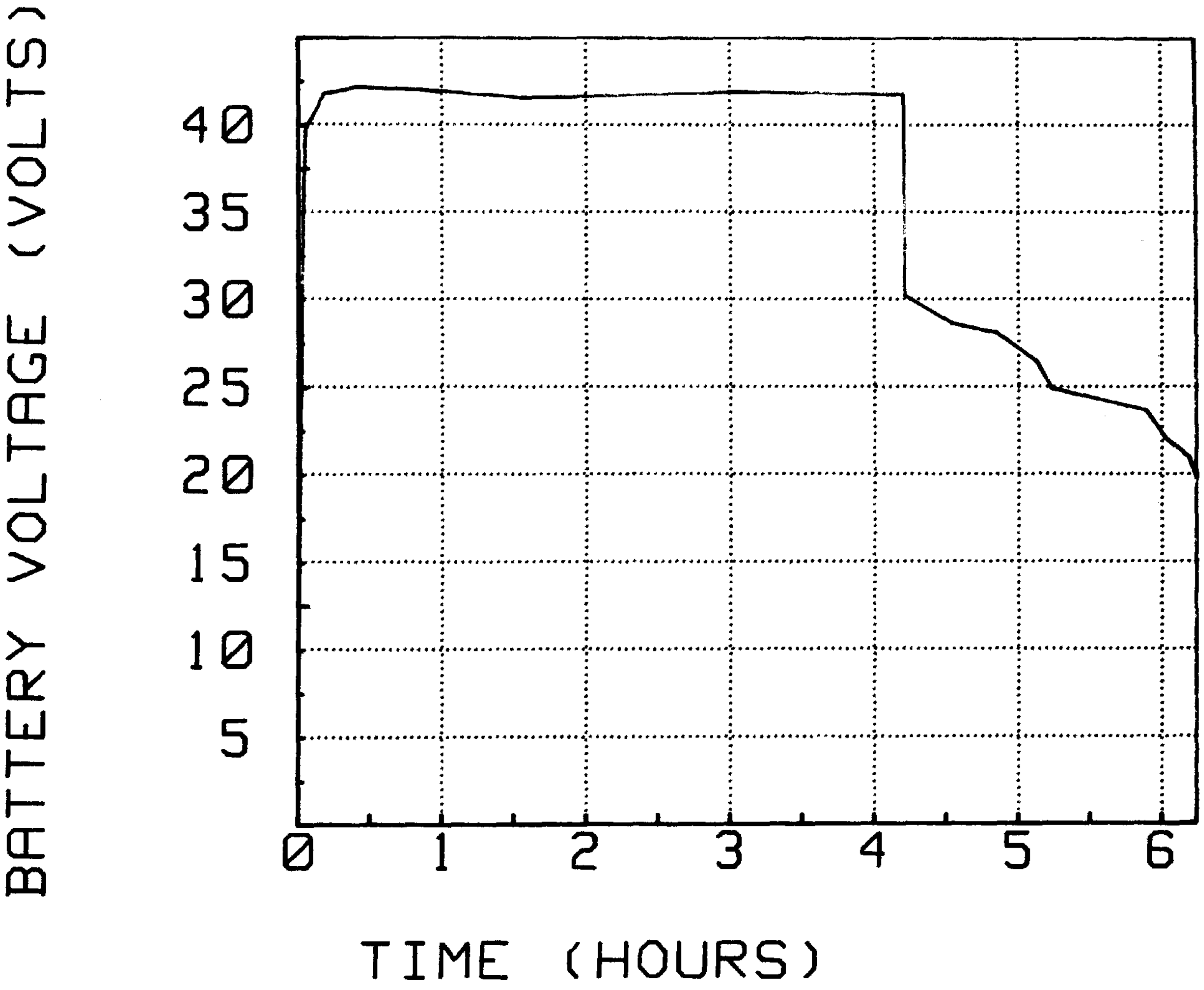

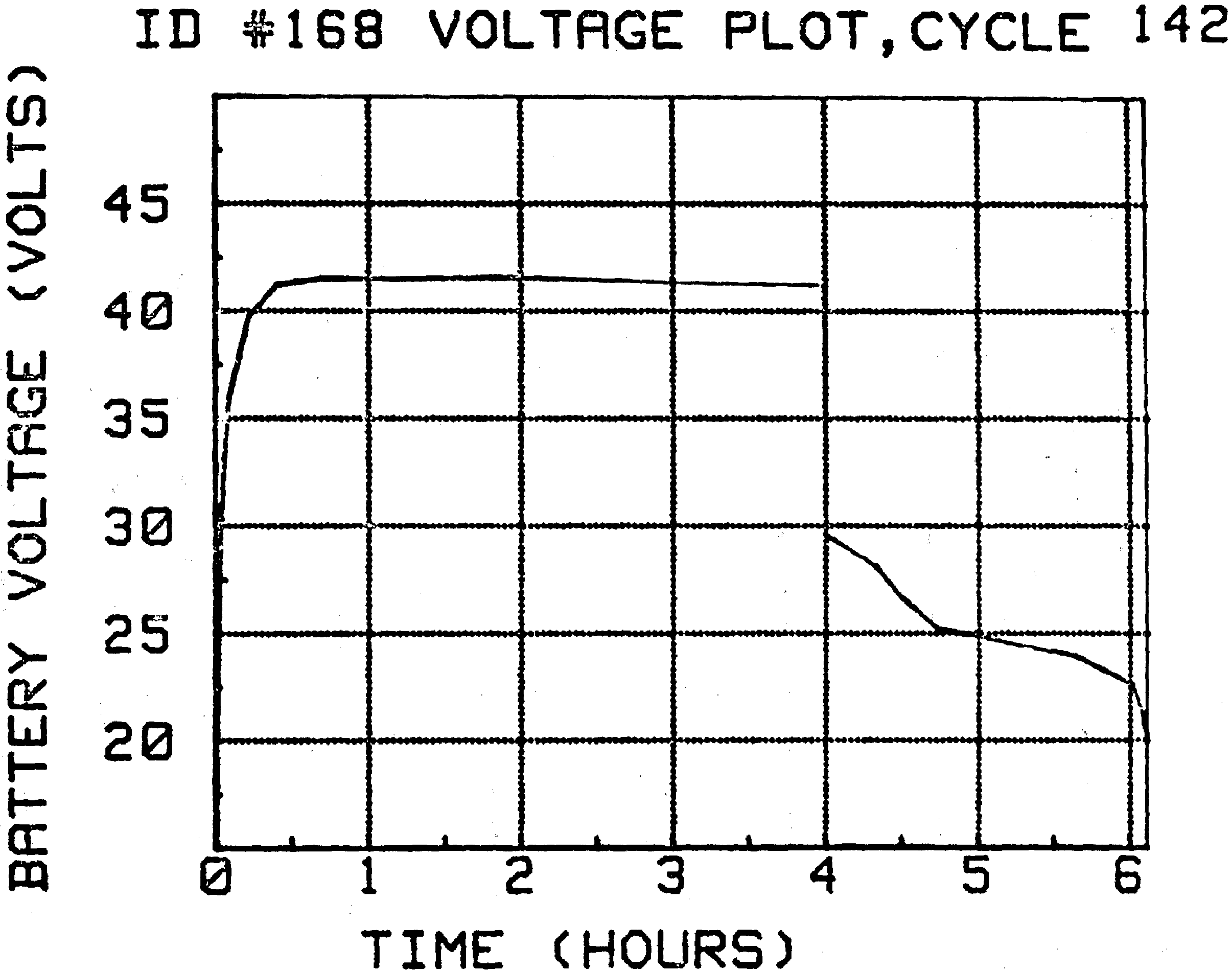

ID #168 VOLTAGE PLOT,CYCLE 142

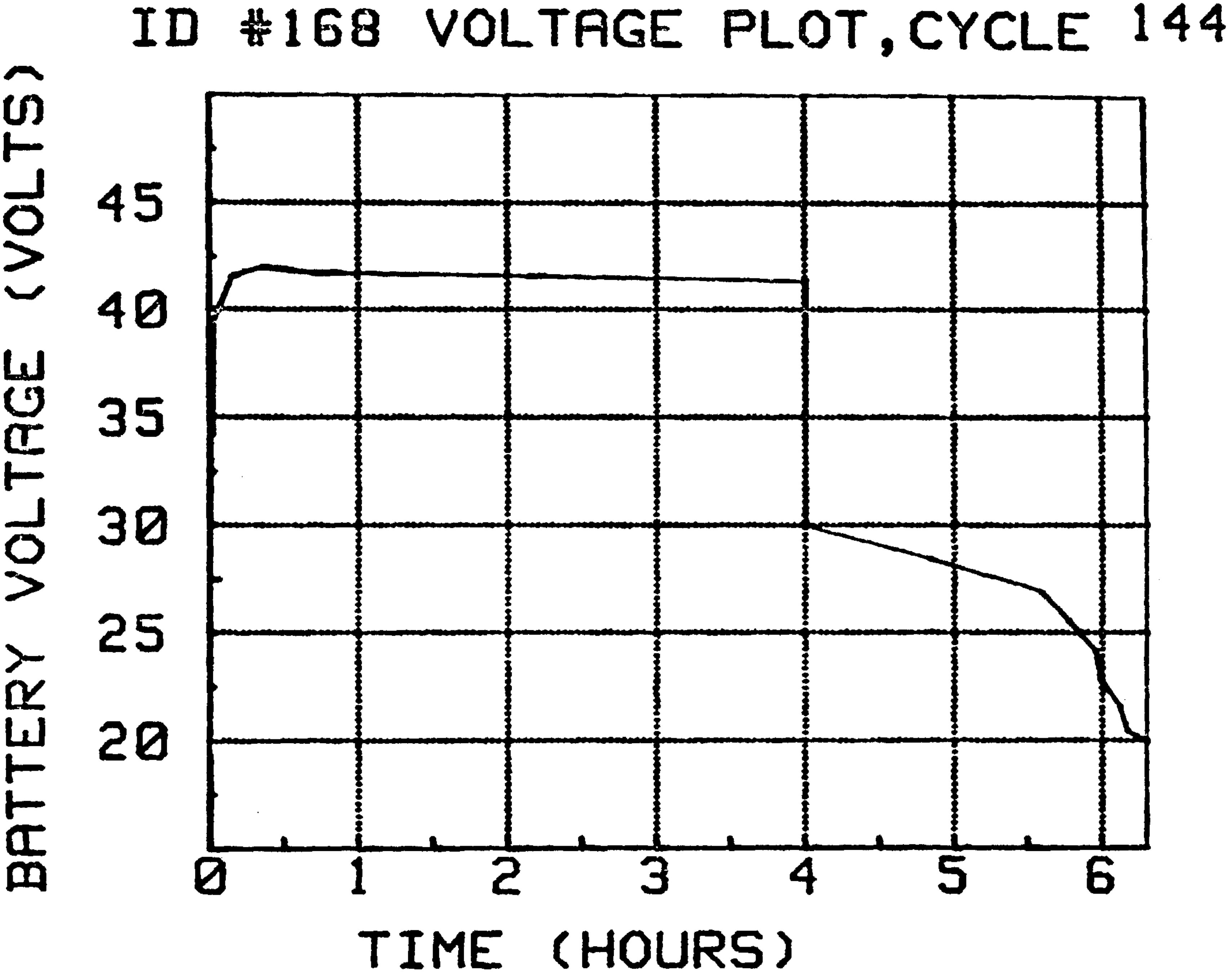
ID #168 VOLTAGE PLOT,CYCLE 144
BATTERY VOLTAGE (VOLTS)
45
40
35
30
25
20
0
1
2
3
4
5
6
TIME (HOURS)

APPENDIX D

Electrolyte Viscosity and Density Measurements

#168 Viscosity Centistoke 25°C
all values ± 0.007

Time	Anolyte	Catholyte	Polybromide
0	1.302	1.200	11.950
1	1.182	1.179	10.655
2	1.125	1.152	10.079
3	1.116	1.123	9.307
4	1.040	1.095	9.242
5	1.094	1.097	9.869
6	1.179	1.131	10.947
7	1.255	1.178	11.048

#168 Density at 20°C (g/cm^3)
all values ± 0.0001

Time	Anolyte	Catholyte	Polybromide
0	1.5710	1.5338	1.9662
1	1.5253	1.5465	1.9971
2	1.4955	1.5448	2.0024
3	1.4753	1.5361	2.0335
4	1.4480	1.5258	2.0485
5	1.5066	1.5103	1.9937
6	1.5561	1.5122	1.9720
7	1.5768	1.5226	1.9641

APPENDIX E

ERC Failure Analysis Notes

$Zn-Br_2$ TEARDOWN ANALYSIS NOTES

1.0 GENERAL

The Gould/ERC 20-cell zinc-bromine battery on test at SNL was taken apart after more than 160 cycles. Performance of the battery toward the end of testing was characterized by low coulombic efficiency (<70%) and excessive electrolyte cross-over between anolyte and catholyte flow loops.

2.0 TEARDOWN PROCEDURE

The submodule was given a 100 Ah charge at 25 Amps on the day prior to the teardown. The unit was drained of electrolyte and filled with D.I. water to reduce corrosion of the zinc deposit overnight.

The frames were numbered 1 through 22, with frames 1 and 22 being the negative and positive end frames respectively. [Note: The current collecting end plates are made of ruthenized titanium, and to prevent corrosion the negative end plate is not used as a working zinc electrode. Instead the negative end plate and first positive electrode constitute a bromine-bromide cell (both electrodes have carbon felt and are separated by Vexar screen with no separator) which is used to introduce current at the negative end of the stack. This extra cell is the reason why the 20-cell stack has 22 frames].

The stack was placed on its side and the negative end backing plate was removed. The electrode/frame assemblies and separators were then examined sequentially and placed in a separate pile. Observations were made, samples were taken, and zinc electrode thicknesses were measured. The following day photographs were taken of all the zinc deposits and separator wraps, some of the cathodes, and the negative and positive end plates.

3.0 RESULTS AND DISCUSSION

3.1 CARBON ELECTRODES AND PLATE TO FRAME BONDS

The carbon electrodes were in excellent condition, with the exception of the plate in frame 21. This electrode appeared to have become roughened in a section in the upper half of the electrode. The roughened area was on the cathode side of the plate. All other electrodes had smooth surfaces.

Plate to frame debonding was seen at the top and bottom of every electrode. The debonding was never apparent until the frame was removed from the stack at which point the electrode would buckle slightly and separate at the top and bottom bonds. The bonds at the sides of the electrodes generally held together during the first day of inspection. However, on the second day many of the side bonds were found to have separated. The initial observation was that the debonding in frame 2 (carbon electrode 1) was the worse bond failure, however this was not quantitatively determined.

None of the carbon electrodes were cracked and no major holes were found in the separator material, which indicates that the crossflow problem was due entirely to the observed debonding.

3.2 ZINC ELECTRODE DEPOSITS

When taken apart, the stack had a zinc electrode loading of 100 mAh/cm^2 minus any zinc lost due to corrosion overnight. Inspection of the stack components indicated that the water had only partially filled the channels, leaving part of the zinc plate dry and the rest of the plate submerged in the bromine loaded water.

The upper (dry) section of the plate had a shiny metallic appearance while the lower (submerged) area had a duller appearance. Thickness measurements were taken about 1" and 5" in from the left side of the plate at various heights. The thickness measurements are diagrammed in the accompanying sheets.

Zinc deposit thickness was the highest on electrode 1, the carbon electrode nearest the negative end plate. All the subsequent plates which were measured had deposits from 2.7 to 6.2 mils less thick than the first plate, with the thinnest deposits occurring in the center of the stack.

The outer perimeter of the electrode surface is not plated with zinc because the anode side of the electrode extends 1/4" in all directions beyond the working cathode area. The unplated area of the electrode varied from plate to plate, as can be seen in the photographs. The area in the bottom-center of the electrode almost always had an unplated region. This may be due to the proximity of this region to the leaking plate-frame bond. Small unplated areas were seen on electrode 8, possibly due to dead spots in the electrode flow.

Small dentrites (< 1/32" high) were observed on electrodes 3, 18 and 20. Major zinc growth was seen on plate 19 (frame 20), with dendrites extending to the separator layer. In all cases where zinc had penetrated the separator, the separator had been deformed and roughened by the penetration.

A glossy black sludge-like material was found in some of the anolyte flow channels. Generally the material was found near areas which had incomplete zinc plates or evidence of zinc shorting.

3.3 SEPARATOR MATERIAL

The separator used in the submodule was DARAMIC, with the outer perimeter filled with silicone to effect flow channel gasket seals. The thickness of the unused film is typically 25 ± 1 mil. Thickness of the separator from the submodule (between frames 18 and 19) was 24.5 mils, indicating that the material had not swelled.

The only physical imperfections seen in the separator were across from zinc dendrite growths, where zinc penetrating had distorted the smooth separator face. No macroscopic thru-holes were observed at shorting points, however, some zinc metal was found in the separator.

The uncycled separator material is light blue, with the sealing perimeter a darker blue color. The cycled separator films all had a uniformly dark appearance, with very little difference between the working cell area and the sealing perimeter.

A Vexar polypropylene screen is used to keep the carbon felt away from the separator and this screen had become fused to the separator.

Like the zinc electrodes, the separator also showed evidence of the partial fill during overnight stand. The submerged section of the separator was clean, however, the dry area exhibited yellowish incrustation from the salts in the evaporating electrolyte. A white, chalklike residue was found in some of the separators.

The separators showed a uniform impression of the sealing ridges around the flow channels, indicating that uniform compression was applied to the stack. The presence of a material which looked like congealed polybromide in the flow frame outside the channels suggested that the channels may not have sealed entirely.

3.4 CARBON FELT CATHODE SUBSTRATE

The carbon felt showed no visible signs of degradation. The area above the liquid level was filled with salts from the dried electrolyte and the submerged area looked normal. A small amount of polybromide was found in most of the plates, however, the felts on both end plates contained considerably more polybromide than the inner electrodes.

The felt is bonded to the bipolar plate with silicone cement along the right and left edges (except at the electrolyte inlets) and spots of cement on the plate itself. The edge bonds had no strength and could be easily peeled apart, while the spot bonds were still very adherent.

3.5 ELECTRODE FRAMES

The polypropylene injection molded frames exhibited some discoloration, with the areas near the lower catholyte flow channels showing the darkest red-orange color. No cracking or warping was observed.

No flow blockages were observed in any of the flow channels, although the black deposit referred to earlier may have impeded flow in the anolyte flow area immediately below the electrode.

A gelled, orange colored material was found in frame 1 (bromine/bromide cell negative end plate) outside the flow channel area. The material is either silicone impreganted with bromine, or gelled polybromide oil. A thin film of a silicone-like material was found on many of the frames around the catholyte inlet manifold.

3.6 ANODE SPACERS

Very little discoloration and no physical degradation was observed in these components.

3.7 RUTHENIZED TITANIUM END PLATES

No degradation of the end plates was apparent on visual inspection.

3.8 ELECTROLYTE

The electrolyte was not inspected by this observer, however, the water used to fill the stack during the overnight stand was. The water from the cathode side had various appearances depending on when it came out of the stack. Some liquid was a clear red color, some a cloudy orange due to emmulsified polybromide and some contained large drops of dark red polybromide oil. The water from the anolyte side was clear yellow with dark particles suspended in it, giving it a greyish appearance.

3.9 SAMPLES TAKEN

The following samples were taken for evaluation:

- Frame 1, Negative End Plate: Gelled orange material
- Frame 3, Electrode 2: Black sludgelike material
- Frame 3, Electrode 2: White crusty residue
- Separator between Frames 3 and 4: White chaulky material
- Frame 4, Electrode 3: Chunk of crystaline material
- Frame 6, Electrode 5: Silicone-like material from flow and locating hole.

4.0 SUMMARY AND CONCLUSIONS

Separator debonding was probably the major cause of failure of the submodule. Certainly the electrolyte crossover problem was due entirely to debonding as no cracks in electrodes or major holes in separators were found.

Zinc dendrite growths were observed, but only in a few of the plates. Uneven plating and unplated spots were also observed, suggesting flow irregularities. Because the extent of self-discharge during overnight stand cannot be quantitatively determined, the measured deposit thicknesses cannot be related to loading level. Many of the unplated areas observed may have had zinc plates prior to the overnight stand, particularly those below the observed liquid level. This may explain the unplated area observed in the bottom center of most of the plates, however, self-discharge stripping of zinc would be expected to be uniform along any horizontal dimension (due to a uniform concentration of settled polybromide or dissolved bromine). The reduced plating in the center suggests either a flow irregularity or self-discharge due to proximity to the leaking electrode-frame bond.

The observed black sludgelike material generally seemed to be associated with either zinc shorting or unplated areas (Note: Many of the observed unplated areas could have been mossy or dendritic deposits which may have self-discharged faster). This suggests that the material is either zinc, or a product of the interaction of zinc shorts with the separator material. The carbon electrode material could also be a source, however, only one electrode exhibited any degradation. The dark particles suspended in the anode side water could also be related to this material.

The one carbon electrode that had an area of roughened surface could represent a manufacturing defect, since the remaining 19 plates had uniformly smooth surfaces. In general the plates looked good, although the observed buckling suggests that some dimensional expansion had occurred.

No degradation was observed in the titanium end plates or carbon felt substrates. The discoloration seen in the polypropylene components (frames and spacers) was typical of polypropylene exposed to this chemical environment.

The presence of encrusted material beyond the flow channels in the frames suggests that the channels did not seal completely. There was not a lot of material in these areas and the leakage did not seem severe.

The separator material did not appear to swell, increase in linear dimension, or warp. The material had darkened with usage and had roughened in areas of zinc penetration. While the darkening is not necessarily an ongoing degradation process, the irreversible roughening due to zinc penetration is certainly a problem.

APPENDIX F

SNL Failure Analysis Notes

ERC/GOULD BATTERY TEARDOWN #168

The battery was charged for 4 hours at 25A, the anolyte and catholyte removed, and D.I. water was placed in the battery and left overnight.

After the battery was taken apart, all pieces were visually inspected and some of the electrodes were measured with a micrometer for thickness. A piece of plastic was placed over the electrodes, adding 3.5 mil. The plastic thickness was subtracted from all measurements. Fig. 1, 2, 3, 4, 10, 11, 12, 17, 18, 20.

Electrode #1

One measurement in area without zinc deposit, the thickness was 0.0365 inch.
Four measurements in areas with zinc deposit, the thickness was from 0.0475 to 0.0495 inch.
Standard deviation was 0.0008, mean is 0.0480.
This electrode had definite debonding top and bottom.

Electrode #2

One measurement in area without zinc deposit, the thickness was 0.0365 inch.
Six measurements in areas with zinc deposit, the thickness was from 0.0395 to 0.0435 inch.
Standard deviation was 0.0013, mean is 0.0421.
The separator had zinc penetration in some areas and a plaster-like residue at the top, near flow channel.

Electrode #3

One measurement in area without zinc deposit, the thickness is 0.0345 inch.
Six measurements in areas with zinc deposit, the thickness is from 0.0385 to 0.0425 inch.
Standard deviation is 0.0015, mean is 0.0408.
Dendrites on lower half of electrode, separator has zinc penetration at bottom.

Electrode #4

One measurement in area without zinc deposit, the thickness is 0.0345 inch.
Six measurements in areas with zinc deposit, the thickness is from 0.0385 to 0.0425 inch.
Standard deviation is 0.0014, mean is 0.0415.

Electrode #8

At least 6 flow dead spots, shown by lack of zinc plating.
Right side of electrode had no zinc--about 2 inches from edge.

Electrode #9
The electrode had full zinc deposit--best in stack.

Electrode #10
Six measurements in areas with zinc deposit, the thickness is from 0.0395 to 0.0430 inch. Standard deviation is 0.0014, mean is 0.0413.

Electrode #11
Eight measurements in areas with zinc deposit, the thickness is from 0.0385 to 0.0435 inch.
Standard deviation is 0.0015, mean is 0.0409.

Electrode #12
Eight measurements in areas with zinc deposits, the thickness is from 0.0405 to 0.0425 inch.
Standard deviation is 0.0007, mean is 0.0419.

Electrode #17
Seven measurements in areas with zinc deposits, the thickness is from 0.0405 to 0.0425 inch. Standard deviation is 0.0007, mean is 0.0418.
Zinc dendrites on lower right of electrode.

Electrode #18
Eight measurements in areas with zinc deposit, the thickness is from 0.0425 to 0.0485 inch.
Standard deviation is 0.0017, mean is 0.0445.

Electrode #19
This electrode had a large amount of dendrites, more black sludge in the flow frame than usual, and clear evidence of zinc shorting.

Electrode #20
Six measurements in areas with zinc deposit, the thickness is from 0.0405 to 0.0455 inch.
Standard deviation is 0.0014, mean is 0.0432.
Bromine electrode, under felt, is rough in the upper half.
A few dendrites in upper corner.

Frame #22
More polybromide in felt of bromine electrode than seen in the middle of the stack.

Silicon-type substance is always around lower catholyte exit and black sludge is always around lower anolyte exit--near each end of flow channel.
All plates had reduction of zinc plating in lower center.
All electrodes had debonding top and bottom when pulled apart--some debonded on sides after handling.
All separators and bromine electrodes had white residue on top half.
One thickness measurement was made on separator #19.
Thickness is 0.0245 inch.

APPENDIX G

Photographs of Failed Battery Components

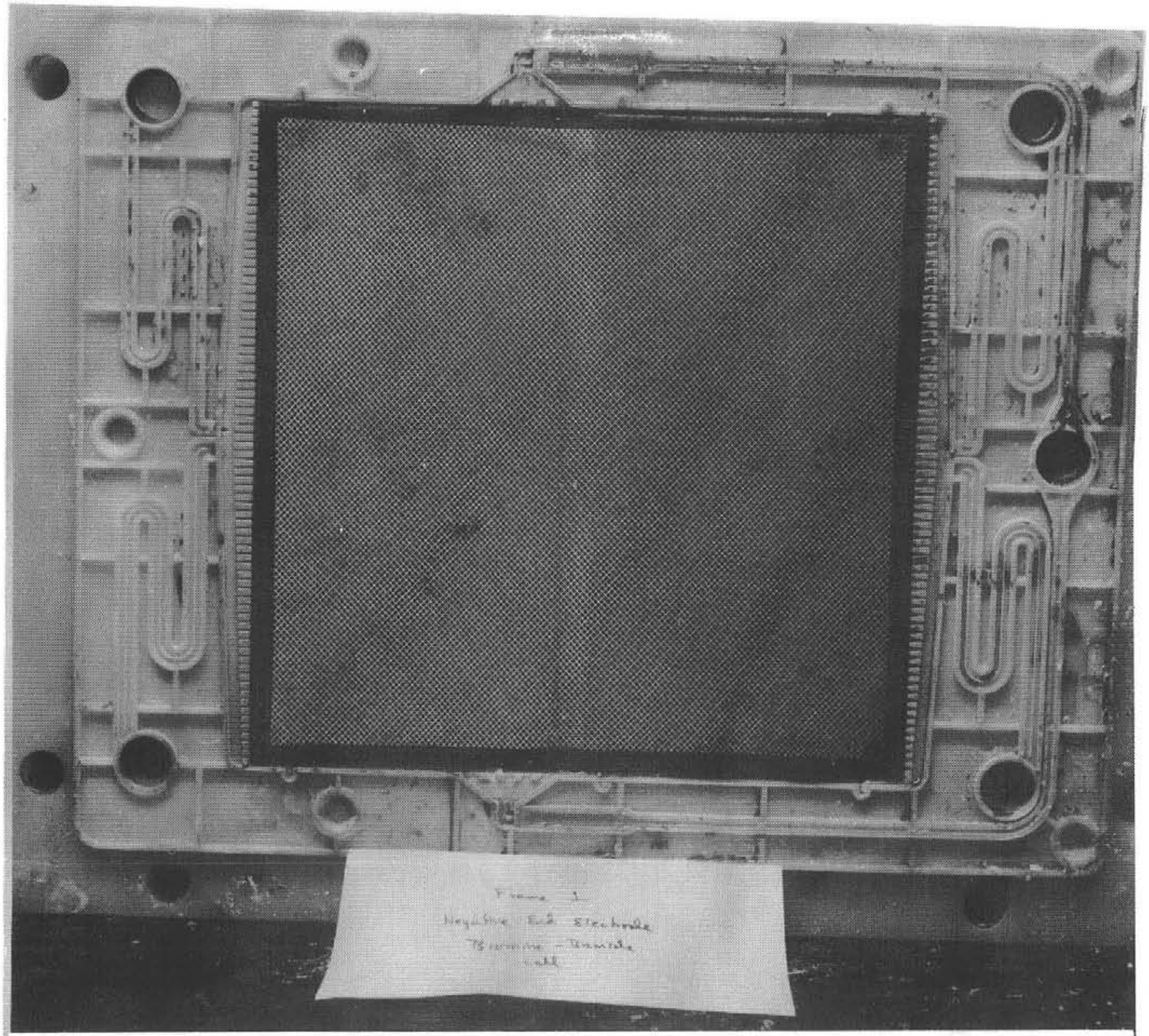

Frame 1

Negative End Electrode Bromine-Bromide Cell

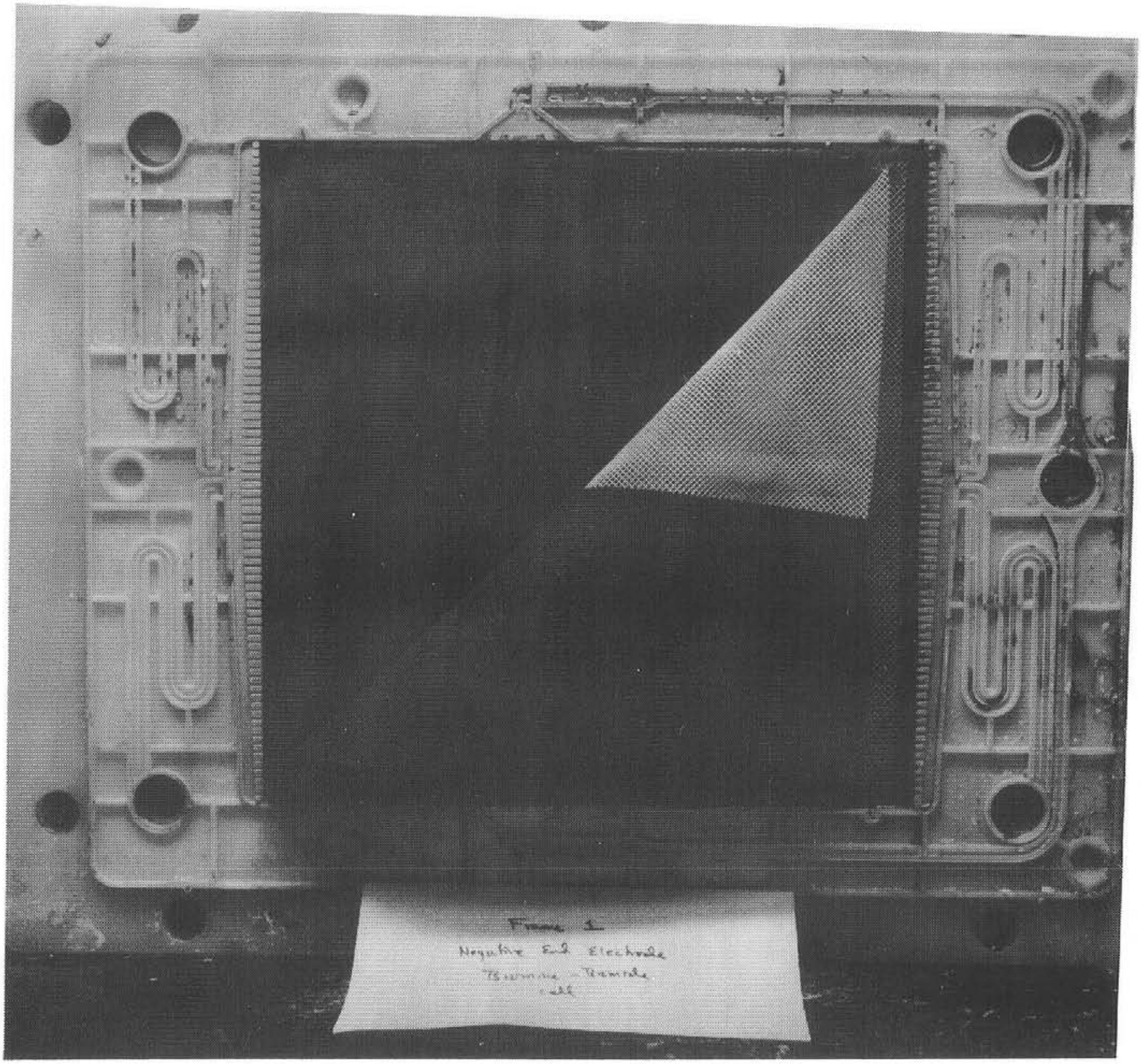

Frame 1
Negative End Electrode Bromine-Bromide Cell

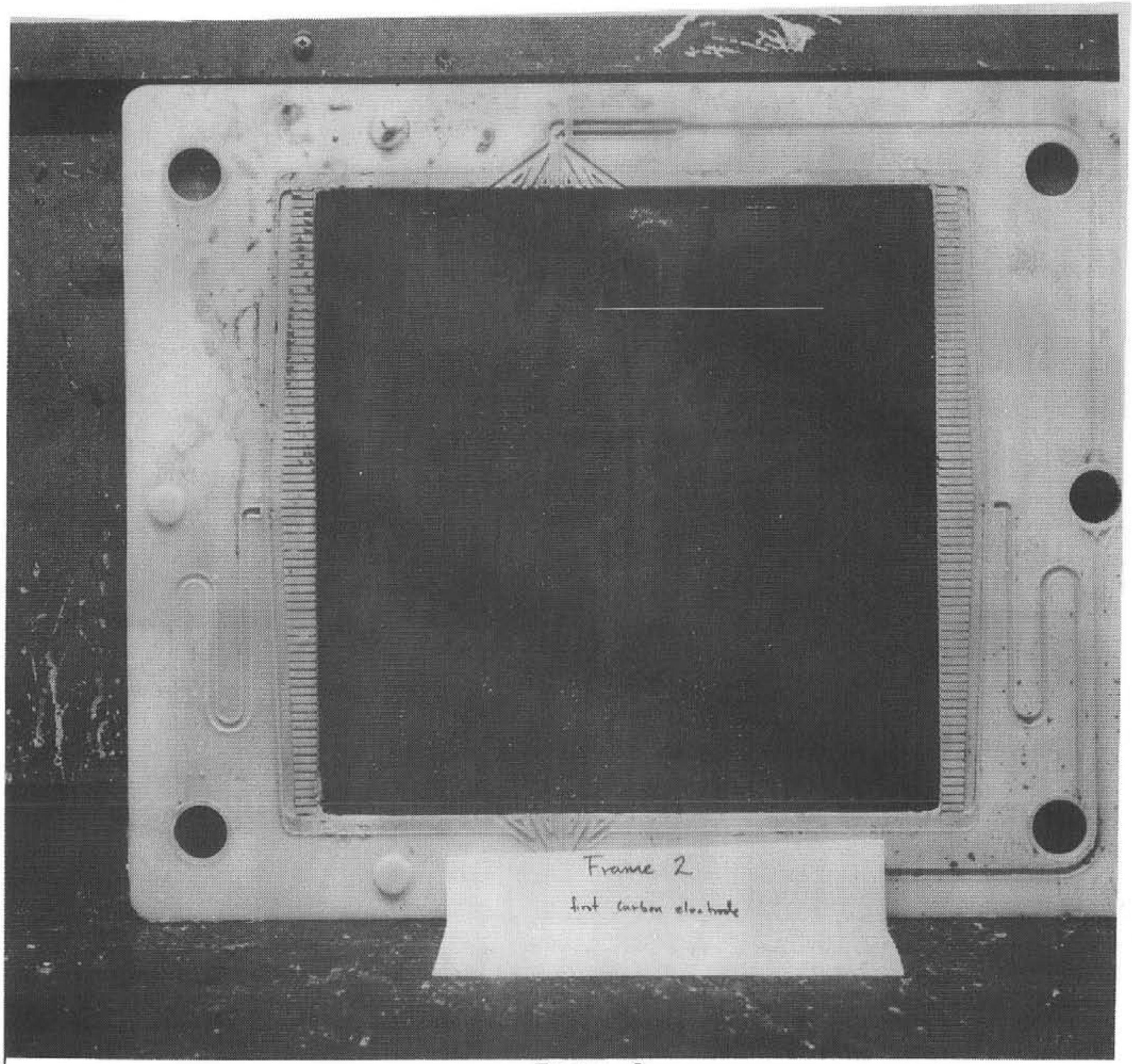

Frame 2
First Carbon Electrode

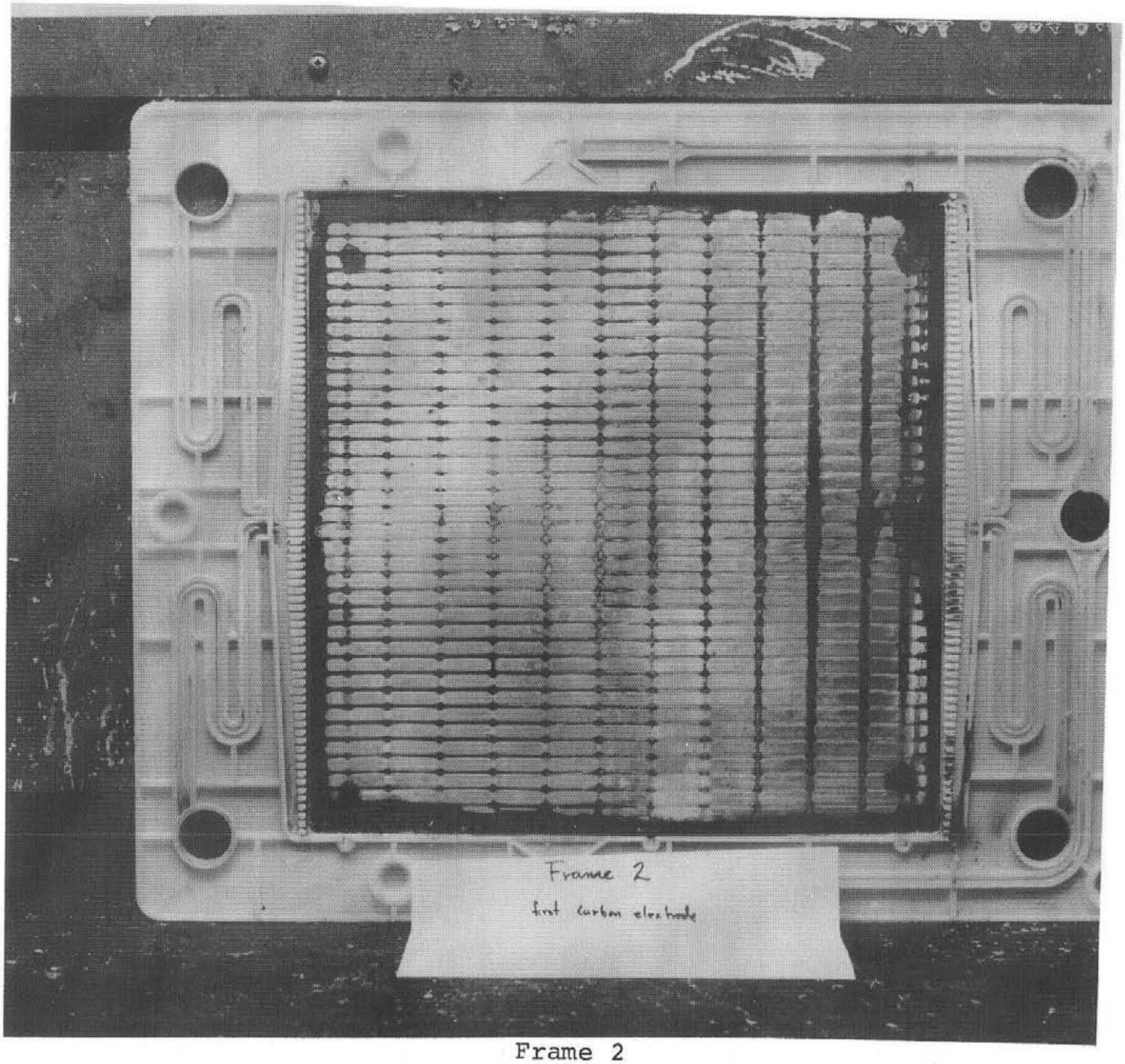

Frame 2
First Carbon Electrode

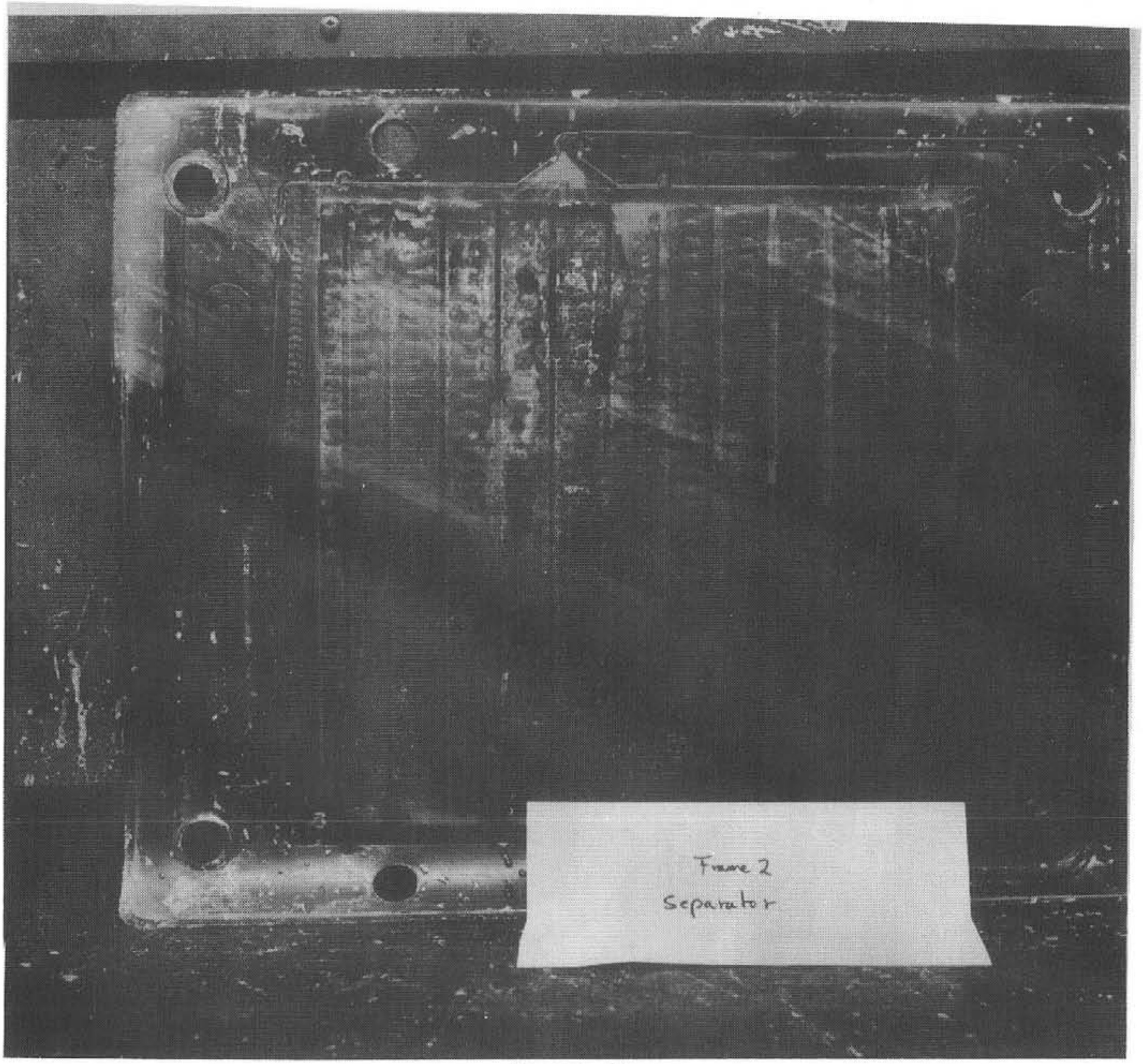

Frame 2
Separator

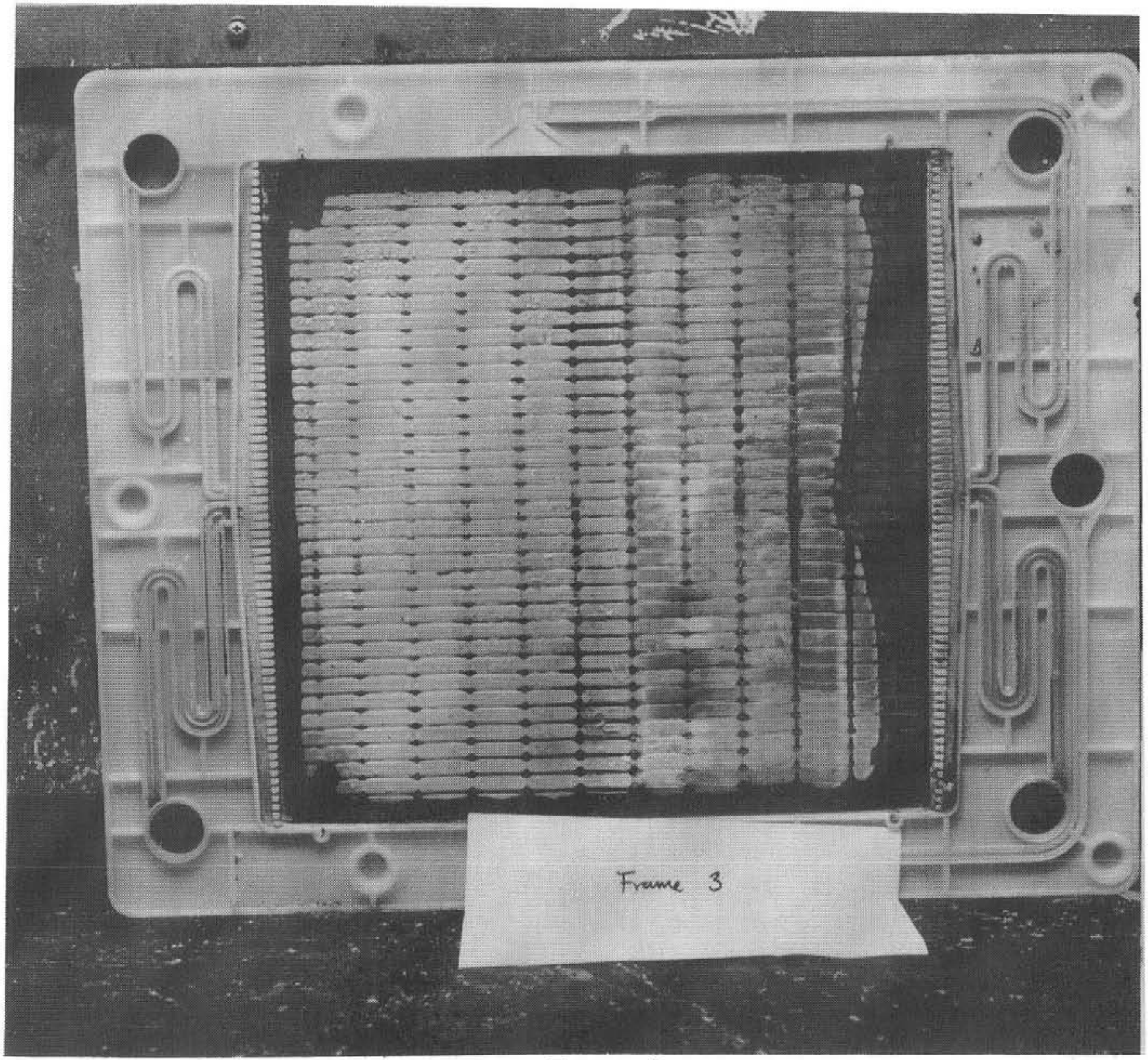

Frame 3

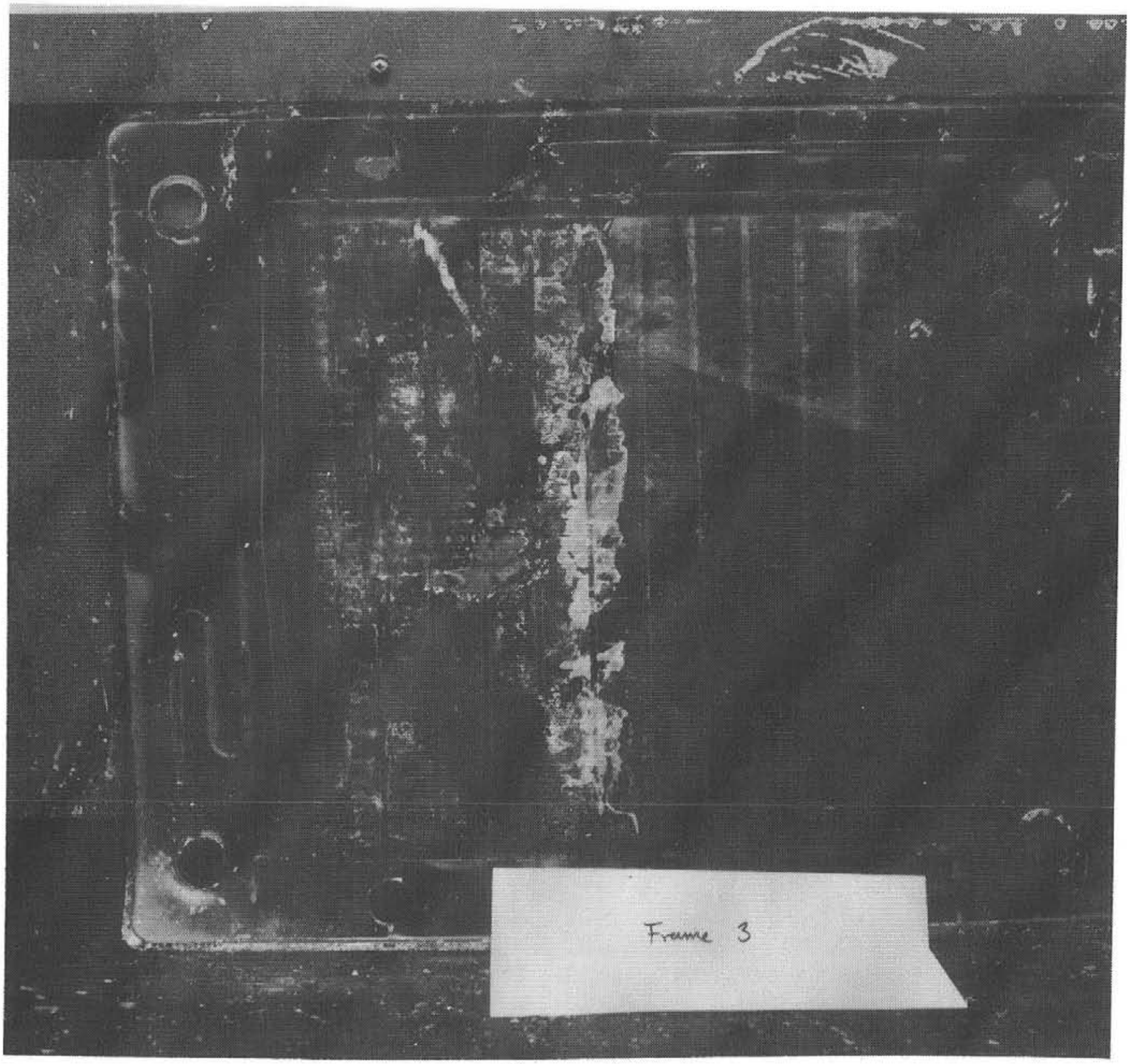

Frame 3

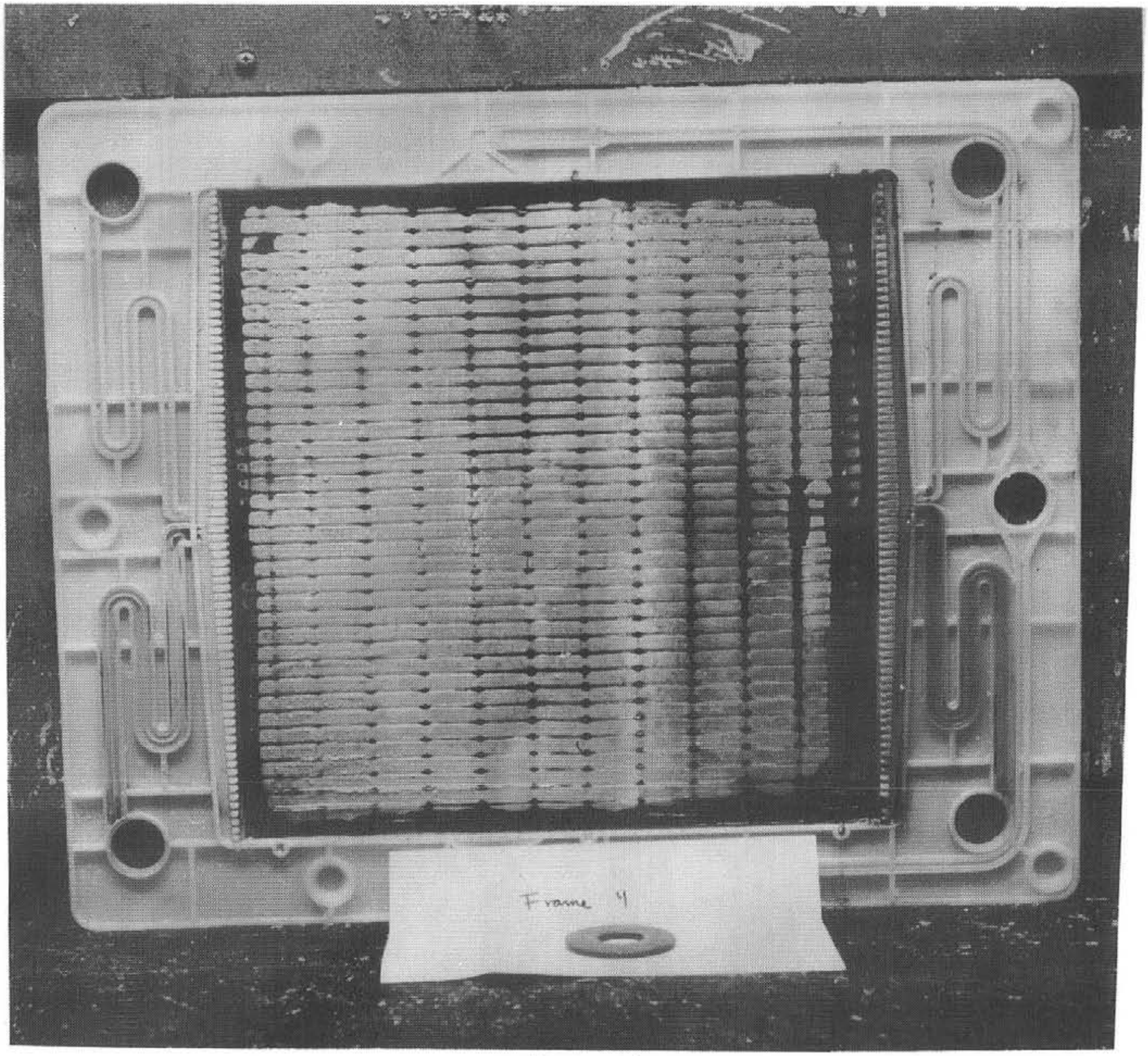

Frame 4

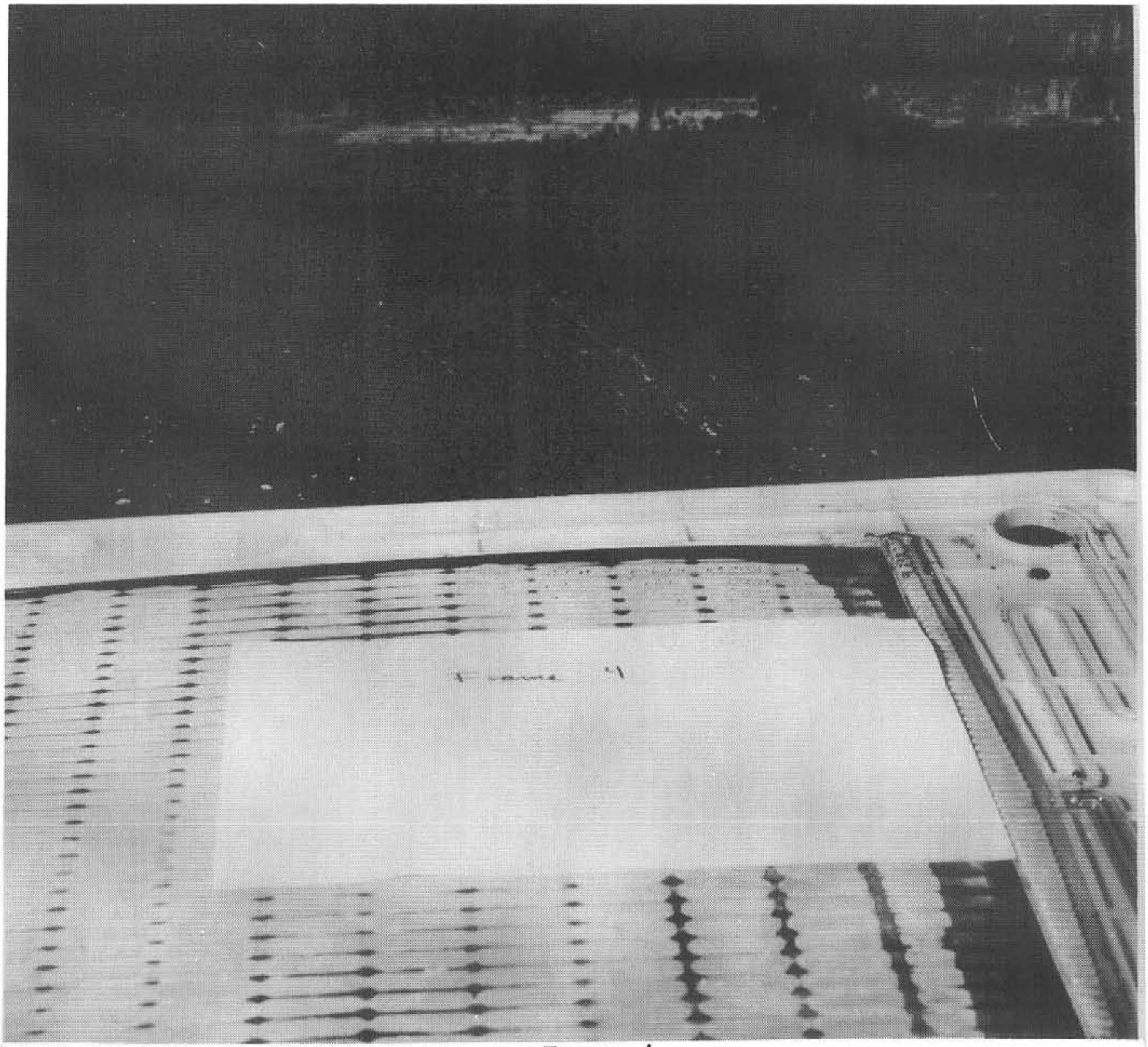

Frame 4

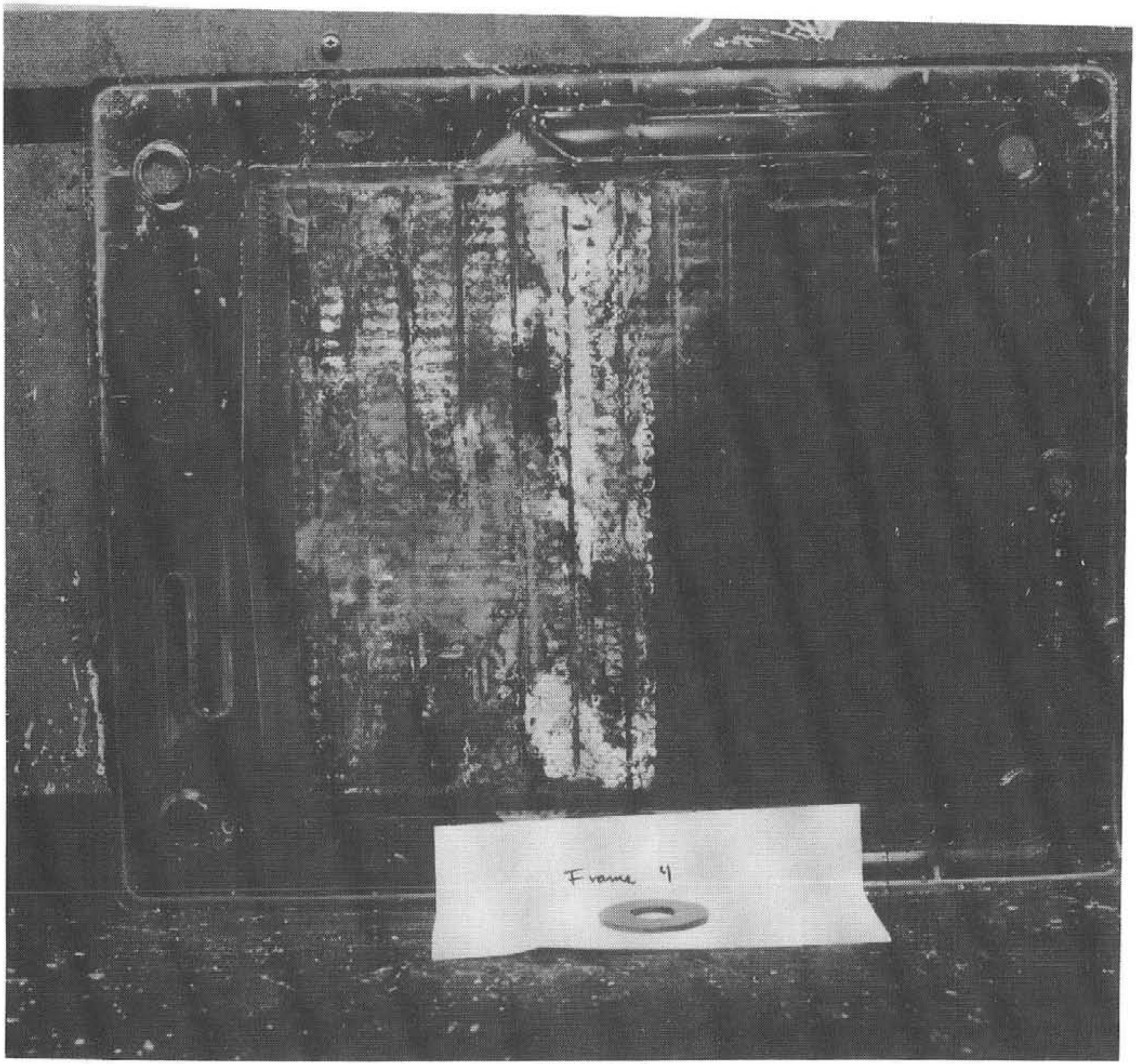

Frame 4

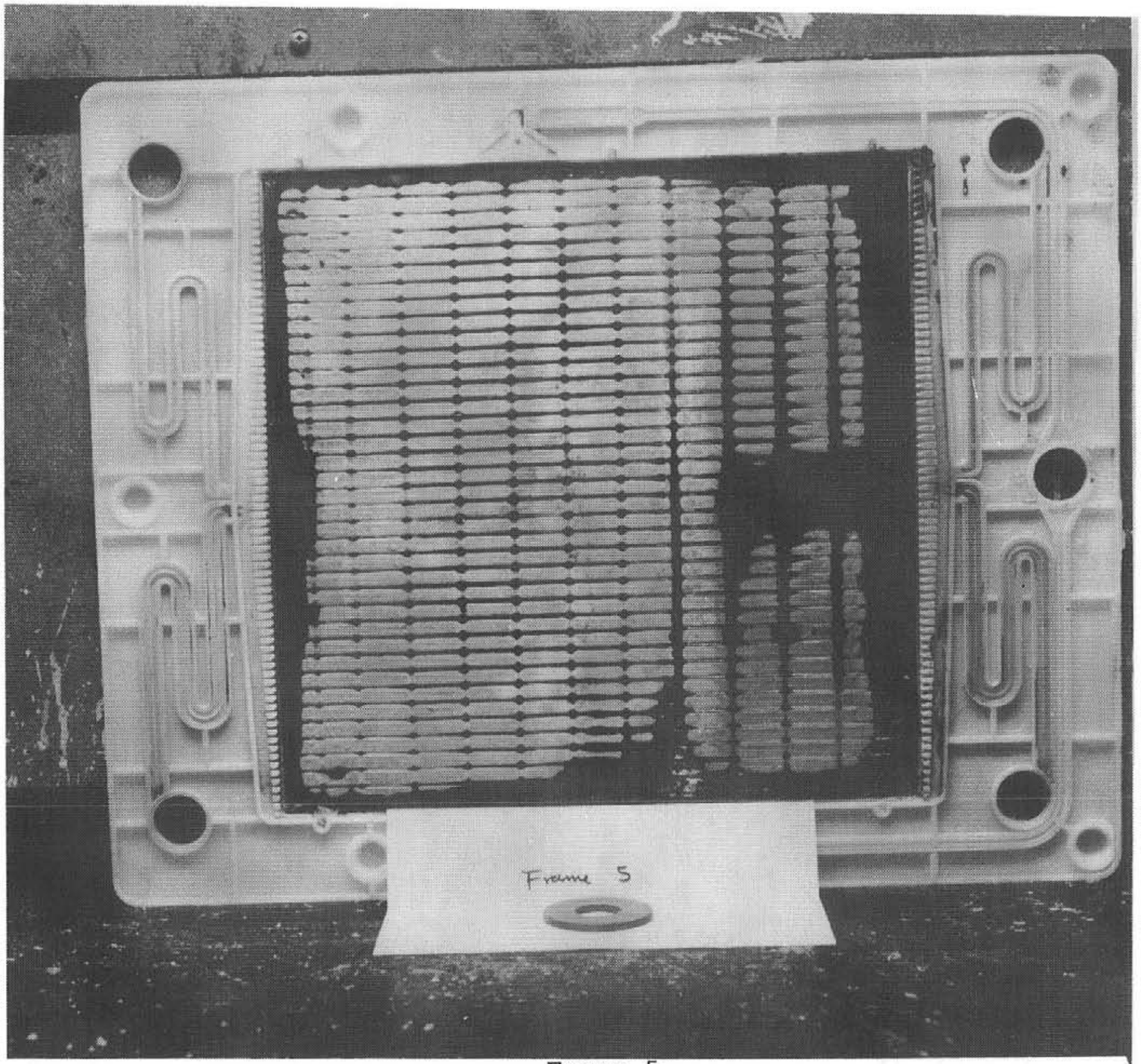

Frame 5

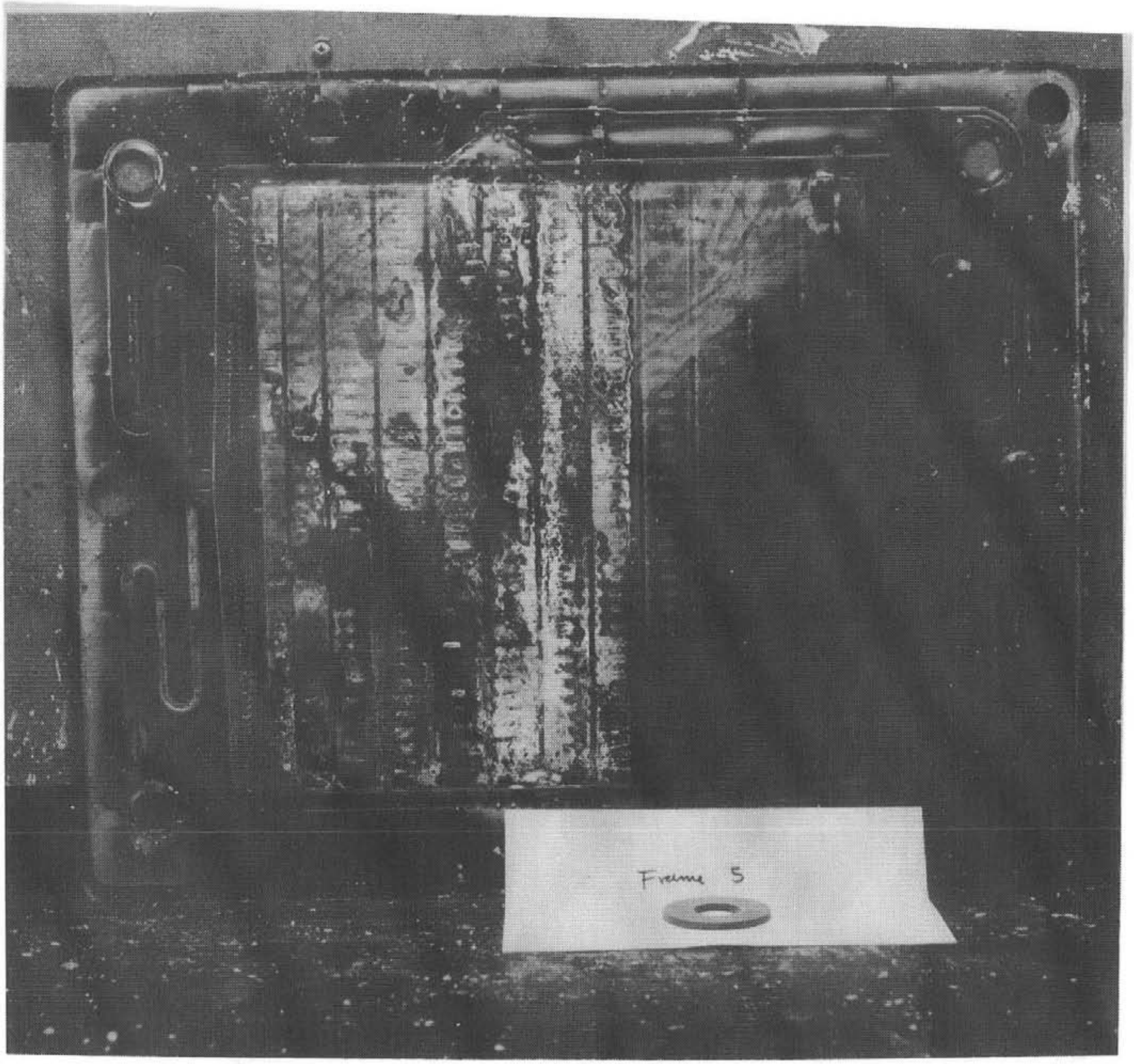

Frame 5

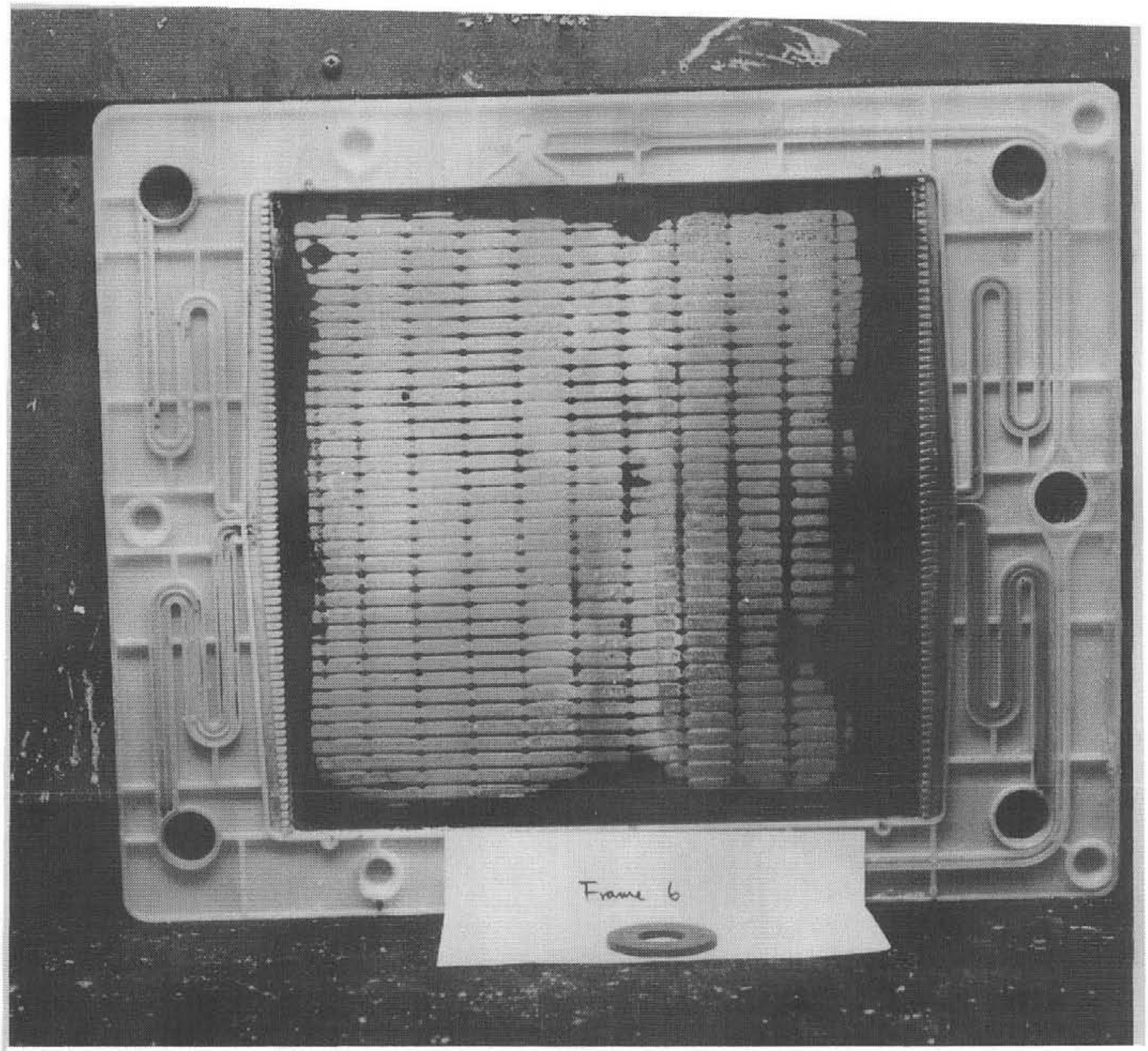

Frame 6

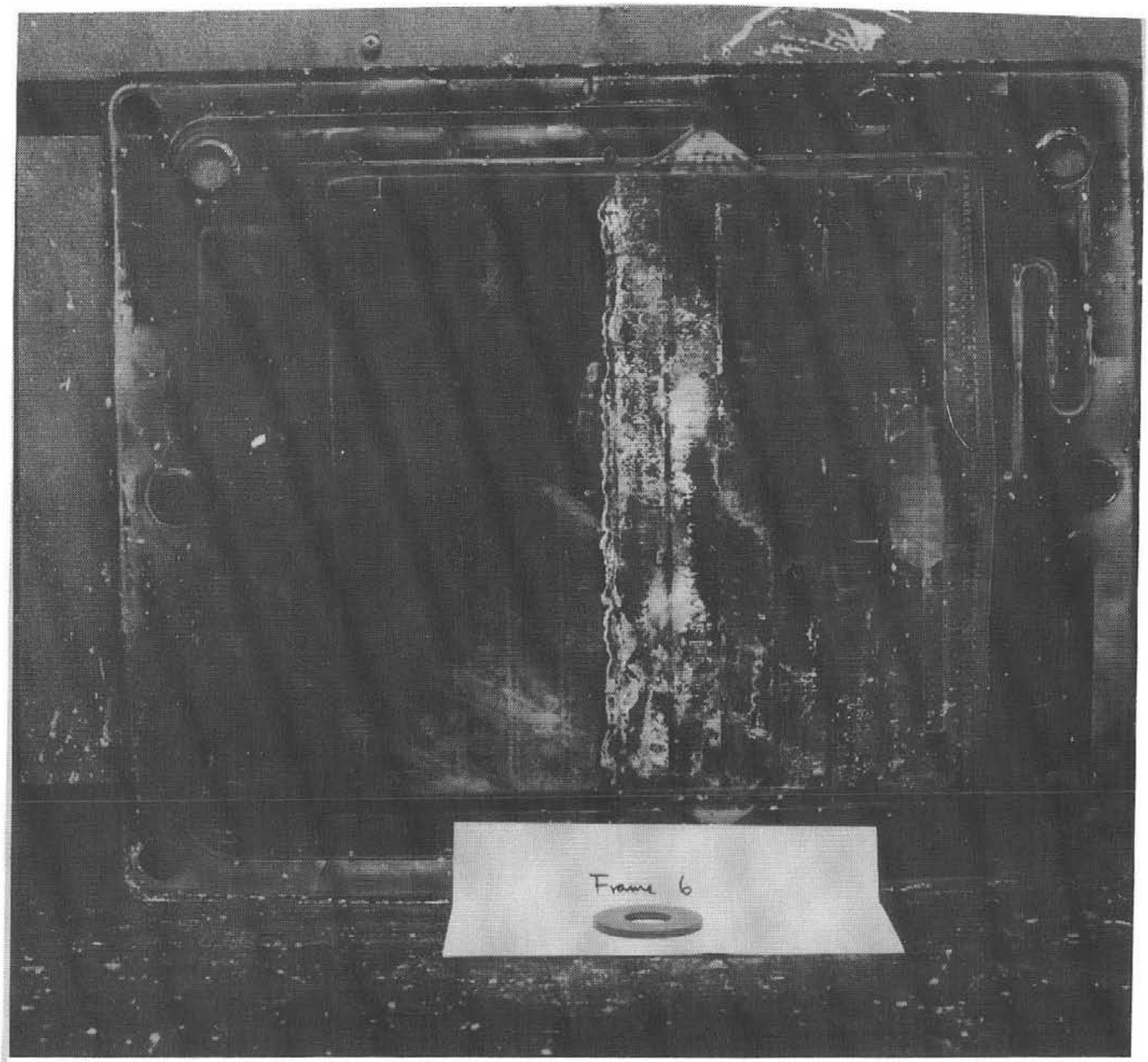

Frame 6

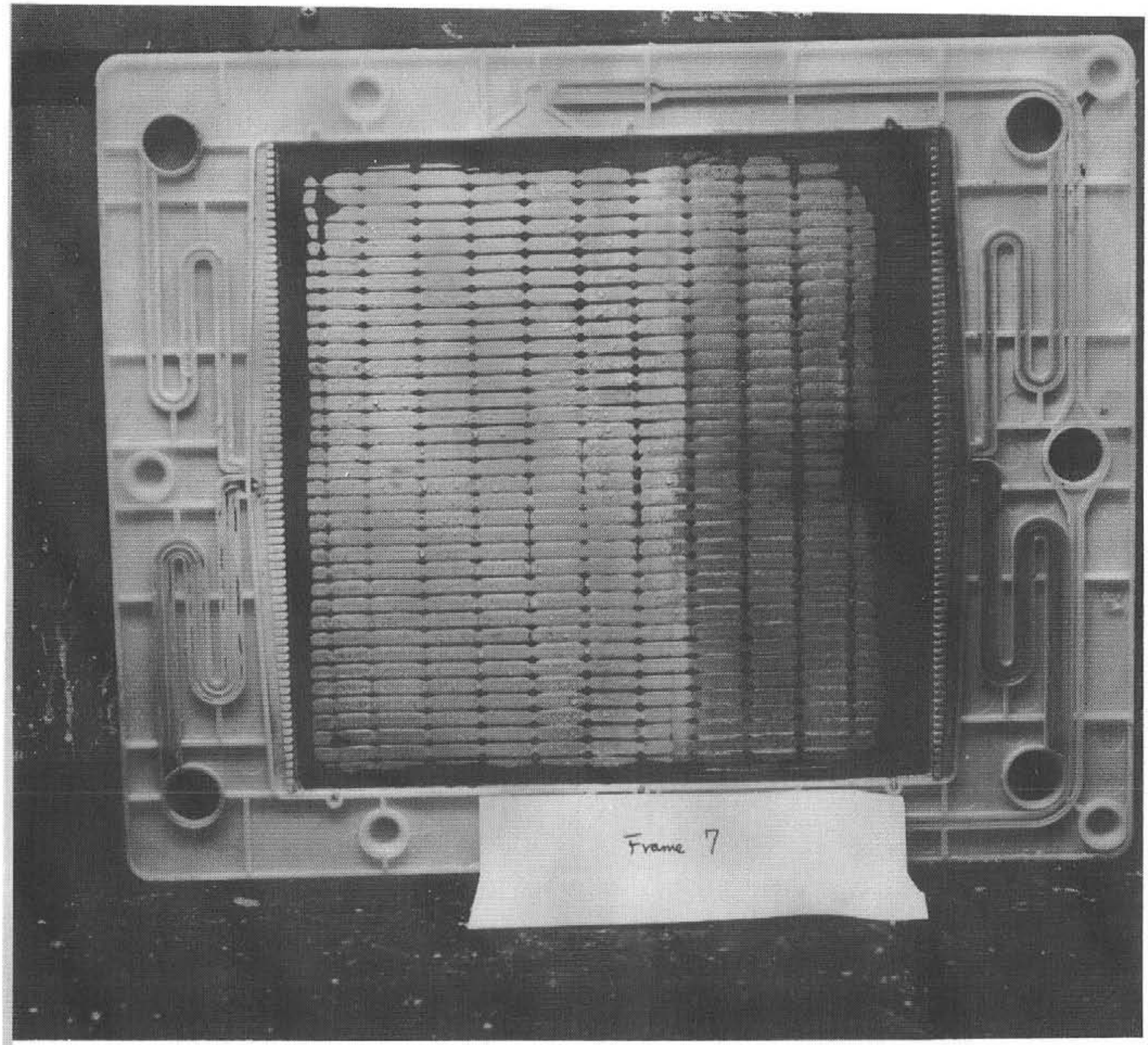

Frame 7

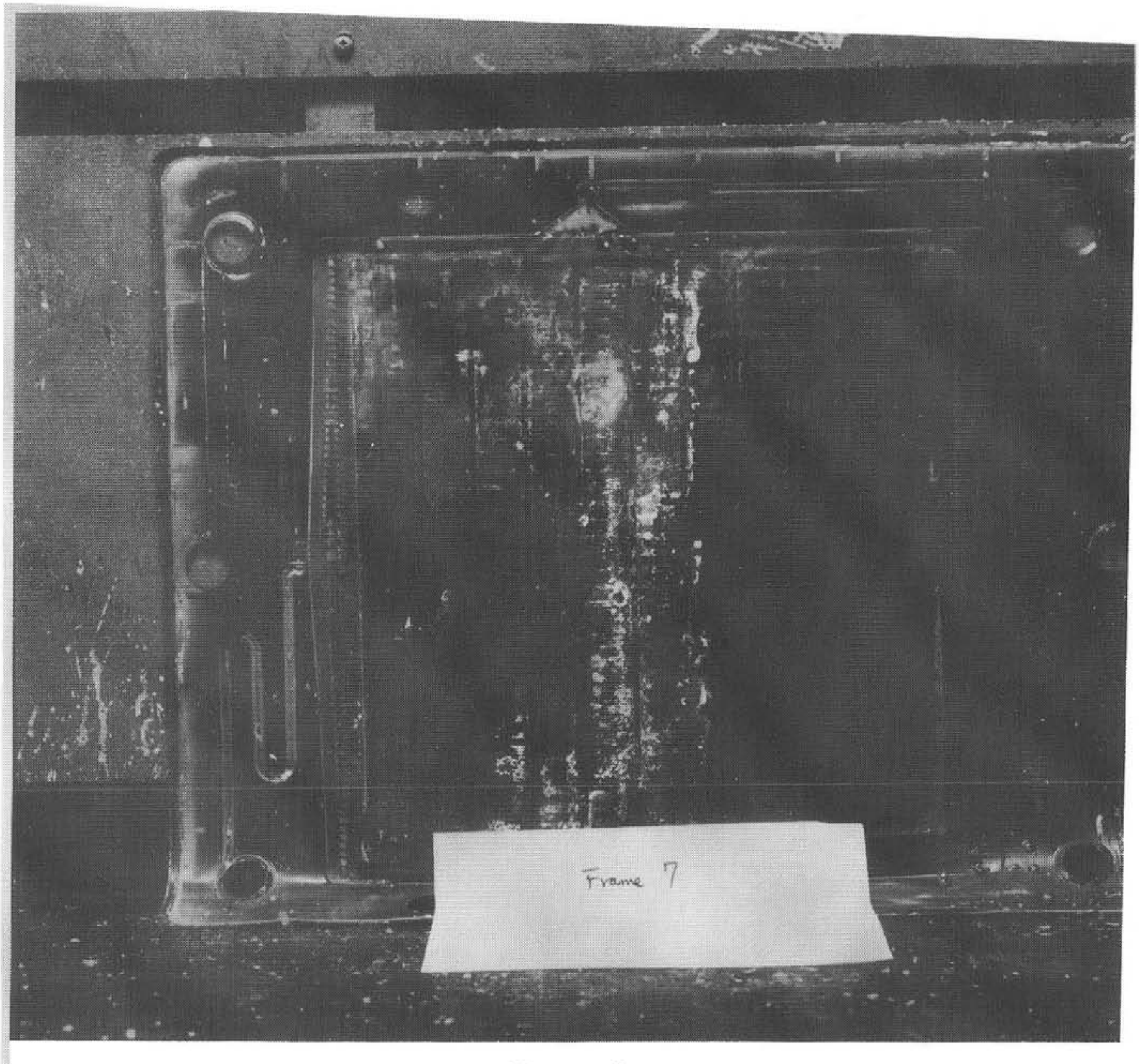

Frame 7

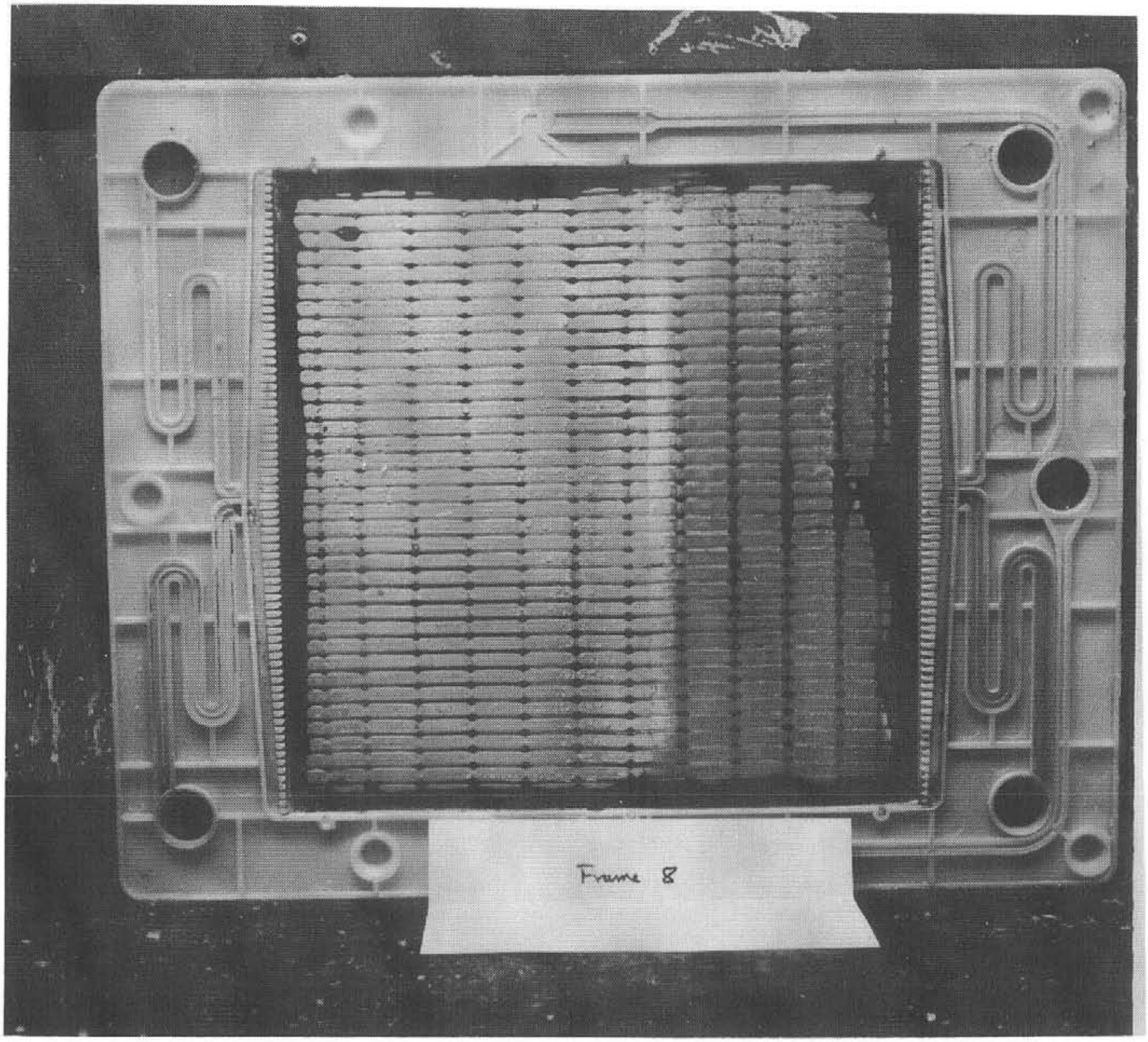

Frame 8

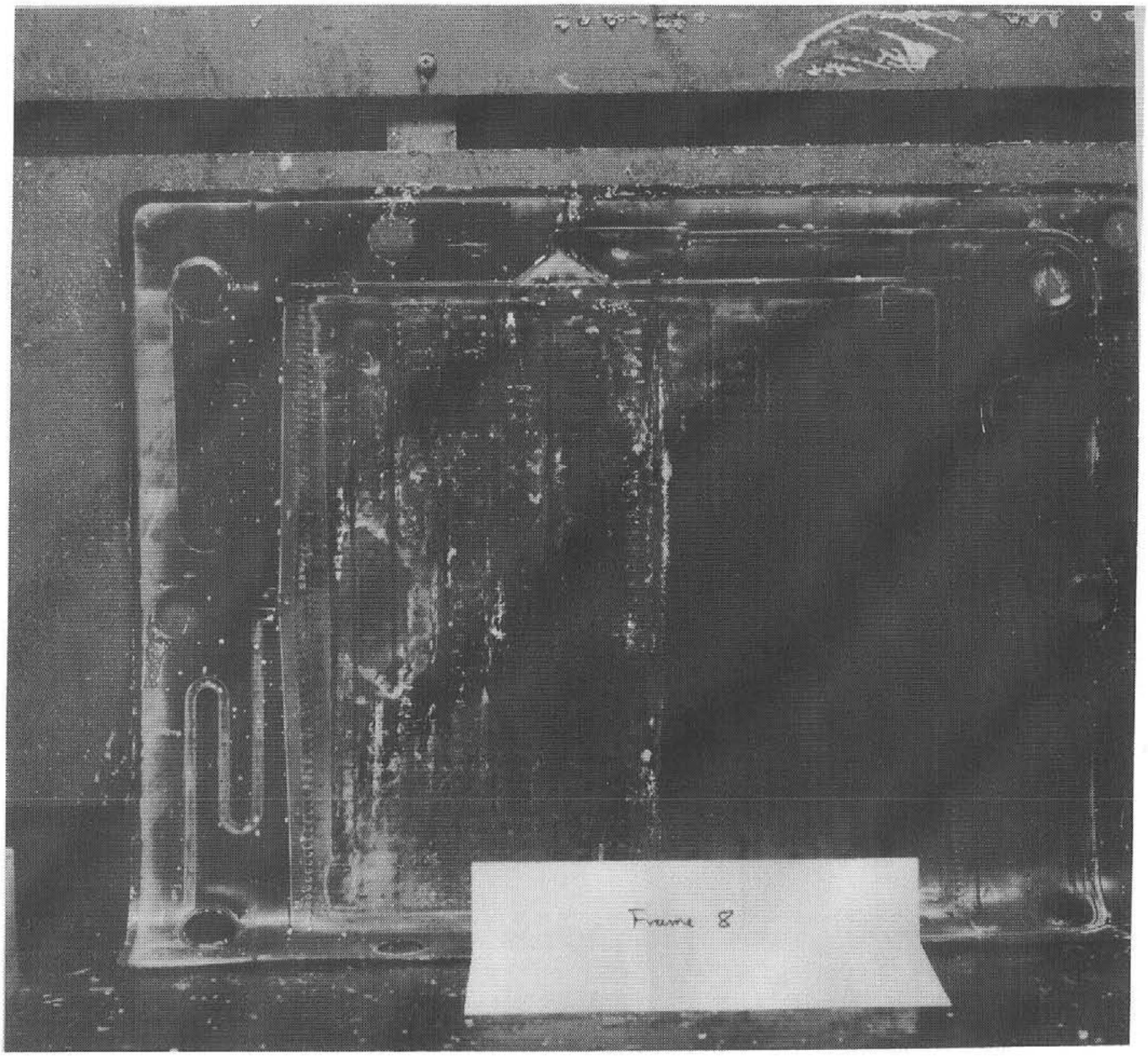

Frame 8

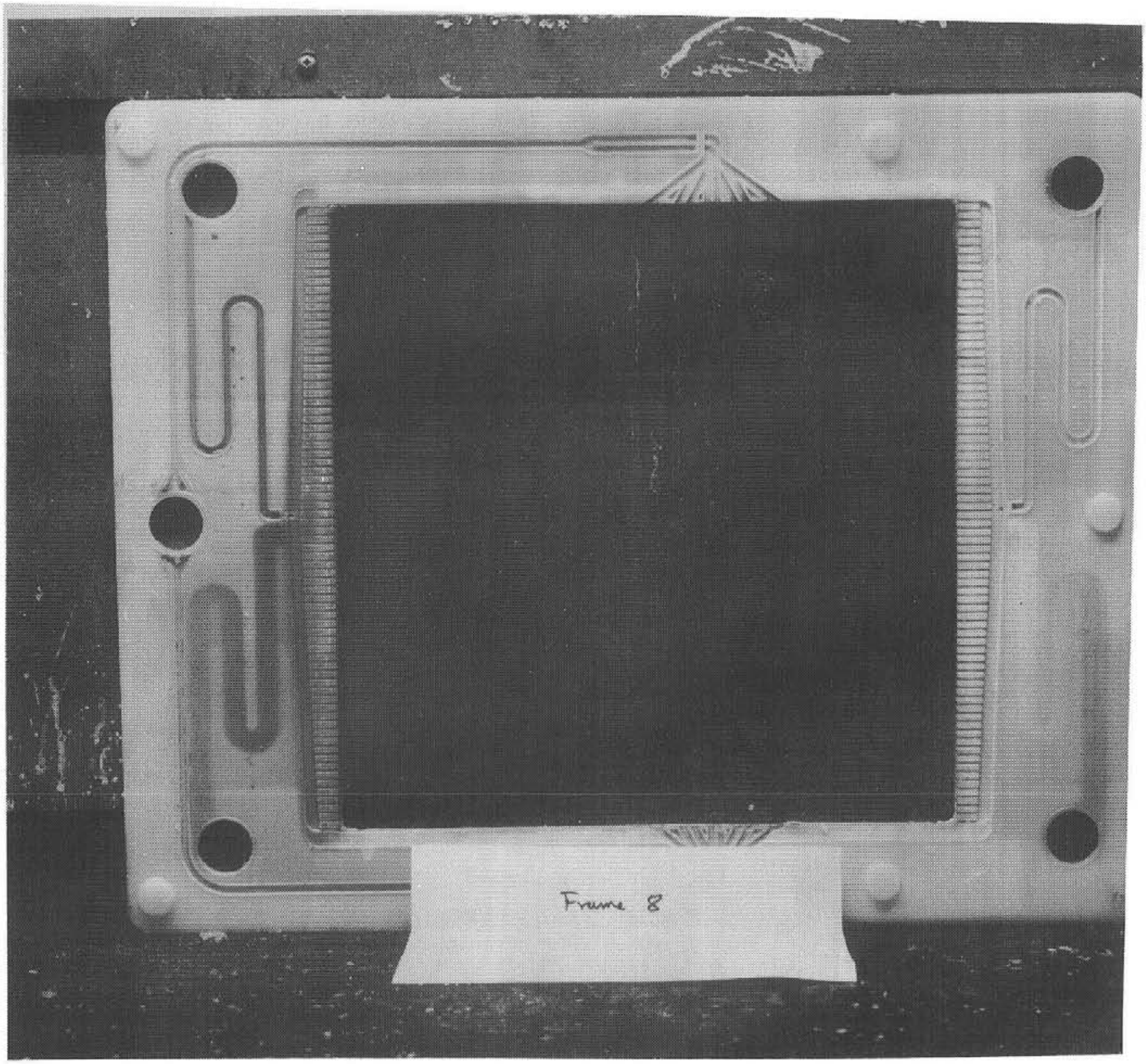

Frame 8

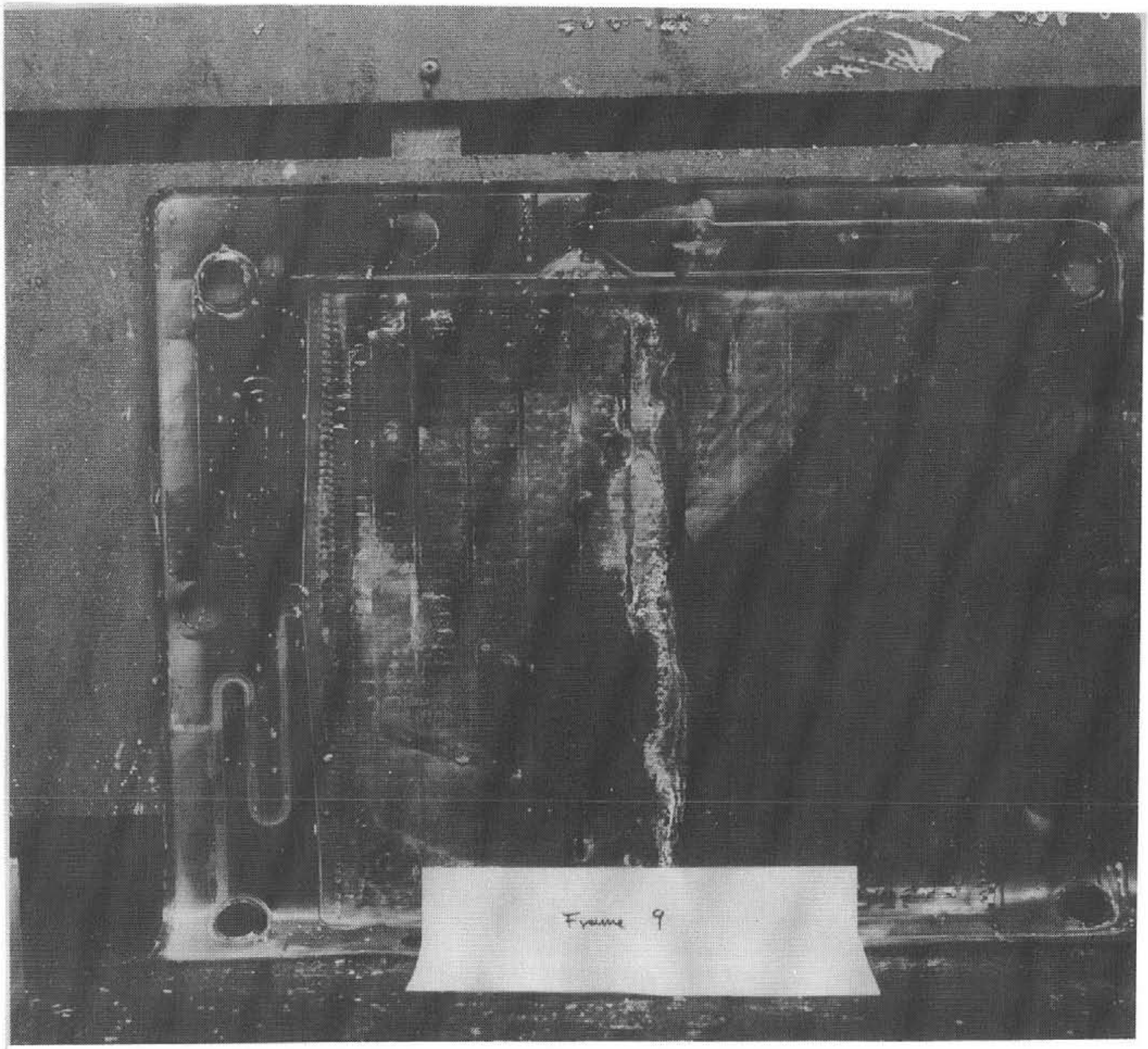

Frame 9

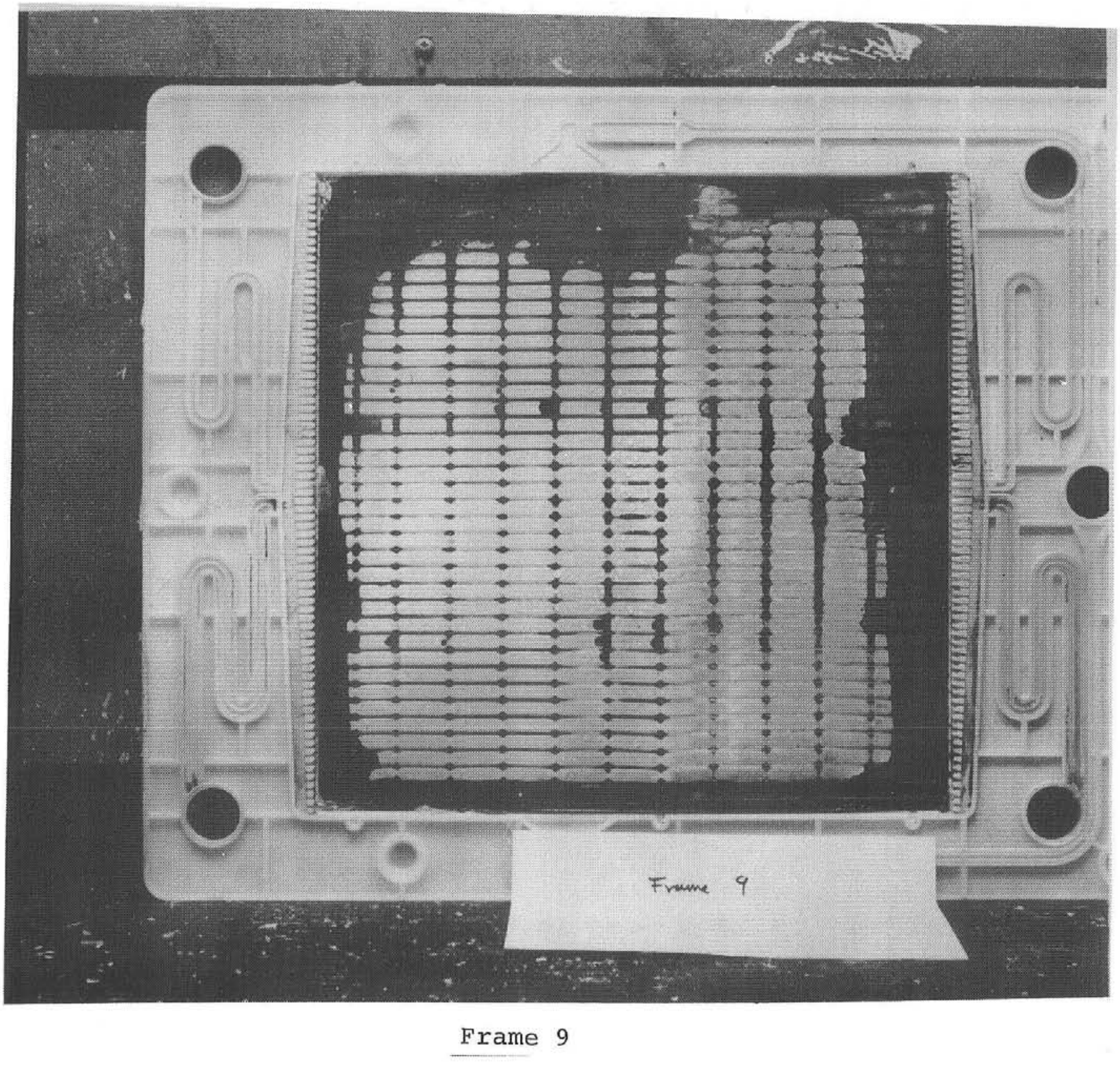

Frame 9

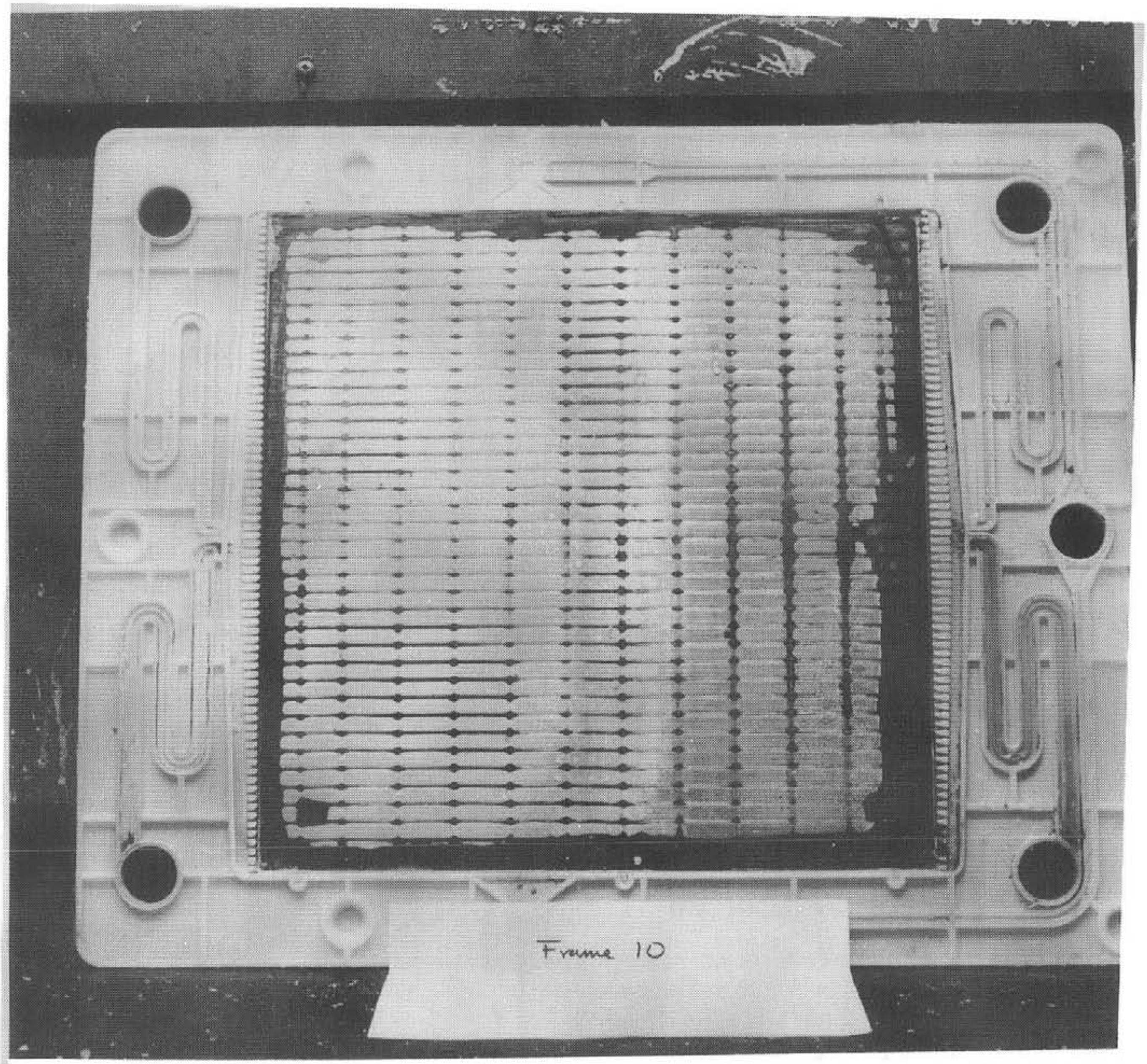

Frame 10

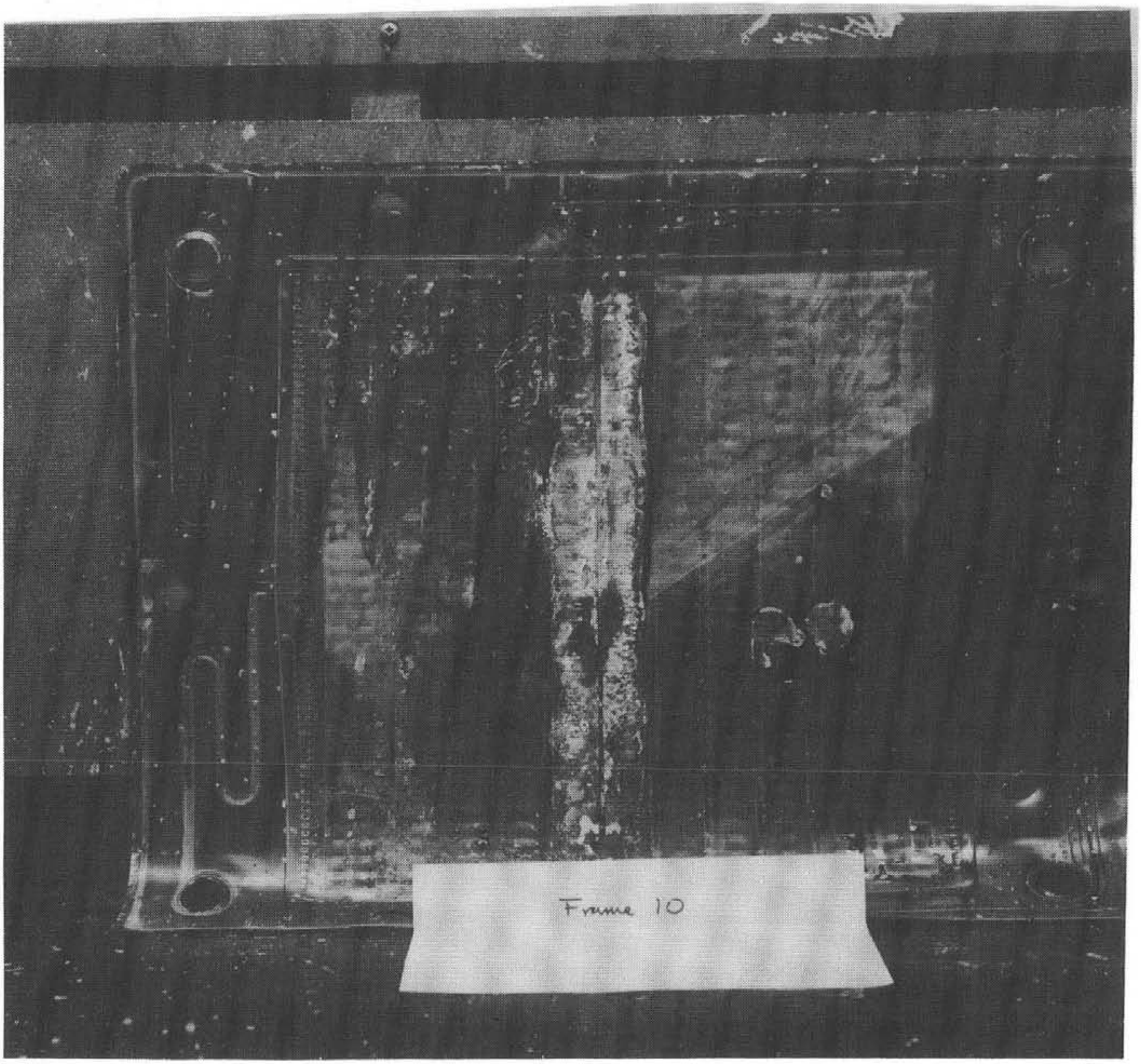

Frame 10

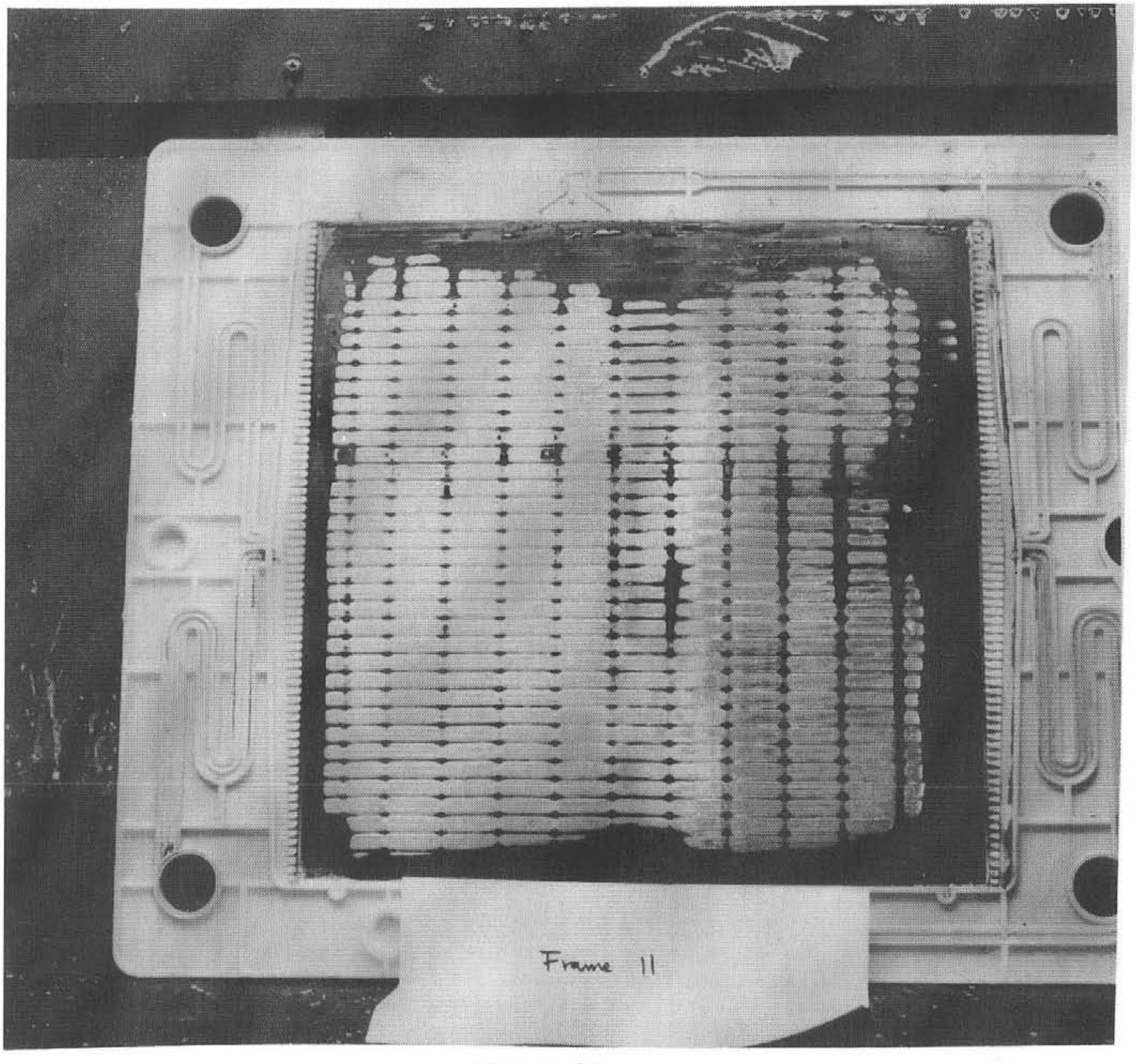

Frame 11

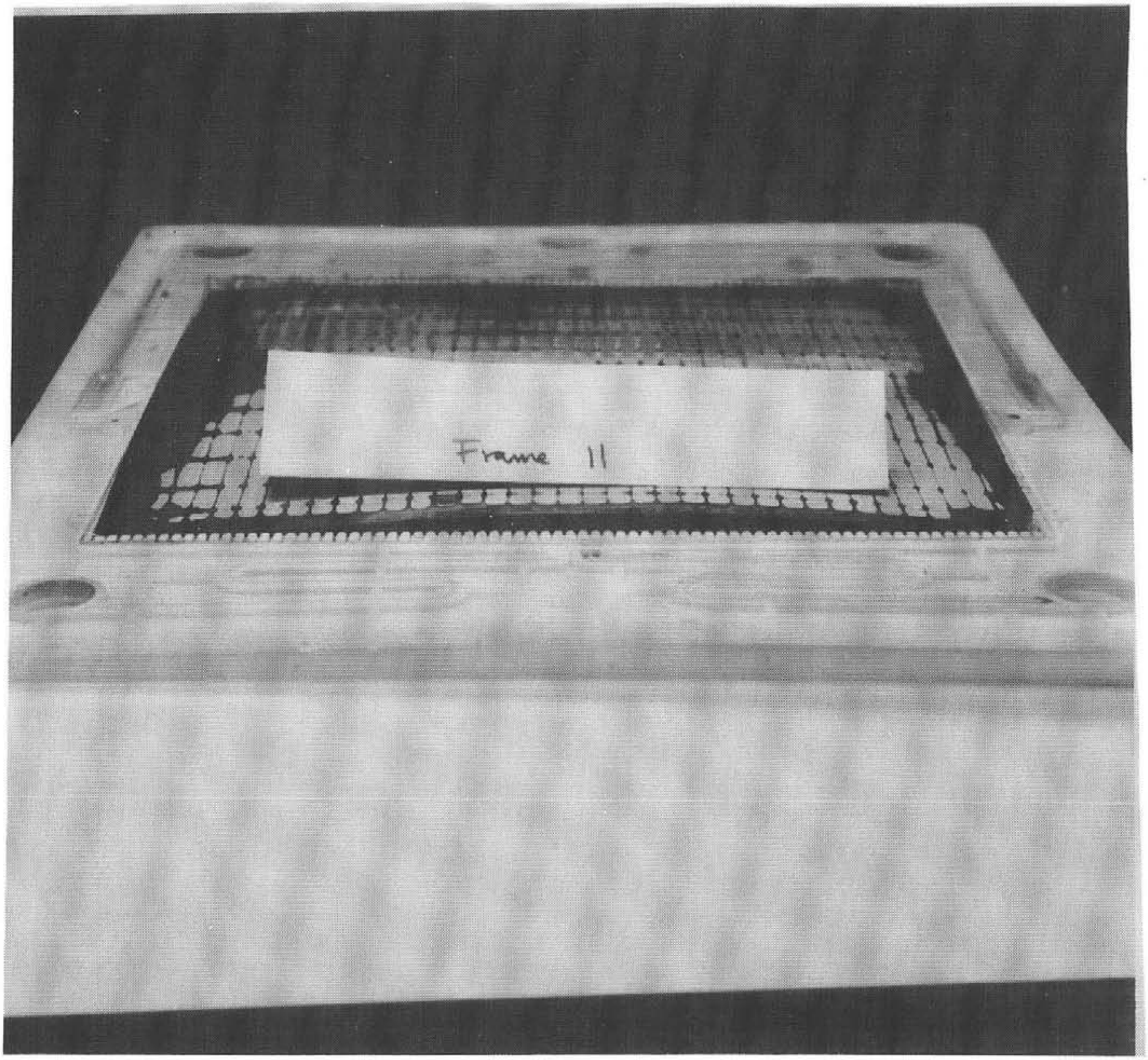

Frame 11

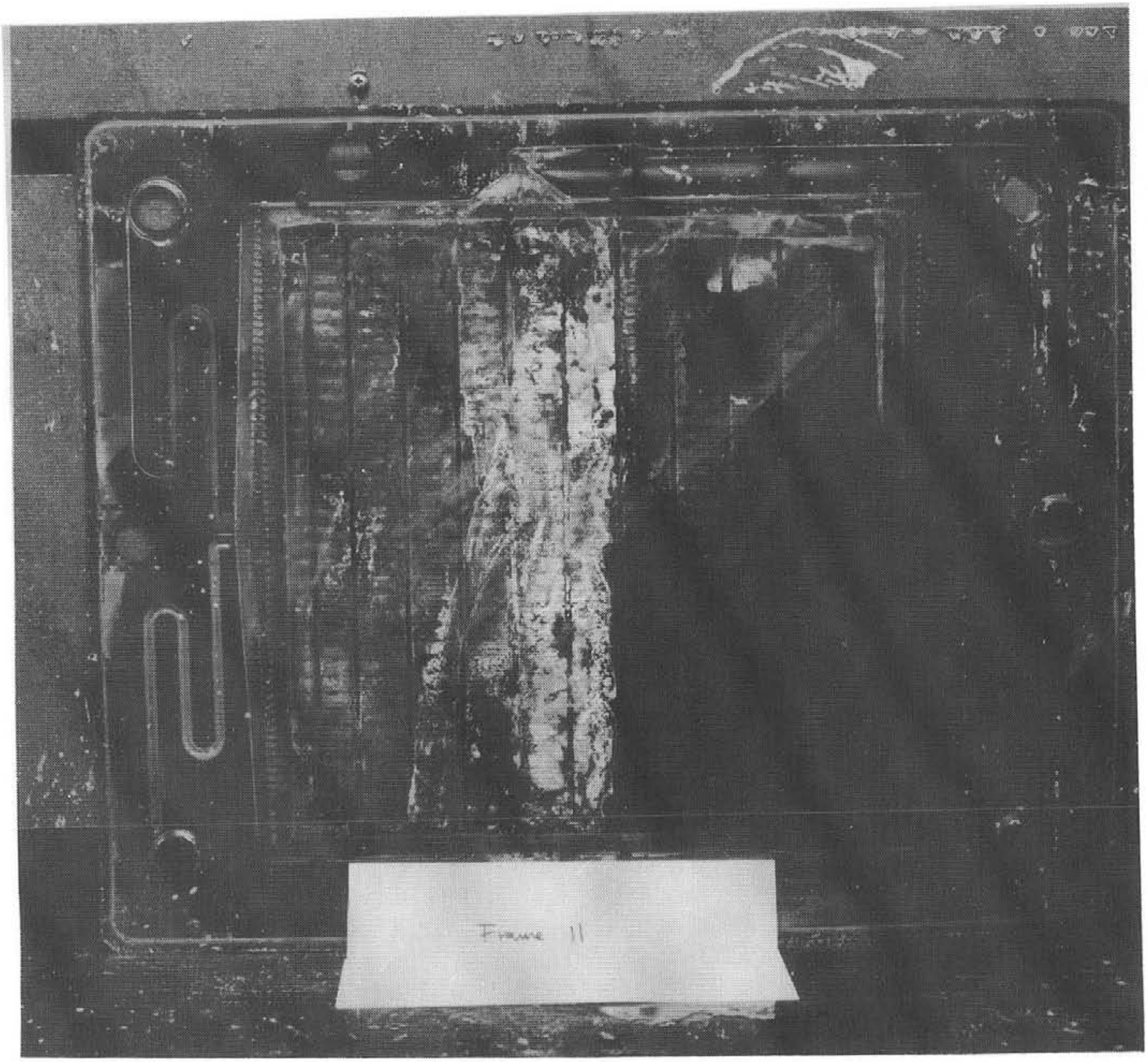

Frame 11

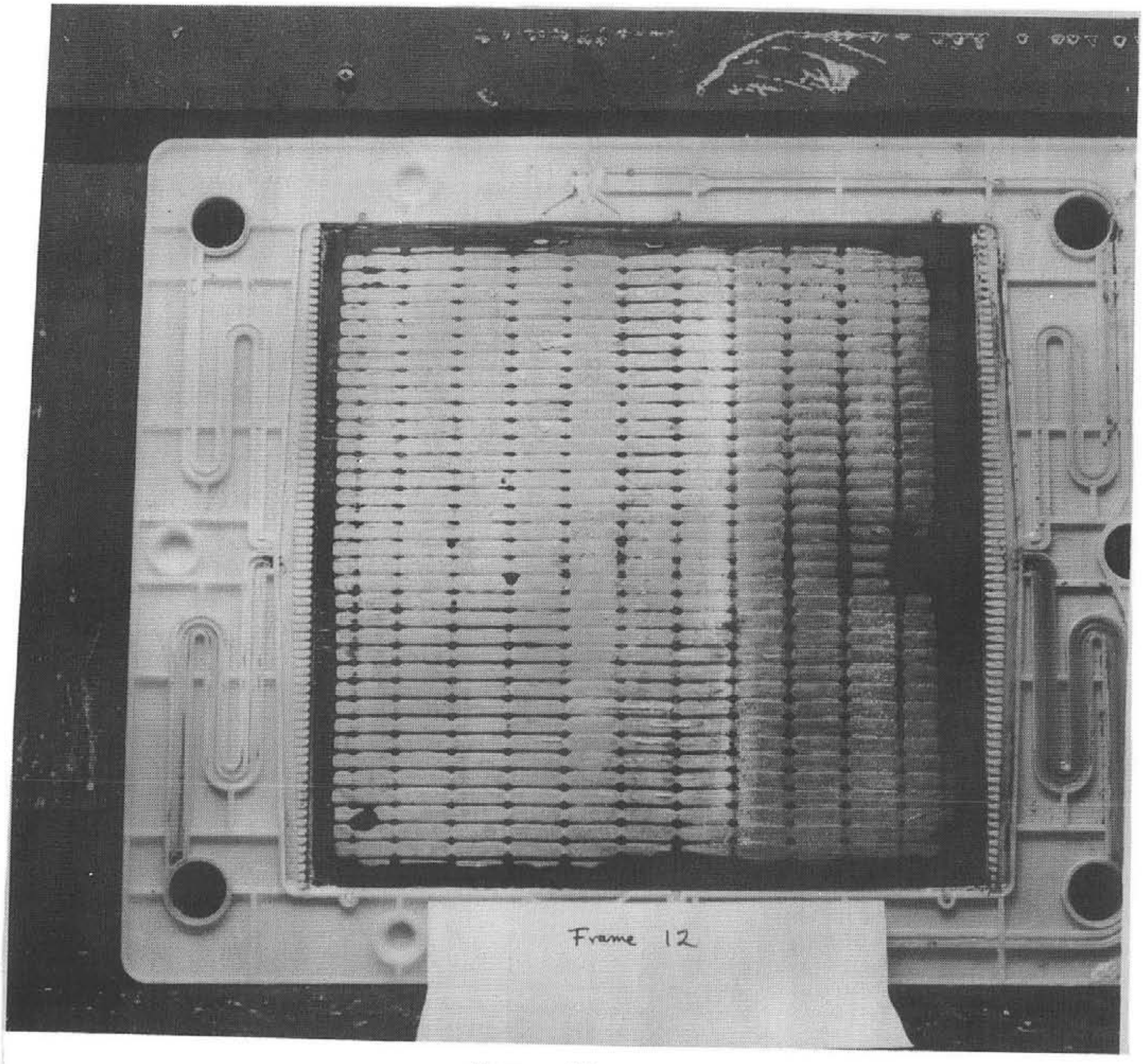

Frame 12

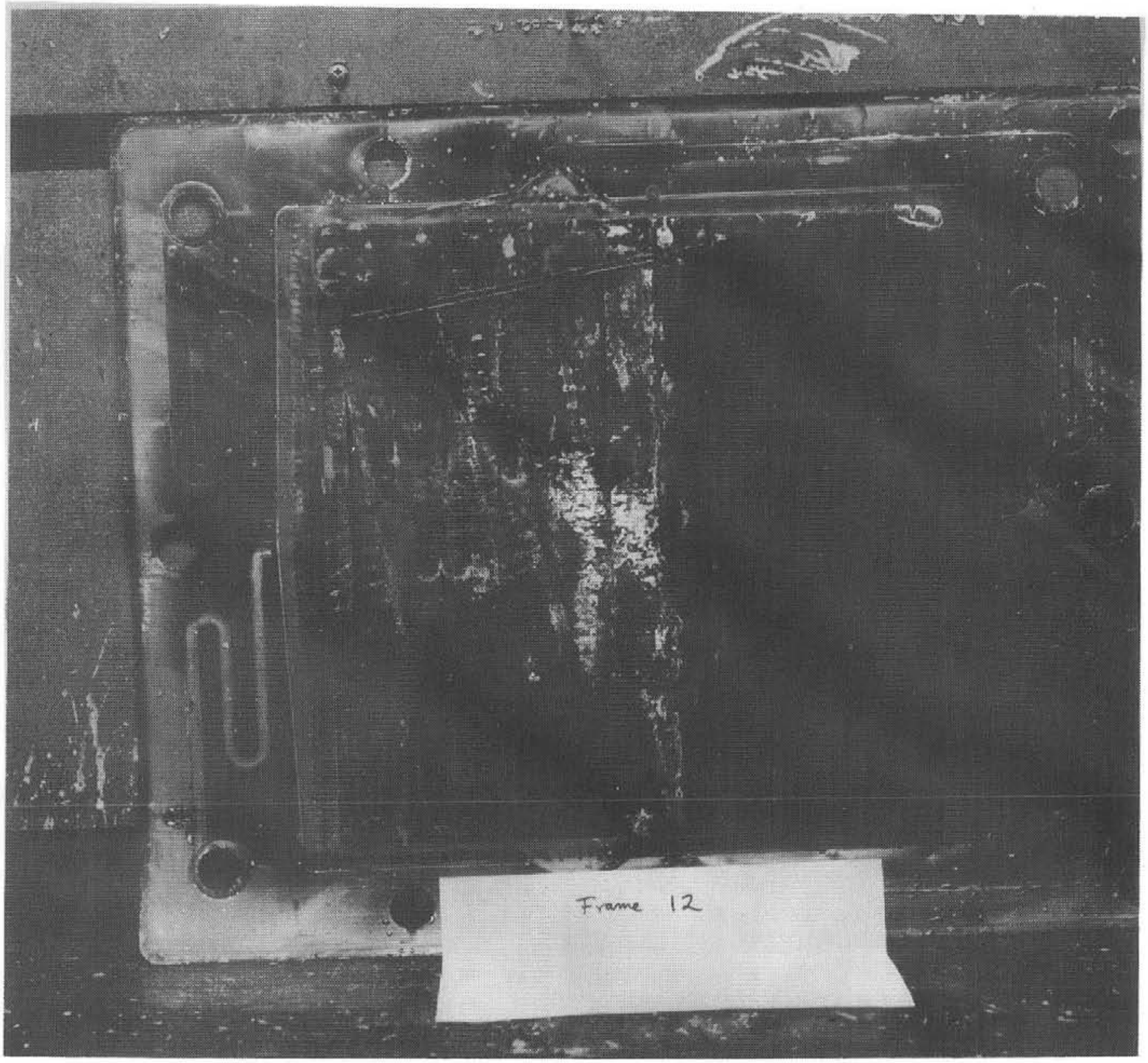

Frame 12

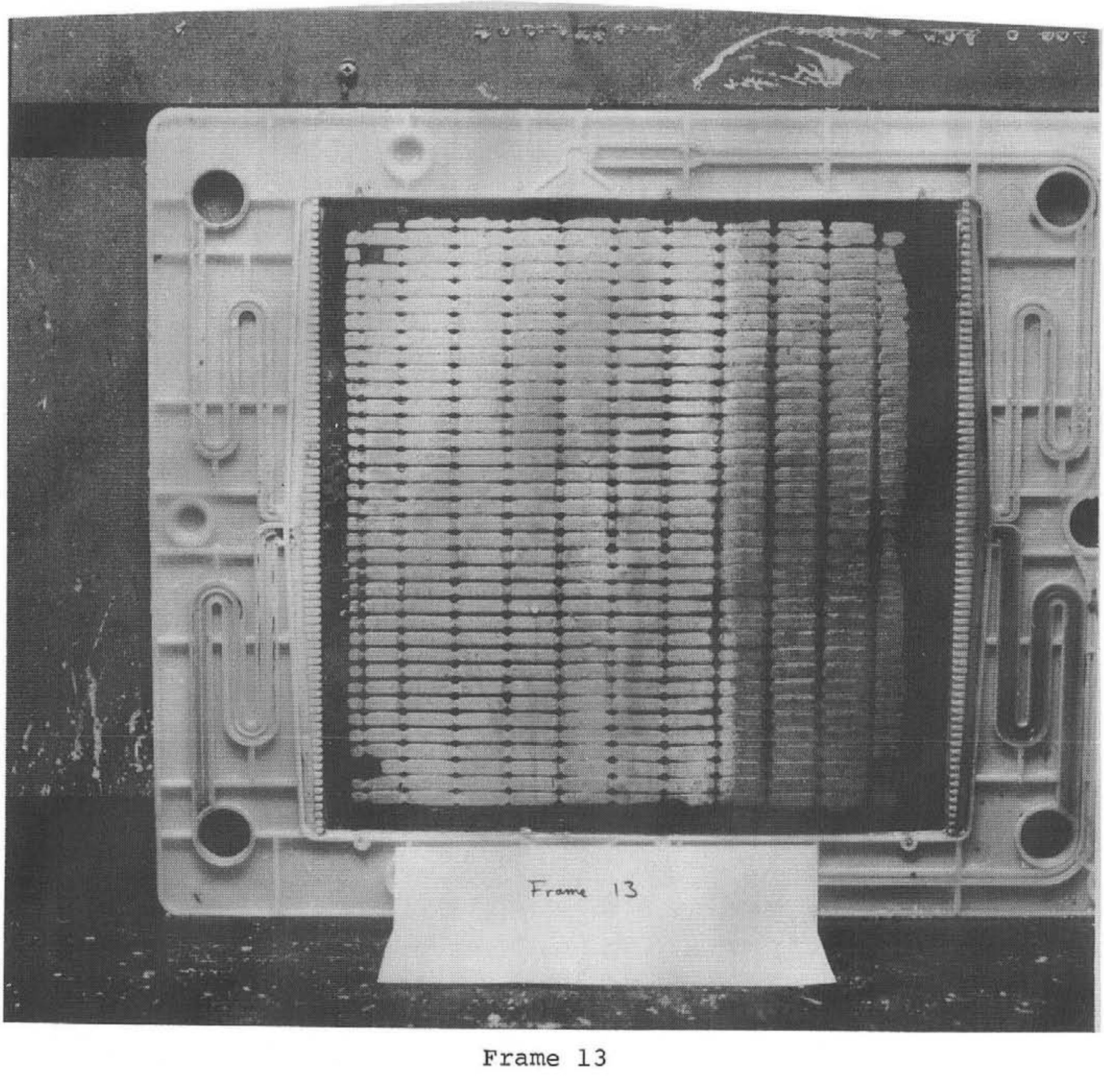

Frame 13

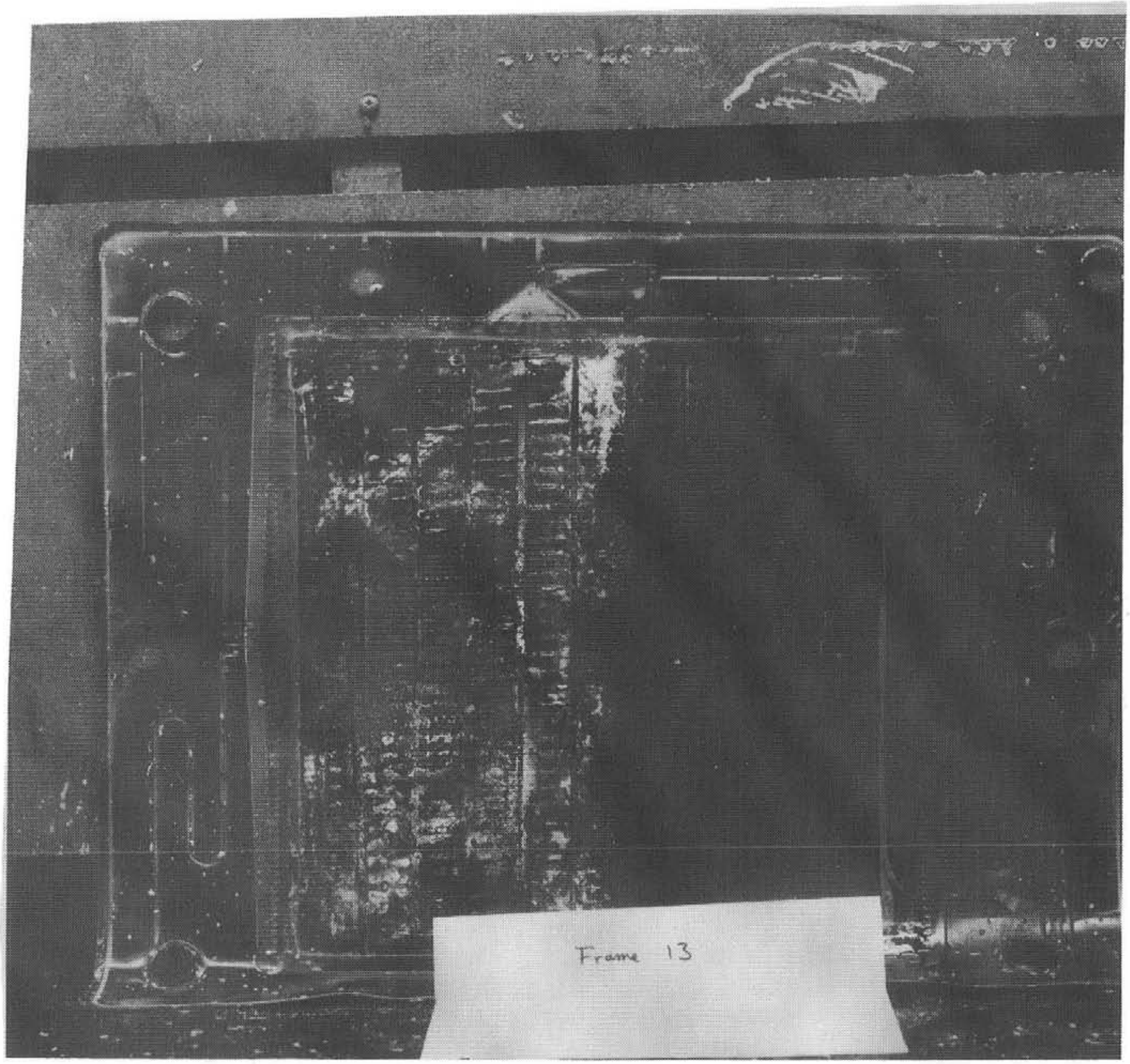

Frame 13

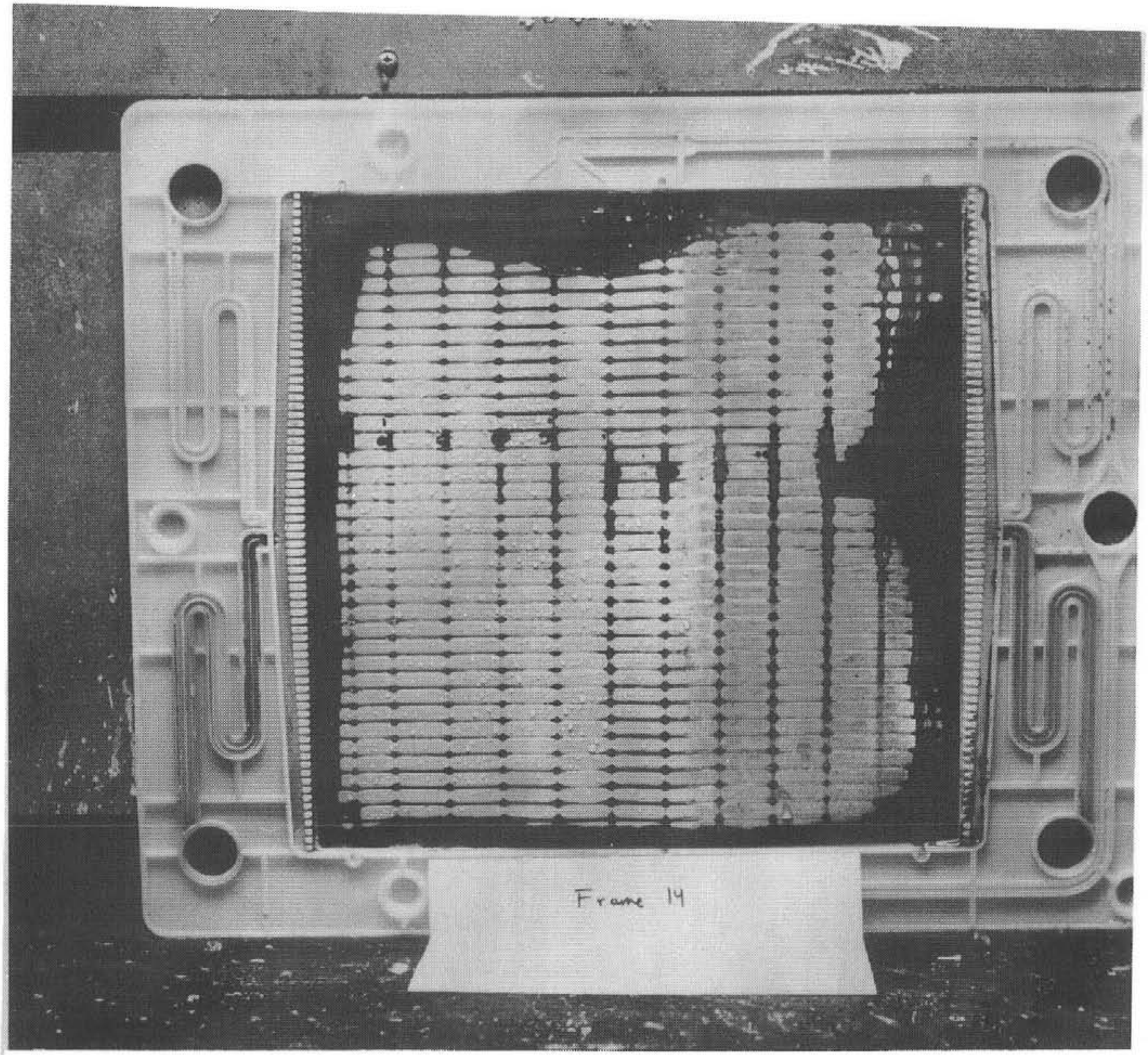

Frame 14

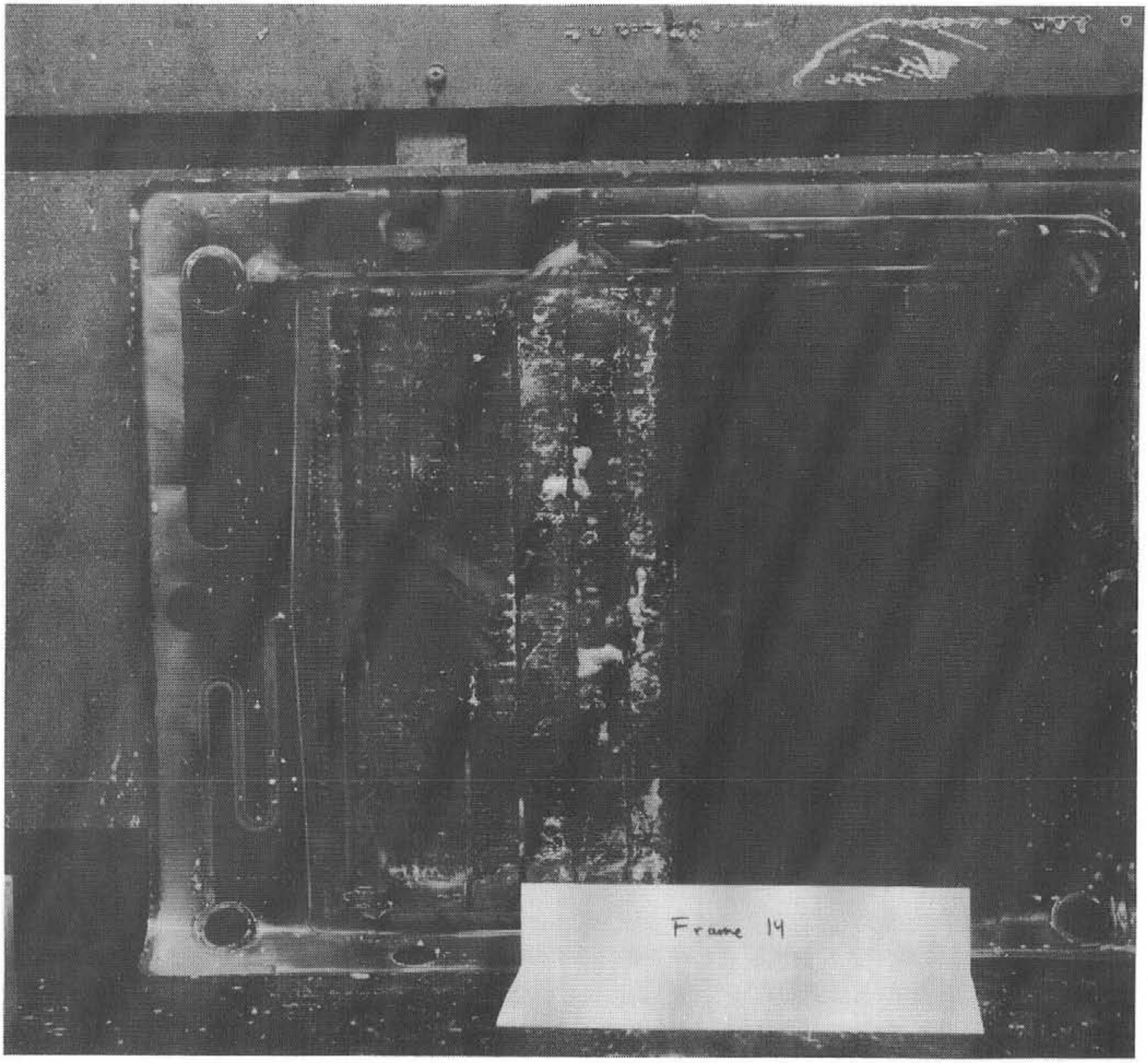

Frame 14

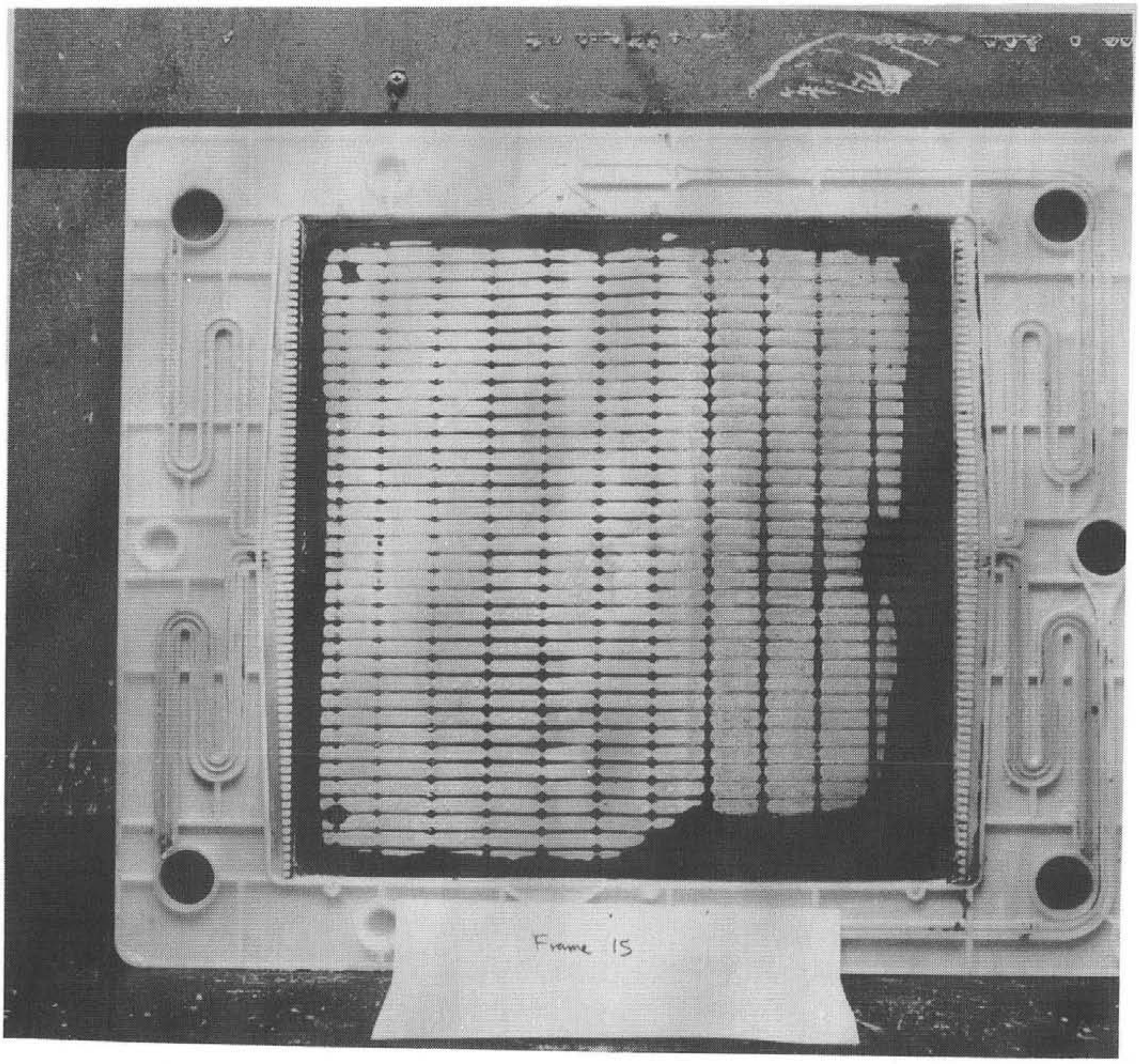

Frame 15

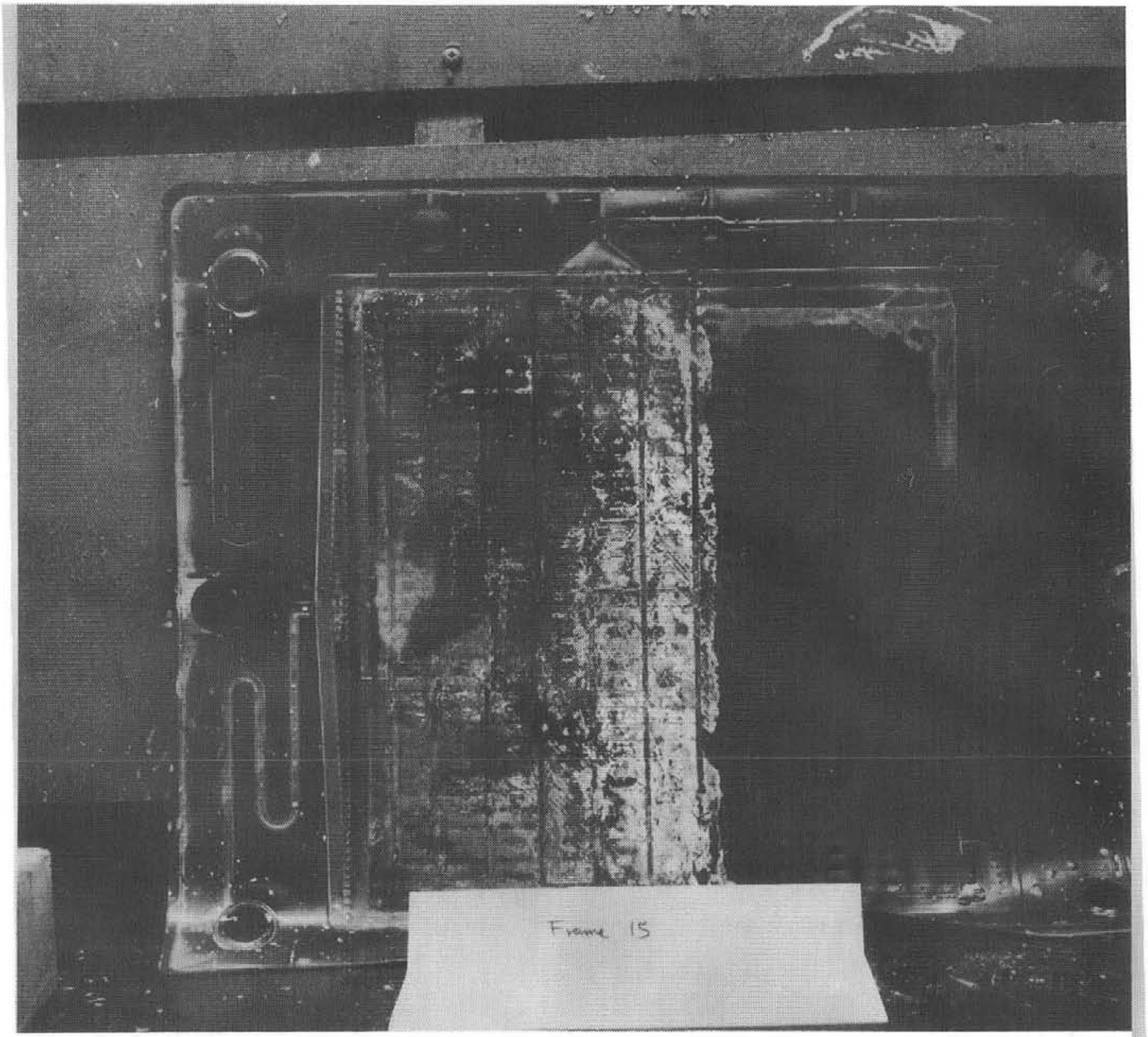

Frame 15

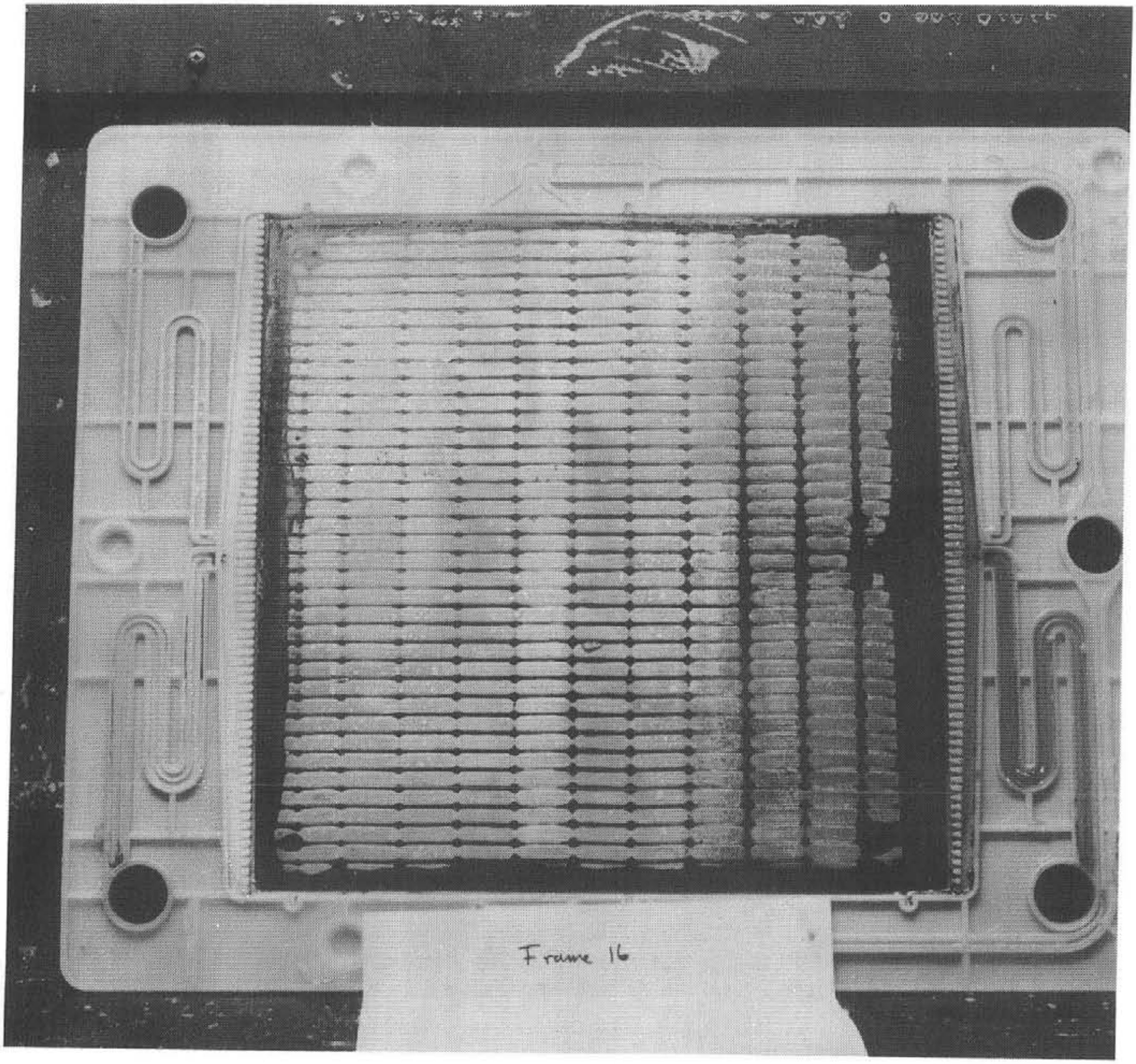

Frame 16

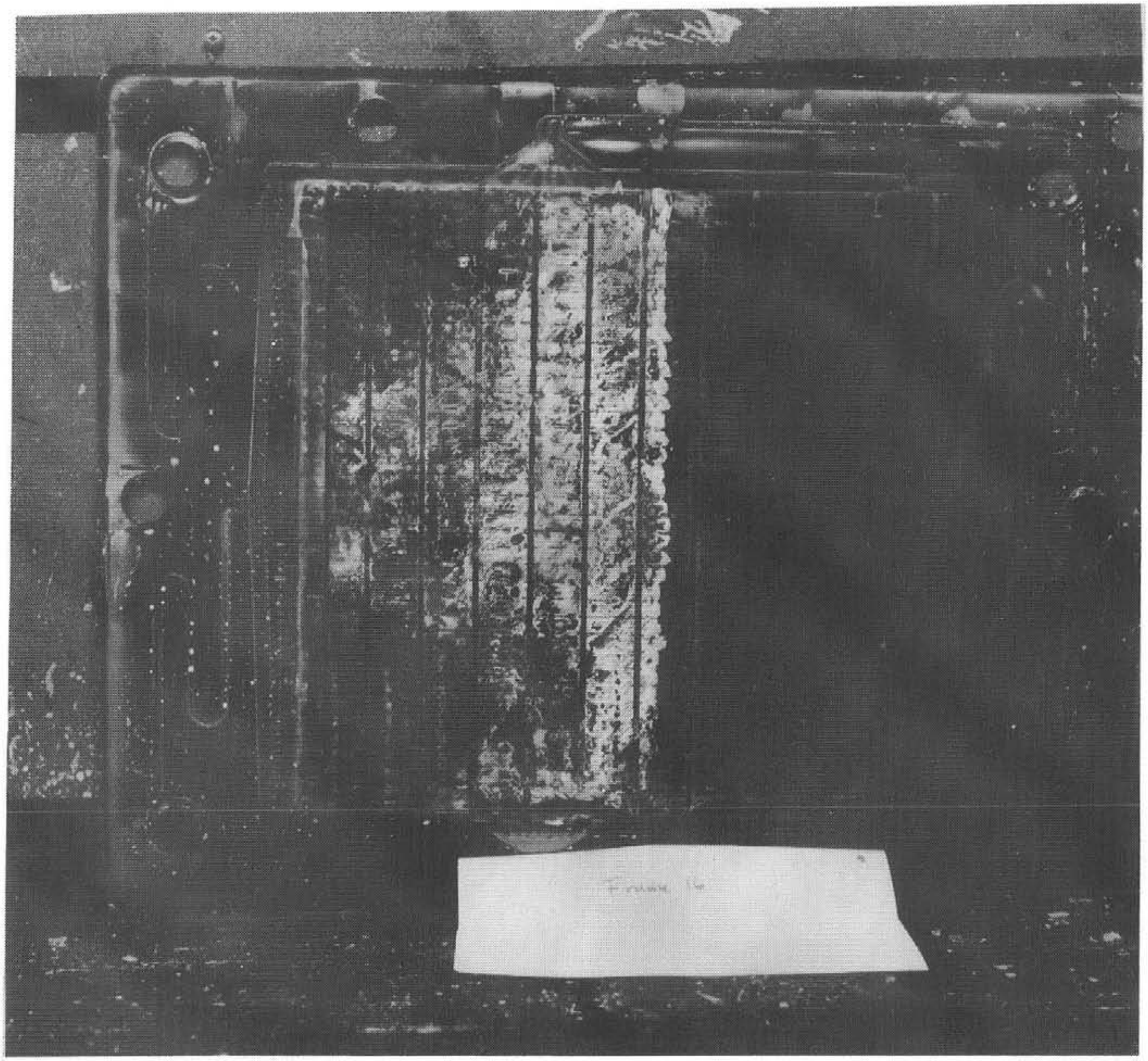

Frame 16

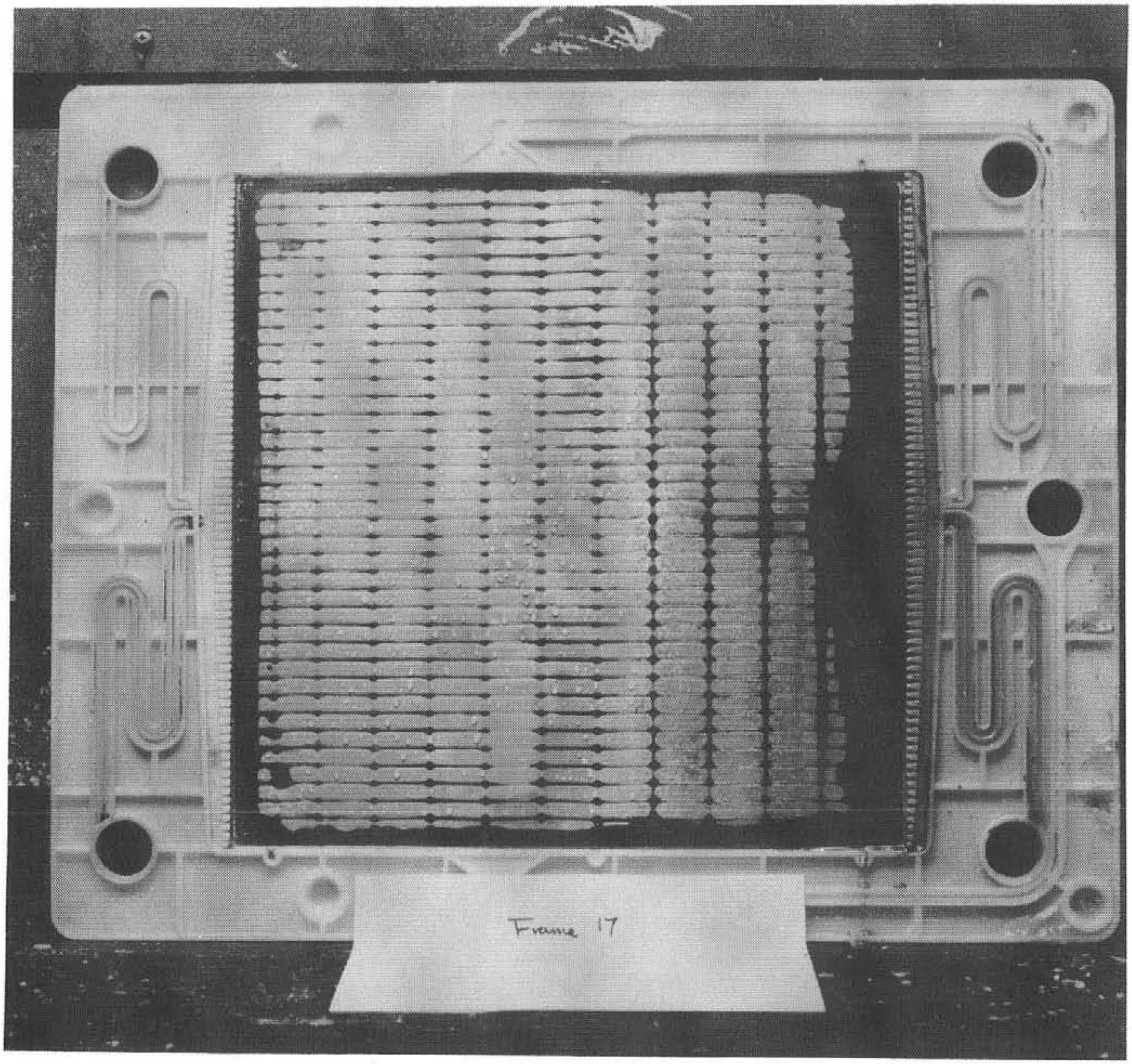

Frame 17

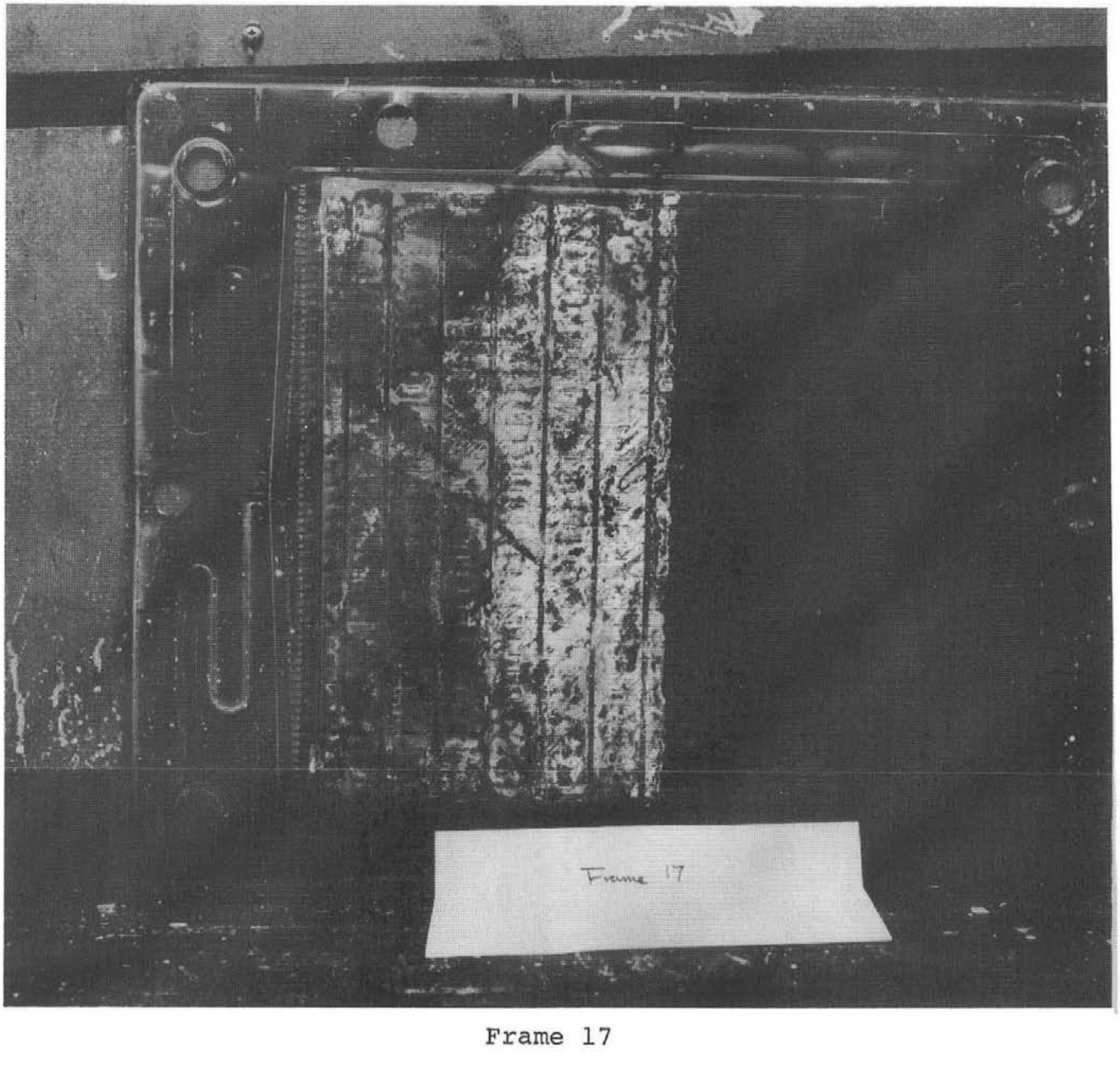

Frame 17

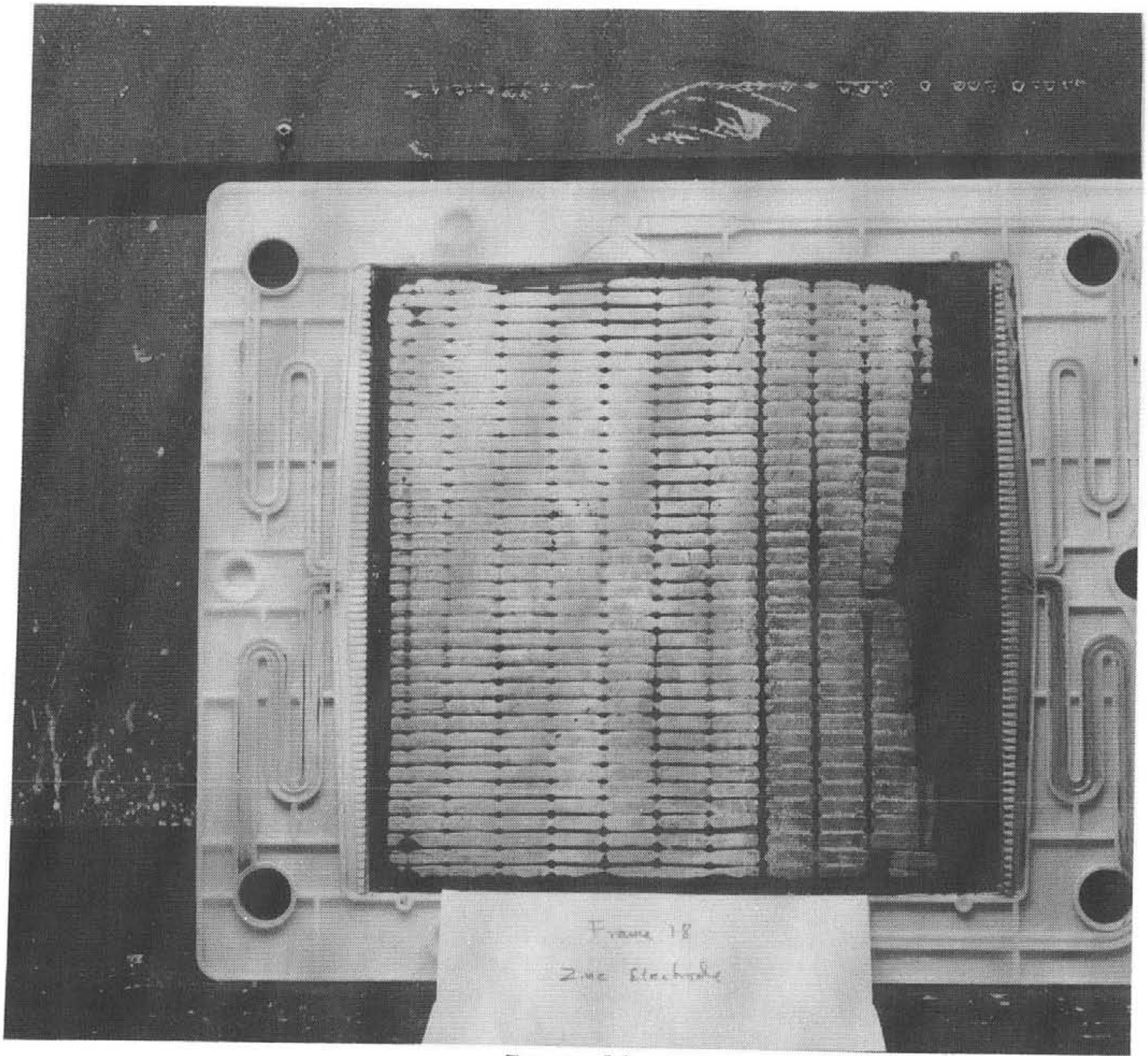

Frame 18
Zinc Electrode

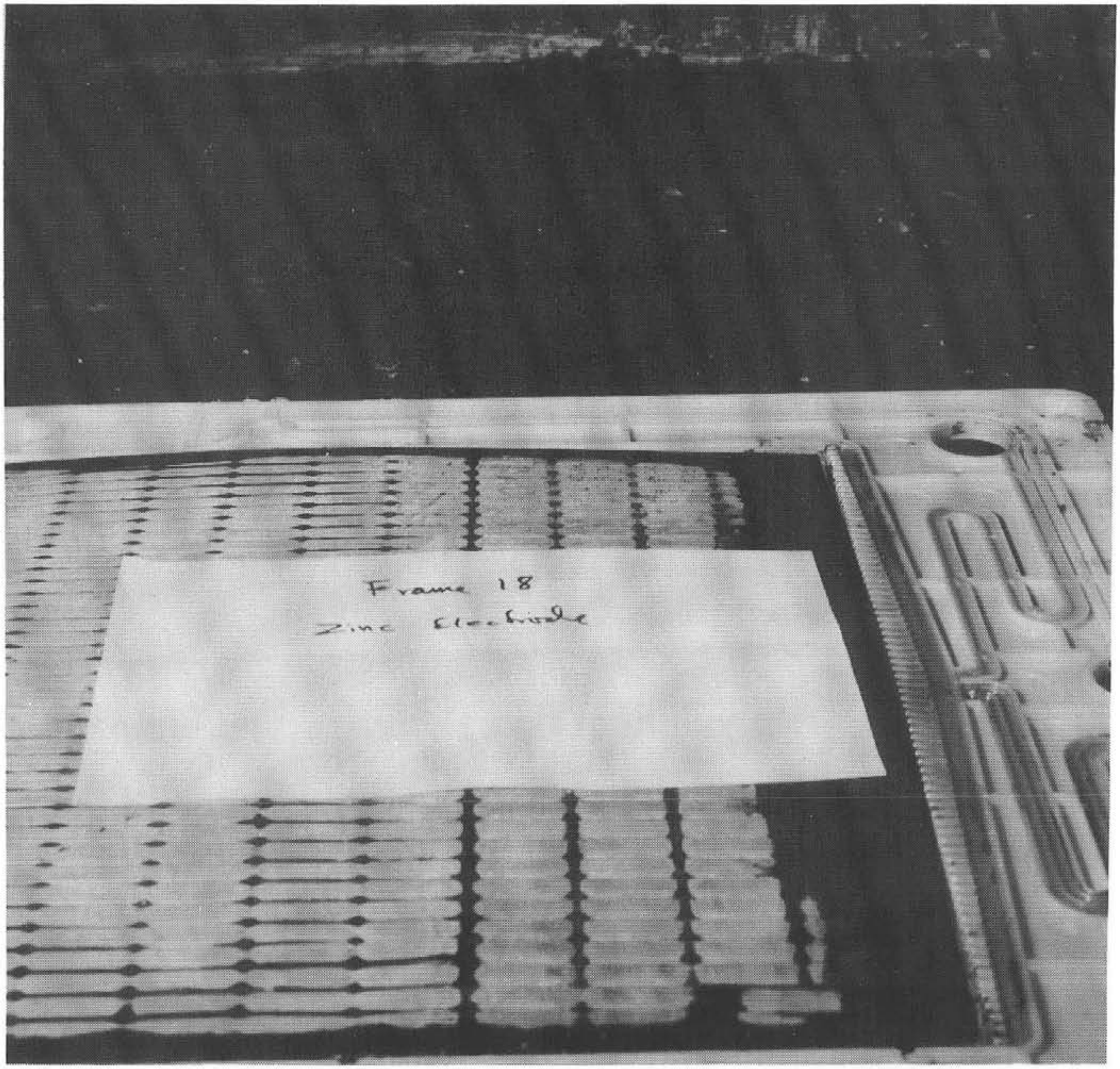

Frame 18
Zinc Electrode

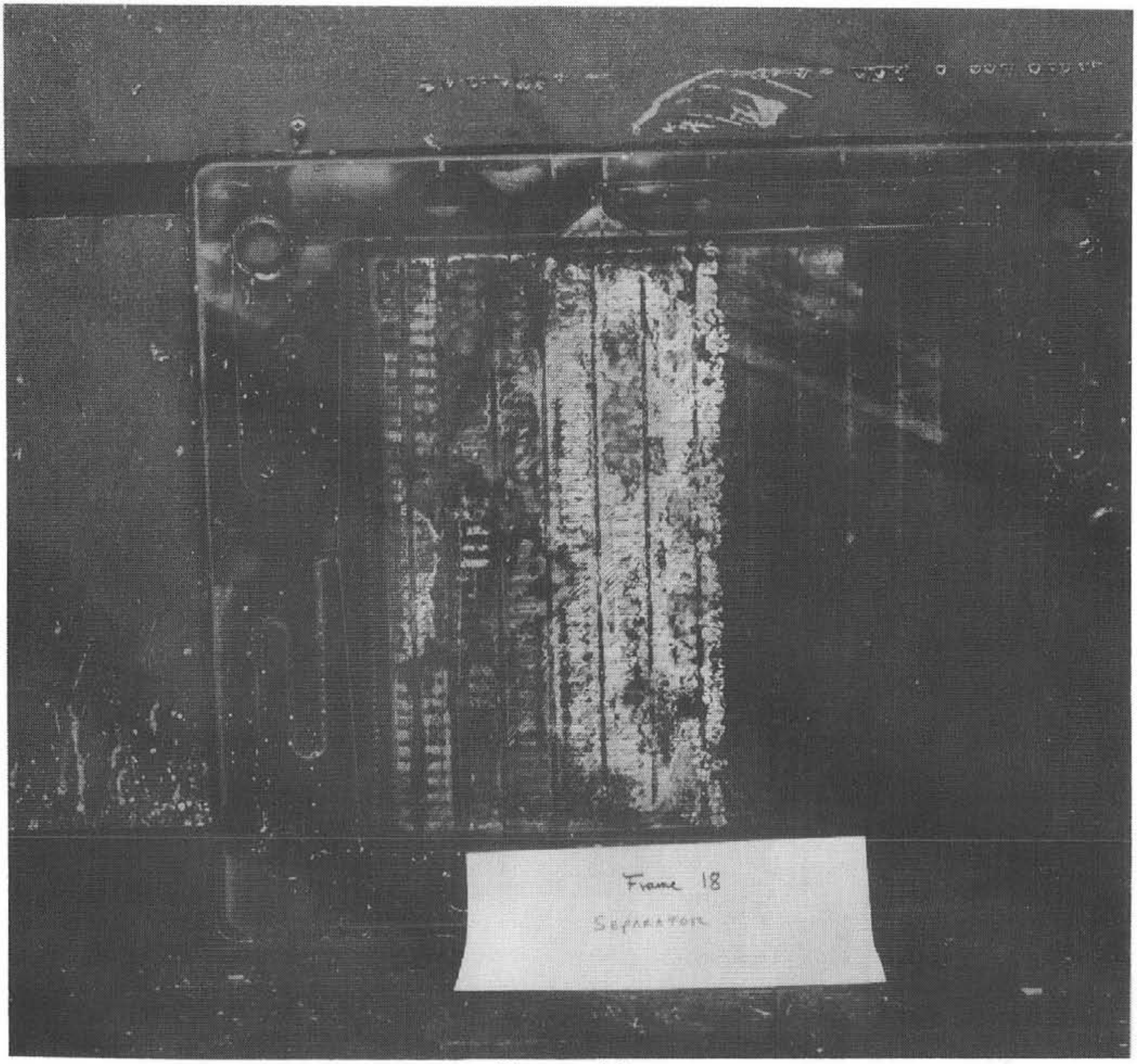

Frame 18
Separator - anode side

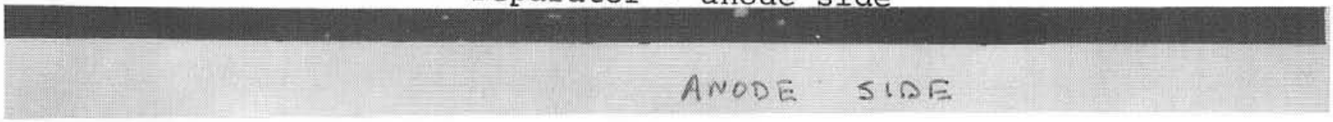

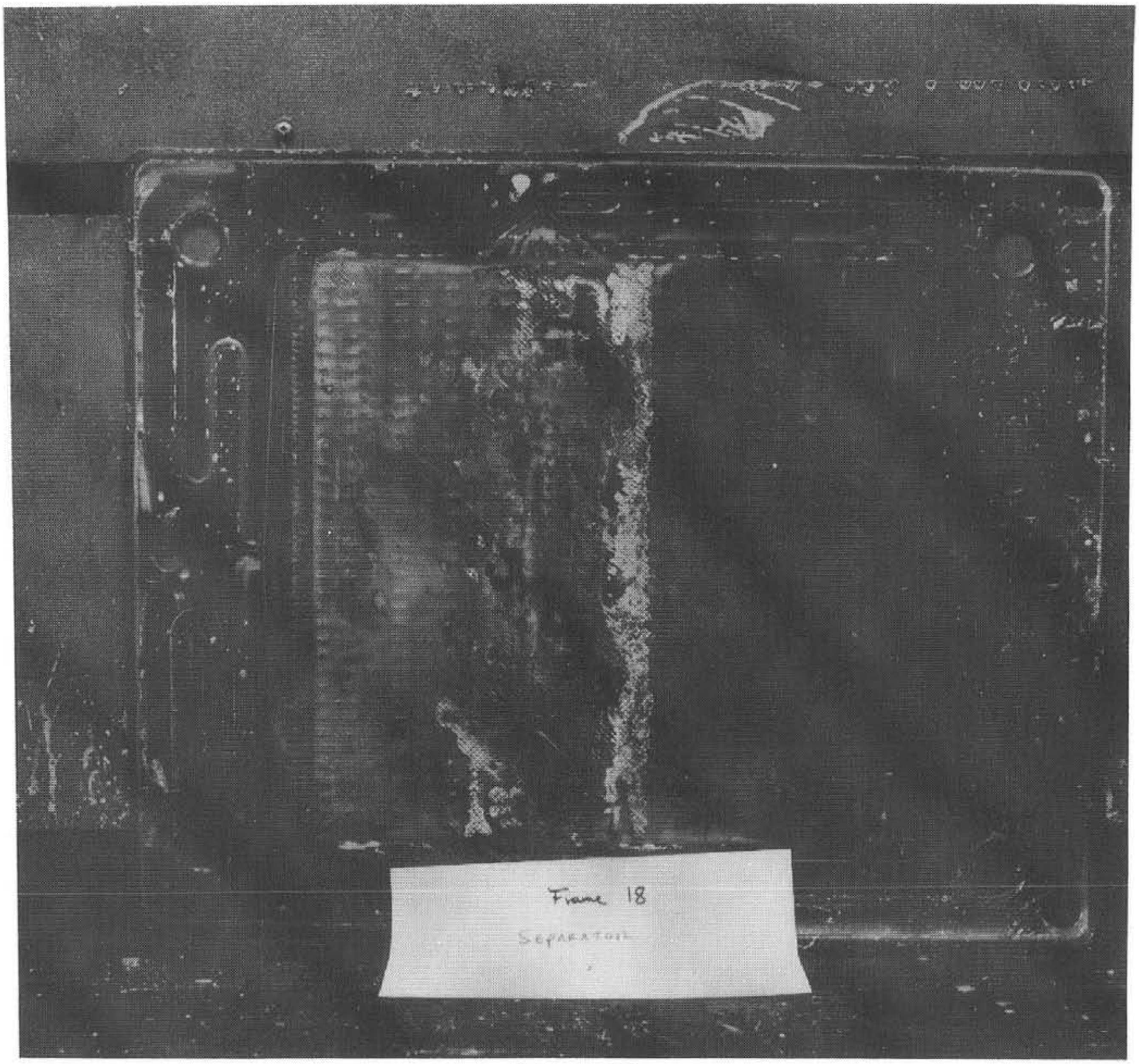

Frame 18
Separator - cathode side

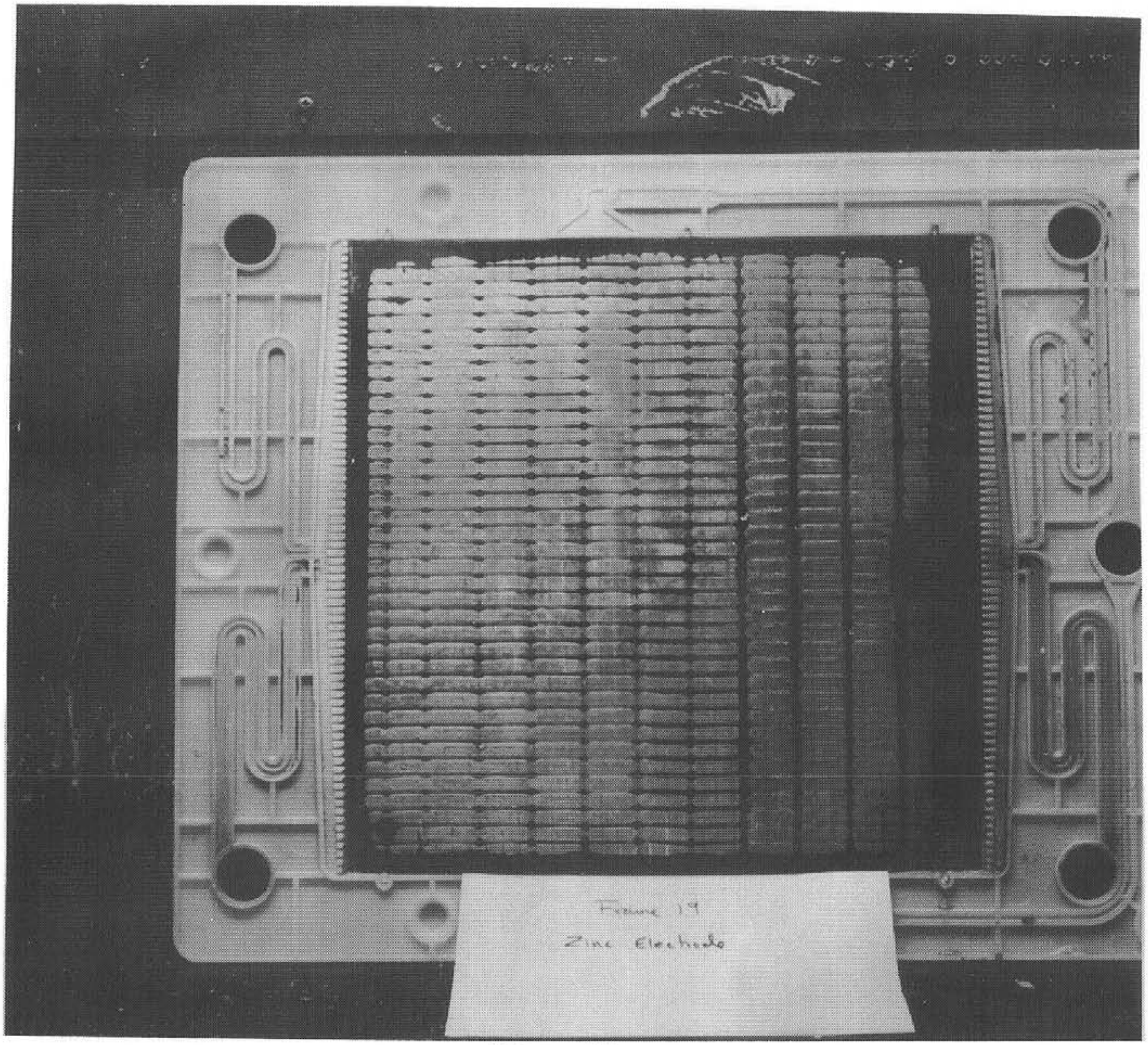

Frame 19
Zinc Electrode

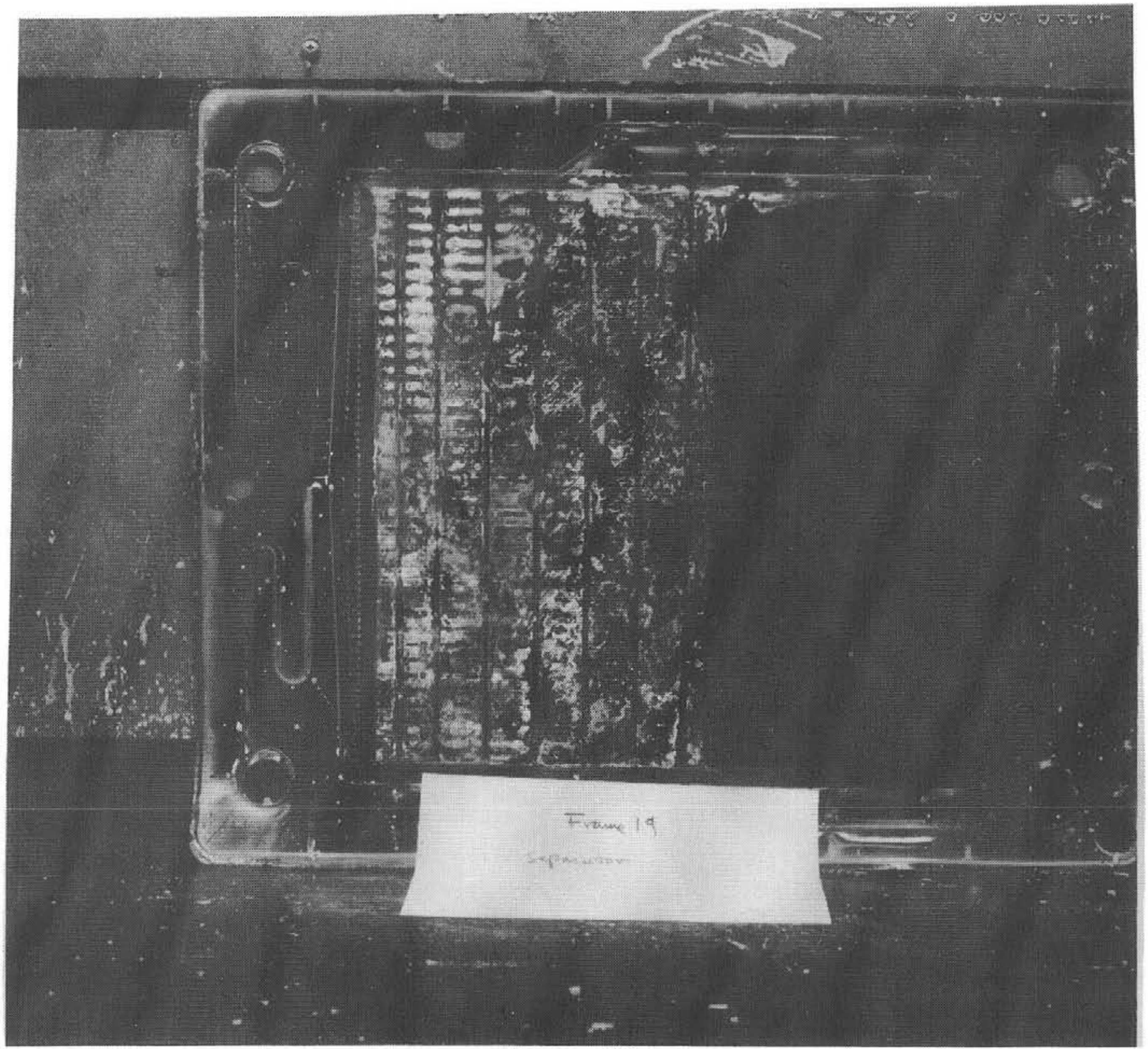

Frame 19
Separator

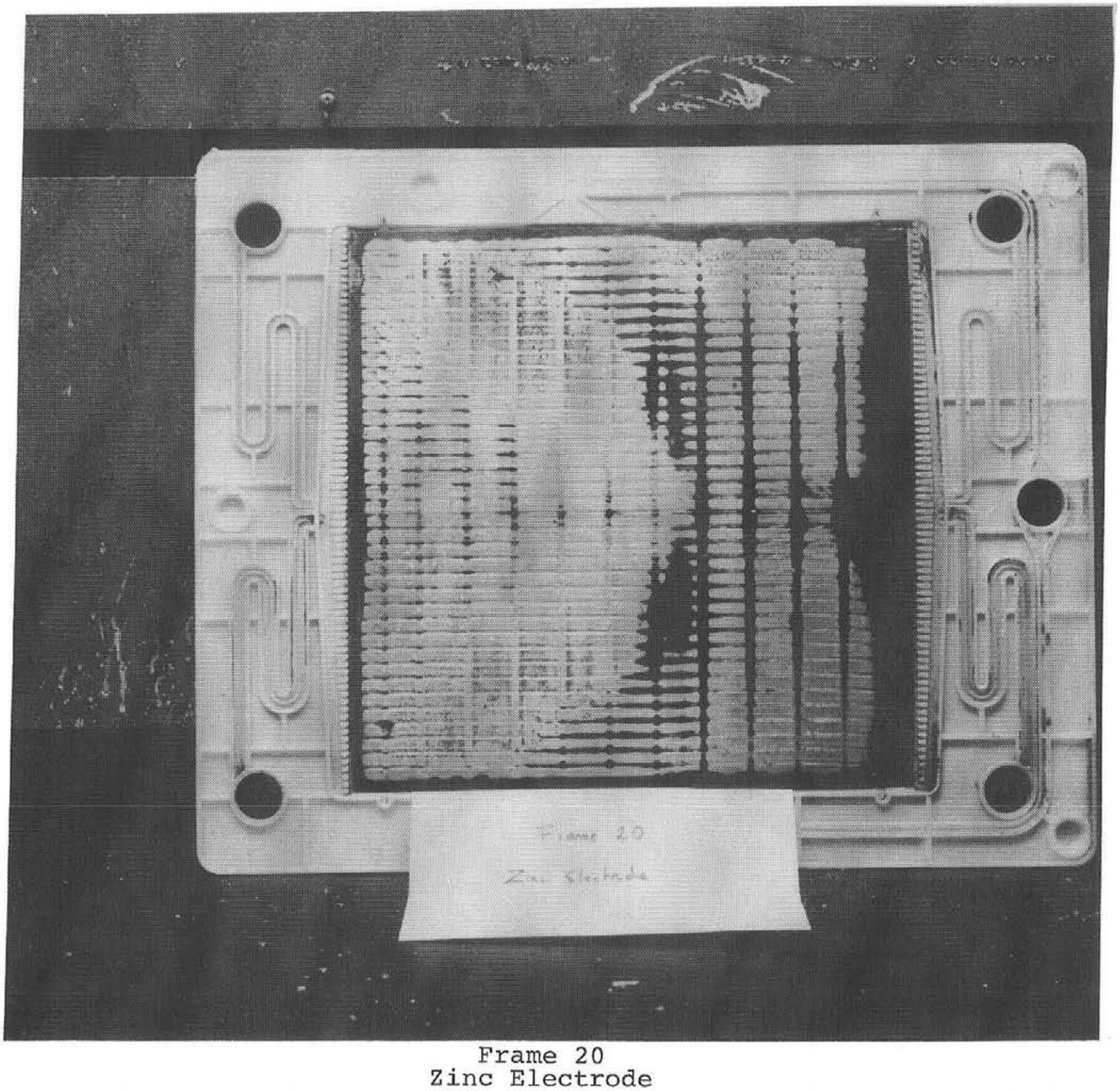

Frame 20
Zinc Electrode

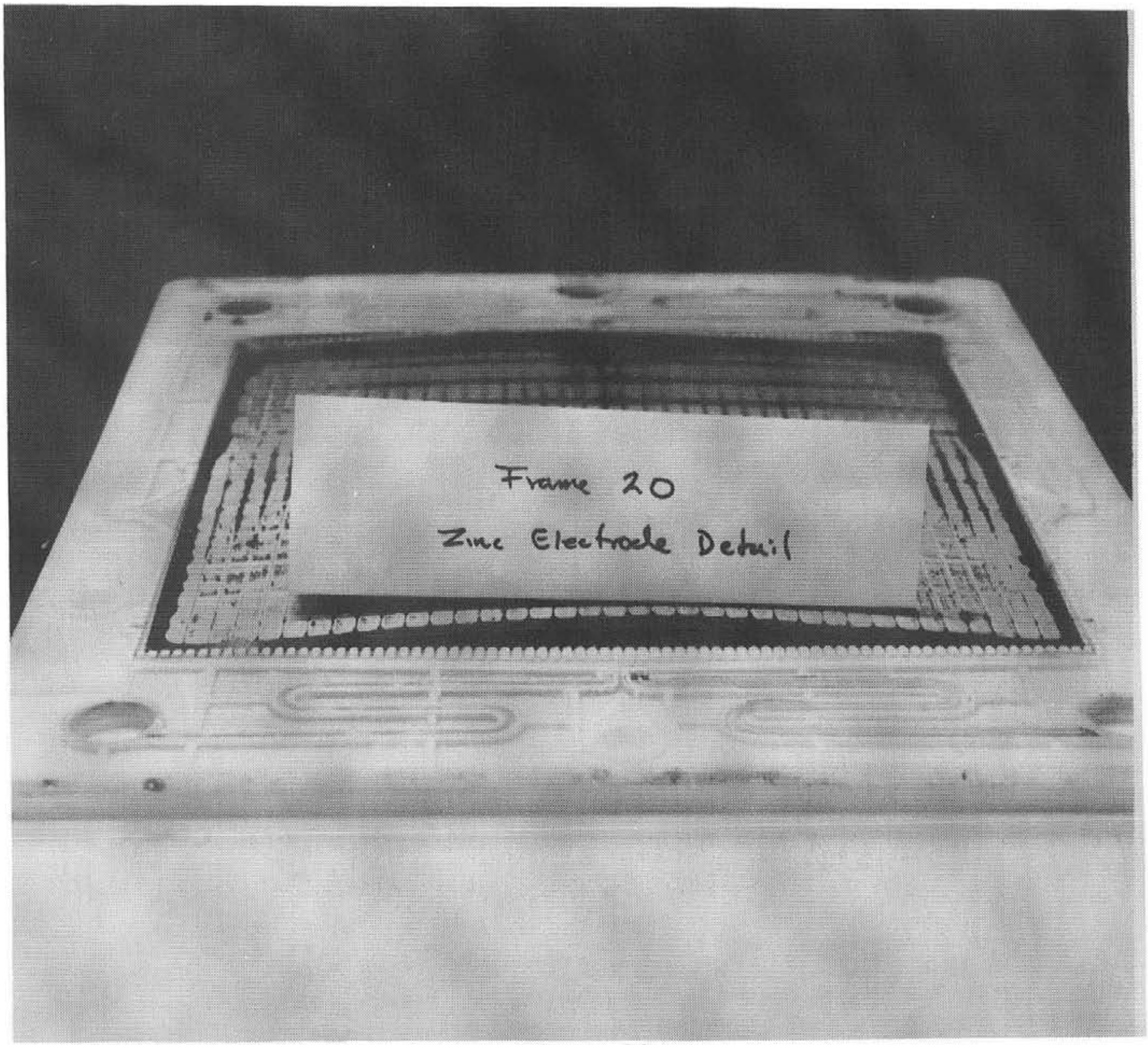

Frame 20
Zinc Electrode Detail

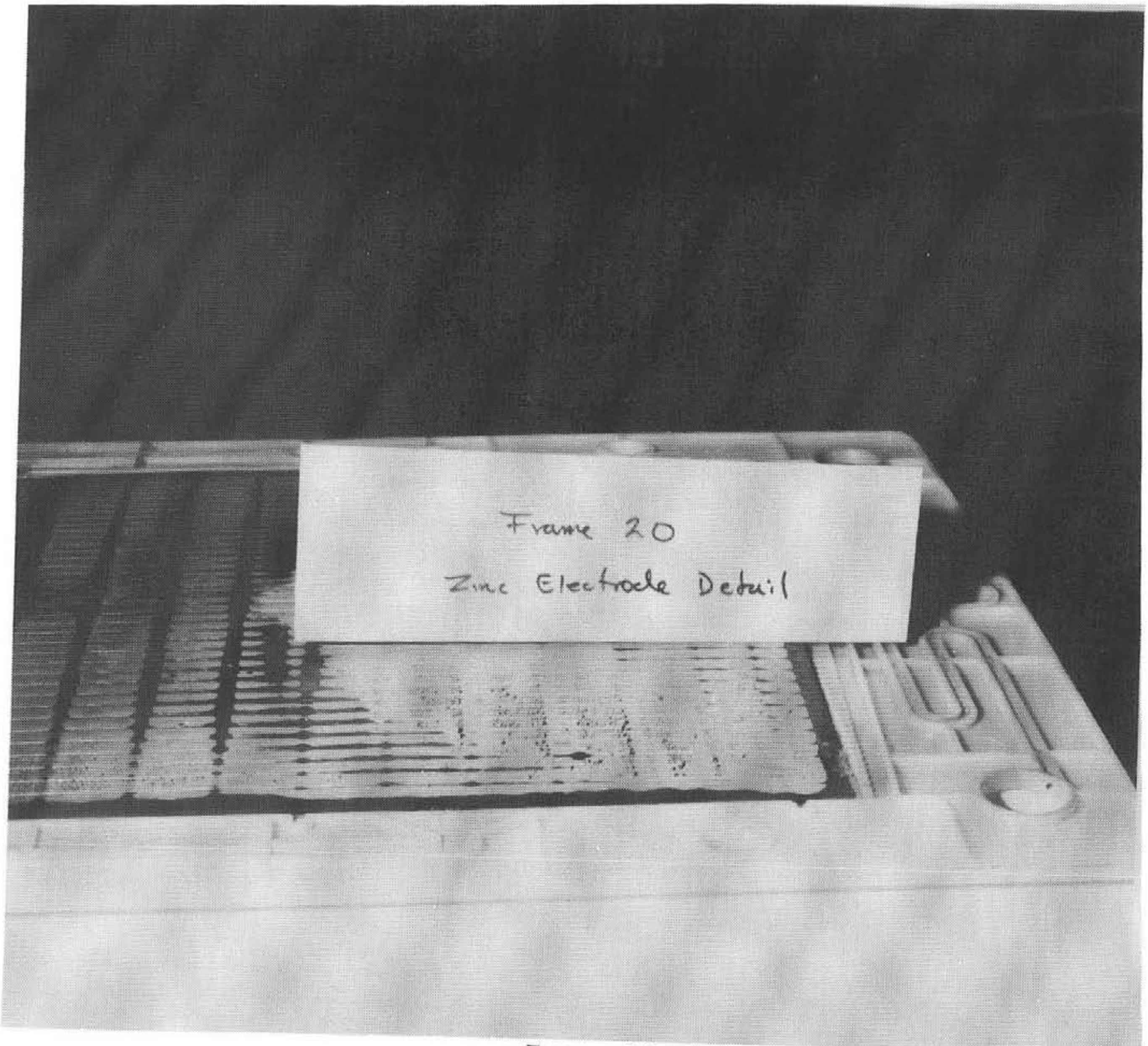

Frame 20
Zinc Electrode Detail

Frame 20
Zinc Electrode Detail

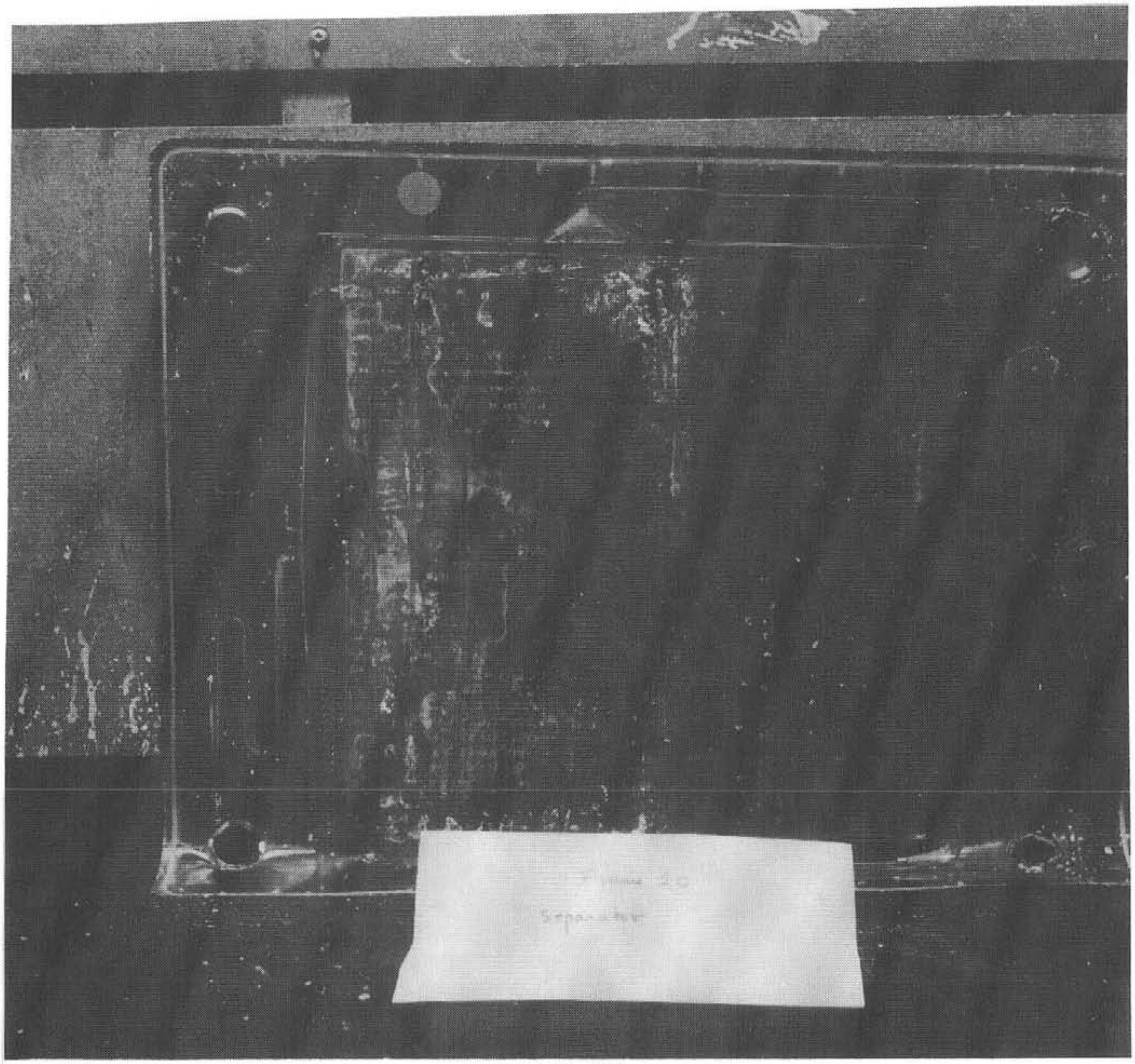

Frame 20
Separator

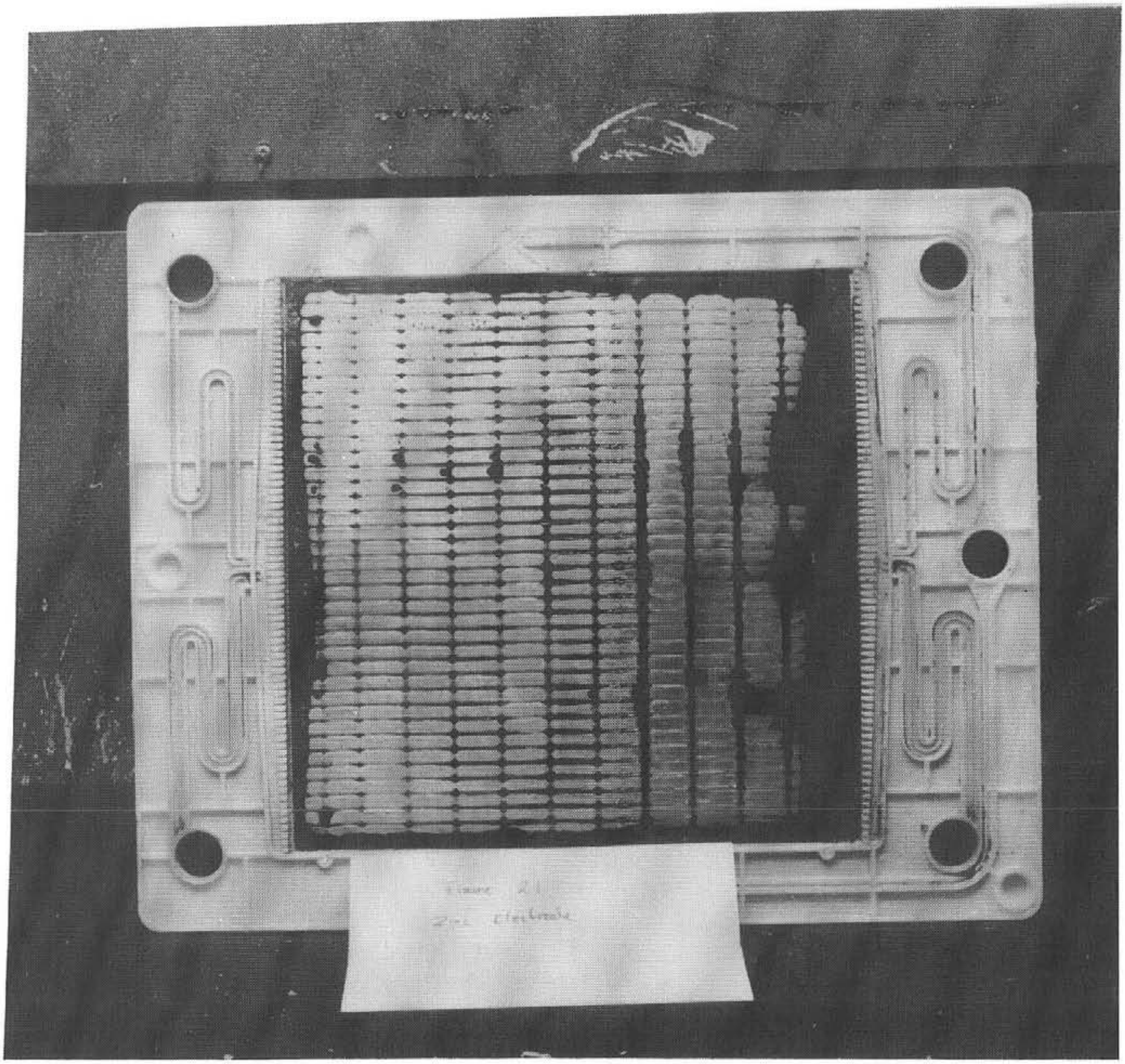

Frame 21
Zinc Electrode

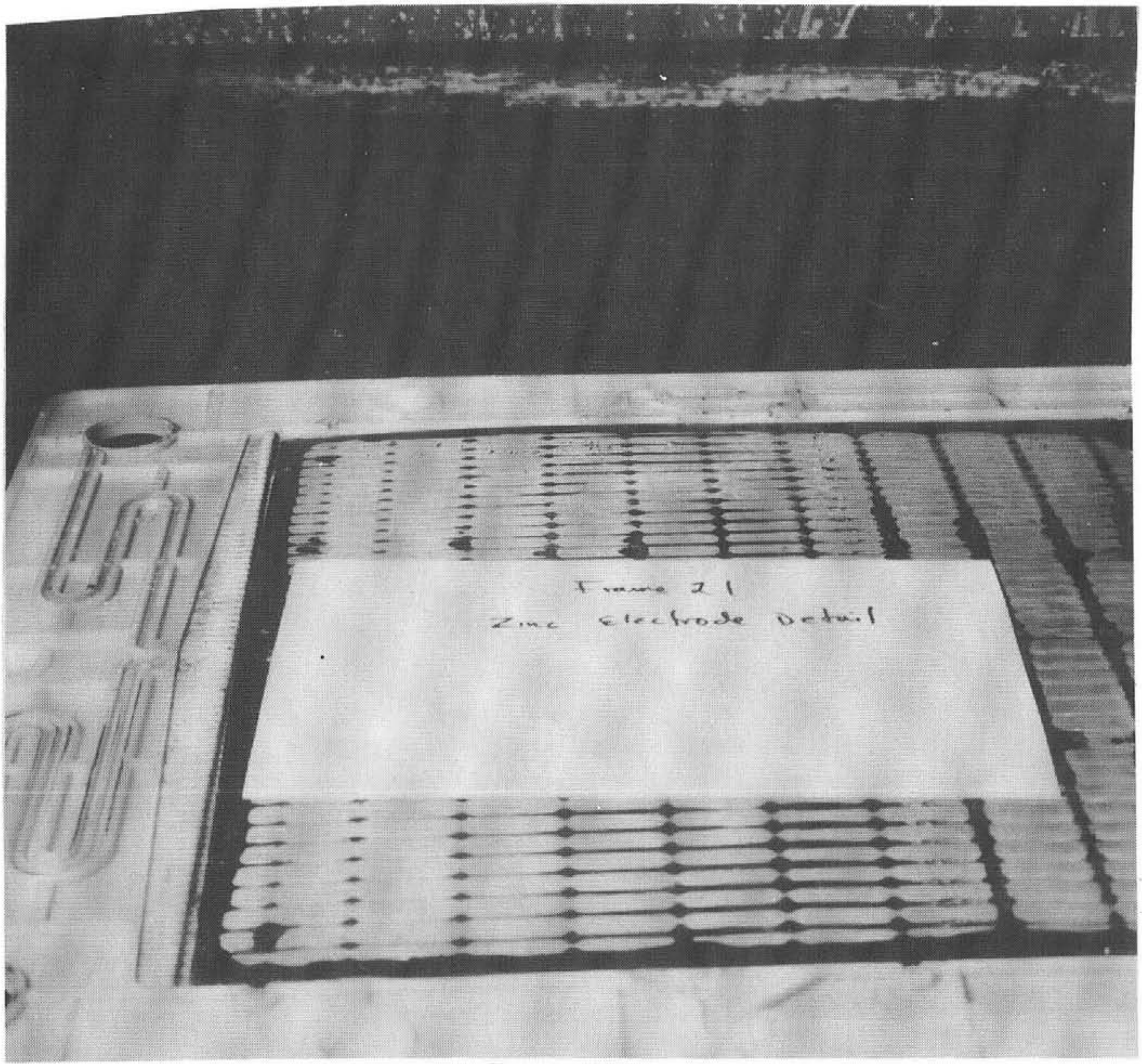

Frame 21
Zinc Electrode Detail

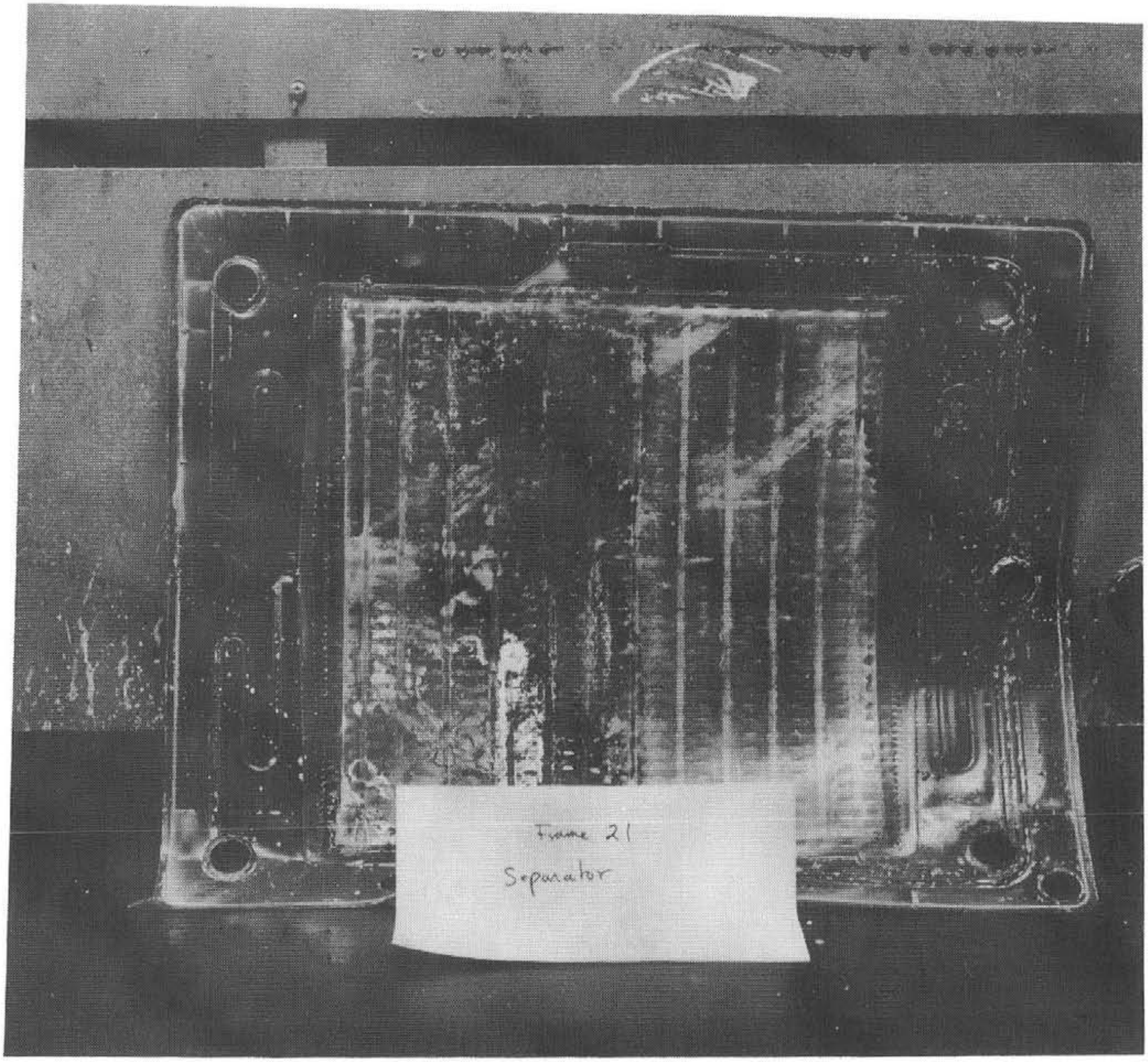

Frame 21
Separator

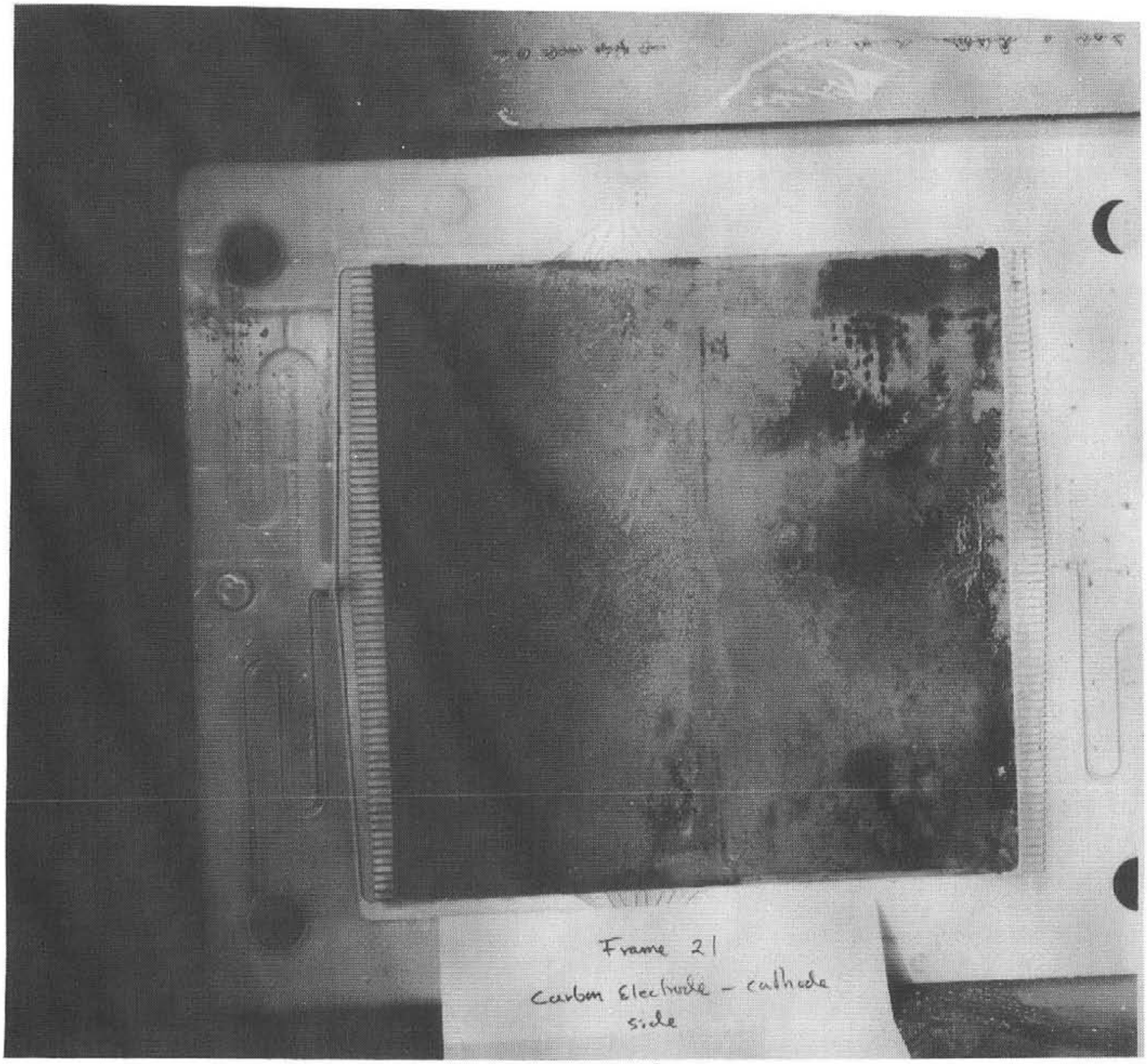

Frame 21
Carbon Electrode - cathode side

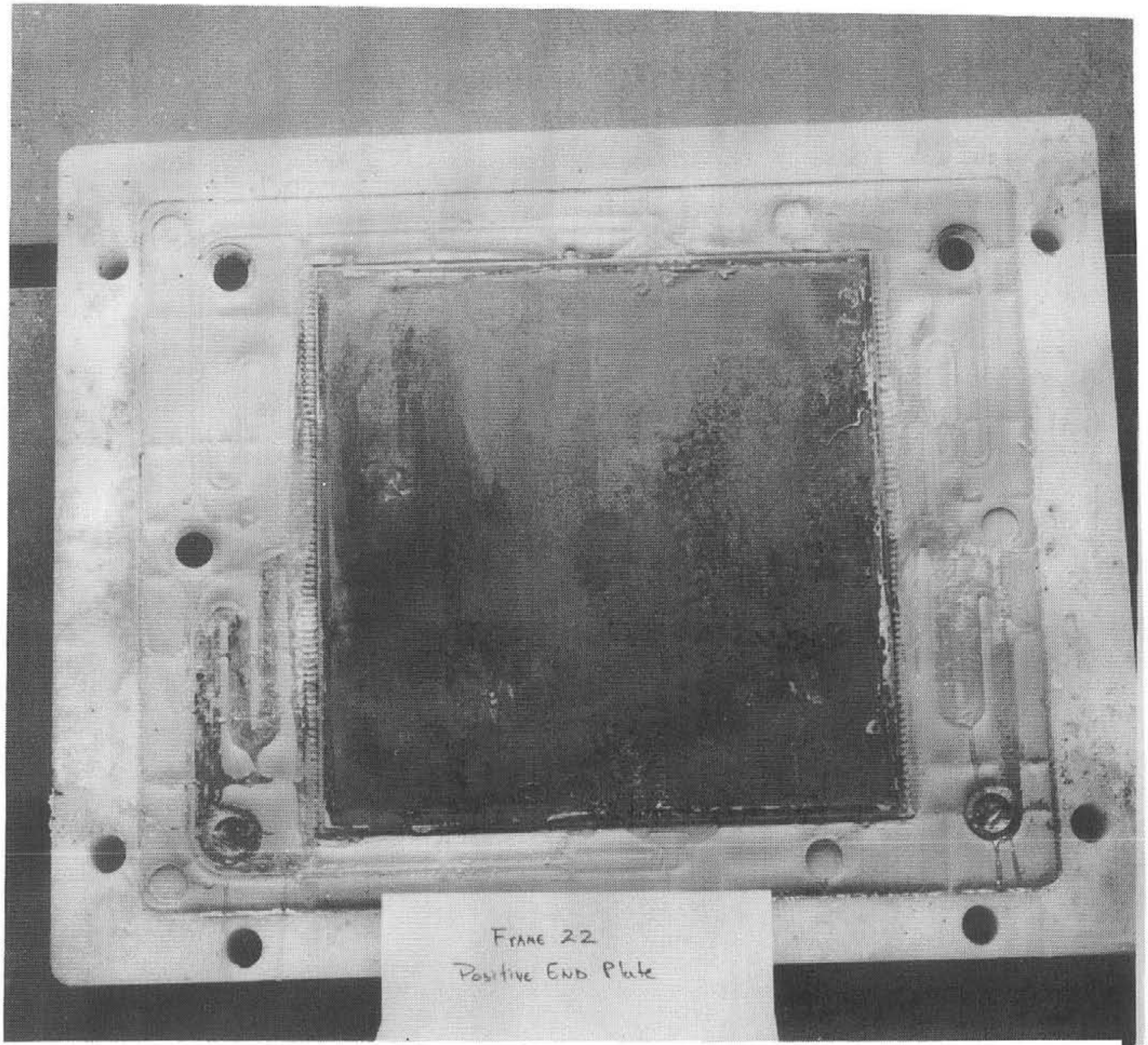

Frame 22
Positive End Plate

REPORT DISTRIBUTION

Alan I. Attia
Gould, Inc., Micro Power Products Div.
2777 Eagendale Blvd.
Eagen, MN 55121

Dr. Richard Bellows
Exxon Research and Engineering Co.
P. O. Box 45
Linden, NJ 07036

Dr. James R. Birk
Electric Power Research Institute
3412 Hillview Ave.
Palo Alto, CA 94303

Mr. Wayne S. Bishop
Wright Aeronautical Laboratories (AFWAL)
Wright-Patterson Air Force Base
Ohio 45433

Dr. Ralph Brodd
AMOCO
P. O. Box 400
Naperville, IL 60566

Dr. Bert Brummet
Energy Development Associates
200 E. Seneca
Greensborough, NC 27406

Kathryn R. Bullock
Johnson Controls, Inc.
P. O. Box 591
Milwaukee, WI 53201

Dr. Elton J. Cairns
Lawrence Berkeley Laboratory
University of California
Berkeley, CA 94720

Charles L. Carter
Tennessee Valley Authority
109 United Bank Building
Chattanooga, TN 37401

Clint Christianson
Argonne National Laboratory
Building 205, CMT, 9700 S. Cass Ave.
Argonne, IL 60439

REPORT DISTRIBUTION

Jack E. Clifford
Battelle Columbus Laboratories
505 King Ave.
Columbus, OH 43201

Dr. William DeLuca
Argonne National Laboratory
Building 205, CMT, 9700 S. Cass Ave.
Argonne, Illinois 60430

Walter Dippold
U. S. Deapartment of Energy, CE-132
FORSTL
Washington, DC 20585

Mr. Ed Dowgiallo
U. S. Department of Energy, CE-132
FORSTL
Washington, DC 20585

David O. Feder
Consultant
35 Ridgedale Ave.
Madison, NJ 07940

D. Thomas Ferrell, Jr.
U. S. Department of Energy
FORSTL
Washington, DC 20585

Dr. Charles W. Fleischmann
C & D Power System
3042 Walton Rd.
Plymouth Meeting, Pennsylvania 19462

Dr. Ed Gay
Argonne National Laboratory
Building 205, CMT, 9700 S. Cass Ave.
Argonne, Illinois 60439

Donald R. Glenn
Energy Research Corporation
Suite 200, 1627 K St. NW
Washington DC 20006

Mr. Norman Hagedorn
NASA Lewis Research Center
21000 Brook Park Rd.
Cleveland, Ohio 44135

REPORT DISTRIBUTION

Jasper Hardin
EG&G Idaho, Inc.
P. O. Box 1625
Idaho Falls, ID 83415

Dr. Gary L. Henriksen
Energy Development Associates
200 E. Seneca
Greensborough, NC 27406

Mr. Roger Hollandsworth
Lockheed Missiles and Space Co., LPARL
3251 Hanover Street
Palo Alto, CA 94304

Mr. Fred Hornstra
Argonne National Laboratory
Building 205, CMT, 9700 S. Cass Ave.
Argonne, Illinois 60430

Jonathan Hurwitch
Battelle Washington Operations
2030 M St. NW
Washington DC 20036

Dr. E. A. Hyman
Public Service Electric and Gas Co.
80 Park Plaza
Newark, NJ 07101

Dr. Ted J. Iltis
Wisconsin Power and Light Company
P. O. Box 192
Madison, WI 53701

Dr. Kim Kinoshita
Lawrence Berkeley Laboratory
1 Cyclotron Rd.
Berkeley, CA 94720

Dr. Robert S. Kirk
U. S. Department of Energy CE-132
FORSTL
Washington, DC 20585

Mr. Martin G. Klein
Energy Research Corp.
3 Great Pasture Road
Danbury, CT 06810

REPORT DISTRIBUTION

Dr. Karl Kordesch
2060 Arthur Avenue
Lakewood, OH 44107

Dr. Albert Landgrebe
U. S. Department of Energy, CE-141
FORSTL
Washington, DC 20585

Mr. Tony Leo
Energy Research Corporation
3 Great Pasture Rd.
Danbury, CT 06810

Dr. Charles Levine
Dow Chemical Company
2800 Mitchell Drive
Walnut Creek, CA 94598

Dr. Arturo Maimoni
LLL, L-367, Bldg. 2401, R. 132
P. O. Box 808
Livermore, CA 94550

Donald E. Mains
Electrochemical Power Sources Division
NAD
Crane, IN 47522

Dr. Paul Malachesky
Exxon Research and Engineering Co.
P. O. Box 45
Linden, NJ 07036

Victor Matricardi
The Aerospace Corp.
955 L'Enfant Plaza SW, Suite 4000
Washington DC 20024

Dr. Frank McLarnon
Lawrence Berkeley Laboratory
University of California
Berkeley, CA 94720

Dr. Peter Pierini
Dow Chemical Company
2800 Mitchell Drive
Walnut Creek, CA 94598

REPORT DISTRIBUTION

Dr. Al Pivec
Public Service Electric and Gas Co.
80 Park Plaza
Newark, NJ 07101

Mr. Ronald Putt
Duracell, Inc.
4261 Communications Drive
Norcross, GA 30093

C. B. Quinn
U. S. Department of Energy
P. O. Box 5400
Albuquerque, NM 87115

Dr. James Quinn
U. S. Department of Energy, CE-141
FORSTL
Washington, DC 20585

Dr. Brad M. Radimer
Public Service Electric & Gas Co.
80 Park Plaza
Newark, NJ 07101

Dr. J. R. Selman
Illinois Institute of Technology
Dept. of Chemical Engineering
Chicago, IL 60616

Mr. William C. Spindler
Electric Power Research Institute
3412 Hillview Ave.
Palo Alto, CA 94304

Philip C. Symons
Electrochemical Engineering Consultants
133 Mission Drive
Palo Alto, CA 94303

Dr. Larry H. Thaller
NASA Lewis Research Center
21000 Brook Park Rd.
Cleveland, Ohio 44135

Dr. William Tiedeman
Johnson Controls, Inc.
P. O. Box 591
Milwaukee, WI 53201

REPORT DISTRIBUTION

G. J. Walker
U. S. Department of Energy
FORSTL
Washington DC 20585

Dr. Charles Warde
Energy Development Associates
200 E. Seneca
Greensborough, NC 27406

Robert D. Weaver
Electric Power Research Institute
3412 Hillview Ave.
Palo Alto, CA 94303

Conrad E. Weinlein
Johnson Controls, Inc.
P. O. Box 591
Milwaukee, WI 53201

Irwin B. Weinstock
The Aerospace Corp.
955 L'Enfant Plaza SW, Suite 4000
Washington DC 20024

Dr. N. P. Yao
Argonne National Laboratory
Building 205, CMT, 9700 S. Cass Ave.
Argonne, Illinois 60430

2500	H. J. Saxton
2520	N. J. Magnani
2522	R. D. Wehrle
2523	J. T. Cutchen
2525	R. P. Clark
2525	P. C. Butler (30)
2525	J. L. Chamberlin
3141	C. M. Ostrander (5)
3151	W. L. Garner (3)
5154-3	C. H. Dalin (25)
8024	M. A. Pound